

## ABSTRACT

Title of Document: REGULATION OF ESTUARINE  
BIOGEOCHEMICAL PROGRESSES BY  
CYANOBACTERIAL BLOOMS

Yonghui Gao, PhD., 2012

Directed By: Prof. Jeffrey C. Cornwell  
Prof. Diane K. Stoecker  
Marine Estuarine Environmental Science

Nutrient supply, including 'new' nitrogen (N) added through N<sub>2</sub>-fixation, nutrient release from sediments and freshwater inflow, can be important in increasing and sustaining estuarine phytoplankton blooms. In return, dense blooms in shallow water estuaries may affect nutrient recycling by elevating the pH and dissolved oxygen (DO) concentrations as well as increasing sedimentation of phytoplankton detritus. My dissertation addressed the interaction between cyanobacterial blooms and biogeochemical nutrient recycling in the tidal-fresh and oligohaline region of the Sassafra River, a tributary of the Chesapeake Bay, Maryland, USA.

When high pH overlying water comes in contact with sediments, the subsequent pH penetration causes desorption of exchangeable NH<sub>4</sub><sup>+</sup> and converts NH<sub>4</sub><sup>+</sup> to NH<sub>3</sub> from both porewater and absorbed NH<sub>4</sub><sup>+</sup> pools. Alkaline pH and the toxicity of NH<sub>3</sub> may inhibit nitrification in the thin aerobic zone. During massive cyanobacterial blooms in summer, high effluxes of SRP and total ammonium from sediments were associated with

reduced nitrification and denitrification rates. Retention of N in the upper estuary and increased dissolved inorganic nitrogen (DIN) release into the water column may facilitate nitrogen assimilation by cyanobacteria in N-limited water. High pH also resulted in a significant increase in soluble reactive phosphate (SRP) flux and lead to relatively high SRP compared to DIN flux rates, which may support the high P demand of N<sub>2</sub>-fixing cyanobacteria.

As N became limiting in summer, the dominant cyanobacterial assemblage changed from non-N<sub>2</sub> fixers (*Microcystis* spp.) to N<sub>2</sub> fixers (*Anabaena* spp., *Pseudanabaena* sp. and *Synechococcus* sp.). Warm temperatures, high P availability and low salinity are environmental factors associated with high rates of N<sub>2</sub> fixation. Dissolved inorganic carbon (DIC) limitation, high pH, and high DO concentrations, mediated by cyanobacterial photosynthesis, can cause decreases in photosynthetic efficiency and daytime N<sub>2</sub> fixation of the cyanobacterial assemblage. Species succession appears to enable the cyanobacterial assemblage to adapt to changing environmental conditions caused by the bloom, including high pH and DO, and to maintain N<sub>2</sub> fixation for sustained growth.

REGULATION OF ESTUARINE BIOGEOCHEMICAL PROCESSES BY  
CYANOBACTERIAL BLOOMS

By

Yonghui Gao

Dissertation submitted to the Faculty of the Graduate School of the  
University of Maryland, College Park, in partial fulfillment  
of the requirements for the degree of  
Doctor of Philosophy  
2012

Advisory Committee:  
Professor Jeffrey C. Cornwell, Chair  
Diane K. Stoecker, Co-chair  
Judith M. O'Neil  
Walter R. Boynton  
Daniel E. Terlizzi

© Copyright by  
Yonghui Gao  
2012

## Acknowledgements

Throughout my dissertation, I have been fortunate enough to have received lots of help, guidance, support and love. This dissertation would not have been possible without them.

I would like to express my appreciation to my dissertation committee. It is a real pleasure to learn and grow from people you respect through the whole process. Their invaluable advice encouraged and inspired me to complete this research. Specifically, I want to thank Jeffrey C. Cornwell and Diane K. Stocker who have helped me since the first day I came to Cambridge and have guided me with endless patience. I benefited tremendously from their teaching in writing, presentation and research. I thank Judy M. O'Neil for providing me with lab space, equipment and many fruitful ideas, and helping to improve the quality of the dissertation. I would like to express my gratitude to Walter R. Boynton and Daniel E. Terlizzi, who were always accessible and willing to help my research.

Besides my committee members, I have reached out to numerous other people for help, and have been rewarded by their generosity. Mike Owens helped with the laboratory experiments and analyses. Todd Kana was instrumental in assisting me with dissolved gas analysis. Ming Li was on my committee for years, acted as a friend and gave me suggestions both in research and life. Patient and helpful technical assistance also came from Alison Weigel, Robert Gutierrez, Lois Lane, Jen O'Keefe and Meg Maddox. A number of other people were also charitable with their time, ideas, and with historical, including Bruce Michael of Maryland DNR, Kascie Herron formerly of the Sassafras River Association, and Gary Shenk of the EPA/ Chesapeake Bay Program. I also

received support from exceptionally bright and motivated undergraduate REU students including Elizabeth Brunel and Zsolt Kormendy. Financial support was provided by a Horn Point Lab Graduate Student Assistantship, Horn Point Laboratory small grant and travel awards for supplies and funds to attend conferences, Maryland Sea Grant (award NA10OAR4170072-NOAA to Stoecker and Cornwell) and a Maryland Sea Grant Graduate Research Fellowship.

Finally, many thanks to my husband, Ji Li, and my parents for all of their love and support.

# Table of Contents

Acknowledgements.....	ii
Table of Contents.....	iv
List of Tables.....	viii
List of Figures.....	ix
Chapter 1 Introduction.....	1
1.1 Introduction.....	1
1.1.1 Cyanobacterial Blooms.....	1
1.1.2 Cyanobacterial Blooms in the Sassafra River.....	3
1.2 Hypotheses.....	5
1.3 Objectives.....	6
References.....	8
Figure.....	12
Chapter 2 Effects of cyanobacterial-driven pH increases on sediment nutrient fluxes and coupled nitrification-denitrification in a shallow fresh water estuary.....	13
2.1 Abstract.....	13
2.2 Introduction.....	14
2.3 Materials and Methods.....	17
2.3.1 Study site and collection of cores.....	17
2.3.2 Experimental design.....	18
2.3.3 Flux rates cross the sediment-water interface.....	19
2.3.4 Sediment pore-water chemistry.....	20
2.3.5 Nitrification potential and nitrification rates.....	20
2.3.6 Molecular diffusive flux rates.....	21
2.3.7 Desorption isotherm of adsorbed ammonium (NH <sub>4</sub> <sup>+</sup> -N).....	22
2.3.8 Chemical analysis.....	24
2.4 Results and Discussion.....	24
2.4.1 Physical conditions.....	24
2.4.2 Effect of pH on the pore water iron profile.....	25
2.4.3 Effect of pH on the pore water SRP profile.....	26
2.4.4 Effect of pH on the pore water ammonium profile.....	26
2.4.5 Adsorbed NH <sub>4</sub> <sup>+</sup> .....	27
2.4.6 Effect of pH on desorption of sediment NH <sub>4</sub> <sup>+</sup> .....	27

2.4.7	Effect of pH on SRP flux .....	28
2.4.8	Effect of pH on DIN flux .....	29
2.4.9	Effect of pH on potential nitrification .....	30
2.4.10	Effect of pH on nitrification rates .....	32
2.4.11	Effect of pH on denitrification .....	33
2.4.12	Effect of pH on oxygen consumption .....	34
2.5	Conclusion and Ecological Implications.....	35
	References.....	37
	Tables.....	45
	Figures.....	49
Chapter 3 Seasonal and spatial changes in sediment-water nutrient exchange: regulating factors in the overlying water .....		
	Abstract.....	54
3.1	Introduction .....	55
3.2	Material and Methods.....	59
3.2.1	Study Sites.....	59
3.2.2	Sediment collection.....	59
3.2.3	Sediment incubation and flux measurement .....	60
3.2.4	Comparison of light and dark core incubation .....	61
3.2.5	Solid phase and pore water processes .....	61
3.2.6	Sample analyses .....	62
3.2.7	Data Analysis .....	63
3.3	Results .....	65
3.3.1	General environment.....	65
3.3.2	Sediment characteristics.....	66
3.3.3	<i>In situ</i> pH and DO status .....	66
3.3.4	Fluxes rates in the light-dark incubations .....	67
3.3.5	Flux rates.....	69
3.3.6	Nitrification efficiency .....	71
3.3.7	Denitrification rates.....	72
3.3.8	Sediment oxygen consumption rates.....	72
3.3.9	Vertical profiles of pore water nutrient concentrations.....	73
3.3.10	Pools of pore water and exchangeable NH <sub>4</sub> <sup>+</sup> .....	74
3.4	Discussion .....	74



3.4.1	Total carbon and total nitrogen in sediments .....	74
3.4.2	Nutrient status in water column .....	75
3.4.3	Light regulation on nutrient exchange .....	76
3.4.4	Ecological implications of Light/dark experiment.....	77
3.4.5	Comparison of dark-incubated fluxes with previous measurements .....	78
3.4.6	Temperature effect on N and P fluxes.....	79
3.4.7	Bloom effects on SRP fluxes .....	80
3.4.8	Organic matter effects on seasonal and spatial changes in NH <sub>4</sub> <sup>+</sup> flux .....	82
3.4.9	pH effects on NH <sub>4</sub> <sup>+</sup> flux .....	83
3.4.10	CO <sub>2</sub> and O <sub>2</sub> .....	84
3.4.11	NO <sub>3</sub> <sup>-</sup> flux and denitrification from winter-spring to early summer.....	84
3.4.12	Summer bloom driven DO effects on penetration depth.....	85
3.4.13	Bloom effects on nitrification .....	85
3.4.14	Bloom influences on N <sub>2</sub> flux.....	87
3.5	Ecological impacts .....	89
	References.....	91
	Tables.....	98
	Figures.....	109
Chapter 4	Photosynthesis and nitrogen fixation during cyanobacterial blooms in an oligohaline / tidal fresh estuary.....	133
	Abstract.....	133
4.1	Introduction .....	134
4.2	Materials and Methods.....	138
	4.2.1 <i>In situ</i> measurements.....	139
	4.2.2 Chl <i>a</i> and cyanobacterial biomass.....	139
	4.2.3 Dissolved and particulate nutrients .....	140
	4.2.4 Laboratory measurement of pH, DO and DIC .....	140
	4.2.5 C and N <sub>2</sub> fixation.....	141
	4.2.6 Data analysis .....	142
4.3	Results .....	143
	4.3.1 <i>In situ</i> conditions .....	143
	4.3.2 Cyanobacterial bloom development and succession.....	143
	4.3.3 Dissolved inorganic nutrients and particulate C, N, P .....	145
	4.3.4 Photosynthesis experiments .....	146

4.3.5	N <sub>2</sub> fixation .....	147
4.3.6	The environmental effects on C and N <sub>2</sub> fixation rates .....	149
4.4	Discussion .....	149
4.4.1	Bloom Stage I.....	149
4.4.2	Bloom Stage II .....	152
4.4.3	Bloom Stage III.....	157
4.5	Conclusions .....	158
	References.....	158
	Tables.....	168
	Figures.....	175
Chapter 5	Summary and Conclusions: Factors contribution to cyanobacterial blooms in the Sassafras River, Maryland .....	187
5.1	Nutrient loading from watershed.....	187
5.2	Hydrological influences .....	188
5.3	Sediment N and P burial in the Sassafras River estuary .....	190
5.4	Contribution of sediment nutrient flux and N <sub>2</sub> fixation in supporting cyanobacteria blooms.....	191
5.5	Factors influencing sediment nutrient regeneration.....	192
5.6	Factors influencing N <sub>2</sub> fixation rates.....	194
5.7	Advantages of cyanobacteria over eukaryotic phytoplankton .....	196
5.8	Conclusions .....	197
	References.....	199
	Tables.....	203
	Figures.....	207
	Complete References .....	215

## List of Table

Table 2-1 Sediment grain sizes, ambient dissolved nutrients in water column and the flux rates before pH mediation .....	45
Table 2-2 Experimental overlying water pH's for experimental incubations of cores from the Powerline (n= 4) and Budds Landing sites. ....	46
Table 2-3 The kinetic parameters used in calculation of diffusion rates and in calculation of ammonium adsorption-desorption in sediments. ....	47
Table 2-4 Efflux rates of SRP and $\Sigma\text{NH}_x$ in control and in high pH treatments in sediment cores from Budds Landing .....	48
Table 3-1 Sampling information in the upper Sassafras River from 2007 to 2010, including dates and number of sediment cores used the nutrient flux measurement. ....	98
Table 3-2 Water column depth and sediment characteristics of the sampling stations in the upper Sassafras River. ....	99
Table 3-3 Mean ( $\pm$ std) of salinity, temperature and dissolved inorganic nutrient concentrations in the bottom water before, during and after bloom seasons .....	100
Table 3-4 Pearson correlation coefficients for the average values of selected bottom-water variables. ....	101
Table 3-5 Mean light and dark fluxes in sandy and muddy sediments( $\pm$ SE), including fluxes of SRP, $\text{NH}_4^+$ , $\text{NO}_3^-$ , $\text{N}_2\text{-N}$ , $\text{O}_2$ and net inorganic nitrogen (DIN), the molar ratio of $\text{O}_2$ : DIN flux rates, denitrification efficiency (DE%) and the calculated nitrogen remineralization. ....	102
Table 3-6 Summary of sediment-water flux rates in the oligohaline and tidal-fresh of the Chesapeake Bay. ....	104
Table 3-7 Multiple regression models used to predict nutrient flux rates in sediments as a function of temperature, pH, salinity, nutrients and Chl a in the water column. ....	106
Table 4-1 The Cyanobacterial species and $\text{N}_2$ fixers observed in the summer of 2010. ....	168
Table 4-2 Three-level nested analysis of variance of effects of station (n= 2), sampling date (n=5 for C and n= 9 for N) and irradiance (n=4) on carbon and nitrogen fixation in laboratory incubations. ....	169
Table 4-3 Photosynthetic efficiency ( $\alpha^{\text{chl}}$ , $\text{mg C mg Chl a}^{-1} \text{h}^{-1}$ ( $\mu\text{mol photon}^{-1} \text{m}^{-2} \text{s}^{-1}$ )), in laboratory incubation of samples collected during bloom stage I, II and III. ....	170
Table 4-4 Response of N-fixation to irradiance in laboratory incubations of samples collected during bloom stage I, II and III. ....	170
Table 4-5 Response of N-fixation to C fixation in the laboratory incubation of samples collected during bloom stage I, II, and III. ....	170
Table 4-6 Correlation among pH, dissolved oxygen (DO), dissolved inorganic carbon (DIC) and irradiance in 24 h incubations. ....	172
Table 4-7 Multiple linear relationship between C fixation rates and environmental parameters, estimated by forward stepwise regression. ....	173
Table 4-8 Multiple linear relationship of $\text{N}_2$ fixation rates with changes in water column, estimated by forward stepwise regression. ....	174

## List of Figure

Figure 1-1 Changes in pH and dissolved oxygen resulting from the cyanobacterial bloom in 2010..	12
Figure 2-1 Budds Landing porewater profiles in the upper 10 cm of sediment under high pH (9.6) and normal pH (7.4) treatments, including vertical changes of pH (A), porewater Fe (B), SRP (D,F), and $\Sigma\text{NH}_x$ (C,E). Changes in ammonium speciation, resulted from surface pH elevation, were calculated by the equilibrium of $\text{NH}_3$ and $\text{NH}_4^+$	49
Figure 2-2 Experimental pH effects on $\text{NH}_4^+$ concentration in solution (A) and desorption of exchangeable $\text{NH}_4^+$ (B), using the 0-2 cm homogenized sediments from Budds Landing collected in November 2008.	50
Figure 2-3 Experimental pH effects on SRP flux rates from sediments at Powerline (black bars) and Budds Landing (gray bars).	51
Figure 2-4 Experimental pH effects on flux rates of total ammonium and nitrate. Sediment cores were taken from Powerline and Budds Landing.	51
Figure 2-5 Experimental pH effects on potential nitrification (A) and intact core nitrification rates (B) from Budds Landing in July 2009.	52
Figure 2-6 Experimental pH effects on denitrification rates (A) and oxygen consumption rates of sediments from the Powerline (black bar) and Budds Landing (grey bar) sites.	53
Figure 2-7 The relationship between the increased $\Sigma\text{NH}_x$ fluxes and the reduced oxygen consumption rates after pH elevation.	53
Figure 3-1 Sampling locations for sediment flux rate measurements in the upper Sassafras River, MD.	109
Figure 3-2 The temporal and spatial changes of pH and dissolved oxygen percentage (DO %) of bottom water during 2008 to 2010.	110
Figure 3-3 Flux rates (a-e) and sediment Chl <i>a</i> concentration (n= 3, upper 1cm). Flux rates of $\text{NH}_4^+$ , $\text{NO}_3^-$ , SRP, $\text{N}_2$ and $\text{O}_2$ were measured under light (white bar) and dark (black bar) incubation for sediments obtained in June 2010 and for sediment 3A' from the same location as 3A but in September 2009	111
Figure 3-4 Relationship of sediment Chl <i>a</i> and the changes in $\text{O}_2$ flux rates, calculated from the difference in $\text{O}_2$ fluxes between light and dark treatments.	112
Figure 3-5 Light and dark effects on $\text{NH}_4^+$ flux versus SOD (A) and SRP flux versus SOD of the fine-grained sediments.	113
Figure 3-6 Effects of light and dark incubation on N remineralization ( $\text{DIN} = \Sigma\text{NH}_4^+ + \text{NO}_3^- + \text{N}_2\text{-N}$ ) through denitrification ( $\text{N}_2$ flux) of the fine-grained sediments.	114
Figure 3-7 Flux rates of $\text{NH}_4^+$ (A), $\text{NO}_3^-$ (B), SRP (C) and $\text{N}_2$ (D) of sediments from the upper Sassafras River during Dec. 2007 to Oct. 2010.	116
Figure 3-8 Comparison of mean of sediment oxygen demand ( $\text{SOD} \pm$ standard deviation) and $\text{CO}_2$ flux ( $\pm$ standard deviation) in dark incubation of sediments from the upper Sassafras River.	117
Figure 3-9 Box and whisker plots of monthly $\text{NH}_4^+$ , $\text{NO}_3^-$ , SRP, $\text{O}_2$ and denitrification fluxes in fine-grained sediments (stations 1A to 3A) and the sandy sediments (station 3B).	119
Figure 3-10 Linear regressions of temperature and the natural logarithm of flux rates.	120
Figure 3-11 Concentration of particulate organic carbon (POC) and particulate organic nitrogen (PON) as a correlation of pH in water column.	121
Figure 3-12 pH effects on SRP flux rates in fine-grained sediments with dark incubation.	122

Figure 3-13 The spatial variation of pH and average $\text{NH}_4^+$ flux rates of sediment cores, taken from the bloom region (Zone I), transitional region (Zone II) and stations outside of bloom (Zone III).....	123
Figure 3-14 Vertical profiles of SRP, $\text{Fe}_2^+$ , $\text{SO}_4^{2-}$ , the ratio of $\text{SO}_4^{2-}$ to $\text{Cl}^-$ , $\text{NH}_4^+$ and $\text{NO}_3^-$ (A to in sediment pore-water in May, August and October 2011 .....	124
Figure 3-15 The fraction of adsorbed and pore-water $\text{NH}_4^+$ in the surface sediments from station 1B (within bloom) and 3A (out of bloom).....	125
Figure 3-16 The spatial variation of denitrification rates ( $\text{N}_2$ -N flux) of sediment cores, taken from the bloom region (Zone I), transitional region (Zone II) and stations out of the bloom (Zone III).....	126
Figure 3-17 Denitrification efficiency (DE%) response to pH elevation in the bloom region (Zone I), transitional region (Zone II) and stations out of bloom (Zone III), when sediments were taken at temperature $> 25^\circ\text{C}$ .....	127
Figure 3-18 The linear relationship of the dark-incubated $\text{CO}_2$ flux rates and sediment oxygen consumption rates ( $K = 1.24$ , $P < 0.05$ ) from spring to summer in 2009 and 2010.....	128
Figure 3-19 Response of oxygen penetration depth to the diel changes of oxygen in the bottom water.....	129
Figure 3-20 Oxygen penetration effects on nitrification efficient during non-bloom (A) and bloom periods (B). Nitrification efficiency were estimated from flux rates of $\text{NO}_3^-$ and $\text{N}_2$ as well as the N remineralization rates from respiration rates when $\text{NO}_3^-$ concentration in the water is less than $25\ \mu\text{M}$ .....	130
Figure 3-21 Oxygen penetration depth effects on denitrification rates (DE %). Data shown are similar to nitrification efficiency in the whole pH range of 7– 9.52 in the bottom water during the sediment core sampling.....	130
Figure 3-22 The box-whisker of the bioavailable inorganic nutrient release (A-C) and the ratio of DIN: SRP flux rates (D) at high and low pH.....	131
Figure 3-23 Mean ( $\pm$ SE) of A) the estimated N flux across the sediment-water interface and the predicted remineralization rates B) the contribution of $\text{NH}_4^+$ and $\text{N}_2$ -N release to total remineralization at bottom water pH $< 9$ and $\geq 9$ .....	132
Figure 4-1 Sampling stations in the upper Sassafras River, Maryland, USA. Budds Landing (BL) and Drawbridge (DB) are located on the upper river, with BL close to the river head and DB slightly downstream from BL.....	175
Figure 4-2 The variation in precipitation at Georgetown, Maryland (A) and Chl <i>a</i> concentrations (B) at Budds Landing (BL, upstream) and Drawbridge (DB, downstream site) from early May to Mid September in 2010.....	176
Figure 4-3 The seasonal patterns of temperature, pH, dissolved oxygen and salinity in the Sassafras River. A) the continuous changes at Budds Landing in 2010. Circles represent the daily average of the continuous records. The daily maximum and minimum values are indicated with solid line and dash lines, respectively (Maryland Department of Natural Resources). B) <i>In situ</i> measurements at Budds Landing (solid circles) and Drawbridge (empty circles).....	177
Figure 4-4 The estimated biomass of phytoplankton at Budds Landing (BL) and Drawbridge in 2010, including non-diazotrophic cyanobacteria (mostly <i>Microcystis sp.</i> ) diazotrophic cyanobacteria (heterocystous <i>Anabaena sp.</i> , unicellular <i>Synechocystis sp.</i> , filamentous non-heterocystous <i>Pseudoanabaena sp.</i> ) and eukaryotic phytoplankton.....	178
Figure 4-5 Weekly or biweekly inorganic nutrient concentrations ( $\text{NH}_4^+$ , $\text{NO}_3^-$ , SRP) and the ratio of dissolved inorganic nitrogen to SRP (DIN: SRP) at Budds Landing (BL) and Drawbridge (DB) in 2010.....	179
Figure 4-6 Particulate molar ratio of C: N: P at Budds Landing (BL) and Drawbridge (DB) in 2010.....	180

Figure 4-7 Photosynthesis and N <sub>2</sub> fixation rates as a function of irradiance in laboratory incubations of samples collected from Budds Landing (BL) and Drawbridge (DB).....	181
Figure 4-8 The mean (± standard deviation) of DIC concentration and carbon fixation rates in laboratory incubations of samples from Budds Landing (BL) and Drawbridge (DB). Samples were taken during bloom Stage I (on June 11 and June 15), Stage II (on July 16 and August 15), and the end of bloom stage III (on September 15).....	182
Figure 4-9 Net photosynthetic rate as a function of average DIC concentration at incubation irradiances of 62.5, 125, 250 μmol photons m <sup>-2</sup> h <sup>-1</sup> .....	183
Figure 4-10 The average of pH and dissolved oxygen (DO) in the laboratory incubations..	184
Figure 4-11 N <sub>2</sub> fixation rates of at Budds Landing (BL) and Drawbridge (DB), including 24 hr dark and dark-light incubation at irradiance of 125 and 250 μmol photons m <sup>-2</sup> h <sup>-1</sup> .....	185
Figure 4-12 Contribution of dark N <sub>2</sub> fixation to daily N <sub>2</sub> fixation at Budds Landing (BL) and Drawbridge (DB). .....	186
Figure 5-1 Cyanobacterial blooms of Drawbridge (DB) and Budds Landing (BL) in the upper Sassafras River, a tributary of Chesapeake Bay. .	207
Figure 5-2 Annual maximum cell density of N <sub>2</sub> -fixing cyanobacteria at two stations on the upper Sassafras River: Drawbridge (DB, 2000 – 2010) and Budds Landing (BL, 2007 – 2010) (MD DNR and our samples in 2009 – 2010).....	208
Figure 5-3 The relationship of nutrient loading and river flow. ....	209
Figure 5-4 Flow rate effects on cyanobacterial abundance (A) and the percentage of diazotrophic cyanobacteria of total cyanobacteria (B)..	210
Figure 5-5 Mean of monthly input of DIN and DIP from the point source and nonpoint diffusion into the Sassafras River. The data shown are the average monthly inputs in 2000-2005, excluding the wet years, 2003 and 2004.....	211
Figure 5-6 The balance between nutrient input from land use and burial rate into the upper Sassafras River.....	212
Figure 5-7 Nutrient release (+) and loss (-) to the shallow water column from sediment due to biogeochemical processes within and outside of bloom area during June to September 2010..	213
Figure 5-8 The summary of mass balance for SRP and DIN demands by a cyanobacterial bloom, accounting from benthic nutrient fluxes and N <sub>2</sub> fixation. ....	214

# Chapter 1 Introduction

## Introduction

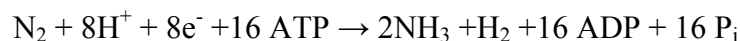
### 1.1.1 Cyanobacterial Blooms

In freshwater, estuarine and coastal ecosystems, cyanobacteria (blue-green algae) can be a major environmental problem and cause negative effects on water quality, human health and aquatic resources (Tango and Butler 2008). Cyanobacterial blooms can form unsightly and smelly scums, which may discourage recreational use of water, foul fishing gear, and directly affect man's activities (Havens 2008). These blooms can disrupt food webs (Dittmann 2005), reduce light penetration in the water column, and inhibit/prevent the growth of sea grasses as well as other submerged aquatic vegetation that provide valuable habitat for fish and wildlife (Kemp et al. 2005). Some cyanobacterial species produce toxins that affect humans and livestock (Huisman and Matthijs 2011).

Cyanobacterial blooms are prevalent in the tidal-fresh and oligohaline zones of Chesapeake Bay, with the maximum density of  $6.3 \times 10^6$  cyanobacteria cells  $\text{ml}^{-1}$  during 1991-2008 (Chesapeake Bay Program, online data). Blooms usually occur in brackish tributaries, such as the Susquehanna River, Potomac River, Choptank River, Nanticoke River, Patuxent River, and Sassafras River (Tango and Butler 2008). The cyanobacterial assemblage is usually composed of a mixture of non- $\text{N}_2$  fixers (mainly *Microcystis* spp.) and  $\text{N}_2$ -fixers (e.g. *Anabaena* spp., *Pseudanabaena* spp., *Synechococcus* spp.) (Maryland Department of Natural Resources).

Nutrient supply can strongly influence the occurrence and maintenance of harmful cyanobacterial blooms in estuarine ecosystems (Kemp et al. 2005). In addition to nutrient loads from land and atmospheric inputs, nutrients released from sediments into the water may support the nutrient demands of phytoplankton blooms (Karl et al. 2002). Particularly in well-mixed shallow water estuaries, the strong benthic-pelagic coupling can enhance eutrophication. Settlement of dead phytoplankton to the bottom can fuel biogeochemical nutrient recycling which can foster blooms in the water column (Hopkinson et al. 1999; Kemp et al. 1999). Nutrient regeneration from the sediments is estimated to supply approximately 80 % of the nitrogen (N, in the Patuxent River) and over 100% of the phosphorus (P, in the Potomac River) demands of primary production during blooms (Kemp and Boynton 1984; Seitzinger 1991).

During the period of low runoff in summer, dissolved N can limit algal growth (Fisher et al. 1992). Nitrogen fixation is variable and relatively high within the cyanobacterial bloom areas in the Chesapeake Bay (Elliston and O'neil 2005). N<sub>2</sub> fixation may provide new 'N' into aquatic environments under N-limited conditions by breaking the triple bond of N<sub>2</sub> through an enzymatically mediated process (Capone et al. 2009):



N<sub>2</sub>-fixing cyanobacteria are able to satisfy their N requirements and may release NH<sub>4</sub><sup>+</sup> and organic N into the water that can be taken up by surrounding bacteria and phytoplankton (Mulholland 2007). The diazotrophic cyanobacteria contribute from 20% to over 100% of community N demand in coastal and marine ecosystems (Paerl and Zehr 2000). Although N<sub>2</sub> fixation is critical for cyanobacterial growth in N limited surface waters, great variation in N<sub>2</sub> fixation rates are reported in estuaries; this is likely due to



variation in the abundance of diazotrophic cyanobacteria, variation in their morphological and physiological attributes, as well as variation in inorganic and organic N input, temperature, light and salinity in estuaries (Gardner et al. 2006; Howarth 2006; Lehtimäki et al. 1997; Lewis 1984).

### 1.1.2 Cyanobacterial Blooms in the Sassafras River

In the upper Sassafras River, a eutrophic, shallow and tidal freshwater tributary of the Chesapeake Bay, dissolved nitrogen is more limiting than phosphate in summer (Chesapeake Bay Program, online data). Based on the observations by Maryland Dept. of Natural Resources (MD DNR), summer cyanobacterial blooms have been increasing in occurrence and biomass in the upper Sassafras River; the maximum density of cyanobacteria has increased ~10 fold from 2000 to 2009. The massive cyanobacterial blooms in the upper river provide a good opportunity to investigate the synergy between cyanobacterial blooms and biogeochemical processes, including nutrient release from sediments and N<sub>2</sub> fixation.

The photosynthetic uptake of inorganic carbon (DIC) and O<sub>2</sub> production by blooms can result in dramatic increases in pH (up to 10.5) and dissolved oxygen (up to 23 mg L<sup>-1</sup>, > 300% DO) in the upper Sassafras River (Fig. 1.1, real-time monitoring at Budds Landing, <http://www.eyesonthebay.com/>). This is partly due to the lower inorganic carbon (DIC) (< 1 mM) and the weaker carbonate buffering capacity in freshwater than in seawater. The maintenance of high pH may be crucial for cyanobacteria dominance in summer. As pH rises, the proportion of CO<sub>2</sub> in the inorganic

carbon pool ( $C_i$ ) generally decreases and the carbonate balance shifts from  $\text{CO}_2$ ,  $\text{HCO}_3^-$  to  $\text{CO}_3^{2-}$  (Badger et al. 2006). Cyanobacteria are more competitive in low dissolved inorganic carbon (DIC) systems than most eukaryotic phytoplankton because of their efficient use of  $\text{CO}_2$  and  $\text{HCO}_3^-$  by  $\text{CO}_2$  concentrating mechanisms (CCM) (Price et al. 2008; Stumm and Morgan 1996).

However, changes in pH, DO and DIC caused by blooms may also influence nutrient regeneration in several ways. High pH increases pore water P solubility and facilitates soluble reactive phosphorus (SRP) release from sediments into the water column. This can be particularly important to meet the high P demand of diazotrophic cyanobacteria (Andersen 1975; Seitzinger et al. 1991; Slomp et al. 1998). Sediments in freshwater contain a large pool of  $\text{NH}_4^+$  that may be influenced by pH elevation. More than 2/3 of ammonium ( $\text{NH}_4^+$ ) is sorbed onto sediment particles rather than dissolved in pore water (Morse and Morin 2005). Part of the sorbed ammonium on the surface sediment is exchangeable and can be easily released through ion exchange (Rosenfeld 1979). Elevated pH leads to the conversion of  $\text{NH}_4^+$  to ammonia ( $\text{NH}_3$ )



This may consequently increase desorption of bound  $\text{NH}_4^+$ . The concentration of  $\text{NH}_4^+$  in pore water and its migration are critical for  $\text{NH}_4^+$  efflux and coupled nitrification-denitrification (Pommerening-Röser and Koops 2005). Meanwhile, super-saturation and diel variation in DO may influence oxygen penetration into sediments, where redox conditions may influence coupled nitrification - denitrification. Despite the potential importance of elevated pH and DO, their effects on N cycling at the sediment-water interface are not described in the literature.

During dense blooms, photosynthesis alters pH and DO concentration in the water column, which may exert control over cyanobacterial physiological processes. As pH rises above 8.5, the proportion of CO<sub>2</sub> in the inorganic carbon pool (C<sub>i</sub>) dramatically decreases and the carbonate balance shifts from CO<sub>2</sub> to HCO<sub>3</sub><sup>-</sup> (Badger et al. 2006). Limited DIC has a negative effect on photosynthetic carbon uptake and N<sub>2</sub> fixation (Boyd et al. 2011; Fu et al. 2008; Tortell et al. 2008). Rising pH also leads to precipitation of essential elements (Cu, Fe, Mo) for photosynthesis and N<sub>2</sub> fixation (Gallon 1992; Strauss et al. 2002). In addition, O<sub>2</sub> elevation caused by photosynthesis may potentially inhibit N reduction by suppression of nitrogenase activity (Berman-Frank et al. 2001; Fay 1992; Staal et al. 2003).

### **Hypotheses**

This study focused on the roles of internal nutrient inputs from sediments and N<sub>2</sub> fixation in the development and maintenance of cyanobacterial blooms in the Sassafra River estuary. Effects of elevated pH and DO on sediment nutrient regeneration and N<sub>2</sub> fixation are emphasized. The following hypotheses were tested:

1. Driven by cyanobacterial photosynthesis, high pH can facilitate the release of N and P from sediments into the water column in shallow water estuaries, and can decrease the loss of N from the system through coupled nitrification-denitrification

2. When the availability of N is low relative to P, N<sub>2</sub> fixation by cyanobacteria can increase and maintain massive blooms in summer. However, during dense blooms, carbon limitation and DO elevation in water may negatively affect photosynthesis and N<sub>2</sub> fixation.
3. In shallow water estuaries, the positive feedbacks between cyanobacterial blooms and sediment N and P recycling may increase nutrient release into the water, which may support the nutrient demands of the bloom.

### **Objectives**

Chapter 2 addresses elevated pH effects on sediment nutrient release. I measured flux rates of NH<sub>4</sub><sup>+</sup>, SRP, oxygen consumption, nitrification and denitrification in pH manipulation experiments with sediment cores. Considering that high pH can penetrate into sediments, the conversion of NH<sub>4</sub><sup>+</sup> to NH<sub>3</sub> was used to calculate the diffusion rates of total ammonium by sampling the pore water nutrient concentration; the equilibrium between pore water and adsorbed NH<sub>4</sub><sup>+</sup> on mineral surfaces was used to estimate the exchangeable ammonium desorption with pH elevation.

In Chapter 3, I present data on seasonal and spatial changes in the dark flux rates of dissolved inorganic nutrients (SRP, NH<sub>4</sub><sup>+</sup> and NO<sub>3</sub><sup>-</sup>), respiration and denitrification in the non-bloom years (2008 and 2009) and the cyanobacterial bloom year (2010). These data were used to analyze the response of biogeochemical processes to environmental factors (temperature, DO, pH and nutrient concentrations). Light-dark experiments were conducted to explore how irradiance alters the magnitude of nutrient release and N loss

through nitrification-denitrification. In summer 2010, pore-water nutrients and exchangeable ammonium were measured in samples taken within and outside of the bloom area to investigate high pH and other bloom related impacts on nutrient exchanges at the sediment-water interface.

In Chapter 4, specific attention was given to photosynthesis and N<sub>2</sub> fixation as well as their responses to changes in pH/DO and other major ecological factors. I conducted field and laboratory studies in 2010 in order to follow the effects of seasonal changes in temperature, N:P ratio and salinity on bloom development. To experimentally investigate the feedback of elevated pH and DO on C and N fixation in the water column, different irradiance levels were used to simulate light changes in the field and to naturally create treatments with differences in pH and DO.

In chapter 5, a preliminary nutrient budget was constructed based on nutrient land loading, sedimentary burial rates, and nutrient supply from biogeochemical recycling during the bloom. The transportation of nutrient land loads with river flow and nutrient sequestration in sediment were analyzed using the output of model generated data and the measurement of burial rates in the upper river. The contribution of N from sediments and N<sub>2</sub> fixation were calculated based on nutrient demand by a cyanobacterial bloom in 2010. The key factors for these biogeochemical processes were evaluated to better understand nutrient budgets in this shallow water estuary.

## References

- Andersen, J. M. 1975. Influence of pH on release of phosphorus from lake sediments. *Archiv für Hydrobiologie* **76**: 411-419.
- Badger, M. R., G. D. Price, B. M. Long, and F. J. Woodger. 2006. The environmental plasticity and ecological genomics of the cyanobacterial CO<sub>2</sub> concentrating mechanism. *Journal of Experimental Botany* **57**: 249-265.
- Berman-Frank, I. and others 2001. Segregation of nitrogen fixation and oxygenic photosynthesis in the marine cyanobacterium *Trichodesmium*. *Science* **294**: 1534-1537.
- Boyd, E. S. and others 2011. Diversity, abundance, and potential activity of nitrifying and nitrate-reducing microbial assemblages in a subglacial ecosystem. *Applied and environmental microbiology* **77**: 4778-4787.
- Capone, D., D. Bronk, M. Mulholland, and E. Carpenter. 2009. Nitrogen in the marine environment. Elsevier.
- Chesapeake Bay Programm, [http://www.chesapeakebay.net/data\\_waterquality.aspx](http://www.chesapeakebay.net/data_waterquality.aspx)
- Dittmann, E. 2005. Genetic contributions to the risk assessment of microcystin in the environment. *Toxicology and applied pharmacology* **203**: 192-200.
- Elliston, K., and J. O'neil. 2005. Nitrogen fixation in various estuarine environments of Chesapeake Bay. Maryland Sea Grant.
- Fay, P. 1992. Oxygen relations of nitrogen-fixation in cyanobacteria. *Microbiological Reviews* **56**: 340-373.
- Fisher, T. R., E. R. Peele, J. W. Ammerman, and L. W. Harding. 1992. Nutrient limitation of phytoplankton in Chesapeake Bay. *Marine Ecology-Progress Series* **82**: 51-63.

- Fu, F. X. and others 2008. Interactions between changing pCO<sub>2</sub>, N<sub>2</sub> fixation, and Fe limitation in the marine unicellular cyanobacterium *Crocospaera*. *Limnology and Oceanography* **53**: 2472-2484.
- Gallon, J. R. 1992. Reconciling the incompatible : N<sub>2</sub> fixation and O<sub>2</sub>. *New Phytologist* **122**: 571-609.
- Gardner, W. S., M. J. McCarthy, S. M. An, D. Sobolev, K. S. Sell, and D. Brock. 2006. Nitrogen fixation and dissimilatory nitrate reduction to ammonium (DNRA) support nitrogen dynamics in Texas estuaries. *Limnology And Oceanography* **51**: 558-568 Part 552.
- Havens, K. E. 2008. Cyanobacterial harmful algal blooms: state of the science and research needs. *Advances in Experimental Medicine and Biology* **619**: 733-747.
- Hopkinson, C. S., A. E. Giblin, J. Tucker, and R. H. Garritt. 1999. Benthic metabolism and nutrient cycling along an estuarine salinity gradient. *Estuaries* **22**: 863-881.
- Howarth, R. W. 2006. Nitrogen as the limiting nutrient for eutrophication in coastal marine ecosystems: Evolving views over three decades. *Limnology and Oceanography* **51**: 364-376.
- Huisman, J., and H. Matthijs. 2011. *Harmful Cyanobacteria*. Springer.
- Karl, D. and others 2002. Dinitrogen fixation in the world's oceans. *Biogeochemistry* **57**: 47-98.
- Kemp, W. M., and W. R. Boynton. 1984. Spatial and temporal coupling of nutrient inputs to estuarine primary production - the role of particulate transport and decomposition. *Bulletin of Marine Science* **35**: 522-535.
- Kemp, W. M. and others 2005. Eutrophication of Chesapeake Bay: historical trends and ecological interactions. *Marine Ecology-Progress Series* **303**: 1-29.
- Kemp, W. M., J. Faganelli, S. Puskarick, E. M. Smith, and W. R. Boynton. 1999. Pelagic-benthic coupling and nutrient cycling. *Ecosystems at the Land-Sea Margin* **55**: 295-339.

- Lehtimäki, J., P. Moisaner, K. Sivonen, and K. Kononen. 1997. Growth, nitrogen fixation, and nodularin production by two Baltic Sea cyanobacteria. *Applied and Environmental Microbiology* **63**: 1647-1656.
- Lewis, W. M. 1984. The light response of nitrogen fixation in Lake Valencia, Venezuela. *Limnology and Oceanography* **29**: 894-900.
- Maryland Department of Natural Resource, data provided by Butler, W. 2009.
- Morse, J. W., and J. Morin. 2005. Ammonium interaction with coastal marine sediments: influence of redox conditions on  $K^*$ . *Marine Chemistry* **95**: 107-112.
- Mulholland, M. R. 2007. The fate of nitrogen fixed by diazotrophs in the ocean. *Biogeosciences* **4**: 37-51.
- Paerl, H., and J. P. Zehr. 2000. Marine nitrogen fixation, p. 387-418. *In* D. Kirchman [ed.], *Microbial Ecology of the Oceans*. Wiley-Liss, Inc.
- Pommerening-Röser, A., and H. P. Koops. 2005. Environmental pH as an important factor for the distribution of urease positive ammonia-oxidizing bacteria. *Microbiological Research* **160**: 27-35.
- Rosenfeld, J. K. 1979. Ammonium adsorption in nearshore anoxic sediments. *Limnology and Oceanography* **24**: 356-364.
- Seitzinger, S. P. 1991. The effect of pH on the release of phosphorus from Potomac estuary sediments - implications for blue-green-algal blooms. *Estuarine Coastal and Shelf Science* **33**: 409-418.
- Seitzinger, S. P., W. S. Gardner, and A. K. Spratt. 1991. The effect of salinity on ammonium sorption in aquatic sediments - implications for benthic nutrient recycling. *Estuaries* **14**: 167-174.
- Slomp, C. P., J. F. P. Malschaert, and W. Van Raaphorst. 1998. The role of adsorption in sediment-water exchange of phosphate in North Sea continental margin sediments. *Limnology and Oceanography* **43**: 832-846.



- Smith, V. H. 2003. Eutrophication of freshwater and coastal marine ecosystems - A global problem. *Environmental Science and Pollution Research* **10**: 126-139.
- Staal, M., S. T. L. Hekkert, F. J. M. Harren, and L. J. Stal. 2003. Effects of O<sub>2</sub> on N<sub>2</sub> fixation in heterocystous cyanobacteria from the Baltic Sea. *Aquatic Microbial Ecology* **33**: 261-270.
- Strauss, E. A., N. L. Mitchell, and G. A. Lamberti. 2002. Factors regulating nitrification in aquatic sediments: effects of organic carbon, nitrogen availability, and pH. *Canadian Journal of Fisheries and Aquatic Sciences* **59**: 554-563.
- Tango, P. J., and W. Butler. 2008. Cyanotoxins in tidal waters of Chesapeake Bay. *Northeastern Naturalist* **15**: 403-416.
- Tortell, P. D., C. Payne, C. Gueguen, R. F. Strzepek, P. W. Boyd, and B. Rost. 2008. Inorganic carbon uptake by Southern Ocean phytoplankton. *Limnology and Oceanography* **53**: 1266-1278.

Figure

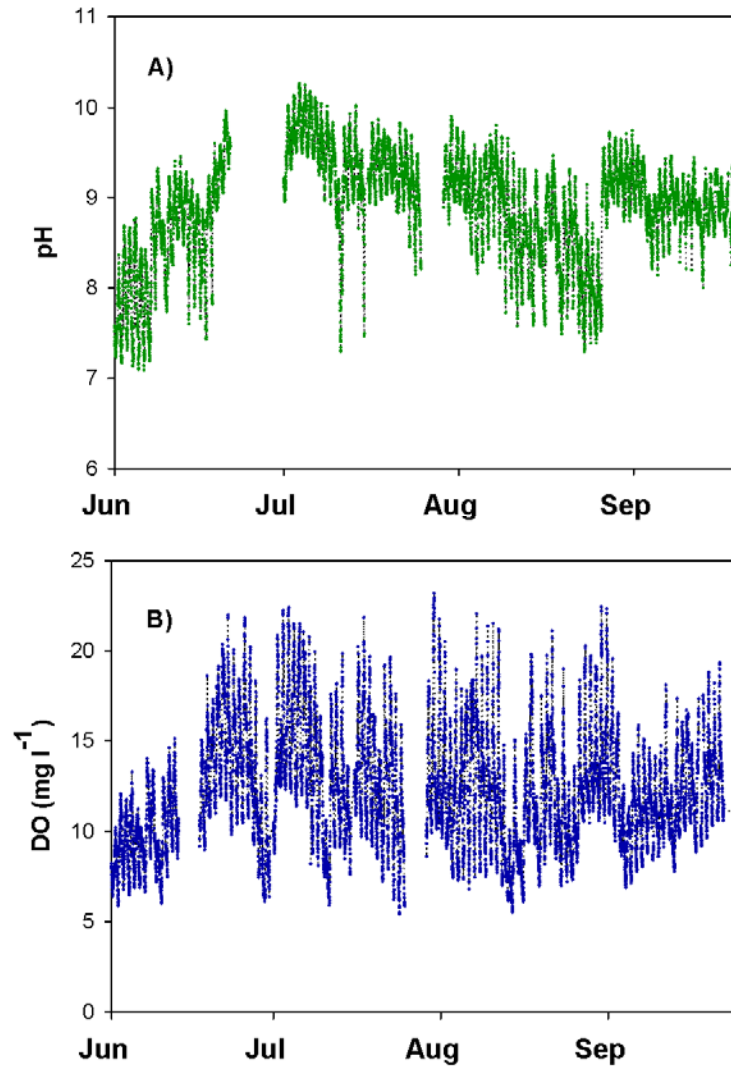


Figure 1-1 Changes in pH and dissolved oxygen resulting from the cyanobacterial bloom in 2010. Data shown from the real time monitoring station at Budds Landing station, probe located at 1 m depth in the upper Sassafas River (Maryland Department of Natural Resource, MD DNR).

## Chapter 2      Effects of cyanobacterial-driven pH increases on sediment nutrient fluxes and coupled nitrification-denitrification in a shallow fresh water estuary

### **Abstract**

Summer cyanobacterial blooms caused an elevation in pH (9 to ~ 10.5) that lasted for weeks in the shallow and tidal-fresh region of the Sassafras River, a tributary of Chesapeake Bay (USA). Elevated pH promoted desorption of sedimentary inorganic phosphorus and facilitated conversion of ammonium ( $\text{NH}_4^+$ ) to ammonia ( $\text{NH}_3$ ). In this study, we investigated pH effects on exchangeable  $\text{NH}_4^+$  desorption, nutrient pore water diffusion and flux rates of  $\text{NH}_4^+$ , soluble reactive phosphorus (SRP), nitrate ( $\text{NO}_3^-$ ), nitrification, denitrification, and oxygen consumption. pH elevation enhanced the desorption of exchangeable  $\text{NH}_4^+$  because of  $\text{NH}_3$  formation from both pore water and adsorbed  $\text{NH}_4^+$  pools. Progressive penetration of high pH from the overlying water into sediment promoted the release of SRP and total ammonium ( $\text{NH}_4^+$  and  $\text{NH}_3$ ) into pore water. At elevated pH, high sediment-water effluxes of SRP and total ammonium were associated with reduction in nitrification, denitrification and oxygen consumption rates. Alkaline pH and the toxicity of  $\text{NH}_3$  may inhibit nitrification in the thin aerobic zone, simultaneously constraining coupled nitrification-denitrification with limited  $\text{NO}_3^-$  supply and high pH penetration into the anaerobic zone. Geochemical feedbacks to pH elevation, such as enhancement of dissolved nutrient effluxes and reduction in  $\text{N}_2$  loss via

denitrification, may be responsible for the persistence of cyanobacterial blooms in shallow water ecosystems.

### **Introduction**

Nutrient releases from sediment to the water column can support a substantial fraction of the primary production in shallow coastal and estuarine ecosystems (e.g., North Carolina estuaries, Fisher et al. 1982; Potomac River Estuary, Kemp and Boynton 1984; Baltic Sea, Koop et al. 1990; Chesapeake Bay, Cowan and Boynton 1996). Enhanced nitrogen and phosphorus fluxes may promote high levels of phytoplankton biomass (Kemp et al. 2005). Such phytoplankton blooms lead to the sustained accumulation of phytodetritus in sediment, fueling nutrient recycling through organic matter remineralization (Cowan and Boynton 1996; Nixon et al. 1996). The consequences, such as decreased water clarity, depletion of bottom-water oxygen and the decomposition of phytodetritus, may enhance sediment respiration, decrease redox potential, limit nutrient uptake by benthic microalgae, and generally increase nutrient fluxes (Kemp et al. 2005).

In the deep, hypoxic region of the Chesapeake Bay and other estuaries, phosphorus flux is usually promoted by the dissolution of Fe-oxides and their conversion to iron sulfides; the increase in ammonium release from sediments tends to coincide with inhibition of nitrification by oxygen depletion and generation of reductants ( $\text{HS}^-/\text{H}_2\text{S}$ ) in sediment, which consequently reduce denitrification (Cornwell and Kana 1999; Kemp et al. 2005). In oxic shallow water ecosystems benthic nutrient releases are generally less redox influenced.

Persistent high pH in shallow water, driven by rapid utilization rates of inorganic carbon for photosynthesis during dense algal blooms (Hansen 2002; Hinga 2002), can influence benthic dynamics by progressive pH penetration from the overlying water into sediments (Bailey et al. 2006). When pH is above a critical threshold (9 – 9.2), inorganic phosphorus desorbs from iron oxides at mineral surfaces (Andersen 1975; Eckert et al. 1997). Elevation of pore water pH (~ 9.8 in tidal-fresh region, Eckert et al. 1997) can release soluble reactive phosphorus (SRP) and support photosynthetic P demand during cyanobacterial blooms in lakes (Xie and Xie 2003) and tidal fresh and oligohaline estuaries (Andersen 1975; Seitzinger 1991).

In contrast to pH-driven P cycling, the effects of pH on sediment N transformations and release are less well understood (Soetaert et al. 2007). During the decomposition of sediment organic matter, remineralized  $\text{NH}_4^+$  may both adsorb onto sediment mineral surfaces and accumulate in pore water. Exchangeable  $\text{NH}_4^+$  is weakly adsorbed at the negatively charged particle surfaces, buffering pore water  $\text{NH}_4^+$  concentrations (Rosenfeld 1979). In estuaries, fine grained sediment generally has a large pool of adsorbed  $\text{NH}_4^+$  (Wang and Alva 2000; Weston et al. 2010), with freshwater sediments having considerably more adsorbed ammonium relative to saline sediments (Seitzinger 1991). Once alkaline pH results in the conversion of ammonium ( $\text{NH}_4^+$ ) to dissolved ammonia ( $\text{NH}_3$ ), formation of non-ionized  $\text{NH}_3$  may decrease  $\text{NH}_4^+$  cation adsorption on sediments and potentially alter the balance between pore water and exchangeable  $\text{NH}_4^+$ .

Remineralized N can be assimilated by plants and bacteria or diffuse/ advect from sediment into the overlying water. Part of the  $\text{NH}_4^+$  can be oxidized sequentially to  $\text{NO}_2^-$  /

$\text{NO}_3^-$  then reduced to  $\text{N}_2$  through coupled nitrification-denitrification (Cornwell and Kana 1999). However, shifts in the  $\text{NH}_4^+$ - $\text{NH}_3$  equilibrium associated with high pH events may change rates of pore water diffusion, nitrification and denitrification. In the tidal-fresh and oligohaline parts of the Potomac River (Chesapeake Bay, USA), Seitzinger (1987) observed both increased SRP and  $\text{NH}_4^+$  fluxes with pH elevation. Experimental  $\text{NH}_4^+$  flux rates increased from  $< 10$  to over  $100 \mu\text{mol m}^{-2} \text{h}^{-1}$  when pH was raised from 8 to 10 in laboratory incubations (Seitzinger 1987a). During an algal bloom in the Potomac estuary, Bailey et al. (2006) observed a three-fold increase of  $\text{NH}_4^+$  efflux when the bottom water pH rose from neutral to above 9. In soil studies, the combined influence of alkaline pH ( $> 8$ ) and  $\text{NH}_3$  production can decrease the  $\text{NH}_4^+$  soil inventory by  $\text{NH}_3$  volatilization, and change the efficiency of nitrification and denitrification by inhibiting bacterial activity (Cuhel et al. 2010; Simek et al. 2002).

We hypothesize that increased sediment pH facilitates not only P desorption but also the conversion of  $\text{NH}_4^+$  to  $\text{NH}_3$  with consequent changes in sediment N cycling. In this study we examined the pH effects on exchangeable  $\text{NH}_4^+$  desorption using the surface sediments. Impacts of high pH conditions on the sediment-water nutrient exchange were estimated with changes in flux rates of SRP,  $\text{NH}_4^+$ ,  $\text{NO}_3^-$ ,  $\text{O}_2$ , and coupled nitrification-denitrification using intact sediment cores. We also calculated the diffusive flux rates of pore water  $\text{NH}_4^+$ ,  $\text{NH}_3$  and SRP to confirm direct flux measurements. Due to the tightly coupled nitrification-denitrification, we independently measured nitrification rates using an inhibitor (Caffrey and Miller 1995) and potential nitrification rates using slurries (Henriksen et al. 1981).

We experimentally addressed these questions using sediment cores in the Sassafras River, a shallow, tidal freshwater tributary of the Chesapeake Bay (USA). As in other parts of the Chesapeake Bay (Tango and Butler 2008), summer cyanobacterial blooms have been observed frequently in the Sassafras River in recent decades. Relative to sea water, tidal fresh and oligohaline water have low pH buffering (Price et al. 2008), facilitating high pH from cyanobacterial photosynthetic carbon uptake. In the Sassafras River, high pH persisted in the range of 9 to 10.5 for several weeks during dense cyanobacterial blooms in the summers of 2007 and 2010. When such high pH is in contact with bottom sediment, pH penetration into sediment can impact nutrient biogeochemical processes (Bailey et al. 2006).

## **Materials and Methods**

### **2.1.1 Study site and collection of cores**

We collected sediments with 7 cm inner diameter, 30 cm long acrylic cores at two sites in the upper Sassafras River. The Powerline site (75°49.712', 39°22.646') was sampled on June 18, 2008 and Budds Landing (75°50.380', 39°22.310') was sampled on July 14, 2009 (Table 1). Dissolved oxygen (DO), salinity, pH and temperature were measured with a YSI 600XLM multiparameter sensor. Vertical irradiance profiles were recorded by a 2  $\pi$  Li-Cor underwater PAR light sensor. Bottom water collected for sediment incubations was filtered to minimize water column autotrophic and microbial respiration and nutrient recycling. Samples were transported to Horn Point Laboratory within 4 hours. Sediment cores were gently bubbled overnight to equilibrate temperature,

O<sub>2</sub>, and N<sub>2</sub>-N in the overlying and near surface pore waters (Kana et al. 2006). The surface sediments from Budds Landing were homogenized for potential nitrification measurements.

### 2.1.2 Experimental design

We incubated experimental cores (at least triplicates) at several pH levels to investigate pH effects on nutrient exchange at the sediment-water interface. Sediment-free blank cores were incubated identically at each pH level to correct for water column metabolism. Consistent with an absence of photosynthetically active radiation at the sediment surface at the time of collection, a dark temperature-controlled environmental chamber was used to maintain the sediments and replacement-water reservoir at *in situ* water temperatures of 25 °C for Powerline and 27 °C for Budds Landing, respectively. The filtered water was bubbled with air to maintain oxygen saturation, adjusted to experimental pH with 0.1 mol L<sup>-1</sup> NaOH, and continuously pumped through the sediment overlying water (~ 500 ml) at 10 ml min<sup>-1</sup>.

For the Powerline experiments, the overlying water pH of 4 replicate sediment cores was increased stepwise from 7.8 ± 0.5 (control) to 9.2 ± 0.05 (pH 1), and 9.6 ± 0.03 (pH 2), with a 5 day equilibration at each elevated pH. An alternative approach was used with sediments from Budds Landing (Table 2). Nine cores were incubated at ambient pH for the initial fluxes, and then triplicate cores were subjected to pH manipulation for each treatment. After 7 days of exposure to higher pH levels, the pH in the overlying water was 7.4 ± 0.3 (control), 9.2 ± 0.05 (pH 1) and 9.5 ± 0.2 (pH 2). Within each sealed core,



suspended magnetic stir bars circulated water gently to keep it mixed below the threshold of sediment resuspension.

For both sites, nutrients fluxes (SRP,  $\text{NH}_4^+$ , and  $\text{NO}_3^-$ ), oxygen consumption ( $\text{O}_2$ ) and coupled nitrification-denitrification (net  $\text{N}_2$  flux) were measured on the 1<sup>st</sup> day of incubation of sediments and after the pH reached the target values. After the termination of flux incubations, the top 11 cm sediments at each pH treatment were sectioned to collect pore water nutrients and to measure sediment pH. Duplicate sediment cores from Budds landing were used to measure nitrification rates, and  $\text{Br}^-$  was added to control cores as tracer to estimate diffusion/advection coefficients (Martin and Banta 1992). The remaining sediment cores were used to estimate the percent water.

### 2.1.3 Flux rates cross the sediment-water interface

Flux rates were measured on the first day of the incubation and after each equilibration period. The pumping of treatment water was interrupted during flux incubations and briefly restarted to collect samples every 1–2 hours with a total of 4 time-points. Solute samples were filtered through a 0.45 $\mu\text{m}$  cellulose acetate syringe filter and frozen at -4 °C. Dissolved  $\text{O}_2$  and  $\text{N}_2$  subsamples were preserved in 7 ml glass tubes by adding 10  $\mu\text{l}$  of 50% saturated  $\text{HgCl}_2$  solution (Kana et al. 2006), and then stored under water at near-ambient temperature until analysis. To preserve total dissolved ammonium ( $\Sigma\text{NH}_x = \text{NH}_4^+ + \text{NH}_3$ ) at higher pH levels, 2.5  $\mu\text{l}$  of 0.1 mol  $\text{L}^{-1}$  sulfuric acid was added into the sample vials. Flux rates were calculated from a regression of the time-concentration data in sediment and water column blank cores.

#### 2.1.4 Sediment pore-water chemistry

Samples for pH and pore water analysis were sectioned over the top ~10 cm into 50 ml centrifuge tubes in a nitrogen-filled glove bag to minimize oxidation artifacts (Bray et al. 1973). Vertical changes of pH were measured immediately with a flat surface pH electrode. Pore water was separated from the solid phase by centrifugation at 2000 G for 10 min. Supernatant solutions were filtered through a 0.45  $\mu\text{m}$  25 mm diameter cellulose acetate syringe filter and appropriately diluted for analysis of  $\text{Br}^-$ , Fe, SRP,  $\text{NH}_4^+$ , and  $\sum\text{NH}_x$ . The total iron, mostly  $\text{Fe}^{2+}$ , was acidified for preservation (Gibb 1979).

#### 2.1.5 Nitrification potential and nitrification rates

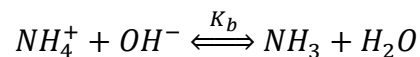
The effect of pH on nitrification was estimated using sediments from Budds Landing. Measurements included slurry incubation for potential nitrification (Henriksen et al. 1981) and  $\text{CH}_3\text{F}$  inhibition of intact sediments (Caffrey and Miller 1995). In  $\text{O}_2$ -saturated Sassafras River water, pH was pre-adjusted to values ranging from 7 to 11 using NaOH. The  $\text{NH}_4\text{Cl}$  concentration was set to 1.0 mM, with triplicates at each pH level. For potential nitrification, the top 2 cm of sediment were homogenized with 1 ml added separately into centrifuge tubes with different pH's. The suspension was gently shaken in darkness at 27 °C and subsamples for  $\text{NO}_3^-$  were taken at 0, 12, and 24 h to calculate rates of potential nitrification. Changes of  $\text{NO}_3^-$  in a sediment-free control were used as a background correction. Although this method homogenizes the redox profile and the  $\text{NH}_4^+$  gradient of the sediment and disrupts the aggregation of aerobic/ anaerobic microbiota (Garcia-Ruiz et al. 1998; Killham 1994), it makes testing pH effects over a large pH gradient relatively simple. c

An alternative to slurries was direct flux measurements using CH<sub>3</sub>F to inhibit nitrification (Caffrey and Miller 1995). The CH<sub>3</sub>F method was carried out immediately after the end of flux measurements. Saturated solutions of CH<sub>3</sub>F were injected into the overlying water of each intact core to a final concentration of ~100 mg L<sup>-1</sup>. After 24 hours of aerobic dark pre-incubation, ammonium flux rates were measured using our standard flux procedure. Increased flux rates of ammonium after CH<sub>3</sub>F treatment were interpreted as the nitrification rate. Shortcomings in the CH<sub>3</sub>F-inhibition method may include increased accumulation of pore water ammonium and non-specific inhibition of other N transformations such as ammonification (Capone et al. 2009).

#### 2.1.6 Molecular diffusive flux rates

Diffusion coefficients in sediment were estimated from Br<sup>-</sup> penetration profile (Martin and Banta, 1992). Bromide (NaBr) was added as a tracer into the overlying water to a concentration of ~6 mM. Pore water Br<sup>-</sup> was sampled after 24 h to estimate a diffusion coefficient ( $D_{Br}$ ), which was corrected for temperature and sediment porosity; the measure  $D_{Br}$  was compared to the theoretical coefficient ( $D_{Br}^*$ ) for to aid in correction of diffusion coefficients for other species (Martin and Banta 1992; Rao and Jahnke 2004; Schulz et al. 2006).

Using the pH-dependent equilibrium (Eq. 1), we calculated pore water NH<sub>3</sub> and NH<sub>4</sub><sup>+</sup> concentrations:



where the equilibrium constant (pK<sub>b</sub>) is 9.25 at 25 °C; we corrected our pore water constants for ionic strength and temperature (Mulholland 2008).

The dissolved NH<sub>3</sub> concentration, [NH<sub>3</sub>], can be calculated (Van Nest and Duce 1987):

$$NH_3 = \frac{[\sum NH_x][OH^-]}{K_b + [OH^-]}$$

where  $[\sum NH_x]$  is for the sum of dissolved NH<sub>3</sub> and NH<sub>4</sub><sup>+</sup>.

The diffusion coefficients (D<sub>i</sub>) of NH<sub>3</sub>, NH<sub>4</sub><sup>+</sup> and SRP were corrected using the Br<sup>-</sup> diffusion estimates in pore water and the theoretical coefficient (D<sub>Br</sub><sup>\*</sup>). Applying Fick's first law, the NH<sub>3</sub>, NH<sub>4</sub><sup>+</sup> and SRP fluxes were calculated by:

$$F_i = -\phi \cdot D_i \times \frac{\partial C_i}{\partial x} \quad (3)$$

where F<sub>i</sub> is the flux of different species (μmol cm<sup>-2</sup> s<sup>-1</sup>). The diffusion coefficient (D<sub>i</sub>) is influenced by tortuosity (θ), temperature and sediment properties.  $\frac{\partial C_i}{\partial x}$  is the gradient of nutrient concentration (C<sub>i</sub>) and depth (x). The diffusion coefficients of NH<sub>3</sub>, NH<sub>4</sub><sup>+</sup> and SRP in sediments were corrected using the D<sub>Br</sub> estimates, and the diffusion coefficients in a particle free solution at *in situ* temperature (Martin and Banta, 1992; Rao and Jahnke, 2004; Schulz et al., 2006). Percent water and the dry sediment density (ρ ~ 2.5 g cm<sup>-3</sup>) were used to calculate porosity (∅) and porosity (ϕ) (Boudreau 1997):

$$\phi = \frac{water\%}{(water\% + \frac{(1-water\%)}{\rho})} \quad (4)$$

$$\theta^2 = 1 - \ln(\phi^2)$$

### 2.1.7 Desorption isotherm of adsorbed ammonium (NH<sub>4</sub><sup>+</sup>-N)

In order to estimate pH effects on ammonium desorption from sediment, surface sediments were collected from Budds Landing in November 2008. Adsorbed NH<sub>4</sub><sup>+</sup> was measured using KCl extraction (Morin and Morse, 1999). Triplicate 1 ml wet samples of

the top 2 cm sediment were extracted twice with 39 ml of 2 mol L<sup>-1</sup> KCl; samples were shaken for 2 hours at the field temperature (10 °C). After centrifugation and filtration, the increase in NH<sub>4</sub><sup>+</sup> concentration relative to the blank was used to quantify adsorbed ammonium. Adsorption coefficients (K) were used to describe this ion exchange following Rosenfeld (1979), Mackin and Aller (1984):

$$K = \rho \cdot \frac{1-\phi}{\phi} \cdot \frac{\hat{C}_N}{C_N} \quad (6)$$

where  $\hat{C}_N$  is exchangeable NH<sub>4</sub><sup>+</sup> on a dry mass basis (μmol g<sup>-1</sup>) and C<sub>N</sub> is the pore water ammonium concentration (μmol L<sup>-1</sup>). Porosity was measured for the top 2 cm of sediment.

To simulate response of adsorbed ammonium to pH elevation, the homogenized sediment (0-2 cm) was suspended in site water with different pH values. We added 1 ml of wet sediment to 39 ml of pH-adjusted water. To inhibit dissimilatory NO<sub>3</sub><sup>-</sup> reduction to NH<sub>4</sub><sup>+</sup>, we used the oxygen-saturated water and left 5 ml headspace in the centrifuge tube.  $\Sigma\text{NH}_x$  was measured after shaking, centrifugation and filtration. Assuming a NH<sub>3</sub> equilibrium between the aquatic and atmospheric phase, the total release of ammonium is estimated as the sum of total dissolved ammonium in the water column ( $\Sigma\text{NH}_{x,l}$ ) and NH<sub>3</sub> gas within the head space (NH<sub>3,g</sub>):

$$\text{NH}_{x,ds} = \Delta\Sigma\text{NH}_{x,l} + \Delta\text{NH}_{3,g} \quad (7)$$

The headspace NH<sub>3</sub> was estimated from 1) the pH at the beginning and end of incubation, 2) ionic strength corrections for NH<sub>3</sub> ( $\gamma_{\text{NH}_3}$ ) and NH<sub>4</sub><sup>+</sup> ( $\gamma_{\text{NH}_4^+}$ ), and 3) the temperature-corrected Henry's law coefficient (K<sub>H</sub>) (Larsen et al., 2001):

$$[\text{NH}_3] = \frac{[\Sigma\text{NH}_x]}{\text{RTK}_H \left( \frac{1}{\gamma_{\text{NH}_3}} + \frac{10^{-\text{pH}}}{K_a \gamma_{\text{NH}_4^+}} \right)} \quad (8)$$

### 2.1.8 Chemical analysis

Concentrations of  $\text{NH}_4^+$ , SRP and Fe were analyzed using colorimetric methods (Gibb 1979; Parsons et al. 1984). Concentrations of  $\text{NO}_3^-$ ,  $\text{NO}_2^-$  and pore water  $\text{Br}^-$  were determined using ion chromatography (Kopp and Mckee 1983).  $\text{NO}_2^-$  concentrations were generally very low. Dissolved  $\text{N}_2$  and  $\text{O}_2$  were measured by the ratios of  $\text{N}_2$ : Ar and  $\text{O}_2$ : Ar using membrane inlet mass spectrometry (Kana et al. 1994; Kana and Weiss 2004). Percent water was determined as the weight loss of wet sediment after drying at 65 °C. After pre-treatment with sodium hypochlorite overnight to remove carbonates and organic matter, grain size was analyzed by wet sieving and followed by pipet analysis of the remaining silt and clay (Folk 1974).

## Results and Discussion

### 2.1.9 Physical conditions

The Powerline and Budds Landing sites had an aerobic water column, low salinity (<1), and fine grain-sized sediment (Table 1). Water depths were 0.8 m at Powerline and 1.3 m at Budds Landing. At the time of collection, bottom water pH was 9.4 at Powerline and 7.3 at Budds Landing. The temperature at Powerline (24.7 °C) was similar to Budds Landing (26.9 °C). Light attenuation coefficients were 4.8  $\text{m}^{-1}$  at Powerline and 4.2  $\text{m}^{-1}$  at Budds Landing, resulting in dim to dark conditions at the sediment surface. Both sites

often have experienced cyanobacterial blooms associated with high pH in summer (Maryland Department of Natural Resources, unpublished data).

#### 2.1.10 Effect of pH on the pore water iron profile

Vertical profiles of pore water pH and iron in the Powerline cores rapidly responded to the diffusion of alkaline overlying pH into the pore water (Fig. 1A, B). The pH profile under ambient condition was nearly constant with depth and generally < 7 below 1 cm; the elevated water column pH treatments resulted in pH > 9.0 in the top 2 cm of sediment, decreasing downward until the pH was similar to the control. Although pH may be buffered by cation exchange (e. g. Ca<sup>2+</sup>, Mg<sup>2+</sup>), sulfate reduction, and anaerobic generation of acid (Cai et al. 2010), such high pore water pH's (pH > 9.5) have been observed during algal blooms in tidal-freshwater estuaries (Magalhaes et al. 2002). Our elevated pH profiles in sediments were similar to a time-series study of pH penetration by Bailey et al. (2006). When Potomac River sediments are incubated at pH (~10) in summer, high pH moves downward with time and maintains pH > 9 at 4 to 8 cm depth in a week incubation (Bailey et al. 2006). In our aerobic incubations, pore water Fe<sup>2+</sup> was undetectable at the surface and peaked in the upper anoxic sediment horizon. Increased pH lead to a reduction in Fe<sup>2+</sup> through hydroxide precipitation (Hutchins et al. 2007). As pH increased to 9.6 in the overlying water, the peak concentration of Fe<sup>2+</sup> simultaneously decreased from 120 μmol L<sup>-1</sup> to 68 μmol L<sup>-1</sup> with its peak position shifting from 1.75 cm downward to 2.5 cm.

### 2.1.11 Effect of pH on the pore water SRP profile

Elevation of pH below the sediment-water interface resulted in SRP release into the pore water, with the peak concentrations increasing from  $< 40 \mu\text{mol L}^{-1}$  to  $102 \mu\text{mol L}^{-1}$  (Fig. 1D, F). Increased SRP concentrations were consistent with pH related P releases from surface metal hydroxide complexes (Seitzinger 1991) due to the increased negative charge of mineral surfaces (Boers 1991). Elevated pH increased upward SRP diffusion from  $5 \mu\text{mol m}^{-2} \text{h}^{-1}$  under neutral pH to  $39 \mu\text{mol m}^{-2} \text{h}^{-1}$  under alkaline pH treatments (Fig. 1E, 1F and Table 4). Under aerobic pH-neutral conditions, iron oxyhydroxides usually adsorb or co-precipitate P, hindering the flux of SRP across the sediment-water interface (Slomp et al. 1998). In contrast to neutral pH conditions, highly alkaline pH's enhanced pore water SRP gradients and increased the diffusion rate (Fig. 1 and 3) by breaking surficial Fe-P bonds.

### 2.1.12 Effect of pH on the pore water ammonium profile

Under ambient pH conditions,  $\text{NH}_4^+$  linearly increased downcore to  $720 \mu\text{mol L}^{-1}$  with negligible  $\text{NH}_3$  present (Fig. 1C). The diffusive flux rate, primarily as  $\text{NH}_4^+$ , was  $149 \mu\text{mol m}^{-2} \text{h}^{-1}$  (Table 4). In contrast, the  $\sum\text{NH}_x$  concentration in high pH cores increased to  $975 \mu\text{mol L}^{-1}$  at  $\sim 4 \text{ cm}$  depth (Fig. 1E). Conversion of  $\text{NH}_4^+$  to  $\text{NH}_3$  in surface horizons resulted in a steeper concentration gradient of  $\text{NH}_4^+$ , increasing  $\text{NH}_4^+$  diffusive fluxes (Table 4). Dissolved  $\text{NH}_3$  exhibited a very sharp peak at  $2 - 3 \text{ cm}$  in the pH 9.6 treatment, yielding a rapid upward flux. Diffusive flux rates were the sum of  $243 \mu\text{mol m}^{-2} \text{h}^{-1}$  for  $\text{NH}_4^+$  and  $234 \mu\text{mol m}^{-2} \text{h}^{-1}$  for  $\text{NH}_3$  (Table 4). Without consideration of  $\sum\text{NH}_x$  speciation at the overlying water pH 9.6, the diffusive rate calculated from the



concentration gradient and diffusion coefficient of  $\text{NH}_4^+$  was only  $271 \mu\text{mol m}^{-2} \text{h}^{-1}$ , less than half of the observed  $\sum\text{NH}_x$  diffusive rate (Fig. 1E).

#### 2.1.13 Adsorbed $\text{NH}_4^+$

Both pore water and adsorbed ammonium are hypothesized to be available for nitrification (Seitzinger et al. 1991). Adsorbed  $\text{NH}_4^+$  is reversibly attracted to negatively charged binding sites on the surface of sediment particles (Rosenfeld, 1979), and can influence pore water  $\text{NH}_4^+$  concentration as well as migration of in sediment (Morse and Morin, 2005). Without pH manipulation, the pH decreased from 7.2 to 6.5 during KCl-extraction, and adsorbed  $\text{NH}_4^+$  in our samples averaged  $3.4 \pm 0.4 \mu\text{mol g}^{-1}$ . It is reasonable to expect higher adsorbed  $\text{NH}_4^+$  in summer due to spring/summer algal deposition and the temperature-related increases in ammonification (Laima 1992; Laima et al. 1999; Vouve et al. 2000). Our adsorption coefficient ( $K = 2.6 \pm 0.4$ ) were similar to the observations of 2.1 – 7.1 in Potomac River sediments (Simon and Kennedy 1987) and in the upper Chesapeake Bay (Cornwell and Owens 2011). The K value in this freshwater estuary is higher than other coastal (1.0 – 1.7, Mackin and Aller, 1984) and marine sediments (1.1 – 1.3, Rosenfeld, 1979). This result is consistent with salinity influences on  $\text{NH}_4^+$  adsorption (Seitzinger et al. 1991b; Weston et al. 2010).

#### 2.1.14 Effect of pH on desorption of sediment $\text{NH}_4^+$

Increased pH stimulated adsorbed ammonium release into pore water by converting  $\text{NH}_4^+$  to  $\text{NH}_3$ . The peak of dissolved  $\text{NH}_4^+$  was  $132 \mu\text{mol L}^{-1}$  at pH 9.3 (Fig. 2A). The increase of dissolved  $\text{NH}_4^+$  at pH's 6.5-13 likely resulted from exchangeable  $\text{NH}_4^+$  desorption. When pH approached or exceeded the  $P_{ka}$  (i.e.  $\text{pH} \geq 9.25$ ),  $\text{NH}_4^+$

concentrations decreased via conversion to  $\text{NH}_3$ . This resulted in a large decrease of dissolved  $\text{NH}_4^+$  when pH rose from 9.3 to 13 (Fig. 2A).

High pH increased the release of  $\text{NH}_3$  and  $\text{NH}_4^+$ , mainly from the exchangeable ammonium pool. As pH increased from 6.5 to 13 (Fig. 2B), the amount of  $\text{NH}_4^+$  desorbed increased from 646 to 2647  $\text{nmol g}^{-1}$ . The elevation of pH above 9.2 resulted in more than 50% of ammonium ( $\sum\text{NH}_x$ ) converting to  $\text{NH}_3$  (Eq. 2). Although mineral surface charges become more and more negative as pH increases, un-ionized  $\text{NH}_3$  does not substantially adsorb to the solid phase. Moreover, drawdown of  $\text{NH}_4^+$  concentration with pH enhancement in the aquatic phase may promote desorption until approximately 80% of KCl-extractable ammonium was desorbed (Fig. 2b).

#### 2.1.15 Effect of pH on SRP flux

Flux rates of SRP increased with pH elevation at both stations ( $P < 0.05$ , student's-*t* test). SRP efflux rates increased from  $< 5 \mu\text{mol m}^{-2} \text{h}^{-1}$  in the control, to 15 – 25  $\mu\text{mol m}^{-2} \text{h}^{-1}$  at pH 9.2, and to 35 – 55  $\mu\text{mol m}^{-2} \text{h}^{-1}$  at pH 9.6 (Fig. 3). Increased SRP flux rates with pH increases were consistent with the molecular diffusive rates of SRP estimated from pore water profiles (Table 4). In the oligohaline region of the Potomac River, SRP release from sediment increased from  $< 10 \mu\text{mol-P m}^{-2} \text{h}^{-1}$  in controls to  $\sim 40 \mu\text{mol m}^{-2} \text{h}^{-1}$  at pH 9.5 and  $\sim 110 \mu\text{mol m}^{-2} \text{h}^{-1}$  at pH 10 (Seitzinger, 1991). Similar large increases in SRP flux rates have been observed at pH's of 9.5 in freshwater sediments (Boers 1991).

#### 2.1.16 Effect of pH on DIN flux

For both Powerline and Budds Landing experimental cores (Fig. 4A), flux rates of  $\Sigma\text{NH}_x$  increased significantly in the high pH treatments (especially pH > 9.5) relative to the control ( $p < 0.05$ , student's - t test), but differences between pH 9.2 and 9.5 were not significant. Compared to the control group, high pH (9.5 – 9.6) increased  $\Sigma\text{NH}_x$  flux rates by about 6-fold at Powerline and by 2-fold at Budds Landing. Increase in  $\Sigma\text{NH}_x$  flux rates were consistent with the pH-induced ammonium desorption at surface sediments and the observed changes in the pore water profile. Similar to observations of salinity-enhanced ammonium desorption (Gardner et al. 1991), ammonium desorption with alkaline pH penetration increased both the  $\Sigma\text{NH}_x$  concentration and the proportion of  $\text{NH}_3$  in pore-water (Fig. 1E). The conversion of  $\text{NH}_4^+$  to  $\text{NH}_3$  and the steeper concentration gradients of these two components all resulted in elevated  $\Sigma\text{NH}_x$  fluxes. At Budds Landing, the flux measurements in the control were similar to the upward diffusion rate of ammonium, primarily as  $\text{NH}_4^+$ . The measured efflux rates of  $\Sigma\text{NH}_x$  at pH 9.6 were equivalent to the sum of the diffusive flux rate of  $\text{NH}_4^+$  and  $\text{NH}_3$  (Table 4). Lack of consideration of  $\text{NH}_3$  production would result in underestimation of ammonium flux rates by 25-35% for the flux measurement and by 50% for the diffusive flux estimation.

Ammonium remineralization, calculated either by stoichiometric oxygen-based N remineralization or measured total inorganic nitrogen flux ( i.e.  $\text{NH}_4^+ + \text{NH}_3 + \text{N}_2\text{-N} + \text{NO}_3^-$ ), suggests elevated pH dramatically promoted N efflux. If we assume that aerobic N remineralization stoichiometry from phytoplanktonic organic matter is 138:16  $\text{O}_2$ : N and denitrification is partly fuelled by the diffusion of water column  $\text{NO}_3^-$  into sediment (Cornwell et al. 1999),  $\Sigma\text{NH}_x$  flux accounted for 20 – 40% of oxygen-based N

rem mineralization in the control and for 68 – 153 % of N rem mineralization in the high pH treatments. Alternatively, if nitrogen rem mineralization rates were evaluated from the sum of  $\Sigma\text{NH}_x$ ,  $\text{NO}_3^-$  and  $\text{N}_2$  flux rates, pH elevation increased ammonium flux as a proportion of total N rem mineralization from 22% to 105% for sediment at Powerline and 44% to 87% at Budds Landing. Both estimates reveal that increased pH enhanced the proportion of ammonium release relative to the total rem mineralized N. However, the difference of  $\text{NH}_4^+$  rem mineralization between two estimates may result from the use of  $\text{O}_2$  consumption rates instead of  $\text{CO}_2$  fluxes. The calculation of oxygen-based ammonium rem mineralization is affected by the production/ reoxidation of reduced inorganic compounds (e.g.  $\text{Fe}^{2+}$ ,  $\text{S}^{2-}$  and  $\text{Mn}^{2+}$ ), potential methanogenesis in organic-matter rich estuaries (Carini and Joye 2008; Martens and Klump 1980), and variable C:N ratios of organic matter.

No significant difference was found for  $\text{NO}_3^-$  flux rates among pH treatments ( $p > 0.05$ , student-t test). Fluxes of  $\text{NO}_3^-$  ranged from -70 to 10  $\mu\text{mol-N m}^{-2} \text{h}^{-1}$ , with most fluxes directed into the sediment (Fig.4B). Concentrations of  $\text{NO}_3^-$  were low in the overlying water and undetectable in pore water.

#### 2.1.17 Effect of pH on potential nitrification

The response of potential nitrification to pH suggests high pH (> 9) inhibited nitrification (Fig. 5A). The potential nitrification rate in the control was  $84 \pm 24 \text{ nmol-N g}^{-1} \text{h}^{-1}$ , similar to rates in other fresh water sediments of 90- 470  $\text{nmol-N g}^{-1} \text{h}^{-1}$  (Cooper 1983). With pH increasing from 9 to 11, potential nitrification rates decreased sharply from 70-110  $\text{nmol-N g}^{-1} \text{h}^{-1}$  to below 10  $\mu\text{mol-N g}^{-1} \text{h}^{-1}$  (Fig. 5A).

Bacterially mediated nitrification is first order or zero-order kinetics with respect to  $\text{NH}_4^+$  /  $\text{NH}_3$  concentrations as nitrifying substrates (Park et al. 2010). However, increases in pH can enhance  $\Sigma\text{NH}_x$  desorption and the total inventories of exchangeable and pore water ammonium may be equal or less than controls because of  $\text{NH}_3$  volatilization. Furthermore, pH-driven  $\text{NH}_3$  accumulation can be toxic or inhibit the growth and enzyme efficiency of nitrifying bacteria (Anthonisen et al. 1976; Kim et al. 2006). In laboratory observations and modeling, both high pH and  $\text{NH}_3$  have negative effects on nitrifying bacteria, ammonium-oxidizing bacteria (AOB, *Nitrosomonas*) and nitrite-oxidizing bacteria (NOB, *Nitrobacter*) (Van Hulle et al. 2007). Elevation of pH above 9 could inhibit enzyme activity of AOB and NOB since the optimal pH range is 6 – 8.5 for AOB and 5.5 – 8 for NOB (Park et al. 2010; Van Hulle et al. 2007). Even though nitrifying bacteria might survive out of the optimal pH range, they would pay an energy cost to maintain their cytoplasmic pH (Wood 1988).

Although few field studies have been conducted on the effect of pH on sediment nitrification relative to water column and soil environments (Carini and Joye 2008; Simek et al. 2002), sediment potential nitrification rates appear to be limited by high pH (> 8) in freshwater and were positively related to exchangeable  $\text{NH}_4^+$  in 36 stream surveys (Strauss et al. 2002). Elevated pH inhibition of nitrification, with decreases of 80% at pH 9 relative to peak nitrification, have been observed in fine-grained sediment in the Arika Sea (Isnansetyo et al. 2011).

### 2.1.18 Effect of pH on nitrification rates

Elevated pH negatively impacted the intact-core nitrification as measured by the changes in  $\sum\text{NH}_4^+$  or  $\text{NH}_4^+$  flux rates after adding  $\text{CH}_3\text{F}$ , an inhibitor of ammonium oxidation (Fig. 5B). Under neutral conditions, no significant difference of nitrification rates existed between the evaluation from  $\sum\text{NH}_4^+$  flux ( $182 \pm 49 \mu\text{mol m}^{-2} \text{h}^{-1}$ ) and from  $\text{NH}_4^+$  flux ( $210 \pm 35 \mu\text{mol m}^{-2} \text{h}^{-1}$ ). Sediments in the upper Sassafras River show considerably higher nitrification rates than the  $< 40 \mu\text{mol m}^{-2} \text{h}^{-1}$  typical of the mesohaline region of the Chesapeake Bay in summer (Kemp et al. 1990), reflecting the aerobic overlying water conditions.

Similar to nitrification potentials (Fig. 5A), increasing pH from neutral to 9.5 exerted a remarkable depression on nitrification, as evidenced by the  $> 50\%$  reduction in nitrification under alkaline water (Fig. 5B). If both dissolved  $\text{NH}_4^+$  and adsorbed  $\text{NH}_4^+$  in sediments are assumed to be the main substrates for nitrification (Seitzinger et al. 1991), high pH related decreases in N availability could functionally suppress nitrification. The reduction of  $\text{NH}_4^+$  concentration in pore water as well as its proportion to  $\sum\text{NH}_x$  may reduce the ammonium availability for nitrification. As a negative function of pH (Fig. 2), adsorbed  $\text{NH}_4^+$  may be reduced, possibly decreasing nitrification (Fig. 5). Following pH penetration into the aerobic sediment surface (typically  $\sim 2 \text{ mm}$ ),  $\text{NH}_3$  toxicity could suppress nitrification (Isnansetyo et al. 2011). In addition, nitrifying bacteria are obligate chemoautotrophs and grow with inorganic carbon in the form of  $\text{CO}_2$  as their sole carbon source (Staner 1970); a reduction in  $\text{CO}_2$  with pH elevation may therefore potentially inhibit nitrifying metabolism.

### 2.1.19 Effect of pH on denitrification

In aerobic Chesapeake Bay sediments, alternative  $N_2$  production via annamox appears inconsequential (Rich et al. 2008), with coupled nitrification-denitrification being the key pathway to transform the rematerialized nitrogen to  $N_2$ -N (Cornwell et al. 1999). Coupled nitrification - denitrification decreased from 180 - 280  $\mu\text{mol-N m}^{-2} \text{h}^{-1}$  to less than 85  $\mu\text{mol -N m}^{-2} \text{h}^{-1}$  as the overlying water pH increased to 9.6 (Fig.6). Denitrification efficiency, the percentage of inorganic nitrogen released from the sediment as  $N_2$ -N (Heggie et al. 2008), decreased from 84% to 35% at Powerline and 64% to 17% at Budds Landing.

Reduction in denitrification with pH elevation may be a consequence of limited  $\text{NO}_3^-$  supply and alkaline pH constraint on denitrifying bacterial activity. The  $\text{NO}_3^-$  supply for denitrification may come from ammonium oxidation and diffusion from the overlying water. In this study, the  $\text{NO}_3^-$  supply from the overlying water (Table 1) was low relative to denitrification rates, an observation consisted with undetectable pore water  $\text{NO}_2^-$  and  $\text{NO}_3^-$  concentrations. Hence, consistent with pH suppression of nitrification (Fig. 5), denitrification at high pH is likely limited by the  $\text{NO}_3^-$  supply (Fig. 6). Moreover, the optimal pH range for denitrification is 7 – 8 in soil and anaerobic sediments (Simek et al. 2002); higher pH may directly inhibit the activity of denitrifying bacteria. Nitrate reducing bacteria, such as *Thioalkalivibrio nitratireducens*, can survive in alkaline sediment and cultivation media at pH 10. However, the nitrite reductase activity of *T. nitratireducens* was maximal when pH ranged from 6.7 – 7.5, and 80% of the activity was inhibited at high pH (9 – 10) (Filimonenkov et al. 2010).

Although dissimilatory nitrate reduction to ammonium (DNRA) in freshwater sediments appears to be minor relative to denitrification (Scott et al. 2008), DNRA usually occurs when  $\text{NO}_3^-$  inputs exceed the availability of carbon substrate for denitrification (Tiedje et al. 1989). As a consequence of pH elevation, limited  $\text{NO}_3^-$  consumption through anaerobic denitrification may provide the potential chances for DNRA and enhance ammonium production. However, DNRA may play a minor role in explaining the enhanced ammonium fluxes. We did not expect high DNRA occurs in the Sassafra River sediment with undetectable free sulfide concentrations.

#### 2.1.20 Effect of pH on oxygen consumption

Oxygen consumption rates in the controls were higher in July at Budds Landing than in June at Powerline, partly a result of the promoted bacteria efficiency of organic matter decomposition with rising temperatures. However, oxygen consumption decreased as pH increased at both sites (Fig. 6). This is likely related to the alkaline pH effects on bacteria production and respiration (Tank et al. 2009). Assuming pH has no effect on organic matter remineralization to ammonium at each sampling site, we postulate that inhibition of nitrification by increased pH resulted in the reduction of oxygen consumption.



The molar ratio of  $\text{O}_2$  to  $\sum\text{NH}_4^+$  is 2 for nitrification. The measured slopes of  $\Delta\sum\text{NH}_4^+$  and  $-\Delta\text{O}_2$  fluxes were consistent with nitrifying stoichiometry (Fig.7), which suggests high pH increased sediment  $\sum\text{NH}_4^+$  diffusion into overlying water rather than enhancing coupled nitrification-denitrification. Deviation of the  $-\Delta\text{O}_2 : \Delta\sum\text{NH}_4^+$  flux rates



from the theoretical 2 : 1 ratio may result from variation in sediment cores, such as oxidation of Mn (II) and Fe (II), and sediment buffering effects on OH<sup>-</sup> penetration in depth and magnitude.

### **Conclusion and Ecological Implications**

Harmful algal blooms, including cyanobacterial blooms, present a clear challenge to the functioning of shallow water coastal ecosystems. Like other blooms, cyanobacterial blooms are increasing in frequency and magnitude over time due to eutrophication. Cyanobacterial blooms can be locally persistent and extensive. However, determining the cause of such blooms can be elusive. Elevated temperature, a long water residence time, and availability and proportions of inorganic and organic nutrients are often cited as 'triggers' (Glibert 2011). Mitigation efforts for eutrophication have not always had success in hindering the development of harmful algal blooms (Glibert 2011). Indeed, cyanobacterial blooms are common in the Potomac River (Chesapeake Bay) despite considerable progress removing P from point sources (Krogmann et al. 1986; Ruhl 2010)(Krogmann et al. 1986; Ruhl and Rybicki 2010). The occurrence of blooms during drought periods with low external nutrient inputs suggests that internal nutrient recycling is a key to the initiation and sustainability of cyanobacterial blooms.

Nutrient release from bottom sediments can be a substantial source in shallow water ecosystems, potentially satisfying nutrient demand of algal growth and enhancing eutrophic conditions. High rates of photosynthesis during dense blooms promote a large

water column pH increase, especially in the low pH buffering water such as lake and freshwater estuaries.

Nutrients, especially N, are limiting to primary production during the extensive summer blooms in Chesapeake Bay (Kemp et al. 2005). In summer, bloom forming cyanobacteria are dominant by diazotrophs, resulting in high pH persistence in the tidal fresh Sassafras River (O'Neil and Maryland DNR, unpublished data). Our study suggests pH elevation can increase inorganic N supply from the sediment into the water column. As pH increased above 9, the N flux from sediments was more than doubled by promoting  $\text{NH}_4^+$  and  $\text{NH}_3$  flux and inhibiting  $\text{N}_2$  loss. Even though  $\text{N}_2$ -fixing cyanobacteria can survive during N deficiency, they prefer to take up dissolved inorganic N rather than consuming energy for  $\text{N}_2$  fixation (Paerl 2008). The pH-induced release of ammonium from sediments may thereby be an important N source for primary productivity during dense blooms in shallow estuaries or lakes. The molar ratio of DIN:SRP sediment efflux decreased from > 70 to 9 – 12 when experimental pH rose from neutral to above 9, which may reinforce N limitation and selectively support  $\text{N}_2$ -fixing cyanobacterial blooms. Given higher P demand for diazotrophs, the augmentation of P flux with pH may boost the growth and persistence of algal blooms (Xie and Xie, 2003; Paerl, 2008).

## References

- Andersen, J. M. 1975. Influence of pH on release of phosphorus from lake sediments. *Archiv für Hydrobiologie* **76**: 411-419.
- Anthonisen, A. C., R. C. Loehr, T. B. S. Prakasam, and E. G. Srinath. 1976. Inhibition of nitrification by ammonia and nitrous-acid. *Journal Water Pollution Control Federation* **48**: 835-852.
- Bailey, E., M. Owens, W. Boynton, and J. Cornwell. 2006. Sediment phosphorus flux: pH interaction in the tidal freshwater Potomac River estuary. Interstate Commission on the Potomac River Basin, UMCES report TS-505-08-CBL: 1-91.
- Boers, P. C. M. 1991. The influence of pH on phosphate release from lake-sediments. *Water Research* **25**: 309-311.
- Boudreau, B. P. 1997. *Diagenetic Models and Their Implementation: Modeling Transport and Reactions in Aquatic Sediments*. Springer.
- Bray, J. T., O. P. Bricker, and B. N. Troup. 1973. Phosphate in interstitial waters of anoxic sediments - oxidation effects during sampling procedure. *Science* **180**: 1362-1364.
- Brunner, E., and J. O'neil. 2010. Factors affecting cyanobacterial nitrogen fixation on the Sassafras River, a tributary of the Chesapeake Bay. 2010 AGU Ocean Sciences Meeting: 22-26.
- Caffrey, J. M., and L. G. Miller. 1995. A comparison of two nitrification inhibitors used to measure nitrification rates in estuarine sediments. *Fems Microbiology Ecology* **17**: 213-220.
- Cai, W. J., G. W. Luther, J. C. Cornwell, and A. E. Giblin. 2010. Carbon cycling and the coupling between proton and electron transfer reactions in aquatic sediments in Lake Champlain. *Aquatic Geochemistry* **16**: 421-446.
- Capone, D., D. Bronk, M. Mulholland, and E. Carpenter. 2009. *Nitrogen in the marine environment*. Elsevier.

- Carini, S. A., and S. B. Joye. 2008. Nitrification in Mono Lake, California: Activity and community composition during contrasting hydrological regimes. *Limnology and Oceanography* **53**: 2546-2557.
- Cooper, A. B. 1983. Population ecology of nitrifiers in a stream receiving geothermal inputs of ammonium. *Applied and Environmental Microbiology* **45**: 1170-1177.
- Cornwell, J., and K. Kana. 1999. Denitrification in coastal ecosystems: methods, environmental controls, and ecosystem level controls, a review. *Aquatic Ecology* **33**: 41-54.
- Cornwell, J., and M. Owens. 2011. Quantifying sediment nitrogen releases associated with estuarine dredging. *Aquatic Geochemistry* **17**: 499-517.
- Cornwell, J. C., W. M. Kemp, and T. M. Kana. 1999. Denitrification in coastal ecosystems: environmental controls and aspects of spatial and temporal scale. *Aquatic Ecology* **33**: 41-54.
- Cowan, J. L. W., and W. R. Boynton. 1996. Sediment-water oxygen and nutrient exchanges along the longitudinal axis of Chesapeake Bay: Seasonal patterns, controlling factors and ecological significance. *Estuaries* **19**: 562-580.
- Cuhel, J. and others 2010. Insights into the effect of soil pH on N<sub>2</sub>O and N<sub>2</sub> emissions and denitrifier community size and activity. *Applied and Environmental Microbiology* **76**: 1870-1878.
- Eckert, W., A. Nishri, and R. Parparova. 1997. Factors regulating the flux of phosphate at the sediment-water interface of a subtropical calcareous lake: A simulation study with intact sediment cores. *Water Air and Soil Pollution* **99**: 401-409.
- Filimonenkov, A. A., R. A. Zvyagilskaya, T. V. Tikhonova, and V. O. Popov. 2010. Isolation and characterization of nitrate reductase from the halophilic sulfur-oxidizing bacterium *Thioalkalivibrio nitratireducens*. *Biochemistry* **75**: 744-751.
- Fisher, T. R., P. R. Carlson, and R. T. Barber. 1982. Sediment nutrient regeneration in 3 north-carolina estuaries. *Estuarine Coastal and Shelf Science* **14**: 101-116.
- Folk, R. 1974. *Petrology of Sedimentary Rocks*. Hemphill Publishing Company.

- Garcia-Ruiz, R., S. N. Pattinson, and B. A. Whitton. 1998. Denitrification in river sediments: relationships between process rate and properties of water and sediment. *Freshwater Biology* **39**: 467-476.
- Gardner, W. S., S. P. Seitzinger, and J. M. Malczyk. 1991. The effects of sea salts on the forms of nitrogen released from estuarine and fresh-water sediments - Does ion-pairing affect ammonium flux. *Estuaries* **14**: 157-166.
- Gibb, M. M. 1979. A simple method for the rapid determination of iron in natural waters. *Water Research* **13**: 295-297.
- Hansen, P. J. 2002. Effect of high pH on the growth and survival of marine phytoplankton: implications for species succession. *Aquatic Microbial Ecology* **28**: 279-288.
- Heggie, D. T., G. A. Logan, C. S. Smith, D. J. Fredericks, and D. Palmer. 2008. Biogeochemical processes at the sediment-water interface, Bombah Broadwater, Myall Lakes. *Hydrobiologia* **608**: 49-67.
- Henriksen, K., J. I. Hansen, and T. H. Blackburn. 1981. Rates of nitrification, distribution of nitrifying bacteria, and nitrate fluxes in different types of sediment from danish waters. *Marine Biology* **61**: 299-304.
- Hinga, K. R. 2002. Effects of pH on coastal marine phytoplankton. *Marine Ecology-Progress Series* **238**: 281-300.
- Hutchins, C. M., P. R. Teasdale, J. Lee, and S. L. Simpson. 2007. The effect of manipulating sediment pH on the porewater chemistry of copper- and zinc-spiked sediments. *Chemosphere* **69**: 1089-1099.
- Isnansetyo, A., N. D. Thien, and M. Seguchi. 2011. Potential of mud sediment of the Ariake Sea tidal flat and the individual effect of temperature, ph, salinity and ammonium concentration on its nitrification rate. *Research Journal of Environmental and Earth Sciences* **3**: 587-599.
- Kana, T. M., J. C. Cornwell, and L. J. Zhong. 2006. Determination of denitrification in the Chesapeake Bay from measurements of N<sub>2</sub> accumulation in bottom water. *Estuaries and Coasts* **29**: 222-231.

- Kana, T. M., C. Darkangelo, M. D. Hunt, J. B. Oldham, G. E. Bennett, and J. C. Cornwell. 1994. Membrane inlet mass spectrometer for rapid high-precision determination of N<sub>2</sub>, O<sub>2</sub>, and Ar in environmental water samples. *Analytical Chemistry* **66**: 4166-4170.
- Kana, T. M., and D. L. Weiss. 2004. Comment on "comparison of isotope pairing and N<sub>2</sub>: Ar methods for measuring sediment denitrification" by B. D. Eyre, S. Rysgaard, T. Dalsgaard, and P. Bondo Christensen. 2002. *estuaries* 25 : 1077-1087". *Estuaries* **27**: 173-176.
- Kemp, W. M., and W. R. Boynton. 1984. Spatial and temporal coupling of nutrient inputs to estuarine primary production - the role of particulate transport and decomposition. *Bulletin of Marine Science* **35**: 522-535.
- Kemp, W. M. and others 2005. Eutrophication of Chesapeake Bay: historical trends and ecological interactions. *Marine Ecology-Progress Series* **303**: 1-29.
- Kemp, W. M., P. Sampou, J. Caffrey, M. Mayer, K. Henriksen, and W. R. Boynton. 1990. Ammonium recycling versus denitrification in Chesapeake Bay sediments. *Limnology and Oceanography* **35**: 1545-1563.
- Killham, K. 1994. *Soil Ecology*. Cambridge University Press.
- Kim, D. J., D. I. Lee, and J. Keller. 2006. Effect of temperature and free ammonia on nitrification and nitrite accumulation in landfill leachate and analysis of its nitrifying bacterial community by FISH. *Bioresource Technology* **97**: 459-468.
- Koop, K., W. R. Boynton, F. Wulff, and R. Carman. 1990. Sediment-water oxygen and nutrient exchanges along a depth gradient in the Baltic sea. *Marine Ecology-Progress series* **63**: 65-77.
- Kopp, J. F., and G. D. Mckee. 1983. *Methods for Chemical Analysis of Water and Wastes*. United States Environmental Protection analysis Agency.
- Laima, M. J. C. 1992. Extraction and seasonal variation of NH<sub>4</sub><sup>+</sup> pools in different types of coastal marine sediments. *Marine Ecology-Progress Series* **82**: 75-84.

- Laima, M. J. C. and others 1999. Distribution of adsorbed ammonium pools in two intertidal sedimentary structures, Marennes-Oleron Bay, France. *Marine Ecology-Progress Series* **182**: 29-35.
- Mackin, J. E., and R. C. Aller. 1984. Ammonium adsorption in marine sediments. *Limnology and Oceanography* **29**: 250-257.
- Magalhaes, C. M., A. A. Bordalo, and W. J. Wiebe. 2002. Temporal and spatial patterns of intertidal sediment-water nutrient and oxygen fluxes in the Douro River estuary, Portugal. *Marine Ecology-progress Series* **233**: 55-71.
- Martens, C. S., and J. V. Klump. 1980. Biogeochemical cycling in an organic-rich coastal marine basin .1. methane sediment-water exchange processes. *Geochimica et Cosmochimica Acta* **44**: 471-490.
- Martin, W. R., and G. T. Banta. 1992. The measurement of sediment irrigation rates - a comparison of the br-tracer and  $^{222}\text{rn}/^{226}\text{ra}$  disequilibrium techniques. *Journal of Marine Research* **50**: 125-154.
- Morin, J., and J. W. Morse. 1999. Ammonium release from resuspended sediments in the Laguna Madre estuary. *Marine Chemistry* **65**: 97-110.
- Mulholland, M. 2008. Gaseous nitrogen compounds (NO, N<sub>2</sub>O, N<sub>2</sub>, NH<sub>3</sub>) in the ocean, p. 52-123. *In* D. Capone, M. Mulholland and E. Carpenter [eds.], *Nitrogen in the Marine Environment*. Elsevier.
- Nixon, S. W. and others 1996. The fate of nitrogen and phosphorus at the land sea margin of the North Atlantic Ocean. *Biogeochemistry* **35**: 141-180.
- Paerl, H. 2008. Nutrient and other environmental controls of harmful cyanobacterial blooms along the freshwater-marine continuum, p. 217-237. *In* K. Hudnell [ed.], *Cyanobacterial Harmful Algal Blooms: State of the Science and Research Needs*. Springer.
- Park, S., W. Bae, and B. E. Rittmann. 2010. Operational boundaries for nitrite accumulation in nitrification based on minimum/maximum substrate concentrations that include effects of oxygen limitation, pH, and free ammonia

and free nitrous acid inhibition. *Environmental Science & Technology* **44**: 335-342.

Parsons, T. R., Y. Maita, and C. M. Lalli. 1984. Fluorometric determination of chlorophylls, p. 107-108. *In* T. R. Parsons [ed.], *A Manual of Chemical and Biological Methods for Seawater Analysis*. Pergamon Press.

Price, G. D., M. R. Badger, F. J. Woodger, and B. M. Long. 2008. Advances in understanding the cyanobacterial CO<sub>2</sub>-concentrating-mechanism (CCM): functional components, Ci transporters, diversity, genetic regulation and prospects for engineering into plants. *Journal of Experimental Botany* **59**: 1441-1461.

Rao, A. M. F., and R. A. Jahnke. 2004. Quantifying porewater exchange across the sediment-water interface in the deep sea with in situ tracer studies. *Limnology and Oceanography-Methods* **2**: 75-90.

Rich, J. J., O. R. Dale, B. Song, and B. B. Ward. 2008. Anaerobic ammonium oxidation (anammox) in Chesapeake Bay sediments. *Microbial Ecology* **55**: 311-320.

Rosenfeld, J. K. 1979. Ammonium adsorption in nearshore anoxic sediments. *Limnology and Oceanography* **24**: 356-364.

Schulz, K. G., U. Riebesell, B. Rost, S. Thoms, and R. E. Zeebe. 2006. Determination of the rate constants for the carbon dioxide to bicarbonate inter-conversion in pH-buffered seawater systems. *Marine Chemistry* **100**: 53-65.

Seitzinger, S. 1987. The effect of pH on the release of phosphorus from Potmac River sediment, p. 1-46. Chesapeake Bay program.

Seitzinger, S. P. 1991. The effect of pH on the release of phosphorus from Potomac estuary sediments - implications for blue-green-algal blooms. *Estuarine Coastal and Shelf Science* **33**: 409-418.

Seitzinger, S. P., W. S. Gardner, and A. K. Spratt. 1991. The effect of salinity on ammonium sorption in aquatic sediments - implications for benthic nutrient recycling. *Estuaries* **14**: 167-174.



- Simek, M., L. Jisova, and D. W. Hopkins. 2002. What is the so-called optimum pH for denitrification in soil? *Soil Biology & Biochemistry* **34**: 1227-1234.
- Simon, N. S., and M. M. Kennedy. 1987. The distribution of nitrogen species and adsorption of ammonium in sediments from the tidal Potomac River and estuary. *Estuarine Coastal and Shelf Science* **25**: 11-26.
- Slomp, C. P., J. F. P. Malschaert, and W. Van Raaphorst. 1998. The role of adsorption in sediment-water exchange of phosphate in North Sea continental margin sediments. *Limnology and Oceanography* **43**: 832-846.
- Soetaert, K., A. F. Hofmann, J. J. Middelburg, F. J. R. Meysman, and J. Greenwood. 2007. The effect of biogeochemical processes on pH (Reprinted from *Marine Chemistry*, vol 105, pg 30-51, 2007). *Marine Chemistry* **106**: 380-401.
- Strauss, E. A., N. L. Mitchell, and G. A. Lamberti. 2002. Factors regulating nitrification in aquatic sediments: effects of organic carbon, nitrogen availability, and pH. *Canadian Journal of Fisheries and Aquatic Sciences* **59**: 554-563.
- Tango, P. J., and W. Butler. 2008. Cyanotoxins in tidal waters of Chesapeake Bay. *Northeastern Naturalist* **15**: 403-416.
- Tank, S. E., L. F. W. Lesack, and D. J. McQueen. 2009. Elevated pH regulates bacterial carbon cycling in lakes with high photosynthetic activity. *Ecology* **90**: 1910-1922.
- Van Hulle, S. W. H., E. I. P. Volcke, J. L. Teruel, B. Donckels, M. C. M. Van Loosdrecht, and P. A. Vanrolleghem. 2007. Influence of temperature and pH on the kinetics of the Sharon nitrification process. *Journal of Chemical Technology and Biotechnology* **82**: 471-480.
- Vouve, F., G. Guiraud, C. Marol, M. Girard, P. Richard, and M. J. C. Laima. 2000.  $\text{NH}_4^+$  turnover in intertidal sediments of Marennes-Oleron Bay (France): effect of sediment temperature. *Oceanologica Acta* **23**: 575-584.
- Wang, F. L., and A. K. Alva. 2000. Ammonium adsorption and desorption in sandy soils. *Soil Science Society of America Journal* **64**: 1669-1674.

- Weston, N. B., A. E. Giblin, G. T. Banta, C. S. Hopkinson, and J. Tucker. 2010. The effects of varying salinity on ammonium exchange in estuarine sediments of the Parker River, Massachusetts. *Estuaries and Coasts* **33**: 985-1003.
- Wood, P. 1988. Monooxygenase and free radical mechanisms for biological ammonia oxidation, p. 219–243. *In* J. Cole and S. Ferguson [eds.], *The Nitrogen and Sulphur Cycles*. Cambridge University Press.
- Xie, L. Q., and P. Xie. 2003. Enhancement of dissolved phosphorus release from sediment to lake water by *Microcystis* blooms - an enclosure experiment in a hyper-eutrophic, subtropical Chinese lake. *Environmental Pollution* **122**: 391-399.

## Tables

Table 2-1 Sediment grain sizes, ambient dissolved nutrients in water column and the flux rates before pH mediation, sampling at the Powerline in June 18, 2008 and Budds Landing in July 14, 2009. Grain size was calculated from the intact core; other measurements are average nutrient  $\pm$  SE (n= 3) and average flux rates  $\pm$  SE (n= 4- 9). Negative rates indicate uptake by the sediment.

Variables	Powerline	Budds landing
<b>Grain size (%)</b>		
sand	3.2	6.7
silt	59.9	58.8
clay	36.9	34.4
<b>Bottom water characterization</b>		
SRP ( $\mu\text{mol L}^{-1}$ )	$0.7 \pm 0.04$	$0.23 \pm 0.07$
$\text{NH}_4^+\text{-N}$ ( $\mu\text{mol L}^{-1}$ )	$2.1 \pm 0.05$	$0.6 \pm 0.1$
$\text{NO}_3^-\text{-N}$ ( $\mu\text{mol L}^{-1}$ )	$7.5 \pm 0.02$	$0.82 \pm 0.02$
Salinity	0.05	0.2
Temperature ( $^{\circ}\text{C}$ )	24.7	26.9
pH	9.4	7.3
DO ( $\text{mg L}^{-1}$ )	10.3	12.48
DO (%)	127.4	158.2
Chl <i>a</i> ( $\text{mg L}^{-1}$ )	78	46.5
<b>Core fluxes</b>		
$\text{NO}_3^-\text{-N}$ flux ( $\mu\text{mol N m}^{-2} \text{hr}^{-1}$ )	$-41 \pm 0.2$	$10 \pm 18$
$\text{NH}_4^+\text{-N}$ flux ( $\mu\text{mol N m}^{-2} \text{hr}^{-1}$ )	$62 \pm 8.5$	$310 \pm 32$
SRP flux ( $\mu\text{mol P m}^{-2} \text{hr}^{-1}$ )	$-0.2 \pm 1.2$	$5.0 \pm 3.7$
$\text{N}_2$ flux rate ( $\mu\text{mol N m}^{-2} \text{hr}^{-1}$ )	$259 \pm 38$	$176 \pm 21$
$\text{O}_2$ flux rate ( $\mu\text{mol O}_2 \text{m}^{-2} \text{hr}^{-1}$ )	$-1614 \pm 62$	$-2240 \pm 293$

Table 2-2 Experimental overlying water pH's for experimental incubations of cores from the Powerline (n= 4) and Budds Landing sites. The Powerline incubations had a sequential change of pH while the Budds Landing incubations had 3 replicate cores at 3 different pH's. For Budds Landing, n= 3 at each pH level except for the control on the first day when n = 9. pH data is the mean value ( $\pm$  SE).

		Powerline		Budds Landing	
Treatment	Time (day)	pH		Time (day)	pH
control	1 <sup>st</sup>	7.8 $\pm$ 0.01	7 <sup>th</sup>	1 <sup>st</sup> and	7.4 $\pm$ 0.3
pH1	6 <sup>th</sup>	9.2 $\pm$ 0.02		7 <sup>th</sup>	9.2 $\pm$ 0.05
pH2	11 <sup>th</sup>	9.6 $\pm$ 0.03		7 <sup>th</sup>	9.5 $\pm$ 0.2

Table 2-3 The kinetic parameters used in calculation of diffusion rates and in calculation of ammonium adsorption-desorption in Budds Landing sediments.

Parameter	Value	Comments	Ref.
pKb	9.25		
Temperature	27 <sup>o</sup> C		
For calculation of the molecular diffusive rates			Stumm and Morgan (1996)
water %	74%	10 cm	
$\rho$	2.50	$\text{g cm}^{-3}$	
$\phi$	0.88		
$\theta^2$	1.26		
D*-Br <sup>-</sup>	20.10		Li and Gregory (1974)
D*-PO <sub>4</sub> <sup>3-</sup>	5.77	The diffusion coefficient in free solution (D*: 10 <sup>-6</sup> cm <sup>2</sup> s <sup>-1</sup> )	
D*-NH <sub>4</sub> <sup>+</sup>	19.80		
D*-NH <sub>3</sub>	24.52		
D-KBr <sup>-</sup>	1.09		
D-SRP	0.30	The corrected diffusion coefficient (D: 10 <sup>-6</sup> cm s <sup>-1</sup> )	
D-NH <sub>4</sub> <sup>+</sup>	1.02		
D-NH <sub>3</sub>	1.29		
For adsorption coefficient of ammonium at top 2 cm sediment			
water %	89%	top 2 cm	
$\phi$	0.95	top 2 cm	
$\hat{C}_N$	1.5 ± 0.2	$\mu\text{mol g}^{-1}$ wet sediment	
C <sub>N</sub>	0.07	$\mu\text{mol mL}^{-1}$	
For ammonium desorption			
R	8.21 × 10 <sup>-5</sup>	atom m <sup>3</sup> mol <sup>-1</sup> K <sup>-1</sup>	
H <sub>-NH3</sub>	7.05 × 10 <sup>-2</sup>	mol atm <sup>-1</sup> m <sup>-3</sup>	Larsen et al. (2001)
H' <sub>s-NH3</sub>	1.72 × 10 <sup>-3</sup>	mol atm <sup>-1</sup> m <sup>-3</sup>	Capone et al.(2009)
I	1.47 × 10 <sup>-3</sup>		
$\gamma_{\text{NH3}}$	1.00		
$\gamma_{\text{NH4}^+}$	0.88		

Table 2-4 Efflux rates of SRP and  $\Sigma\text{NH}_x$  in control and in high pH treatments in sediment cores from Budds Landing. Net flux rates were compared to rates estimated from molecular diffusion of pore water.

pH levels	SRP flux rates ( $\mu\text{mol-P m}^2 \text{ h}^{-1}$ )		Ammonium flux rates ( $\mu\text{mol-N m}^2 \text{ h}^{-1}$ )			
	Diffusive rate	Flux rate	$\text{H}_4^+$	$\text{H}_3$	Diffusive rate $\text{NH}_4^+ + \text{NH}_3$	Flux rate $\Sigma\text{NH}_x$
control	4.6	$3 \pm 3.2$	49.5	0.2	$\frac{149.}{7}$	$61.7 \pm 8.5$
pH= 9.6	39.2	$43.5 \pm 7.4$	43.1	34.2	$\frac{477.}{3}$	$440.9 \pm 19.1$

## Figures

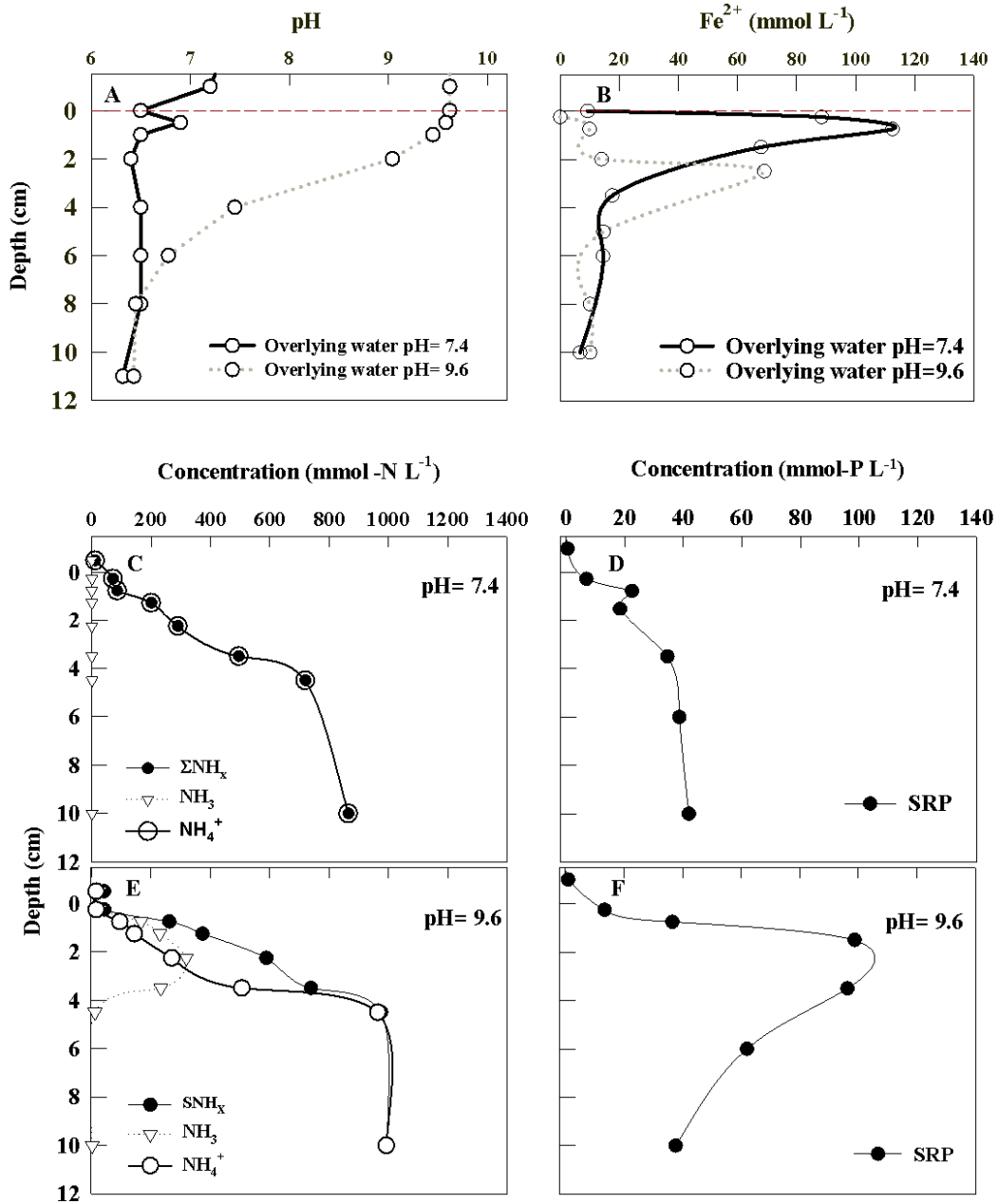


Figure 2-1 Budds Landing porewater profiles in the upper 10 cm of sediment under high pH (9.6) and normal pH (7.4) treatments, including vertical changes of pH (A), porewater Fe (B), SRP (D,F), and  $\Sigma NH_x$  (C,E). Changes in ammonium speciation, resulted from surface pH elevation, were calculated by the equilibrium of  $NH_3$  and  $NH_4^+$ .

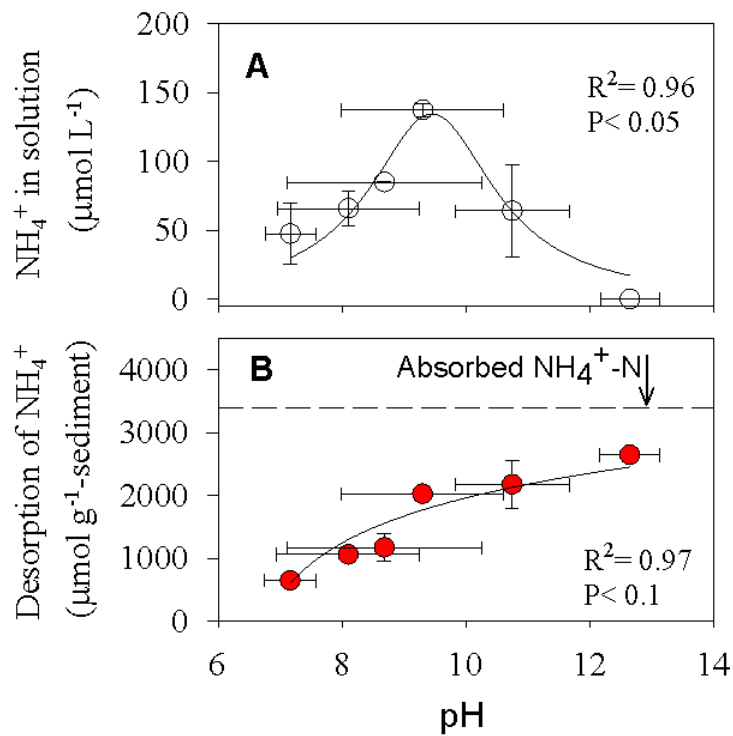


Figure 2-2 Experimental pH effects on  $\text{NH}_4^+$  concentration in solution (A) and desorption of exchangeable  $\text{NH}_4^+$  (B), using the 0-2 cm homogenized sediments from Budds Landing collected in November 2008. Dissolved  $\text{NH}_4^+$  concentration was estimated from the  $\Sigma\text{NH}_x$  concentrations and pH in the aquatic phase. Desorbed  $\text{NH}_4^+$  was the sum of  $\Sigma\text{NH}_x$  in water and the volatilized  $\text{NH}_3$  in the headspace of the sealed centrifuge tubes. The dashed line represents 'total' adsorbed  $\text{NH}_4^+$ , estimated by KCl extraction of pH-neutral sediment.



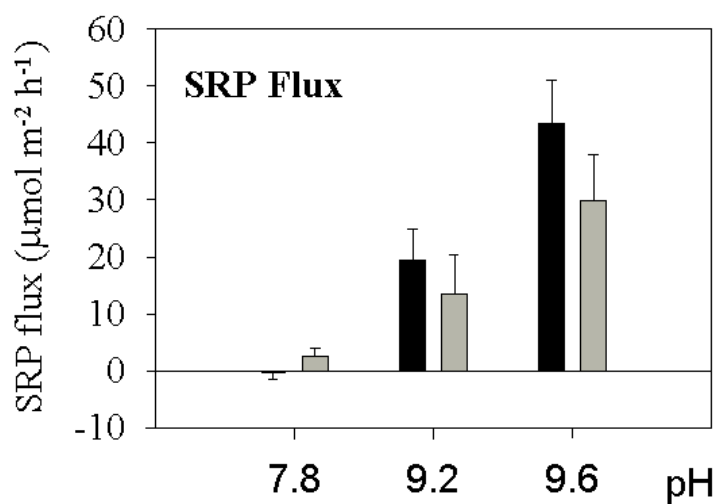


Figure 2-3 Experimental pH effects on SRP flux rates from sediments at Powerline (black bars) and Budds Landing (gray bars). Error bars are the standard deviation.

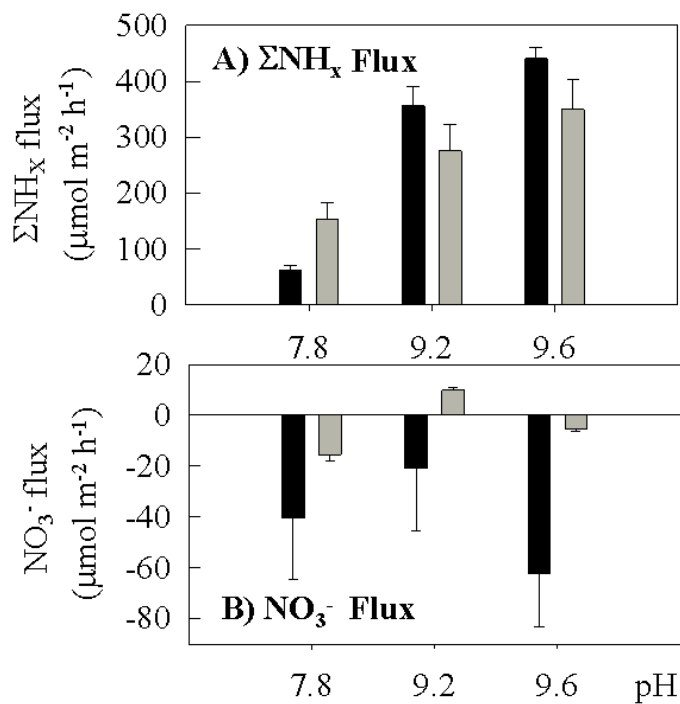


Figure 2-4 Experimental pH effects on flux rates of total ammonium and nitrate. Sediment cores were taken from Powerline (black bars) and Budds Landing (gray bars). Data are presented as the mean of flux rate ± standard deviation.

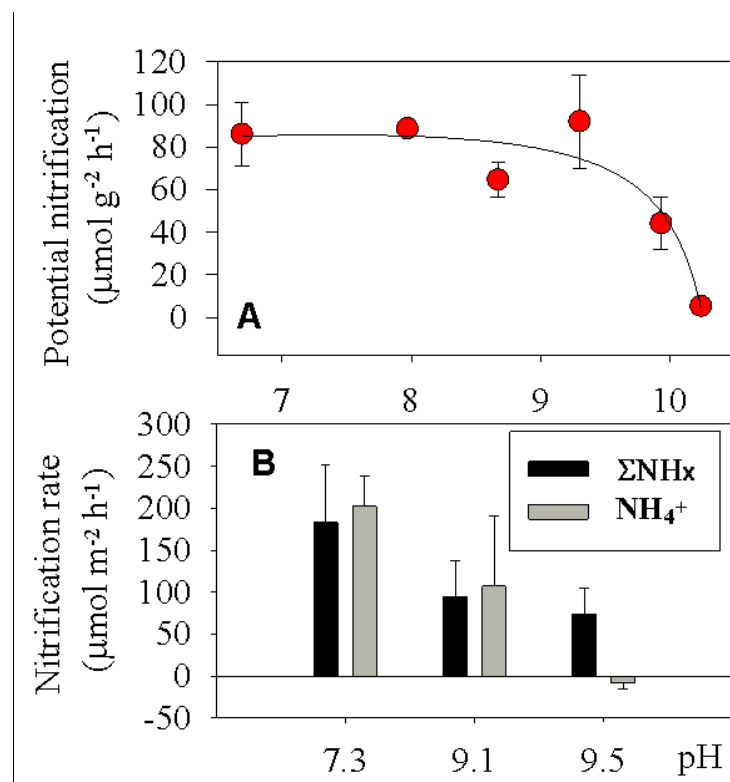


Figure 2-5 Experimental pH effects on potential nitrification (A) and intact core nitrification rates (B) from Budds Landing in July 2009. The potential nitrification rates (A) are calculated from nitrate production in  $\text{NH}_4^+$ -amended slurries from surficial sediments (0– 2 cm). Nitrification rates (B) are estimated by inhibition of nitrification using  $\text{CH}_3\text{F}$ . Bars show the average flux rates of  $\Sigma\text{NH}_x$  (black bars) and  $\text{NH}_4^+$  (gray bars) as well as the standard error for triplicate samples.

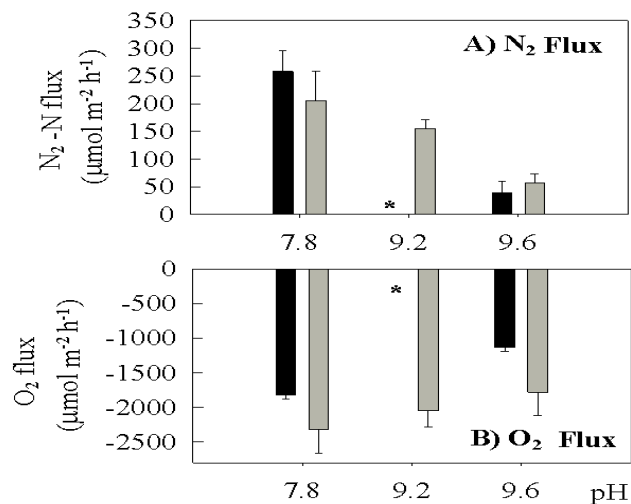


Figure 2-6 Experimental pH effects on denitrification rates (A) and oxygen consumption rates (B) of sediments from the Powerline (black bar) and Budds Landing (grey bar) sites. ‘\*’ indicates where measurements were not taken. Bars show the mean of triplicate cores, error bars are the standard error.

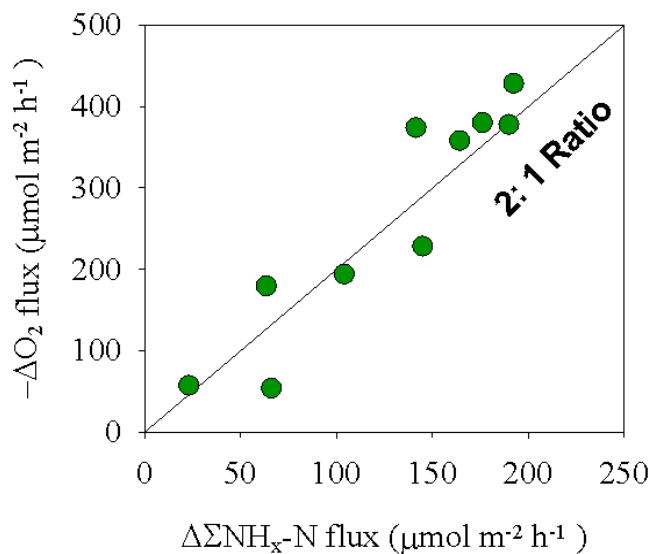


Figure 2-7 The relationship between the increased  $\Sigma \text{NH}_x$  fluxes and the reduced oxygen consumption rates after pH elevation. Data from Powerline are the changes of  $\Sigma \text{NH}_4^+$  and  $\text{O}_2$  flux rates in the same core after pH was elevated from 7.8 to 9.5. Data from Budds’ Landing are the changes of flux rates between control cores and cores at a pH of 9.2 and 9.5 after 6 days incubation. The slope (K) of solid line is 2:1, which is equal to the molar ratio of ammonium to oxygen for nitrification (Eq. 8).

## Chapter 3      Seasonal and spatial changes in sediment-water nutrient exchange: regulating factors in the overlying water

### **Abstract**

In the upper SassafRAS River, a tidal fresh and shallow tributary of the Chesapeake Bay, sediment cores were collected for nutrient flux measurements before, during and after cyanobacterial blooms and from locations within and downstream of the bloom region. Dense cyanobacterial bloom in summer 2010, but not in 2008 or 2009, resulted in elevated pH (9 – 10.5) and O<sub>2</sub> (10 – 24 mg L<sup>-1</sup>) persisting in the water column for weeks. Standard incubations were conducted in the dark for flux measurements of ammonium (NH<sub>4</sub><sup>+</sup>), nitrate (NO<sub>3</sub><sup>-</sup>), soluble reactive phosphate (SRP), denitrification (N<sub>2</sub>) and sediment oxygen demand (SOD). Flux rates of NH<sub>4</sub><sup>+</sup>, SRP and high SOD were positively associated with temperature increase from spring to summer. In the cyanobacterial bloom zone, spring sedimentation of phytoplankton debris added organic matter to sediments where it could be rapidly remineralized in summer. Because of pH-driven NH<sub>4</sub><sup>+</sup> conversion to NH<sub>3</sub> and desorption of exchangeable ammonium on the ratios of pore water: exchangeable NH<sub>4</sub><sup>+</sup> in sediments increased with bloom development from June to September in 2010. Release of NH<sub>4</sub><sup>+</sup> with pH elevation coupled with the persistent organic matter input from algae in the bloom area. High pH/DO penetration into sediments may inhibit nitrification-denitrification by enhancing the oxic layer thickness and perhaps also due to high NH<sub>3</sub> concentrations and high pH which

may suppress bacterial activity. Relative to non-bloom summers, high pH (> 9) resulted in an increase of 2 – 5 folds in SRP efflux, 19 – 30 % in  $\text{NH}_4^+$  efflux and a reduction of 28 - 41% in the loss of N as  $\text{N}_2$  in the bloom region. With approximately 62% of observations of DIN : SRP flux rates below the Redfield ratio during high pH (> 9) conditions, the released nutrients can increase water column N limitation in summer. To determine how light penetration to the bottom affects nutrient recycling, light-dark experiments were conducted with cores obtained during periods when irradiance at the sediment water interface was  $\sim 50 \mu\text{mol photons m}^{-2} \text{ s}^{-1}$ . Compared with light-incubations, flux rates of  $\text{NH}_4^+$  and SRP in the dark were higher by 17% -70% and by - 88%, respectively; oxygen consumption and denitrification rates were enhanced significantly due to sediment respiration in darkness. Water column turbidity and algal blooms in the upper Sassafras River reduce irradiance reaching the sediment surface and thus may promote DIN and SRP release from sediments into the water column. The positive feedbacks between cyanobacterial blooms and biogeochemical nutrient cycles, including pH-driven higher effluxes of  $\text{NH}_4^+$  and SRP, lower denitrification efficiency and decrease DIN: SRP flux ratios < 16, and may partially sustain  $\text{N}_2$  fixing cyanobacterial blooms in summer.

### **Introduction**

With the increased nutrient loads into the Chesapeake Bay region over the last century, deposition of particulate nutrients and organic debris has made sediments a large sink for phosphorus (P) and nitrogen (N) in the estuary (Boynton et al. 1995; Kemp et al.

2005). Higher nutrient burial rates are generally found in tidal freshwater and oligohaline environments relative to the lower parts of estuaries such as the Potomac River, Patuxent River and Maryland Mainstem Bay (Boynton et al. 1995). In the shallow and oligohaline regions of Chesapeake Bay tributaries, particulate P has a high accumulation rate in sediments due to the proximity to P inputs (Hartzell et al. 2010). Burial rates of N are 12-fold higher in the oligohaline region than that in the mesohaline region of the estuary (Okeefe 2007). Sediment nutrient release can strongly support primary production in the water column (Seitzinger 1987b; Sharp et al. 2009) and reinforce eutrophication (Gardner and McCarthy 2009). Therefore, it is critical to quantify nutrient fluxes at the sediment-water interface and to evaluate factors regulating nutrient regeneration.

The efficiency of P regeneration in the upper Chesapeake Bay is much lower than in the anoxic regions (Cornwell et al. 1996). In freshwater estuaries, sediments with an oxidized surface layer can effectively retain soluble P by re-adsorption/precipitation onto iron oxide minerals (Boers et al. 1998). In contrast, remobilization of P in anoxic sediments is rapid through reductive dissolution of Fe-oxides (Anschutz et al. 1998). For instance, sulfide-rich sediments in mid-Chesapeake Bay do not show increased P accumulation in recent (< 80 ) years, indicating P remobilization to counteract the accelerated P input from lands and atmosphere (Cornwell et al. 1996). Previous studies suggest high pH (> 9 – 9.2) can increase the solubility of Fe-bound P compounds and thus facilitate P release from sediments (Eckert et al. 1997). Photosynthesis during dense algal blooms causes the dramatic increases in pH, partly due to photosynthetic carbon removal in the low carbonate buffering in freshwater estuaries. Once high pH waters

comes in contact with the sediments, it may trigger release of sequestered P from sediments (Bailey et al. 2006).

Dissolved inorganic nitrogen (DIN, i.e.,  $\text{NH}_4^+$ ,  $\text{NO}_2^-$  and  $\text{NO}_3^-$ ) derived from sediments and released into the water column may partially support algal blooms in coastal ecosystems (Cowan and Boynton 1996; Fisher et al. 1988). Sediment  $\text{NH}_4^+$  recycling represents about 60-80% of plankton assimilative N demand in Chesapeake Bay tributaries (e.g. Patuxent River) (Kemp and Boynton 1984). In particular, sediment DIN supply is critical in estuaries when biologically available N demand is high during blooms and the ratio of DIN: SRP concentration is low in summer (Fisher et al. 1988; Paerl 2008). Moreover, in aerobic and freshwater systems a substantial proportion of remineralized ammonium ( $\text{NH}_4^+$ ) may be nitrified to  $\text{NO}_2^-$  and  $\text{NO}_3^-$  and then denitrified to  $\text{N}_2$ , representing a loss of N from the system (Seitzinger et al. 1991). Coupling between nitrification and denitrification, as the main pathway for  $\text{N}_2$  formation, results from nitrate transport across the oxic/anoxic boundary (Rysgaard et al. 1994). Nitrogen remineralization rates can be influenced by a variety of environmental parameters, including temperature, organic matter input, substrate availability, redox condition, the presence of inhibitors (e.g.,  $\text{H}_2\text{S}$ ,  $\text{S}^{2-}$ ), pH and salinity (An 2001; Mayer et al. 1990; Seitzinger et al. 1991).

Algal blooms are a symptom of chronic eutrophication (Kemp et al. 2005) and are responsible for alteration of biogeochemical cycles in shallow water estuaries. Accumulation of massive phytoplankton blooms at the water surface can reduce irradiance reaching the bottom, and thus decrease benthic photosynthesis, oxygen production and nutrient assimilation. Decomposition of phytoplanktonic debris can

increase benthic oxygen consumption and reduce the redox potential in surface  
Deposits of phytoplankton can also be grazed, supporting a benthic community that can cause bioturbation and bioirrigation of sediments (Magni and Montani 2006). In shallow water, increased pH and dissolved oxygen (DO) concentrations related to phytoplankton photosynthesis may influence chemical and redox conditions at the surface sediment. High pH can cause the formation of  $\text{NH}_3$ , which is toxic to most organisms in sediments, resulting in a reduction in macrofaunal metabolism and can even cause the death of macrofauna such as amphipods (Kater and Dubbeldam 2006). All these changes should directly or indirectly effect N and P recycling, but the responses of biogeochemical processes are expected to vary seasonally, spatially and with sediment properties.

Seasonal and spatial investigations of sediment flux rates of soluble reactive phosphate (SRP),  $\text{NH}_4^+$  and nitrate ( $\text{NO}_3^-$ ) and measurements of sediment oxygen demand (SOD), respiration ( $\text{CO}_2$ ), and denitrification ( $\text{N}_2$ ) were conducted in the tidal-freshwater region of the upper Sassafras River. Light-dark incubations were carried out to investigate the effects of episodic changes in bottom irradiance due to turbidity or algal blooms on sediment biogeochemical processes. Pore water nutrients, surface sediment exchangeable ammonium and other sediment properties were measured in cores from inside and outside the bloom area in summer 2010. Sediment nutrient recycling was evaluated before, during and after the bloom.



## Material and Methods

### 3.1.1 Study Sites

In the Sassafras River, six sites are categorized into three zones starting at the upper freshwater regions of the river and going downstream: Zone I (1A and 1B), Zone II (2A and 2B), and Zone (III) (3A and 3B) (Table 1 and Fig. 1). Biomass of algal blooms tended to decrease from upstream (Zone I) to downstream (Zone III). Zone I has often experienced cyanobacterial blooms in recent years, with higher biomass than in downstream stations (Sassafras River Association 2010). Zone II is the transitional region for bloom dispersion and nutrient transport between the tidal-fresh water and oligohaline waters. Summer blooms were either low in density or short lived in Zone III, which was close to a marina and the Galena *Wastewater Treatment Plant* (WWTP). Sampling sites in each zone were on both sides of main river channel, which were similar in overlying water depth and presence of blooms.

### 3.1.2 Sediment collection

Field investigations were conducted in the upper Sassafras River estuary during 2007, 2008, 2009 and 2010 (Table 1). We collected sediment cores for sediment flux measurements 3 times between winter 2007 and autumn 2008 and 6 times in 2009; at least one sampling were conducted in spring, summer, and winter during each period. In 2010, in which the highest biomass bloom occurred within our study, sampling was monthly from March to October (excluding April).

To qualify the nutrient release from sediment, we took intact 10- 15 cm sediment cores ( $> 2$ ) at each site using a pole corer, equipped with 7 cm diameter, 30 cm long

acrylic cylinders. *In situ* profiles of salinity, DO, pH, and water temperature were measured using a YSI XLM 600 sonde. Light attenuation coefficients were calculated from the vertical changes of irradiance measured by a Li Cor  $2\pi$  photosynthetically active radiation (PAR) sensor. Approximately 30 L of bottom water from each zone was pumped through an inline water filter (equivalent to 0.8  $\mu\text{M}$  filter) for use in the core incubations. The water was filtered to reduce nutrient assimilation and  $\text{N}_2$  fixation by algae. Samples were transported to Horn Point Laboratory within 4 hours after collection. Sediment cores were submersed in filtered water in a temperature-controlled environmental chamber.

### 3.1.3 Sediment incubation and flux measurement

We quantified nutrient fluxes of  $\text{NO}_3^-$ ,  $\text{NH}_4^+$ , SRP, sediment oxygen demand (SOD) and denitrification ( $\text{N}_2$ ), following methods of Kana *et al.* (2006). We routinely incubated the sediment cores in the dark at ambient water temperatures to simulate *in situ* conditions at the bottom of the river. Usually the irradiance at the bottom was very low due to turbidity from both algae and suspended inorganic particulates. After gently bubbling overnight on the day of collection, the cores were sealed with a gas tight stirring top. To deduct the rates of microbial processes in the water column (e.g., respiration, nutrient uptake,  $\text{N}_2$  fixation), the blank cores without sediment were incubated identically to sediments cores. Net flux measurements were generally conducted 4-6 times during the ~ 6 hours of incubations; ~ 24 hours incubation were performed at temperatures  $< 10^\circ$  C. Dissolved inorganic nutrients ( $\text{NO}_3^-$ ,  $\text{NH}_4^+$  and SRP) were collected with 20 ml syringes, filtered with 0.45  $\mu\text{m}$  cellulose acetate syringe filters, and frozen at  $\sim 20^\circ$  C until

analysis. When the measured pH was above 9, extra samples were preserved for total ammonium by adding 0.025 ml 1 M H<sub>2</sub>SO<sub>4</sub> to minimize NH<sub>3</sub> volatilization. HgCl<sub>2</sub> was immediately added in subsamples for dissolved gases (N<sub>2</sub> / O<sub>2</sub> and CO<sub>2</sub>) to a final concentration of 10 mg L<sup>-1</sup> as an inhibitor of microbial activity. The sample glass tubes were stopped with top sealer and stored under water at the incubation temperature; samples were analyzed within 3 days.

#### 3.1.4 Comparison of light and dark core incubation

Sediment cores from site 3A in September 2009 and from all stations in June 2010 were used for the light and dark incubations. Usually irradiance at the sediment surface was very low, but during these sampling times irradiance in the bottom waters reached around 50 μmol photons m<sup>-2</sup> s<sup>-1</sup>. After the flux measurements in the dark, surface sediment irradiances of ~ 100 μmol photons m<sup>-2</sup> s<sup>-1</sup> were maintained for sediment incubations. Subsamples were taken at 1-1.5 hour intervals, following same procedure as dark measurements. The incubation temperatures were 28 °C in September 2009 and 26 °C in June 2010, close to *in situ* bottom water temperatures.

#### 3.1.5 Solid phase and pore water processes

After the nutrient flux incubations, the overlying water from each core was siphoned off prior to sediment sectioning to avoid disturbance of the surface layer. Using a N<sub>2</sub>-filled glove bag to minimize oxidation effects (Bray et al. 1973), sediment cores were sectioned into 0-0.5 cm, 0.5-1 cm, 1-1.5 cm, 1.5-2 cm, 2-3 cm, 3-4 cm, 5-7 cm, and 9-11 cm segments. Pore water was separated from sediment by centrifuging at 2000 G for 10 min, and filtered through a 0.45 μm 25 mm diameter cellulose acetate syringe filter.

Subsamples for  $\text{SO}_4^{2-}$ , Fe,  $\text{PO}_4^{3-}$ ,  $\text{NH}_4^+$ , and  $\sum\text{NH}_x$  were appropriately diluted according to instrument detection limits. Total iron, primarily from dissolved  $\text{Fe}^{2+}$  in pore water, was acidified with 0.2 ml of HCl in 5 ml diluted samples. After they were dried at 60 °C, sediments were ground with a mortar and pestle and analyzed for total C, N and P

One core was occasionally used for sediment porosity and Chl *a* measurements. Surface wet sediments (1 ml) were collected for Chl *a* using a cut-off syringe barrel and stored at -20 °C in 15 ml centrifuge tubes wrapped in aluminum foil. Sediments for water content and solid phase analysis were placed in aluminum pans. Water content was calculated from the dry and wet weights of sediments after being dried at 60 °C. Organic content were determined by weight loss upon combustion (550 °C) in a muffle furnace. In addition, exchangeable  $\text{NH}_4^+$  samples were taken from sections of cores from stations 1B and 3A in summer of 2010. Wet sediments (0.5 ml) from each segment was added into centrifuge tubes, and extracted with KCl to measure adsorbed  $\text{NH}_4^+$  on sediment particles.

### 3.1.6 Sample analyses

Concentration of  $\text{NH}_4^+$  and SRP were analyzed by the phenol hypochlorite method (Parsons et al. 1984) and by the molybdate-ascorbic acid reduction method (Murphy and Riley 1962), respectively. Pore water Fe was analyzed colorimetrically (Gibb 1979).

Concentrations of  $\text{Cl}^-$ ,  $\text{SO}_4^{2-}$  and  $\text{NO}_3^-$  were determined with ion chromatography (US EPA 1983). Dissolved  $\text{N}_2$  and  $\text{O}_2$  concentrations were analyzed from  $\text{O}_2 : \text{Ar}$  and  $\text{N}_2 : \text{Ar}$  ratios using membrane inlet mass spectrometry (Kana et al. 1994). DIC samples were

acidified and analyzed using gas chromatography (Shimadzu GC-14) in 2009 (Stainton 1973) and a IR-based DIC analyzer in 2010 (Apollo SciTech, Inc. ModelAS-C3) in

### 3.1.7 Data Analysis

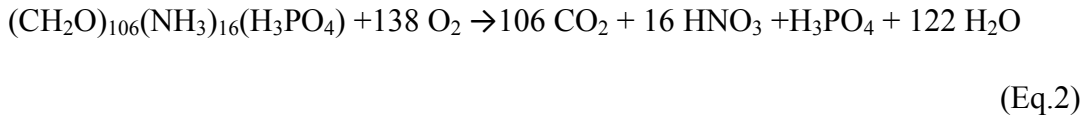
Net flux rates of nutrients, SOD, respiration and denitrification were calculated from the linear regression of changes in concentration with time for each sediment core, with slope adjusted for water column metabolism in control cores. Calculations were performed separately for dark and light incubations. Fluxes of  $N_2-N$  represented the net exchange of  $N_2-N$  at the sediment-water interface since no specific identification can be made among the reactions of denitrification, anammox, and  $N_2$  fixation (Kana et al. 1998; Kana and Weiss 2004).

All statistical analysis was performed using SAS (version 9.1, SAS Institute, Cary, NC). Significance for all of the reported data was determined at  $\alpha = 0.05$ . The Pearson correlation coefficient was calculated to determine the significance of nutrient-time relationships. Linear regression and stepwise multiple linear regression analyses were used to examine flux rates and environmental variables in the overlying water, presented as the linear regression coefficient ( $k$ ). The correlation of fluxes in fine-clay sediments with environmental factors were normalized and determined by multiple linear regression analysis. Station SR\_6 was excluded from this analysis because of coarse grain size. The effects of changes in pH on  $NH_4^+$  and  $N_2$  flux rates were analyzed using linear regressions of data from each station. Differences in the flux rates between high pH conditions and the relatively lower pH conditions in summer were compared by one-way ANOVA.

We examined flux data with respect to water temperature to determine the temperature coefficient ( $Q_{10}$ ), which is the factor by which the rate increases when the temperature is raised by 10 degrees.

$$Q_{10} = \left(\frac{F_2}{F_1}\right)^{\frac{10}{(T_2-T_1)}}; \text{ or } \ln Q_{10} = \frac{\ln(F_2) - \ln(F_1)}{(T_2-T_1)} \times 10 \quad (\text{Eq. 1})$$

Assuming nutrients are regenerated by respiration from a Redfield composition of sediment organic matter with the minimal influence of other decomposition processes, the stoichiometric analysis for N recycling was based on the relationship of oxygen consumption and nutrient release from algae in aerobic decomposition:



Here we assume that the sum of DIN flux rates (DIN=  $\text{NH}_4^+$ ,  $\text{NO}_3^-$ ,  $\text{N}_2\text{-N}$  flux) is equal to the remineralized N in this equation; the negative  $\text{NO}_3^-$  flux, which presents a possible contribution to denitrification from the overlying water rather than organic matter decomposition, is deducted from total DIN flux. The presumed ratio of 138  $\text{O}_2$  : 106  $\text{CO}_2$  : 16 DIN : 1 SRP flux was used to predict flux rates for regenerated nutrients in sediment.

Oxygen penetration depth is defined as the thickness of the oxic zone in sediments, which is regulated by organic matter decomposition and the transportation of bottom water oxygen into sediment (Cai and Sayles 1996). Although bioirrigation and bioturbation may affect this process, oxygen penetration depth (L) can be estimated from benthic oxygen flux ( $F_{\text{O}_2}$ ), and bottom water oxygen concentration ( $[\text{O}_2]_{\text{BW}}$ ) (Cai and Sayles 1996):

$$L = 2\Phi D_s [O_2]_{BW} / (F_{O_2}) \quad (\text{Eq. 3})$$

where  $\Phi$  is the porosity of 0.88;  $D_s$  is the diffusion coefficient of  $O_2$  in sediment.  $D_s$  is a temperature related coefficient ( $D_s = 0.0453 \times \text{Temp } (^{\circ}\text{C}) + 1.0043$ ) (Schulz and Zabel 2000), and corrected using  $Br^-$  diffusivity in the fine-grain sediment of the upper Sassafras River (Chapter 2). We assume SOD rates in the day were the same as in night due to light limitation in the bottom layer. Dissolved oxygen in the bottom water ( $[O_2]_{BW}$ ) and temperature either come from ambient DO measurements during sampling or from the continuous real time records at Budds Landing (in 2010, [www.eyesonthebay.com](http://www.eyesonthebay.com)).

## Results

### 3.1.8 General environment

The average depth of sampling stations in the upper Sassafras River ranged from 0.68 to 3.4 m, becoming deeper along the salinity gradient from Zone I to Zone III. According to the tidal records at Drawbridge, tidal range can be 0.3 m and even higher due to meteorologic changes. In this turbid water, the average light attenuation coefficient was  $4.5 \text{ m}^{-1}$ . During our sampling, 89% of the time bottom water irradiances were below  $15 \mu\text{mol photons m}^{-2} \text{ s}^{-1}$ .

Salinity, temperature and dissolved nutrients exhibited pronounced seasonal changes (Table 3). Temperature ranged from  $4.2 \pm 3.5 \text{ }^{\circ}\text{C}$  in winter to  $27.2 \pm 3.2 \text{ }^{\circ}\text{C}$  in summer. Salinity, increasing from the river head (Zone I) to further downstream (Zone III), was relatively lower in summer ( $< 1.5$ ) than in other seasons. Concentrations of  $\text{NO}_3^-$  the main fraction of DIN in Sassafras River inputs, substantially decreased from  $> 50$

$\mu\text{mol L}^{-1}$  in spring to  $< 1 \mu\text{mol L}^{-1}$  in summer; the average  $\text{NH}_4^+$  and SRP decreased from 8.4 to  $0.5 \mu\text{mol L}^{-1}$  and from 1.0 to  $0.3 \mu\text{mol L}^{-1}$  during summer blooms, respectively. Meanwhile, dissolved N: P ratios in the water column declined from spring to summer, resulting in nitrogen limitation in most cases during the summer. As bloom developed, dissolved nutrient concentrations ( $\text{NH}_4^+$ ,  $\text{NO}_3^-$  and SRP) decreased from spring to summer, which reflected on the negative relations between nutrient concentrations and water column changes, such as Chl *a*, DO and pH elevation (Table 4).

#### 3.1.9 Sediment characteristics

Our study region was covered with fine-grained clays except for sandy sediment at site 3B (Table 2). All of the fine-clay sediment cores had a distinctly oxidized surficial layer and no smell of  $\text{H}_2\text{S}$ . In 2011, the year with the biggest algal blooms, organic matter in fine sediments was 1.4 – 2.6 times higher for C and up to 2.7 times higher for N than at the sandy site (3B). The carbon content in the top 1 cm fine-grained sediments increased 20% to 47% from June to September. Meanwhile, the molecular ratio of C: N decreased from 9.3 – 17.2 to 8.6 – 13.3 in the bloom area (Zone I) and adjacent region (Zone II), respectively (Table 2).

#### 3.1.10 *In situ* pH and DO status

In the water column, pH varied from 6.4 to 10.2. Elevated pH ( $> 9$ ) was observed during spring 2010 and most of summer when the cyanobacterial blooms occurred (Table 3). Dissolved oxygen (DO) ranged from 4.7 to  $20.3 \text{ mg L}^{-1}$ , with a higher average of  $15.6 \text{ mg L}^{-1}$  during bloom conditions in the summer (Table 3). Dissolved oxygen concentrations were affected by oxygen release due to photosynthesis during summer



blooms and the higher solubility of oxygen at low temperature in winter (Table 4). In general, the temporal and spatial patterns of pH were more similar to the percent DO saturation rather than DO concentrations (Figure 2). pH and percent DO show a downstream decrease as cyanobacterial biomass decreased. Fewer blooms were found in 2008 and 2009 than in 2010. In 2009, high pH values (9-9.5) were only observed in a short period of time in early September within Zone I and II. In 2010, pH and DO rose dramatically to  $> 9.2$  and over 200%, respectively, during the short-period spring bloom in May and during the summer blooms from June to the early September. In Zone I especially, the daily average pH and DO% were maintained in the range of 9.2 to 10.2 and 200 – 300%, respective, for several weeks (eyesonthebay.com; Chapter 3). pH values were positively related to Chl *a* , DO % and O<sub>2</sub> in the overlying water (Table 3).

#### 3.1.11 Fluxes rates in the light-dark incubations

Sediments for light and dark treatments were incubated at field temperatures (25-27 °C) and pH (7.5 – 8.4) in September 2009 and June 2010. Benthic microalgae, as evaluated by Chl *a* concentration in the top 1 cm sediment, varied temporally (Fig. 3F). Sediment Chl *a* showed a gradual downstream decrease from  $\sim 210 \pm 28 \text{ mg m}^{-3}$  at 1B to  $17 \pm 6.9 \text{ mg m}^{-3}$  at the sandy site 3B.

In response to dark respiration and light photosynthesis in sediment, production of O<sub>2</sub> in the light decreased net oxygen consumption by 58~86% in Zone I and led to net O<sub>2</sub> evolution of up to  $1208 \mu\text{mol m}^{-2} \text{ h}^{-1}$  in Zone II and III (Fig 3E). The net increase of O<sub>2</sub> between light and dark incubations was positively related to sediment Chl *a* (Fig. 4).

Flux rates of dissolved inorganic nitrogen under light-dark incubations (Fig. 3 A-C) had negative rates, indicating uptake by sediments. DIN was primarily released as  $\text{NH}_4^+$  from sediment into the water column. Fluxes of  $\text{NO}_3^-$  were generally low, but with great variation; while  $\text{NO}_2^-$  flux was negligible at all stations.  $\text{NH}_4^+$  fluxes (Fig. 3A) varied from 46 to 174  $\mu\text{mol m}^{-2} \text{h}^{-1}$  in the dark and from -88 to 44  $\mu\text{mol N m}^{-2} \text{h}^{-1}$  in the light, with significantly higher effluxes in the dark than in the light ( $P < 0.05$ , Student's *t* test). Illumination turned 71% of net  $\text{NH}_4^+$  release into negative flux rates, indicating ammonium uptake with photosynthesis. Compared with the recycled N from organic matter decomposition at a ratio of 138  $\text{O}_2$  : 16 N (Fig. 5),  $\text{NH}_4^+$  fluxes in our study were close to the predicted N remineralization value.

Illumination resulted in a general increase of  $\text{NO}_3^-$  flux, enhanced on average by 24.3  $\mu\text{mol m}^{-2} \text{h}^{-1}$  at all stations (Table 5). Dark-incubated  $\text{NO}_3^-$  flux rates ranged from -120 to 16  $\mu\text{mol N m}^{-2} \text{h}^{-1}$ , with 71% of observations showing  $\text{NO}_3^-$  diffusion from the overlying water into sediments despite negative  $\text{NO}_3^-$  fluxes in some cases. There was general higher  $\text{NO}_3^-$  fluxes exhibited in the light than in the dark, which was consistent with oxygen production by sediment photosynthesis and potentially increase in nitrification (Fig. 3B).

SRP flux rates (Fig. 3C) varied from -10 to 12  $\mu\text{mol m}^{-2} \text{h}^{-1}$  in the dark and from -28 to 7  $\mu\text{mol m}^{-2} \text{h}^{-1}$  in the light, respectively. SRP flux rates significantly decreased from an average uptake of -0.2  $\mu\text{mol m}^{-2} \text{h}^{-1}$  in the dark to -7  $\mu\text{mol P m}^{-2} \text{h}^{-1}$  in the light at all stations ( $P < 0.01$ , Student's *t* test). For SRP flux, the light and dark incubated fluxes were close to or below the P remineralization calculated from SOD fluxes (Fig 5).

Denitrification rates were relatively lower in sandy sediments than fine-grained sediments, ranging from 150 to 320  $\mu\text{mol m}^{-2} \text{h}^{-1}$  (Fig. 3C). In muddy sites,  $\text{N}_2$  flux in the light decreased by 48 to 72% compared to dark rates. In sandy sediments, dark denitrification rates were low ( $< 100 \mu\text{mol N m}^{-2} \text{h}^{-1}$ ) and did not show significant decreases in the light. Denitrification efficiency (DE) was estimated from the fraction of  $\text{N}_2$  in the total DIN flux. Dark-incubated DE indicated 46 – 76% of the remineralized N was denitrified, while DE in the light treatments showed a greater variation of 34 – 92 %. The slope of  $\text{N}_2$  versus DIN flux (Fig. 6) indicated a slightly higher DE in the dark ( $K = 0.64$ ) than in the light incubations ( $K = 0.56$ ).

#### 3.1.12 Flux rates

Nutrient exchange at the sediment-water interface was measured in the dark because most of time PAR was low at the sediment surface due to light attenuation by phytoplankton and suspended particles. SRP flux rates were generally low with an average of  $0.3 \mu\text{mol m}^{-2} \text{h}^{-1}$  ( $n = 74$ ) and ranged from - 20 to  $43 \mu\text{mol m}^{-2} \text{h}^{-1}$  (Fig. 7). Multiple regression analysis (Table 7) suggested SRP flux rates were positively related to pH, temperature and Chl *a* ( $\text{SRP} = 5.2 \times \ln(\text{Temp}) + 5.3 \text{ pH} + 8.52 \ln(\text{Chl } a)$ ;  $P = 0.03$ ,  $n = 74$ ). Water temperature accounted for ~ 60% of the seasonal variation in SRP release. The estimated  $Q_{10}$  was 2.3 in the temperature range of 10 - 30 °C (Fig. 10A). In summer, SRP fluxes were below  $10 \mu\text{mol m}^{-2} \text{h}^{-1}$  at  $\text{pH} < 9$ , but dramatically rose to  $42 \mu\text{mol m}^{-2} \text{h}^{-1}$  when pH of the water was  $> 9$  (Fig. 10A).

Flux rates of  $\text{NH}_4^+$  changed with sediment properties and temperature.

Ammonium flux in the fine-grained sediments ranged from an uptake of  $-42 \mu\text{mol N m}^{-2}$

$\text{h}^{-1}$  to an efflux of  $720 \mu\text{mol N m}^{-2} \text{h}^{-1}$  (Fig 7); while  $\text{NH}_4^+$  flux rates in sand were less than  $200 \mu\text{mol N m}^{-2} \text{h}^{-1}$  (Fig. 7A and 9). Sediment types, changing from fine-grained sediment to sand, caused significant reduction in  $\text{NH}_4^+$  release ( $p < 0.001$ , t-student). Moreover, the  $\text{NH}_4^+$  flux rates increased from winter-spring to summer, with maximum release in August and September (Fig. 8). A positive relationship existed between  $\text{NH}_4^+$  flux rates and temperature ( $Q_{10} = 1.6$ ,  $P < 0.05$ ,  $n = 173$ , Fig. 10). Fine-clay sediments showed a higher  $Q_{10}$  value of 1.59 than in sandy sediments ( $Q_{10} = 0.92$ ).

The pH effects on the variation of  $\text{NH}_4^+$  fluxes differed in spring and in summer. Although high pH ( $> 9$ ) was observed during spring blooms in 2010, no significant enhancement of  $\text{NH}_4^+$  flux rates happened in the bloom zone (zone I) in 2010 relative to the measurements in non-bloom years. However, the release of  $\text{NH}_4^+$  in summer was temporally and spatially related to the bloom-driven changes in pH and organic matter deposition. The  $\text{NH}_4^+$  fluxes in summer generally declined from Zone I to Zone III, partly correlated to the decreasing cyanobacterial biomass in the water and Chl *a* concentrations in sediments. Compared with the pH changes in the overlying water in the summer bloom season,  $\text{NH}_4^+$  fluxes tended to have a positive response to pH elevation within or close to the bloom zone (Fig. 11), in which high pH had lasted for weeks. In the linear regression of pH and  $\text{NH}_4^+$  flux rates of sediments from 6 locations, the positive linear coefficients were 144.2 in 1A ( $R^2 = 0.65$ ,  $P < 0.05$ ,  $n = 6$ ), 345.2 in 1B ( $R^2 = 0.68$ ,  $P < 0.01$ ,  $n = 5$ ); 100.7 in 1C ( $R^2 = 0.65$ ,  $P < 0.05$ ,  $n = 5$ ), but no significant pH influence existed outside the bloom region (Fig.11).

Nitrate flux rates varied greatly, ranging from an uptake of  $-328 \mu\text{mol N m}^{-2} \text{h}^{-1}$  to a release of  $212 \mu\text{mol N m}^{-2} \text{h}^{-1}$  (Fig. 7).  $\text{NO}_2^-$  fluxes were undetectable in this aerobic

ecosystem. In the seasonal pattern,  $\text{NO}_3^-$  flux into sediments occurred in early spring with high  $\text{NO}_3^-$  concentrations in the overlying water, and became close to zero or positive in summer (Fig. 8).

### 3.1.13 Nitrification efficiency

We used the measured rates of coupled nitrification-denitrification ( $\text{N}_2$  loss) and the  $\text{NO}_3^-$  fluxes to determine the rates of nitrification. To examine nitrification response to pH and DO changes, we used  $\text{NO}_3^-$  release into water and denitrification as an indication of  $\text{N}_2$ -N flux minus  $\text{NO}_3^-$  flux into sediment. Nitrification efficiency was estimated as the sum of  $\text{N}_2$  flux and  $\text{NO}_3^-$  flux and then divided by the  $\text{CO}_2$  based N remineralization rates.

To elucidate bloom effects on nitrification, we used nitrification efficiency under low  $\text{NO}_3^-$  concentrations ( $< 20 \mu\text{mol L}^{-1}$ ) in the overlying water to minimize the substrate influence from the water rather than sediment N ammonification. When pH values were less than 8.5 in the bottom water, a weak positive relationship existed between nitrification efficiency and the estimated oxic layer depth (0 - 3mm) (Fig. 20); however, photosynthesis of cyanobacterial blooms can lead to simultaneous oxygen and pH increases. Thus, alkaline pH penetration into the thin oxic layer may have co-occurred with the increased oxic layer thickness. Even though the depth of the aerobic zone increased in sediments, nitrification efficiency linearly declined with the increased oxic zone under bottom water pH ( $> 9$ ), an pattern opposite of that observed during non-bloom periods (Fig. 20).

#### 3.1.14 Denitrification rates

Denitrification rates were generally 2~3 times higher in fine-grained sediments than sandy sediments (Fig. 7). Net N<sub>2</sub>-N flux rates in the fine sediment sites showed a clear seasonal pattern, with low rates ( $< 100 \mu\text{mol m}^{-2} \text{h}^{-1}$ ) in winter and rate up to  $370 \mu\text{mol m}^{-2} \text{h}^{-1}$  in early summer; rates tended to be depressed in the bloom season from summer to autumn (Fig. 9). In summer, denitrification rates (Fig. 15) and DE (Fig. 16) were negatively related to pH elevation in the bloom area and transition zone ( $P < 0.05$ ). Coupled nitrification and denitrification may have been inhibited by the deepened oxic zone (Fig. 21).

#### 3.1.15 Sediment oxygen consumption rates

Both SOD and net CO<sub>2</sub> flux rates (Fig. 8) showed similar seasonal patterns, with maximum SOD during the summer and minimum rates during the cold season. In the fine-grained sediments, oxygen uptake rates ranged from  $300 \mu\text{mol m}^{-2} \text{h}^{-1}$  at  $5^\circ\text{C}$  to  $2,000\text{-}2,960 \mu\text{mol m}^{-2} \text{h}^{-1}$  at  $\sim 30^\circ\text{C}$  in summer. Net CO<sub>2</sub> flux rates varied from 456 to  $4900 \mu\text{mol m}^{-2} \text{h}^{-1}$ , being highest in summer. At the sandy sites (3B), we observed low SOD and CO<sub>2</sub> production of less than 1000 and  $1700 \mu\text{mol m}^{-2} \text{h}^{-1}$ , respectively (Fig. 5). Temperature was positively related to SOD ( $Q_{10} = 1.3$ ) and CO<sub>2</sub> fluxes ( $Q_{10} = 1.5$ ) at 15-32 °C. Assuming CO<sub>2</sub> and O<sub>2</sub> were regenerated by respiration from a Redfield composition of algal matter source, the linear coefficient of CO<sub>2</sub> fluxes versus SOD was 1.24, which exceeded the predicted ratio of 106 CO<sub>2</sub> to 138 SOD (Fig.15).

### 3.1.16 Vertical profiles of SRP, Fe<sup>2+</sup>, Cl<sup>-</sup>, SO<sub>4</sub><sup>2-</sup> and NO<sub>3</sub><sup>-</sup> concentrations in sediments

Pore water SRP concentrations increased with depth in sediments to generate an upward flux at both stations 1B and 3B (Fig.14A). The time series of pore water profiles showed that the slope of SRP concentrations with depth increased from May to August, with larger gradients in sediments within blooms (1B) than outside of the blooms (3B).

Pore water Fe<sup>2+</sup> profiles (Fig.14B) exhibited a peak of 100 - 184 μmol L<sup>-1</sup> at the surface and declined in the deeper anaerobic sediments. The upward diffusion of Fe<sup>2+</sup> along the pore water gradient and the sharp decrease of Fe<sup>2+</sup> at the surface indicated the precipitation of Fe oxides when passing through the aerobic layer in sediments (Fig. 14). In addition, the time changes in concentration gradient and peak of Fe<sup>2+</sup> showed a reverse pattern with SRP: a decrease of Fe<sup>2+</sup> from May to August at 1B, corresponding with iron oxidation and precipitation with the increase of DO and pH in the overlying water. Meanwhile, pore water gradients of Fe<sup>2+</sup> were enhanced under non-bloom conditions.

Pore water SO<sub>4</sub><sup>2-</sup> in the sediment surface of the upper river was 500 – 1000 μmol L<sup>-1</sup>, lower than at the more saline downstream site (3A). The vertical profile of SO<sub>4</sub><sup>2-</sup> showed a rapid decrease across the oxic layer to a low and constant level in deeper sediments. Using Cl<sup>-</sup> penetration into sediment to minimize the effects of changes salinity, the SO<sub>4</sub><sup>2-</sup>/ Cl<sup>-</sup> gradient varied little in sediments at both stations.

Pore water profiles of NO<sub>3</sub><sup>-</sup> in spring showed a response to NO<sub>3</sub><sup>-</sup> concentrations in the overlying water with a penetration gradient from surface sediment at 10 – 30 μmol L<sup>-1</sup> to zero (Fig. 12 F). In summer, pore water NO<sub>3</sub><sup>-</sup> and NO<sub>2</sub><sup>-</sup>, as intermediate products of nitrification at oxic layer, did not accumulate in sediments at 1B and 3B and corresponded to negligible molecular diffusive mobility of NO<sub>3</sub><sup>-</sup>.

### 3.1.17 Pools of pore water and exchangeable $\text{NH}_4^+$

The vertical profiles of pore water  $\text{NH}_4^+$  indicated higher diffusion rates during blooms (1B, August), compared with the non-bloom times in 1B (May and October) and profiles out of the bloom region (3B) (Fig. 14). In order to estimate bloom effects on N regeneration, pore water and exchangeable  $\text{NH}_4^+$  were compiled (Table 5). The exchangeable  $\text{NH}_4^+$  of sediments in the bloom zone was higher than in the sediments out of blooms. Pore water and exchangeable  $\text{NH}_4^+$  were considered as supply in the N balance between flux and nitrification-denitrification (both calculated per sediment volume using sediment porosity and density). The percent of exchangeable pool increased by 25% in the bloom zone from May to June, and decreased from 78% to 52% with pH elevation due to massive blooms. This absence is consistent with experimental cores (Chapter 2). The ratios between pore water and exchangeable  $\text{NH}_4^+$  were almost constant in sediments outside of the bloom area (Fig. 13).

## **Discussion**

### 3.1.18 Total carbon and total nitrogen in sediments

Sediment TC and TN contents increased from spring to autumn and changed with bloom distribution in summer. Sediment TC : TN ratios in fine-grained stations were intermediate between molar elemental composition of phytoplankton (6.62) and terrestrial organic matter (e. g., 17-27 after litter decomposition in sediments) (Baldock et al. 2004), which suggests the organic matter sources included phytoplankton deposition and terrestrial runoff. Sediment TC: TN ratios decreased from spring and



became closer to the Redfield ratio in Zone I (1A and 1B), where cyanobacterial blooms lasted for the whole summer in 2010. Due to low river flow and low terrestrial inputs in summer, sediments within the bloom region might have more opportunity to receive sedimented phytoplanktonic matter (Table 2). Relatively higher sediment C: N ratios further downstream were consistent with the potential influence of bloom distribution and a sewage treatment plant in the lower estuary.

In shallow estuaries, high rates organic matter decomposition and the associated nutrient regeneration can influence nutrient concentrations and support primary production in the water column. The seasonal decrease in C: N from spring to autumn also suggested more efficient benthic recycling of N compared to C, similar to the trends in the main channel of Chesapeake Bay and other coastal environments (Boynton et al. 1985).

#### 3.1.19 Nutrient status in water column

In winter/spring DIN and SRP are higher than other seasons due to freshwater runoff and low nutrient consumption in the water during this period. With lowest dissolved nutrient concentrations in summer, the upper Sassafras River appeared to be N limited during over 60% of observations, based on the Redfield N: P ratio. Nutrient release from sediments may be important in mediating nutrient supply for phytoplankton production during cyanobacterial blooms. In the oxygen-saturated water, low  $\text{SO}_4^{2-}$  and small variations in salinity are not likely to have accounted for the N and P recycling (e.g. inhibition of nitrification by sulfide; sulfate reduction and salinity related P desorption). pH elevation was usually associated with increased particulate organic matter content in

the water (Fig. 11), which can be sedimented and rapidly remineralized during the warm season.

### 3.1.20 Light regulation on nutrient exchange

If relatively high light irradiances reach the bottom, microphytobenthos (MPB) can limit nutrient fluxes from the sediment to the water column by assimilating nutrients, changing pH and oxygen concentrations by photosynthesis, and consequently influence biogeochemical cycles at the sediment-water interface (Risgaard-Petersen 2003; Risgaard et al. 1995). The light incubations conducted in September 2010 and June 2009 indicated that MPB in the surface layer could greatly reduce N and P release rates due to their own nutrient demand (Newell et al. 2002). Illumination can increase nutrient assimilation of benthic microalgae, which can reduce sediment nutrients which would otherwise be available for the water column and pelagic communities (Krausejensen et al. 1996; Sundback and Miles 2000). The light treatments can reduce  $\text{NH}_4^+$  and SRP flux out of the sediments or, in some cases, reverse the direction of flux by taking up nutrients from the water column (Fig. 3).

Benthic microalgae also can change redox conditions through photosynthesis and in the dark by respiration, with SOD consistently higher in the dark than in the light (Fig. 3). Moreover, oxygen production in the light was positively related to sediment chlorophyll *a* (Fig. 4). Oxygen production at the surface sediment may broaden the oxic zone, which would favor nitrification as well as the release of  $\text{NO}_3^-$  (An 2001). With relatively higher Chl *a* in the sediments within or close to the bloom zone than that observed at downstream stations, the slight increase of  $\text{NO}_3^-$  in the light was consistent

with previous studies that showed light incubations increased nitrification in sediments (Rysgaard et al. 1994). In spite of the increased  $\text{NO}_3^-$  fluxes in the light, the negative  $\text{NO}_3^-$  fluxes in some cases may have resulted from increased  $\text{NO}_3^-$  assimilation by microalgae in the light; this also may be related to tightly coupled nitrification-denitrification, quickly reducing the produced  $\text{NO}_3^-$  in the aerobic layer.

Consistent with previous observations (Rysgaard et al. 1994; Seitzinger 1988; Tomaszek and Czerwieniec 2003), dark  $\text{N}_2$  flux rates and denitrification efficiency in fine-grained sediments were generally higher than that in the light (Fig. 3 and Fig. 6). Although sediment photosynthesis in the light may increase nitrification, however the expansion of the oxic zone may have inhibited anaerobic denitrification (Henriksen et al. 1981).

### 3.1.21 Ecological implications of Light/dark experiment

Sassafras River has experienced cyanobacterial blooms and seagrass loss within the past decades (Sassafras River Action Plan 2010). The observations from this study of low bottom water irradiance ( $< 15 \mu\text{mol photons m}^{-2} \text{s}^{-1}$ ) were generally coincident with the Secchi depth measurement  $\sim 0.2$  m reported in monthly investigations during 1985-2010 (Maryland DNR). Irradiance is a limiting factor for microphytobenthic biomass and their photosynthetic activities. Especially in summer, the high biomass and buoyancy of cyanobacteria during blooms creates dim to dark conditions in the bottom water and at the sediment surface; this can result in a decreased nutrient uptake by benthic microalgae, cause dark respiration and favor anaerobic denitrification. In the dark incubations, the average  $\text{NH}_4^+$  release from sediments into the overlying water was 70% higher in the

fine-grained sediments and 17% higher in sand compared to incubations in the light. Flux rates of SRP in the dark incubations increased by 60% to 88% compared to the light (Table 3). Compared with oxygen-based nutrient remineralization, only part of the remineralized N is released as  $\text{NH}_4^+$  (Fig. 5A) in the dark (Fig. 5A). This result is consistent with the observed high denitrification rates in the dark. Although in oxygen saturated water, SRP may be adsorbed onto iron rich mineral surfaces, the dark SRP flux rates (Fig. 3) and predicted SRP release (Fig. 5B) exceeded the P release in the light. Therefore, the dark bottom water may be one of factors that facilitate N release into the water.

### 3.1.22 Comparison of dark-incubated flux rates with previous measurements

Considering the low irradiance status at the bottom of the Sassafras River, dark-incubated flux rates may reflect the average *in situ* conditions. Dissolved inorganic nutrient release ( $\text{NH}_4^+$ ,  $\text{NO}_3^-$  and SRP) from sediments were comparable to those measured in the tidal-fresh zone of Chesapeake Bay (Table 6). In summer, a decreasing pattern of  $\text{NH}_4^+$  and SRP flux (Fig. 7) from Zone I to III in the upper Sassafras River are in agreement with the much lower flux observation in the lower estuary (Table 6), which suggest a general decrease in  $\text{NH}_4^+$  fluxes from river head to further downstream. The seasonal pattern of nutrient release and SOD in the upper Sassafras River (Fig. 7) was consistent with data from the upper Chesapeake Bay (Boynton 1996; Kemp et al. 1990; Mayer et al. 1990). Denitrification rates ( $12 \sim 370 \mu\text{mol N m}^{-2} \text{h}^{-1}$ ) in the upper river (Zone I) were somewhat higher than those observed in sediments in most tidal-fresh areas

of Chesapeake Bay (Table 6), but were in the range of the observations ( $0 - 345 \mu\text{mol N m}^{-2} \text{h}^{-1}$ ) in freshwater streams (Seitzinger 1988).

### 3.1.23 Temperature effect on N and P exchange at the sediment-water interface

Increased water temperature is usually associated with increased microbial activity, which can lead to rapid remineralization of nutrients, accelerate  $\text{NH}_4^+$  and SRP release and respiration in sediments. Significantly increased remineralization rates of N were found in Chesapeake Bay when the water temperature was higher than  $10^\circ\text{C}$  (Cowan and Boynton 1996).

Flux rates in this study were positively related to temperature.  $Q_{10}$  values of SRP flux (Fig. 10) were close to the estimated  $Q_{10}$  of 3.0 in the Potomac River (Bailey et al. 2006) and 1.9 in a eutrophic lake (Liikanen et al. 2002). The responses of  $\text{NH}_4^+$  flux and SOD to temperature were similar to Bailey's estimation of  $\text{NH}_4^+$  flux ( $Q_{10} = 2.9$ ) and SOD ( $Q_{10} = 1.8$ ) in the Potomac River (2006).

Coincident with high  $\text{NO}_3^-$  availability in the overlying water during spring to early summer, denitrification rates were positively enhanced by increased temperature. The  $Q_{10}$  for  $\text{N}_2$  flux was 2.4 at temperatures below  $22^\circ\text{C}$  based on a linear relationship between temperature and  $\text{N}_2$  flux ( $P < 0.05$ ,  $R^2 = 0.42$ ). No significant relationship between  $\text{N}_2$  flux and temperature was found during summer - autumn at temperatures of  $22-31^\circ\text{C}$ . Hence, changes in nitrification efficiency, overlying water  $\text{NO}_3^-$  concentration and oxygen concentration, taking place as temperature enhancement, made it difficult to isolate the effect of temperature on the denitrification (Seitzinger 1988).

### 3.1.24 Bloom effects on SRP fluxes

During cyanobacterial blooms in the upper river, high pH can be maintained over weeks during dense blooms, which is attributable to photosynthetic carbon uptake and low carbonate buffering in fresh water estuaries. In particular, when high pH is associated with settlement of detritus (POC and PON) from dense blooms (Fig. 11), increased SRP fluxes were found when the overlying water pH exceeded 9 (Fig. 12).

Pore water profiles showed increased SRP concentrations and a sharper SRP gradient with bloom development, which is consistent with the observed pH-driven flux rates. Relative to sediments sampled at sites outside of bloom area, the concentration gradients of SRP in pore water in the bloom area were significantly higher in August when the water column pH was 9 – 10.3 due to cyanobacterial blooms (Fig. 2 and 12). Iron-bound P is the largest fraction of particulate phosphorus in Chesapeake Bay sediments and accounts for 20% – 50% of the pool of total inorganic P in sediments (Hartzell et al. 2010). High pH (> 9 – 9.2) facilitates P desorption from sediments and accelerated SRP molecular diffusion (Seitzinger 1991; Wang and Alva 2000).

The magnitude and duration of blooms may be a key for pH persistence, which is critical in controlling the penetration depth and duration of high pH, and consequently the amount of P desorption and efflux. In generally, pH effect may be restricted to the surface layer due to high pH buffering capacity of sediments. As a consequence of increasing cyanobacterial abundance in the overlying water, pH increased dramatically and showed diel changes of increases with high carbon consumption in daytime and decreases with CO<sub>2</sub> production in night. So penetration of high pHs were progressive into sediment with a diel fluctuation. However, phosphorus desorption can initially have a fast

reaction time (2 – 4 h), followed by a slow release that continues up to 20 h (Cabrera et al. 1981). The closer to the surficial sediment layer, the more labile P may have been removed by the rapid desorption with high pH movement in sediment. Meanwhile, high pH in the water column is likely to extract P from suspended particulate P before sedimentation. Thus, the inventory of labile P in sediments during blooms may not be as high as in sediment cores sampled during a non-bloom year.

These data showed that field SRP fluxes during bloom events are lower than the flux measurement in experimental pH manipulations (Chapter 2), suggesting P depletion by high pH. The maximum SRP flux rates during high pH events in 2009 and 2010 were  $23 \pm 4$  and  $42 \pm 5 \mu\text{mol m}^{-2} \text{h}^{-1}$ , respectively, in Zone I (Fig. 8), which is 20% ~ 40% of the estimated SRP flux using sediments from same location sampled pre-summer blooms for high pH (~ 9.5) incubations in 2008 and 2009 (Chapter 2). In the tidal fresh zone of the Potomac River, a similar mismatch was found between the  $20 \mu\text{mol m}^{-2} \text{h}^{-1}$  *in situ* measurement during a *Microcystis* bloom (Bailey et al. 2006) and the  $> 100 \mu\text{mol m}^{-2} \text{h}^{-1}$  SRP flux measured in a high pH flux stimulation experiment (Seitzinger 1991).

In spring there was no significant difference in SRP fluxes between sediment cores collected in May 2010 (bloom year) and during the same period in 2008-2009 (when there wasn't a pronounced spring bloom) (Fig. 7). The influence of short-term pH (> 9) elevation in the water column on sediments may be limited and not strong enough to maximize the P desorption.

### 3.1.25 Organic matter effects on seasonal and spatial changes in $\text{NH}_4^+$ flux

In spring, nutrient effluxes are likely limited by the amount of labile organic matter available for remineralization and the temperature dependence of decomposition rates of phytoplanktonic debris. Those combined effects may result in low flux rates of  $\text{NH}_4^+$  (Fig. 7). Similar to SRP flux, high pH ( $> 9$ ) in the spring bloom did not significantly enhance  $\text{NH}_4^+$  release in 2010 (Fig. 2 and 7).

However, sediments may act as a reservoir for spring phytodetritus to fuel summer N fluxes. By comparing the total Chl *a* in surface sediment (an indicator of organic matter availability during day 80 to 220 in the year) and the average warm season flux rates of  $\text{NH}_4^+$  and SRP (day 120 and 220), the estimated time lag was about one month between the deposition of organic matter into sediment and the large increases of  $\text{NH}_4^+$  and SRP fluxes (Cowan and Boynton 1996; Cowan et al. 1996). In spring, low water temperatures may hinder the response time of OM decomposition (Boynton et al. 2008). The warmer the temperature, the higher the bacterial activity which may accelerate the remineralization of stored organic matter. This may explain the coherence between phytoplankton blooms in spring and increased nutrient release from sediments in summer (Rauch and Denis 2008).

The quantity and quality of organic matter may be responsible for the temporal and spatial distribution of  $\text{NH}_4^+$  fluxes in summer, with decreasing rates along the salinity gradient of 0 to 2 (Fig. 7A). With bloom development during the warm summer, settlement of PON and POC from the water column into sediments may coincidentally increase with water column pH elevation in the river head (Fig. 11). Enhanced  $\text{NH}_4^+$  flux is expected with organic matter remineralization and pH elevation in the bloom area



(Zone I) (Fig. 13). Even though part of the cyanobacteria detritus may be advected downstream, land runoff from agricultural land and sewage plant discharge in the downstream area may continue to provide organic inputs, which may be responsible for the decreased  $\text{NH}_4^+$  flux out of bloom region (Zone III).

Similar to the seasonal pattern observed by Smith and Kemp (2001),  $\text{NH}_4^+$  fluxes decline in the early fall despite temperature remaining high. Boynton (1986) explained the reduction in  $\text{NH}_4^+$  release from Chesapeake Bay sediments after mid-summer by the exhaustion of organic matter available for remineralization.

#### 3.1.26 pH effects on $\text{NH}_4^+$ flux

Highly significant positive relationships (Fig.13) exist between pH and  $\text{NH}_4^+$  efflux in the bloom area (zone I). This relationship tends to weaken with lower cyanobacterial density downstream. Pore water  $\text{NH}_4^+$  concentrations were consistent with bloom development from May to August at site 1B and with differences in pore water  $\text{NH}_4^+$  between sediments within and outside of the bloom area (Fig. 14).

Elevation of pH in sediments can have a profound effect on N desorption in sediments (Chap. 2). As pH in sediments progressively increased with bloom development, the  $\text{NH}_3$  proportion of total ammonium ( $\text{NH}_4^+ + \text{NH}_3$ ) increased in pore water. Once dissolved, un-ionized  $\text{NH}_3$  is formed in pore water at high pH and does not readily adsorb onto negatively charged sediment surfaces. Meanwhile, decreased  $\text{NH}_4^+$  concentrations accelerated the release of  $\text{NH}_4^+$  loosely bound to clay particles (Morin and Morse 1999). Accordingly, the ratios of adsorbed- $\text{NH}_4^+$  to pore water  $\text{NH}_4^+$  decreased in sediments (site 1B) within the bloom region, a consequence of the exposure of sediments

to high pH during July to September in 2010 (Fig. 15). In high pH events, the accelerated ammonium desorption thus accounts for flux increase from the sediments in the bloom zone.

### 3.1.27 CO<sub>2</sub> and O<sub>2</sub>

The ratio of benthic respiration to SOD is 1.22 in late spring to summer (Fig. 18), similar to 138 O<sub>2</sub> : 106 CO<sub>2</sub> of aerobic algal decomposition. Storage of solid phase Fe (II), Mn (II) and S (II) may account for delayed oxygen consumption and result in a relatively high CO<sub>2</sub> to SOD flux rate. In general, flux rates of CO<sub>2</sub> are a better parameter than SOD for the calculation of N and P regeneration from organic matter remineralization.

### 3.1.28 NO<sub>3</sub><sup>-</sup> flux and denitrification from winter-spring to early summer

The rising water temperatures from spring to early summer were weakly correlated with NO<sub>3</sub><sup>-</sup> flux rates ( $P > 0.05$ ) and N<sub>2</sub> flux rates ( $P < 0.05$ ,  $R^2 = 0.42$ ), partly because temperature stimulated increases in ammonium oxidation and denitrifying bacterial activity (Martin et al. 2001; Pfenning and McMahon 1997). Similar to the seasonal changes in terrestrial NO<sub>3</sub><sup>-</sup> flux in the upper Chesapeake Bay (Kemp et al. 1990), the high concentration of NO<sub>3</sub><sup>-</sup> in spring may account for the negative NO<sub>3</sub><sup>-</sup> flux rates (Fig. 9), which consequently support increased N<sub>2</sub> loss through coupled nitrification-denitrification (Fig. 9). In addition, heterotrophic respiration increased with temperature at all stations, which, decreased the depth interval of aerobic conditions in the sediments and facilitated NO<sub>3</sub><sup>-</sup> reaching the zone of denitrification (Risgaardpedersen et al. 1994). At the fine-grained sediment sampling sites (1A to 3A), denitrification accounted for 66 % to 94% of N remineralization based on the oxygen consumption rates.

### 3.1.29 Summer bloom driven pH and DO effects on oxygen penetration depth

The coupling of nitrification-denitrification, which coexists with ammonium oxidation in the oxic zone and nitrate reduction in the deeper anaerobic zone, often removes a substantial proportion of sediment N (Seitzinger 1988). Changing depths of the oxic-anoxic boundary layer depends on the sediment oxygen consumption and water column oxygen changes (Rysgaard et al. 1994).

During dense cyanobacterial blooms in summer, water column DO concentrations were enhanced and showed great diel fluctuations, partly as a result of high light photosynthesis and dark respiration (Fig. 19). This consequently influenced the aerobic zone thickness; the aerobic zone moved on average from 1 – 2 mm to 4 – 5 mm down between bloom initiation and the peak of the bloom (Fig. 19). For example, with diel changes of DO from 8 to 22 mg/L in early July (Budds Landing, eyesonthebay.net), assuming no difference of sediment respiration in this turbid river, the redox boundary moved upward at night (1 – 2 mm) and downward during the day (3 – 4 mm). In some cases, the oxic layer may even move deeper during the day due to light-stimulated photosynthesis at the sediment surface. As DO changed in the overlying water, alteration of the redox regime may therefore minimize the habitat for nitrification and denitrification in sediments, disrupting coupled nitrification-denitrification (Risgaardpedersen et al. 1994).

### 3.1.30 Bloom effects on nitrification

With an increase in the nitrifying bacteria activity with rising temperatures and increases in the concentration of the substrate ( $\text{NH}_4^+$ ) through organic matter degradation, nitrification may be consequently enhanced (Stief et al. 2002). However, coupled

nitrification-denitrification may hinder  $\text{NO}_3^-$  efflux in the summer. At all stations, efflux of  $\text{NO}_3^-$  from sediments (Fig. 7) was rarely observed, indicating a large fraction of  $\text{NO}_3^-$  produced from nitrification in the sediments was simultaneously reduced through denitrification (e.g. >99% of  $\text{NO}_3^-$  produced during spring in the Patuxent River is denitrified) (Jenkins and Kemp 1984).

Henriksen and Kemp (1988) suggested nitrification was influenced by the combination of ammonium limitation, oxygen production and high pH in the upper few millimeters of sediment. Here we divided the data that was collected at temperature > 22°C and when the overlying water  $\text{NO}_3^-$  concentrations was below 20  $\mu\text{mol L}^{-1}$  into two group: pH > 9 and pH < 8.5, to compare the responses in nitrification. The relationship of nitrification efficiency to the calculated oxic depth was negative during the bloom (indicated by pH > 9 in the overlying water), but it was weakly positive at lower pH during the non-bloom season (pH < 8.5) (Fig. 19). Slight changes of pH (when the pH is below 8.5) in the overlying water may cause minimal changes in sediment pH and may not exert effects on N recycling. Oxygen increases in pore water during the day may theoretically enhance nitrification, and result in increased nitrification efficiency (Fig. 19). However, expansion of oxic layer usually occurred with high pH in the aerobic zone (Fig. 19), which may reduce the chance for  $\text{NH}_4^+$  and  $\text{NH}_3$  oxidation (nitrification). Relative to non-bloom periods, long-term high pH (> 9) maintenance during blooms tends to decrease both dissolved and exchangeable ammonium, which are assumed to be the substrates for nitrification (Seitzinger 1991). Nitrification rates may decrease with decreases in ammonium availability, following Michaelis-Menten kinetics (Henriksen and Kemp 1988). Formation of un-ionized  $\text{NH}_3$  reduces the sorption of ammonium in

solids, which is evidenced by the percent contribution of exchangeable- $\text{NH}_4^+$  in sediments (Fig. 15). Meanwhile, conversion of  $\text{NH}_4^+$  to  $\text{NH}_3$  at high pH, along with low  $\text{NH}_4^+$  in the overlying water, may create a sharp gradient in the anoxic layer of sediments and thereby favor the rapid release of soluble ammonium over nitrification (Strauss et al. 2002). In addition, most studies showed that pH outside of an optimum range of 7 – 8.5 inhibited the enzyme activity of both ammonia oxidizing bacteria and nitrifying oxidizing bacteria, which are involved in the oxidation of  $\text{NH}_3$  and  $\text{NO}_2^-$  to  $\text{NO}_3^-$  (Pommerening-Röser and Koops 2005).

### 3.1.31 Bloom influences on $\text{N}_2$ flux

During summer, there was a spatial pattern in denitrification rates caused by pH and DO elevation. In this study,  $\text{N}_2$  fluxes linearly decreased with pH elevation in the bloom regions (Fig. 14), an observation consistent with high pH incubations in the laboratory (Chapter 2). The massive bloom related changes may be responsible for reduction in coupled nitrification-denitrification.

In general, a decrease in denitrification in fine-grained sediments during blooms (Fig. 9D) may be attributable to a limited  $\text{NO}_3^-$  supply. Increases in organic matter are not directly linked to denitrification rates in field observations (Kemp et al. 1990). Experimental addition of organic matter: 1) showed no significant response of denitrification (Lamontagne et al. 2002); 2) exhibited a negative response to amount of organic matter added (moderate and high) and incubation time (2 day and 27 days) (Oakes Jm Oakes et al. 2011; Sloth et al. 1995). However, nitrate concentrations during blooms were generally low in the overlying water (Fig. 16 and Table. 3). Similar to the

$\text{NO}_3^-$  distribution described in other estuaries (Kemp et al. 1990; Trimmer et al. 1998),  $\text{NO}_3^-$  and  $\text{NO}_2^-$  concentrations were negligible in pore-water below the surface of the sediments (Fig. 14). Moreover, the main  $\text{NO}_3^-$  supply for denitrification comes from  $\text{NH}_4^+/\text{NH}_3$  oxidation in sediments, which may be directly inhibited with pH elevation in sediments.

In summer, the temperature effect on  $\text{N}_2$  flux was weakened by the penetration of alkaline pH, which may mediate nitrifying bacterial activity. A similar optimum pH range of 7 ~ 8.5 was found for denitrifying bacteria (Liu et al. 2010; Park et al. 2010). Even though pore water and exchangeable ammonium increased in the thin oxic layer, high pH may have restricted  $\text{NO}_3^-$  supply due to the limited growth and activity of nitrifying bacteria. Along with the high pH, the toxicity of dissolved  $\text{NH}_3$  may decrease nitrification (Cuhel et al. 2010).

Denitrification in sediments may be inhibited by increasing the oxic layer thickness (Fig. 19 and 21). Denitrifying bacteria are anaerobes and usually congregate at the interface of oxic-anoxic layers to intercept  $\text{NO}_3^-$  (Kemp and Dodds 2001). Denitrification is inhibited by  $\text{O}_2$  concentrations above a critical threshold (~10  $\mu\text{M}$ ) (Tiedje et al. 1989). Moreover, diel DO changes may disturb the living conditions for bacteria for denitrification and consequently reduce  $\text{N}_2$  flux during bloom. In response to diel oxygen changes, fluctuation of oxic zone caused sediments to experience the switch between aerobic-anaerobic conditions below ~ 2 mm depths (Eq. 3). Previous studies suggest denitrification declines during the switches between aerobic and anaerobic conditions in response to reduction in the population of denitrifying bacteria, which experience disappearance of denitrifying activity and substrate for denitrification

(e. g.  $\text{NO}_2^-$ ,  $\text{N}_2\text{O}$ ) in the presence of oxygen, as well as time delays of the nitrite reductase under anaerobic conditions (Baumann et al. 1996; Davies et al. 1989).

In addition, benthic nitrogen fixation during N limited conditions may account for the reduction in  $\text{N}_2$  fluxes, a processes difficult to identify from flux data (Kana et al. 1998; Kana and Weiss 2004). In the lower Sassafras River,  $\text{N}_2$  fixation was found in both sediments and associated with the sea grasses *Vallisnaria americana* and *Myriophyllum* sp. (Elliston and O'neil 2005).

### **Ecological impacts**

In spring, settlement of particulate and organic compounds from land runoff and spring blooms may increase the sediment nutrient inventory in the upper Sassafras River. Due to high adsorption of phosphate by oxic sediments (Slomp et al. 1998) and a P burial rate of  $1.8 \text{ g m}^{-2} \text{ yr}^{-1}$  in the upper river (Cornwell, unpublished), sediments act as a large sink for P in this tidal-fresh water estuary. Low DIN and SRP flux rates at the sediment-water interface suggest temperature limitation of nutrient remineralization (Fig. 22).

In the non-bloom region, SRP released from the sediment under normal pH conditions was 2 to 5 times lower than at high pH, while  $\text{NH}_4^+$  release rates at normal pH were almost half that at high pH (Fig.22) and denitrification efficiency did not change significantly (Fig. 16). Moreover, the concentrations of dissolved inorganic N and P become low or even undetectable during the summer (Table 3 and 4). Limited nutrient diffusion from the overlying water makes the benthic microbiota act as an efficient filter, consuming  $\text{NH}_4^+$  and SRP in pore water and hindering their release across the sediment-water interface.

During N-limited periods in the Sassafras River, an increase in  $\text{NH}_4^+$  efflux coupled with a decrease in denitrification rate could increase DIN concentrations in the system, which may lead to more cyanobacterial biomass. Comparison between high and normal pH groups showed  $\text{NH}_4^+$  fluxes in the bloom region (Zone I) were significantly enhanced by pH elevation during blooms than in non-bloom periods, with average values increasing from 176 to 285  $\mu\text{mol m}^{-2} \text{h}^{-1}$ . At the same time, average  $\text{N}_2\text{-N}$  losses through denitrification were reduced from 172 to 110  $\mu\text{mol m}^{-2} \text{h}^{-1}$  during blooms in zone (I) and from 103 to 51  $\mu\text{mol m}^{-2} \text{h}^{-1}$  in the transition zone (II) (Fig. 16). Based on the estimation of  $\text{CO}_2$  and SOD based N remineralization, high pH during the bloom resulted in an increase of 19 - 30 % in  $\text{NH}_4^+$  and reduction of 28 - 41% in loss of N as  $\text{N}_2$  in the bloom region.

Benthic fluxes of  $\text{NH}_4^+$ ,  $\text{NO}_3^-$  and SRP changed the amount and the N: P ratio of nutrients in the water column, creating a positive feedback mechanism for maintenance of the  $\text{N}_2$ -fixing cyanobacterial blooms. High pH in the bloom region resulted in an increase of 2-5 times in P fluxes, and appeared to play an important role in meeting phytoplankton P demand during dense blooms. Relative to observations under normal pH (< 9) in the overlying water, DIN: SRP flux rates under high pH (> 9) conditions were significantly lower, and approximately 62% of the observations were below the Redfield ratio (Fig. 23). This may facilitate the persistence of N-fixing cyanobacterial blooms.



## References

- An, S. 2001. Enhancement of coupled nitrification-denitrification by benthic photosynthesis in shallow estuarine sediments. *Limnol. Oceanogr.* **46**: 62-74.
- Anschutz, P., S. J. Zhong, B. Sundby, A. Mucci, and C. Gobeil. 1998. Burial efficiency of phosphorus and the geochemistry of iron in continental margin sediments. *Limnol. Oceanogr.* **43**: 53-64.
- Bailey, E., M. Owens, W. Boynton, and J. Cornwell. 2006. Sediment phosphorus flux: pH interaction in the tidal freshwater Potomac River estuary. Interstate Commission on the Potomac River Basin, UMCES report TS-505-08-CBL: 1-91.
- Baldock, J. A., C. A. Masiello, Y. Gelinas, and J. I. Hedges. 2004. Cycling and composition of organic matter in terrestrial and marine ecosystems. *Mar. Chem.* **92**: 39-64.
- Baumann, B., M. Snozzi, A. J. B. Zehnder, and J. R. Vandermeer. 1996. Dynamics of denitrification activity of *Paracoccus denitrificans* in continuous culture during aerobic-anaerobic changes. *J. Bacteriol.* **178**: 4367-4374.
- Boers, P. C. M., W. Van Raaphorst, and D. T. Van Der Molen. 1998. Phosphorus retention in sediments. *Water Sci. Technol.* **37**: 31-39.
- Boynton, W. R. 1996. Sediment-water oxygen and nutrient exchanges along the longitudinal axis of Chesapeake Bay: Seasonal patterns, controlling factors and ecological significance. *Estuar. Coast.* **19**: 562-580.
- Boynton, W. R., J. H. Garber, R. Summers, and W. M. Kemp. 1995. Inputs, transformations, and transport of nitrogen and phosphorus in Chesapeake Bay and selected tributaries. *Estuaries* **18**: 285-314.
- Boynton, W. R. and others 2008. Nutrient budgets and management actions in the Patuxent River estuary, Maryland. *Estuar. Coast.* **31**: 623-651.
- Bray, J. T., O. P. Bricker, and B. N. Troup. 1973. Phosphate in interstitial waters of anoxic sediments - oxidation effects during sampling procedure. *Science* **180**: 1362-1364.

- Cabrera, F., P. Dearambarri, L. Madrid, and C. G. Toca. 1981. Desorption of phosphate from iron-oxides in relation to equilibrium pH and porosity. *Geoderma* **26**: 203-216.
- Cai, J., and F. L. Sayles. 1996. Oxygen penetration depths and fluxes in marine sediments. *Mar. Chem.* **52**: 123-131.
- Cornwell, J. C., D. J. Conley, M. Owens, and J. C. Stevenson. 1996. A sediment chronology of the eutrophication of Chesapeake Bay. *Estuaries* **19**: 488-499.
- Cowan, J. L. W., and W. R. Boynton. 1996. Sediment-water oxygen and nutrient exchanges along the longitudinal axis of Chesapeake Bay: Seasonal patterns, controlling factors and ecological significance. *Estuaries* **19**: 562-580.
- Cowan, J. L. W., J. R. Pennock, and W. R. Boynton. 1996. Seasonal and interannual patterns of sediment-water nutrient and oxygen fluxes in Mobile Bay, Alabama (USA): Regulating factors and ecological significance. *Mar. Ecol. Prog. Ser.* **141**: 229-245.
- Cuhel, J. and others 2010. Insights into the effect of soil pH on N<sub>2</sub>O and N<sub>2</sub> emissions and denitrifier community size and activity. *Appl. Environ. Microbiol.* **76**: 1870-1878.
- Eckert, W., A. Nishri, and R. Parparova. 1997. Factors regulating the flux of phosphate at the sediment-water interface of a subtropical calcareous lake: A simulation study with intact sediment cores. *Water Air Soil Pollut.* **99**: 401-409.
- Elliston, K., and J. O'neil. 2005. Nitrogen fixation in various estuarine environments of Chesapeake Bay. Maryland Sea Grant.
- Fisher, T. R., L. W. Harding, D. W. Stanley, and L. G. Ward. 1988. Phytoplankton, nutrients, and turbidity in the Chesapeake, Delaware, and Hudson estuaries. *Estuar. Coast. Shelf Sci.* **27**: 61-93.
- Gardner, W., and M. Mccarthy. 2009. Nitrogen dynamics at the sediment-water interface in shallow, sub-tropical Florida Bay: why denitrification efficiency may decrease with increased eutrophication. *Biogeochemistry* **95**: 185-198.

- Gibb, M. M. 1979. A simple method for the rapid determination of iron in natural waters. *Water Res.* **13**: 295-297.
- Hartzell, J. L., T. E. Jordan, and J. C. Cornwell. 2010. Phosphorus burial in sediments along the salinity gradient of the Patuxent River, a subestuary of the Chesapeake Bay (USA). *Estuar. Coast.* **33**: 92-106.
- Henriksen, K., J. I. Hansen, and T. H. Blackburn. 1981. Rates of nitrification, distribution of nitrifying bacteria, and nitrate fluxes in different types of sediment from danish waters. *Mar. Biol.* **61**: 299-304.
- Henriksen, K., and M. J. Kemp. 1988. Nitrification in estuarine and coastal marine sediments: Methods, patterns and regulating factors. *In* H. Blackburn and J. Sorensen [eds.], *Nitrogen cycling in coastal marine environments*. Wiley.
- Jenkins, M. C., and W. M. Kemp. 1984. The coupling of nitrification and denitrification in 2 estuarine sediments. *Limnol. Oceanogr.* **29**: 609-619.
- Kana, T. M., M. B. Sullivan, J. C. Cornwell, and K. Groszkowski. 1998. Denitrification in estuarine sediments determined by membrane inlet mass spectrometry. *Limnol. Oceanogr.* **42**: 334-339.
- Kana, T. M., and D. L. Weiss. 2004. Comment on "comparison of isotope pairing and N<sub>2</sub>: Ar methods for measuring sediment denitrification" by B. D. Eyre, S. Rysgaard, T. Dalsgaard, and P. Bondo Christensen. 2002. *estuaries* 25 : 1077-1087". *Estuaries* **27**: 173-176.
- Kater, B. J., and M. Dubbeldam. 2006. Ammonium toxicity at high pH in a marine bioassay using *corophium volutator*. *Arch. Environ. Contam. Toxicol.* **51**: 347-351.
- Kemp, M. J., and W. K. Dodds. 2001. Centimeter-scale patterns in dissolved oxygen and nitrification rates in a prairie stream. *J. North. Am. Benthol. Soc.* **20**: 347-357.
- Kemp, W. M., and W. R. Boynton. 1984. Spatial and temporal coupling of nutrient inputs to estuarine primary production - the role of particulate transport and decomposition. *Bull. Mar. Sci.* **35**: 522-535.

- Kemp, W. M. and others 2005. Eutrophication of Chesapeake Bay: historical trends and ecological interactions. *Mar. Ecol. Prog. Ser.* **303**: 1-29.
- Kemp, W. M., P. Sampou, J. Caffrey, M. Mayer, K. Henriksen, and W. R. Boynton. 1990. Ammonium recycling versus denitrification in Chesapeake Bay sediments. *Limnol. Oceanogr.* **35**: 1545-1563.
- Krausejensen, D., K. Mcglathery, S. Rysgaard, and P. B. Christensen. 1996. Production within dense mats of the filamentous macroalga *Chaetomorpha linum* in relation to light and nutrient availability. *Mar. Ecol. Prog. Ser.* **134**: 207-216.
- Lamontagne, M., V. Astorga, A. E. Giblin, and I. Valiela. 2002. Denitrification and the stoichiometry of nutrient regeneration in Waquoit Bay, Massachusetts. *Estuaries* **25**: 272-281.
- Liikanen, A., L. Flojt, and P. Martikainen. 2002. Gas dynamics in eutrophic lake sediments affected by oxygen, nitrate, and sulfate. *J. Environ. Qual.* **31**: 338-349.
- Liu, B. B., P. T. Morkved, A. Frostegard, and L. R. Bakken. 2010. Denitrification gene pools, transcription and kinetics of NO, N<sub>2</sub>O and N<sub>2</sub> production as affected by soil pH. *FEMS Microbiol. Ecol.* **72**: 407-417.
- Magni, P., and S. Montani. 2006. Seasonal patterns of pore-water nutrients, benthic chlorophyll a and sedimentary AVS in a macrobenthos-rich tidal flat. *Hydrobiologia* **571**: 297-311.
- Martin, L. A., P. J. Mulholland, J. R. Webster, and H. M. Valett. 2001. Denitrification potential in sediments of headwater streams in the southern Appalachian Mountains, USA. *J. North. Am. Benthol. Soc.* **20**: 505-519.
- Mayer, M., K. Henriksen, and W. R. Boynton. 1990. Ammonium recycling versus denitrification in Chesapeake Bay sediments. *Limnol. Oceanogr.* **35**: 1545-1563.
- Morin, J., and J. W. Morse. 1999. Ammonium release from resuspended sediments in the Laguna Madre estuary. *Mar. Chem.* **65**: 97-110.

- Newell, R. I. E., J. C. Cornwell, and M. S. Owens. 2002. Influence of simulated bivalve biodeposition and microphytobenthos on sediment nitrogen dynamics: A laboratory study. *Limnol. Oceanogr.* **47**: 1367-1379.
- Oakes Jm Oakes, J. M., B. D. Eyre, and D. J. Ross. 2011. Short-term enhancement and long-term suppression of denitrification in estuarine sediments receiving primary- and secondary-treated paper and pulp mill discharge. *Environ. Sci. Technol.* **45**: 3400-3406.
- Okeefe, J. 2007. Sediment biogeochemistry across the Patuxent River estuarine gradient: Geochronology and Fe-S-P interactions. Master Thesis.
- Paerl, H. 2008. Nutrient and other environmental controls of harmful cyanobacterial blooms along the freshwater-marine continuum, p. 217-237. *In* K. Hudnell [ed.], *Cyanobacterial Harmful Algal Blooms: State of the Science and Research Needs*. Springer.
- Park, S., W. Bae, and B. E. Rittmann. 2010. Operational boundaries for nitrite accumulation in nitrification based on minimum/maximum substrate concentrations that include effects of oxygen limitation, pH, and free ammonia and free nitrous acid inhibition. *Environ. Sci. Technol.* **44**: 335-342.
- Pfenning, K. S., and P. B. McMahon. 1997. Effect of nitrate, organic carbon, and temperature on potential denitrification rates in nitrate-rich riverbed sediments. *Journal Of Hydrology* **187**: 283-295.
- Pommerening-Röser, A., and H. P. Koops. 2005. Environmental pH as an important factor for the distribution of urease positive ammonia-oxidizing bacteria. *Microbiol. Res.* **160**: 27-35.
- Rauch, M., and L. Denis. 2008. Spatio-temporal variability in benthic mineralization processes in the eastern English Channel. *Biogeochemistry* **89**: 163-180.
- Risgaard-Petersen, N. 2003. Coupled nitrification-denitrification in autotrophic and heterotrophic estuarine sediments: On the influence of benthic microalgae. *Limnol. Oceanogr.* **48**: 93-105.

- Risgaardpedersen, N., S. Rysgaard, L. P. Nielsen, and N. P. Revsbech. 1994. Diurnal-variation of denitrification and nitrification in sediments colonized by benthic microphytes. *Limnol. Oceanogr.* **39**: 573-579.
- Rysgaard, S., P. B. Christensen, and L. P. Nielsen. 1995. Seasonal-variation in nitrification and denitrification in estuarine sediment colonized by benthic microalgae and bioturbating infauna. *Mar. Ecol. Prog. Ser.* **126**: 111-121.
- Rysgaard, S., N. Risgaard-Petersen, and N. P. Sloth. 1994. Oxygen regulation of nitrification and denitrification in sediments. *Limnol. Oceanogr.* **39**: 1643-1652.
- Seitzinger, S. 1988. Denitrification in freshwater and coastal marine ecosystems: ecological and geochemical significance. *Limnol. Oceanogr.* **33**: 702-724.
- Seitzinger, S. P. 1987. The effect of pH on the release of phosphorus from Potmac River sediment, p. 1-46. Chesapeake Bay Programm Report.
- . 1991. The effect of pH on the release of phosphorus from Potomac estuary sediments - implications for blue-green-algal blooms. *Estuar. Coast. Shelf Sci.* **33**: 409-418.
- Seitzinger, S. P., W. S. Gardner, and A. K. Spratt. 1991. The effect of salinity on ammonium sorption in aquatic sediments - implications for benthic nutrient recycling. *Estuaries* **14**: 167-174.
- Sharp, J. H. and others 2009. A Biogeochemical view of estuarine eutrophication: seasonal and spatial trends and correlations in the Delaware estuary. *Estuar. Coast.* **32**: 1023-1043.
- Slomp, C. P., J. F. P. Malschaert, and W. Van Raaphorst. 1998. The role of adsorption in sediment-water exchange of phosphate in North Sea continental margin sediments. *Limnol. Oceanogr.* **43**: 832-846.
- Sloth, N. P., H. Blackburn, L. S. Hansen, N. Risgaardpetersen, and B. A. Lomstein. 1995. Nitrogen cycling in sediments with different organic loading. *Mar. Ecol. Prog. Ser.* **116**: 163-170.
- Smith, E. M., and W. M. Kemp. 2001. Size structure and the production/respiration balance in a coastal plankton community. *Limnol. Oceanogr.* **46**: 473-485.

- Stainton, M. P. 1973. Syringe gas-stripping procedure for gas-chromatographic determination of dissolved inorganic and organic carbon in fresh water and carbonates in sediments. *J. Fish. Res. Board Can.* **30**: 1441-1445.
- Stief, P., D. De Beer, and D. Neumann. 2002. Small-scale distribution of interstitial nitrite in freshwater sediment microcosms: The role of nitrate and oxygen availability, and sediment permeability. *Microb. Ecol.* **43**: 367-378.
- Strauss, E. A., N. L. Mitchell, and G. A. Lamberti. 2002. Factors regulating nitrification in aquatic sediments: effects of organic carbon, nitrogen availability, and pH. *Can. J. Fish. Aquat. Sci.* **59**: 554-563.
- Sundback, K., and A. Miles. 2000. Balance between denitrification and microalgal incorporation of nitrogen in microtidal sediments, NE Kattegat. *Aquat. Microb. Ecol.* **22**: 291-300.
- Tiedje, J. M., S. Simkins, and P. M. Groffman. 1989. Perspectives on measurement of denitrification in the field including recommended protocols for acetylene based methods. *Plant Soil* **115**: 261-284.
- Tomaszek, J. A., and E. Czerwieńec. 2003. Denitrification and oxygen consumption in bottom sediments: factors influencing rates of the processes. *Hydrobiologia* **504**: 59-65.
- Trimmer, M., D. Nedwell, and D. Sivyer. 1998. Nitrogen fluxes through the lower estuary of the river Great Ouse, England: the role of the bottom sediments. *Mar. Ecol. Prog. Ser.* **163**: 109-124.
- Wang, F. L., and A. K. Alva. 2000. Ammonium adsorption and desorption in sandy soils. *Soil Sci. Soc. Am. J.* **64**: 1669-1674.

**Tables**

Table 3-1 Sampling information in the upper Sassafras River from 2007 to 2010, including dates and number of sediment cores used the nutrient flux measurement.

<b>year</b>	<b>Time Date</b>	<b>No. of cores in each station</b>						<b>Total cores</b>
		1A	1B	2A	2B	3A	3B	
<b>2007</b>	12/20/2007					6		6
<b>2008</b>	5/7/2008	3	4			3		10
	6/18/2008		4			3		7
	9/4/2008	6	3			3		12
<b>2009</b>	3/27/2009	3	3					6
	4/9/2009	3	3					6
	5/21/2009	2	2	2	2	2	2	12
	7/9/2009		7					7
	9/20/2009	2	2	2	2	2	2	12
	11/18/2009	2	2	2	2	2	2	12
<b>2010</b>	3/25/2010	2	2	2	2	2	2	12
	5/11/2010	2	2	2	2	2	2	12
	6/4/2010	2	2	2	2	2	2	12
	7/1/2010	2	2	2	2	2	2	12
	8/4/2010	2	2	2	2	2	2	12
	9/2/2010	2	2	2	2	2	2	12
	10/5/2010	2	2	2	2	2	2	12
	<b>Total</b>	35	44	20	20	35	20	174



Table 3-2 Water column depth and sediment characteristics of the sampling stations in the upper Sassafras River. Depth represents the average value for each station over the 2 years study. Grain sizes were measured in Sept. 2009. The content and molar ratios of C N P were presented as the average value of surface sediments (0-1 cm) taken during June to September in 2010.

Location	depth	Grain Size			June			August		
	mean (m)	Sand %	Silt %	Clay %	TC ( $\mu\text{g C g}^{-1}$ )	TN ( $\mu\text{g N g}^{-1}$ )	C:N	TC ( $\mu\text{g C g}^{-1}$ )	TN ( $\mu\text{g N g}^{-1}$ )	C:N
1A	0.78	6%	58%	36%	32.4	2.2	17.2	38.8	3.4	13.3
1B	1.35	7%	59%	34%	29.8	2.8	12.4	44.1	6.0	8.6
2A	2.4	3%	59%	37%	40.2	4.6	10.2	41.3	5.5	8.8
2B	2.8	9%	58%	33%	39.8	5	9.3	59.4	7.9	8.8
3A	1.9	12%	26%	62%	39.8	3.8	12.2	45.9	4.5	11.9
3B	3.4	75%	13%	12%	24.4	2.7	10.5	26.4	2.1	14.7

Table 3-3 Mean ( $\pm$  std) of salinity, temperature and dissolved inorganic nutrient concentrations in the bottom water before, during and after bloom seasons. Data shown from all stations during 2007-2010 (n = sample size).

<b>Parameters</b>		<b>Before Bloom (Mar-May, n = 25)</b>			<b>Bloom (Jun.-Sept., n = 36)</b>			<b>After Bloom (Oct. -Dec., n = 13)</b>		
Salinity	Mean $\pm$ Std	0.54	$\pm$	0.38	0.38	$\pm$	0.34	0.98	$\pm$	0.79
	Range	0.12	—	1.37	0.00	—	1.44	0.12	—	2.91
Temp ( $^{\circ}$ C)	Mean $\pm$ Std	15.72	$\pm$	4.26	27.64	$\pm$	1.88	10.32	$\pm$	5.52
	Range	9.40	—	22.65	24.30	—	31.30	4.76	—	17.18
DO ( $\text{mg L}^{-1}$ )	Mean $\pm$ Std	10.72	$\pm$	4.26	15.64	$\pm$	3.88	10.32	$\pm$	5.52
	Range	5.40	—	14.65	10.30	—	20.30	4.76	—	17.18
$\text{NO}_3^-$ ( $\mu\text{mol L}^{-1}$ )	Mean $\pm$ Std	75.11	$\pm$	35.06	4.47	$\pm$	15.36	56.76	$\pm$	41.81
	Range	31.80	—	142.99	0.32	—	52.50	17.60	—	151.40
$\text{NH}_4^+$ ( $\mu\text{mol L}^{-1}$ )	Mean $\pm$ Std	8.39	$\pm$	9.85	0.47	$\pm$	0.62	4.92	$\pm$	3.23
	Range	0.26	—	38.50	0.26	—	2.17	10.86	—	10.86
SRP ( $\mu\text{mol L}^{-1}$ )	Mean $\pm$ Std	0.94	$\pm$	0.69	0.27	$\pm$	0.79	0.47	$\pm$	0.25
	Range	0.12	—	2.74	0.01	—	1.67	0.08	—	0.89
DIN : SRP	Mean $\pm$ Std	79.22	$\pm$	22.12	37.52	$\pm$	24.72	104.73	$\pm$	47.12
	Range	34.13	—	112.44	0.99	—	50.99	50.36	—	350.36

Table 3-4 Pearson correlation coefficients for the average values of selected bottom-water variables. Corr is the correlation coefficient; N is the sample size and P is the significant level (Note \* P < 0.05, \*\* P < 0.01 and \*\*\* P < 0.001).

Variables		pH	Temp (°C)	Salinity	DO (mg L <sup>-1</sup> )	Chl <i>a</i> (µg L <sup>-1</sup> )	DO (%)	[NH <sub>4</sub> <sup>+</sup> ] (µmol L <sup>-1</sup> )	[NO <sub>3</sub> <sup>-</sup> ] (µmol L <sup>-1</sup> )	SRP (µmol L <sup>-1</sup> )		
<b>pH</b>	Corr	1										
	P											
	N	73										
<b>Temp</b>	Corr	0.495	1									
	P	<.0001	***									
	N	73	74									
<b>Salinity</b>	Corr	-0.093	-0.259	1								
	P	0.432	0.026	*								
	N	73	74	74								
<b>DO</b>	Corr	-0.019	-0.307	0.114	1							
	P	0.871	0.008	**	0.332							
	N	73	74	74	74							
<b>Chl <i>a</i></b>	Corr	0.648	0.662	-0.259	0.146	1						
	P	<.0001	***	<.0001	***	0.052	0.279					
	N	57	57	57	57	57						
<b>DO (%)</b>	Corr	0.543	0.411	-0.199	-0.387	0.552	1					
	P	<.0001	***	0.0003	***	0.0888	0.0007	***	<.0001	***		
	N	73	74	74	74	74	57	74				
<b>[NH<sub>4</sub><sup>+</sup>]</b>	Corr	-0.369	-0.263	-0.049	0.026	-0.146	-0.218	1				
	P	0.0014	**	0.0246	*	0.679	0.827	0.284	0.064			
	N	72	73	73	73	73	56	73	73			
<b>[NO<sub>3</sub><sup>-</sup>]</b>	Corr	-0.526	-0.648	-0.040	0.151	-0.510	-0.426	0.554	1			
	P	<.0001	***	<.0001	***	0.7332	0.1999	<.0001	***	0.0002	***	
	N	73	74	74	74	74	57	74	73	74		
<b>SRP</b>	Corr	-0.245	-0.076	-0.133	-0.089	-0.316	-0.156	0.030	0.337	1		
	P	0.0383	*	0.523	0.261	0.452	0.0176	*	0.188	0.799	0.0036	**

Table 3-5 Mean light and dark fluxes in sandy and muddy sediments( ± SE), including fluxes of SRP, NH<sub>4</sub><sup>+</sup>, NO<sub>3</sub><sup>-</sup>, N<sub>2</sub>-N, O<sub>2</sub> and net inorganic nitrogen (DIN), the molar ratio of O<sub>2</sub>: DIN flux rates, denitrification efficiency (DE%) and the calculated nitrogen remineralization. Net DIN flux presents the sum of positive fluxes of NH<sub>4</sub><sup>+</sup>, NO<sub>3</sub><sup>-</sup> and N<sub>2</sub>-N; denitrification efficiency (DE%) is the N<sub>2</sub>-N flux as a fraction of DIN; N remineralization is calculated based on the consumption of oxygen consumption rates the Red field ratio in dark.

Sediment property		Sandy station		Muddy station			
Parameters	Treatment	Mean	± SE	Daily rates	Mean	± SE	Daily rates
		μmol m <sup>-2</sup> h <sup>-1</sup>		mmol m <sup>-2</sup> d <sup>-1</sup>		μmol m <sup>-2</sup> h <sup>-1</sup>	
SRP Flux	Dark	-2.2	± 16.0	-0.3	3.6	± 13.2	0.0
	Light	-19.5	± 10.4		-5.6	± 17.8	
NH <sub>4</sub> <sup>+</sup> Flux	Dark	46.7	± 24.6	1.0	114.3	± 53.5	1.6
	Light	38.0	± 123.8		34.7	± 61.9	
NO <sub>3</sub> <sup>-</sup> Flux	Dark	-25.9	± 57.0	-0.3	-39.7	± 79.4	0.1
	Light	-1.6	± 41.4		32.4	± 83.1	
N <sub>2</sub> -N Flux	Dark	14.3	± 3.7	0.6	188.3	± 121.9	2.7
	Light	29.7	± 16.3		61.5	± 52.0	
O <sub>2</sub> Flux	Dark	1475.9	± 533.9	-7.5	1625.9	± 680.0	-14.2
	Light	515.3	± 358.8		146.1	± 956.3	
Net DIN Flux	Dark	147.8	± 63.5	3.4	294.5	± 138.0	5.7
	Light	136.0	± 101.9		193.3	± 134.1	
O <sub>2</sub> /DIN	Dark	10.1	± 0.8		6.4	± 2.9	
	Light	-6.6	± 7.6		0.6	± 14.0	
DE%	Dark	16.3	± 10.4		66.2	± 21.4	
	Light	20.2	± 10.1		43.2	± 11.5	
N Remineralization	Dark	222.8	± 80.6		245.4	± 102.6	



Table 3-6 Summary of sediment-water flux rates in the oligohaline and tidal-fresh of the Chesapeake Bay. Flux rates include nutrient release of SRP,  $\text{NH}_4^+$  and  $\text{NO}_3^-$ , denitrification ( $\text{N}_2$ ) and sediment oxygen demand (SOD). Note: The unit difference between nutrient flux rates and SOD.

Flux Rate	Chesapeake Bay <sup>1</sup>			Corsica River <sup>2</sup>	Lower Sassafras River <sup>3</sup>
		n=241		n=41	n=12
SOD ( $\text{mmol m}^{-2} \text{d}^{-1}$ )	average	-60		-24	-39
	std	30		19	18
	max	-9		-7	-26
	min	-209		-73	-89
$\text{NH}_4^+$ flux ( $\mu\text{mol m}^{-2} \text{h}^{-1}$ )	average	295		51	105
	std	297		174	116
	max	1616		808	359
	min	-86		-105	-28
SRP ( $\mu\text{mol m}^{-2} \text{h}^{-1}$ )	average	10		4	3
	std	21		13	4
	max	171		35	12
	min	-38		-20	0
$\text{NO}_3^-$ and $\text{NO}_2^-$ ( $\mu\text{mol m}^{-2} \text{h}^{-1}$ )	average	-62		6	5
	std	105		17	16
	max	288		69	33
	min	-607		-23	-27
$\text{N}_2$ flux <sup>4</sup> ( $\mu\text{mol m}^{-2} \text{h}^{-1}$ )	average	70		61	
	std	213		31	
	max	21		145	
	min	62		10	

Flux rates of the low salinity (< 5) and shallow water (< 5 m) sites in Chesapeake Bay in 1980 - 2006 (Boynton, Chesapeake Bay sediment water flux database <http://www.gonzo.cbl.umces.edu/data.htm>) ; 2. Flux rates in the Corsica river estimated in summer 2007 (Cornwell, unpublished data) 3. June-August in 2000 (Boynton, unpublished data); 4. Denitrification rates in the Chesapeake Bay (Boynton, 2008).



Table 3-7 Multiple regression models used to predict nutrient flux rates in sediments as a function of temperature, pH, salinity, nutrients and Chl a in the water column. All independent variables, the normalized environmental factors, left in each model are significant at the 0.15 level. RMSE: root mean square deviation; n is the number of statistically related independent factors; df: Estimated degree freedom; Cp is the Mallows' Cp criterion.

Dependent variable	RMS E	Intercept	pH	ln (Temp)	Ln (Salinity)	Ln (NO <sub>3</sub> <sup>-</sup> )	Ln (N:P)	Ln (Chl a)	n	df	R <sup>2</sup>	C(p)
NH <sub>4</sub> -Nflux	104.5	-81.6	30.8			-23.9	-24.9	32.3	4	3	0.39	3.16
N <sub>2</sub> -Nflux	58.9	-126.6		50.5		-31.0	14.9		4	3	0.32	0.54
SRP flux	11.6	-58.4	5.3	5.2				8.52	3	4	0.22	-0.87
SOD	515.6	-1258.5			404.0	120.8		265.7	4	3	0.38	3.99



Appendix. Adsorbed-NH<sub>4</sub><sup>+</sup>, pore-water NH<sub>4</sub><sup>+</sup> and sediment characteristics of sediment taken from stations within bloom (A) and out of bloom (B) from May to September 2010. Adsorbed NH<sub>4</sub><sup>+</sup>, pore-water NH<sub>4</sub><sup>+</sup> concentration (PW), sediment percent water (% water) and porosity ( $\phi$ ) were measured in each section. K\* is the adsorption coefficients; Abs (%) is the adsorbed-NH<sub>4</sub><sup>+</sup> fraction in both adsorbed and pore-water phase. Average values of K\* and Abs% were integrated with the depth in top 3 cm sediments.

A)	Time	Sections	NH <sub>4</sub> <sup>+</sup>		% water	$\phi$	K*	K*	NH <sub>4</sub> <sup>+</sup>		Abs%	Abs %
			Adsorbed $\mu\text{M/g wet}$	PW $\mu\text{mol L}^{-1}$					Adsorbed $\text{mM L}^{-1}$	PW $\text{mM L}^{-1}$		
<b>Within bloom (1B)</b>	May	0-0.5	1513.96	84.68	0.78	0.90	1.99	1.19	151.76	76.19	0.67	0.53
		0.5-1.0	1086.42	132.65	0.75	0.88	1.09		127.22	117.12	0.52	
		1.0-2.0	1370.94	208.20	0.71	0.86	1.06		189.96	179.35	0.51	
		2.0-3.0	1926.04	381.39	0.68	0.84	0.96		308.25	320.35	0.49	
	Jul.	0-0.5	1240.23	150.29	0.86	0.94	0.55	2.89	77.60	140.89	0.36	0.70
		0.5-1.0	6095.72	267.86	0.81	0.91	2.14		523.95	244.84	0.68	
		1.0-2.0	12199.77	477.62	0.75	0.88	3.34		1411.68	422.36	0.77	
		2.0-3.0	16777.80	595.10	0.74	0.88	3.97		2071.16	521.64	0.80	
	Aug.	0-0.5	1832.60	357.97	0.72	0.87	0.78	2.06	243.18	310.47	0.44	0.59
		0.5-1.0	2653.87	611.55	0.59	0.78	1.23		584.57	476.84	0.55	
		1.0-2.0	4481.39	848.46	0.66	0.83	1.10		773.38	702.03	0.52	
		2.0-3.0	6598.84	1686.16	0.35	0.58	4.09		2794.05	972.21	0.74	
	Sept.	0-0.5	2077.06	209.50	0.86	0.94	0.67	3.13	131.15	196.27	0.40	0.59
		0.5-1.0	4184.47	249.00	0.80	0.91	1.66		376.51	226.60	0.62	
		1.0-2.0	6375.24	194.31	0.76	0.89	4.25		731.69	172.01	0.81	
		2.0-3.0	3018.04	666.55	0.68	0.84	0.85		475.42	561.55	0.46	

B)	Time	Sections	NH <sub>4</sub> <sup>+</sup>		% water	φ	K*	K*	NH <sub>4</sub> <sup>+</sup>		Abs%	Abs %
			Adsorbed μM/g wet	PW μmol L <sup>-1</sup>					Adsorbed mM L <sup>-1</sup>	PW mM L <sup>-1</sup>		
<b>Out of bloom (3B)</b>	May	0-0.5	2018.87	84.68	0.85	0.93	1.68	1.52	132.72	79.11	0.63	0.60
		0.5-1.0	956.23	132.65	0.67	0.84	1.40		155.46	111.09	0.58	
		1.0-2.0	1651.70	208.20	0.69	0.85	1.44		253.04	176.31	0.59	
		2.0-3.0	1964.53	381.39	0.57	0.76	1.58		462.11	291.67	0.61	
	Jul.	0-0.5	921.16	142.82	0.85	0.93	0.47	1.50	62.22	133.17	0.32	0.57
		0.5-1.0	2017.11	211.91	0.81	0.92	0.87		168.74	194.18	0.46	
		1.0-2.0	7052.95	448.58	0.79	0.90	1.69		684.02	405.07	0.63	
		2.0-3.0	12421.73	699.52	0.77	0.89	2.14		1338.34	624.15	0.68	
	Aug.	0-0.5	1649.48	242.29	0.83	0.92	0.57	1.18	127.37	223.58	0.36	0.53
		0.5-1.0	2099.65	312.82	0.76	0.89	0.86		239.18	277.18	0.46	
		1.0-2.0	3790.98	604.91	0.64	0.81	1.44		708.48	491.86	0.59	
		2.0-3.0	4505.43	810.58	0.62	0.80	1.39		899.48	648.76	0.58	
	Sept.	0-0.5	1580.83	141.71	0.81	0.91	1.08	1.25	139.07	129.24	0.52	0.45
		0.5-1.0	2788.95	193.73	0.87	0.94	0.88		161.28	182.53	0.47	
		1.0-2.0	3239.58	371.08	0.82	0.92	0.77		263.17	340.93	0.44	
		2.0-3.0	4906.11	701.85	0.79	0.90	0.75		474.10	634.02	0.43	

## Figures

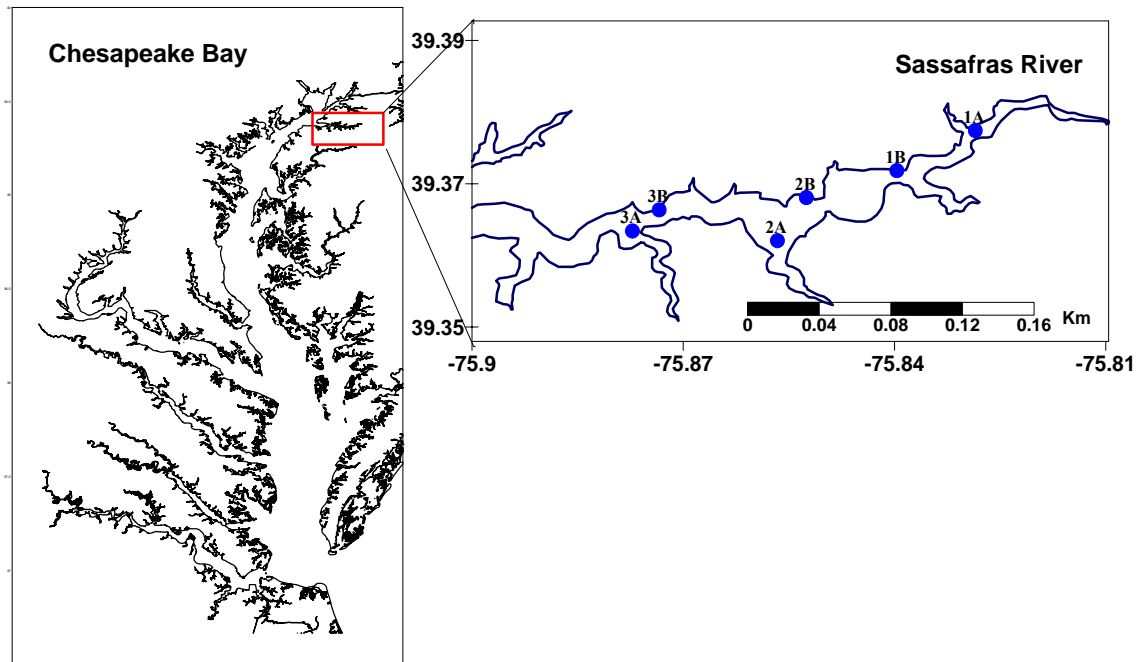


Figure 3-1 Sampling locations for sediment flux rate measurements in the upper Sassafras River, MD. Budds Landing, the continuous monitoring water quality station of Maryland Department of Natural Recourse, is less than 20 m from station 1B.

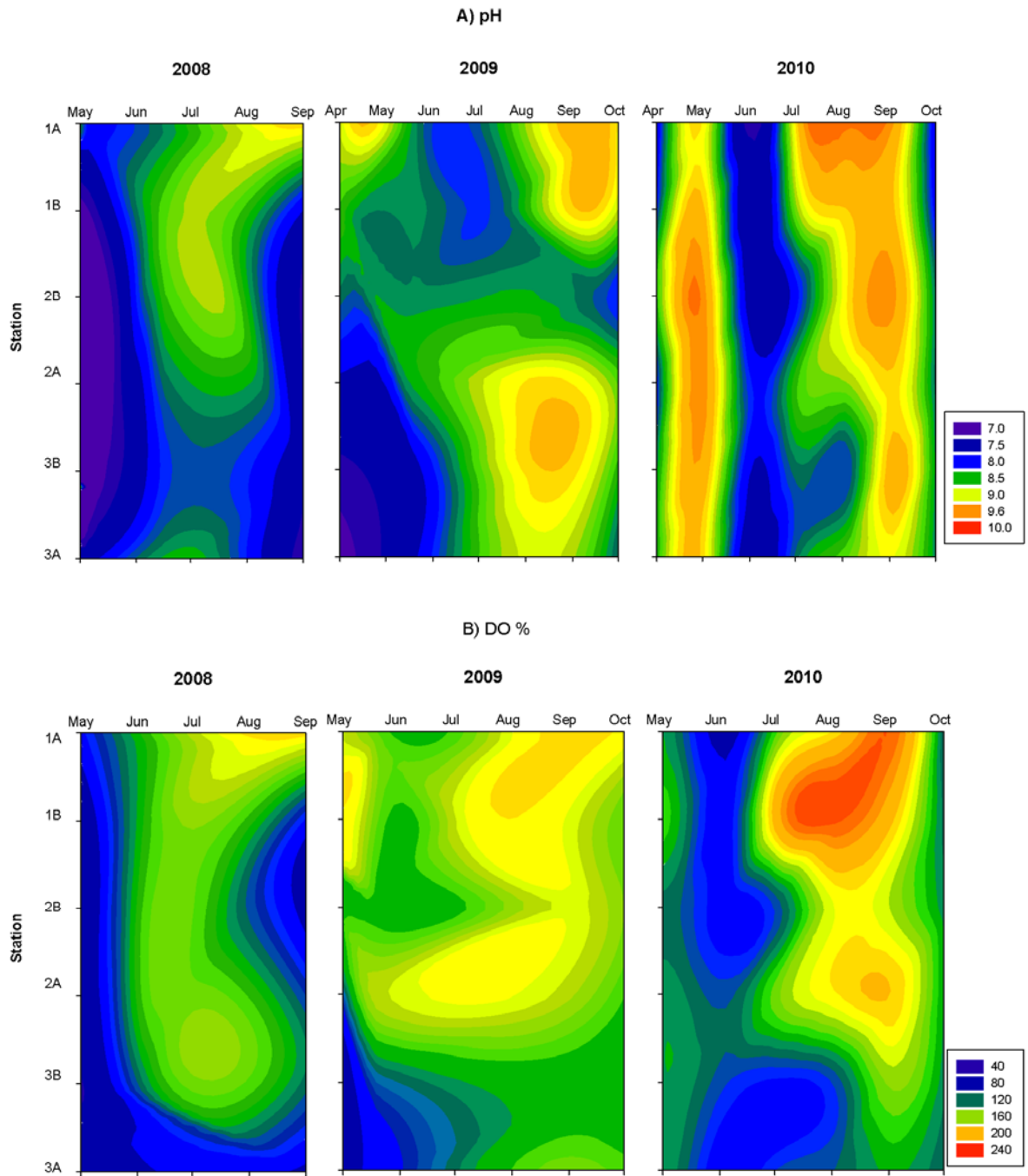


Figure 3-2 The temporal and spatial changes of pH and dissolved oxygen percentage (DO %) of bottom water during 2008 to 2010. Stations shown are from the riverhead to downstream.

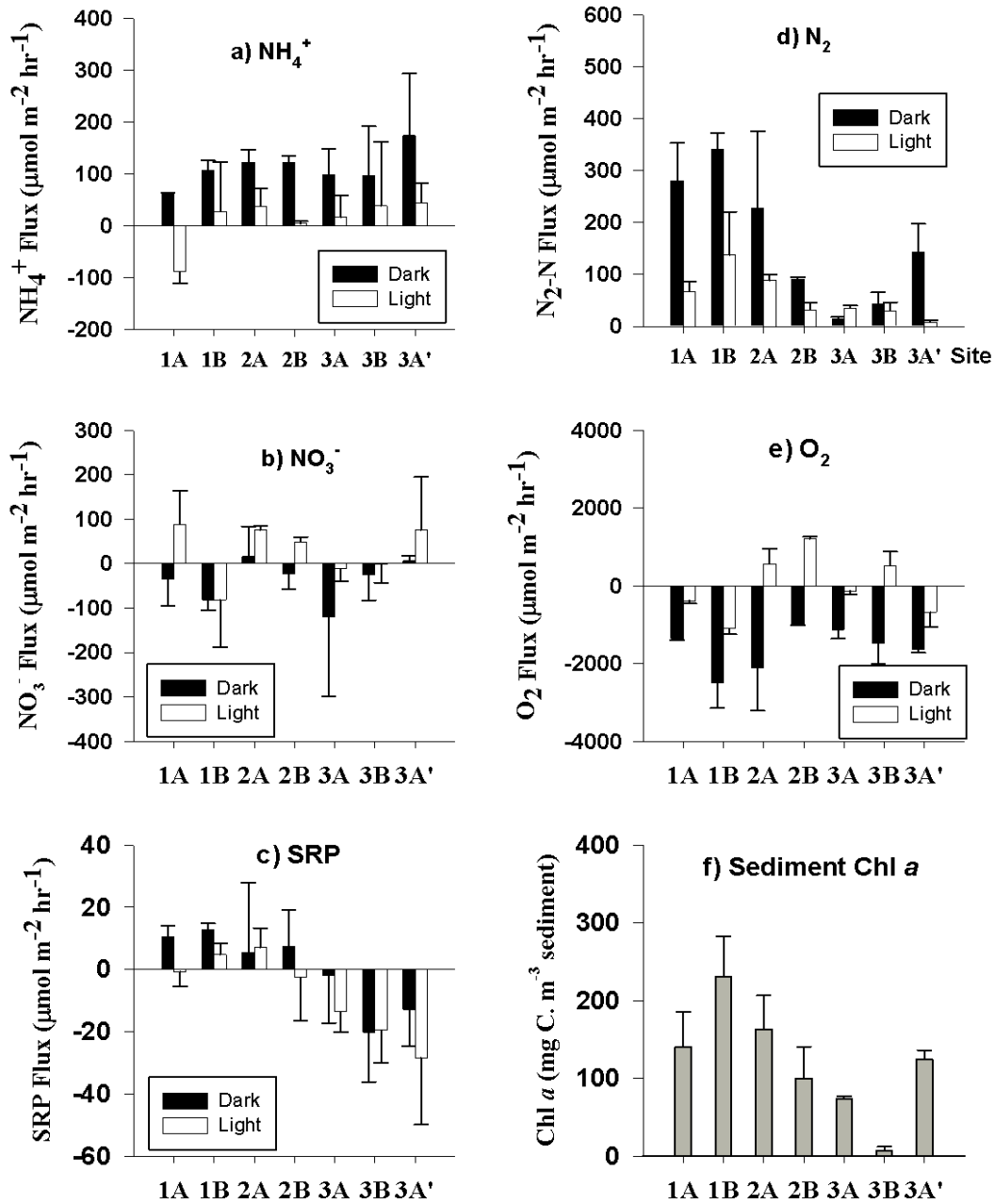


Figure 3-3 Flux rates (a-e) and sediment Chl *a* concentration (n= 3, upper 1cm). Flux rates of  $\text{NH}_4^+$ ,  $\text{NO}_3^-$ , SRP,  $\text{N}_2$  and  $\text{O}_2$  were measured under light (white bar) and dark (black bar) incubation for sediments obtained in June 2010 and for sediment 3A' from the same location as 3A but in September 2009. The bars are mean  $\pm$  SE.

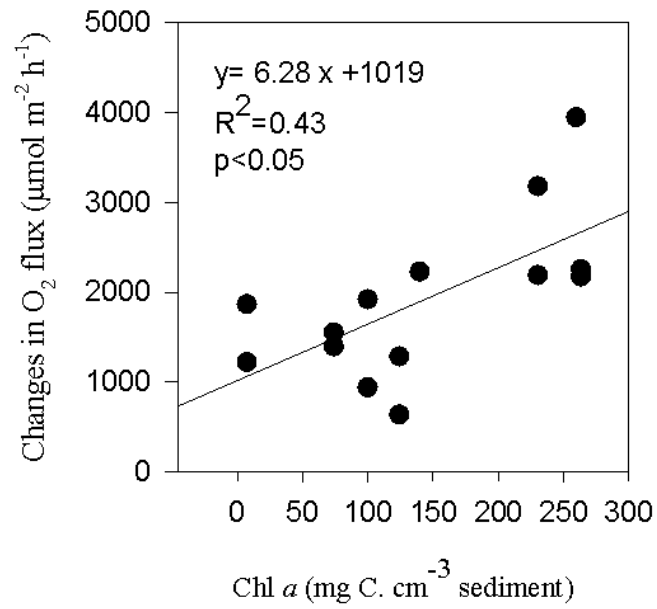


Figure 3-4 Relationship of sediment Chl *a* and the changes in O<sub>2</sub> flux rates, calculated from the difference in O<sub>2</sub> fluxes between light and dark treatments. Data shown from the light-dark incubation in September 2009 and June 2010 (Figure 3).

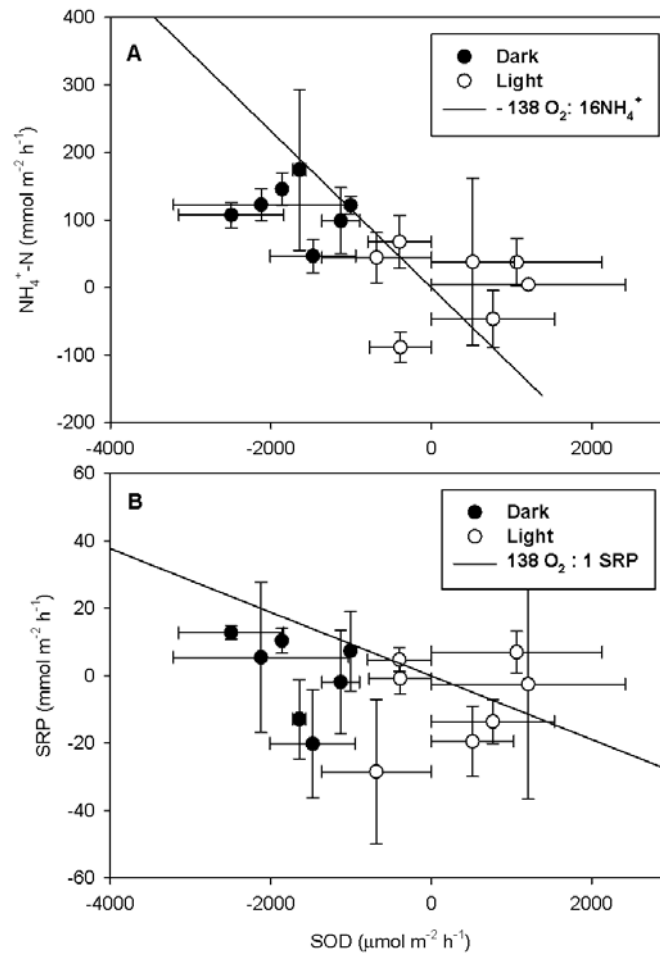


Figure 3-5 Light and dark effects on  $\text{NH}_4^+$  flux versus SOD (A) and SRP flux versus SOD of the fine-grained sediments. Mean ( $\pm$  SE) flux rates of  $\text{NH}_4^+$  and SRP shown from measurements in September 2009 and June 2010 in Figure 3. Solid lines present the stoichiometric ratio of  $\text{O}_2$ : N and  $\text{O}_2$ : P as predicted from Redfield ratios (138  $\text{O}_2$  : 16N : 1P).

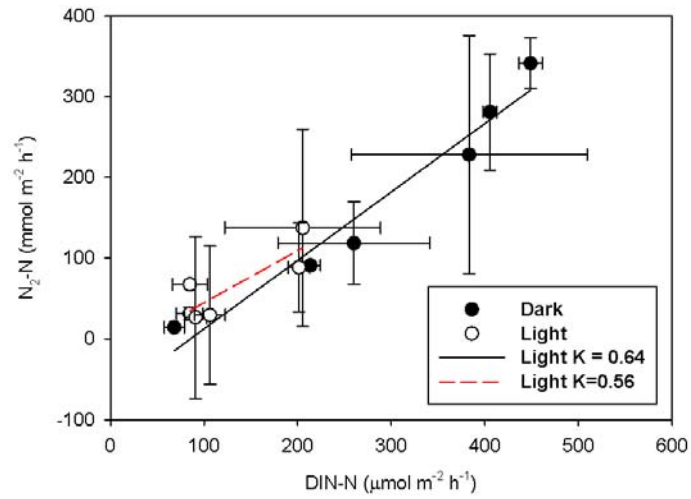
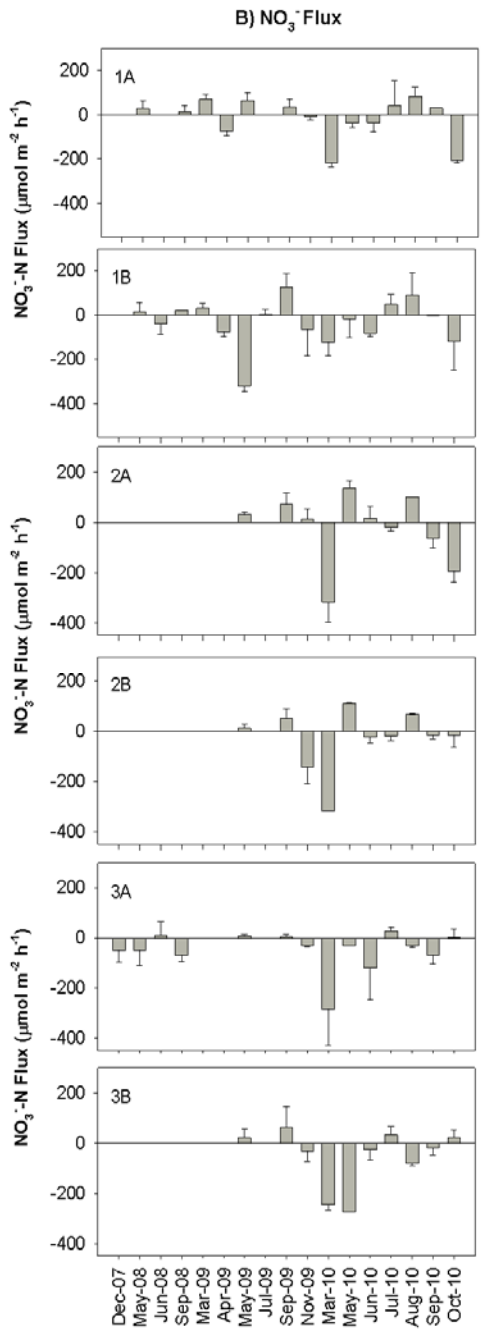
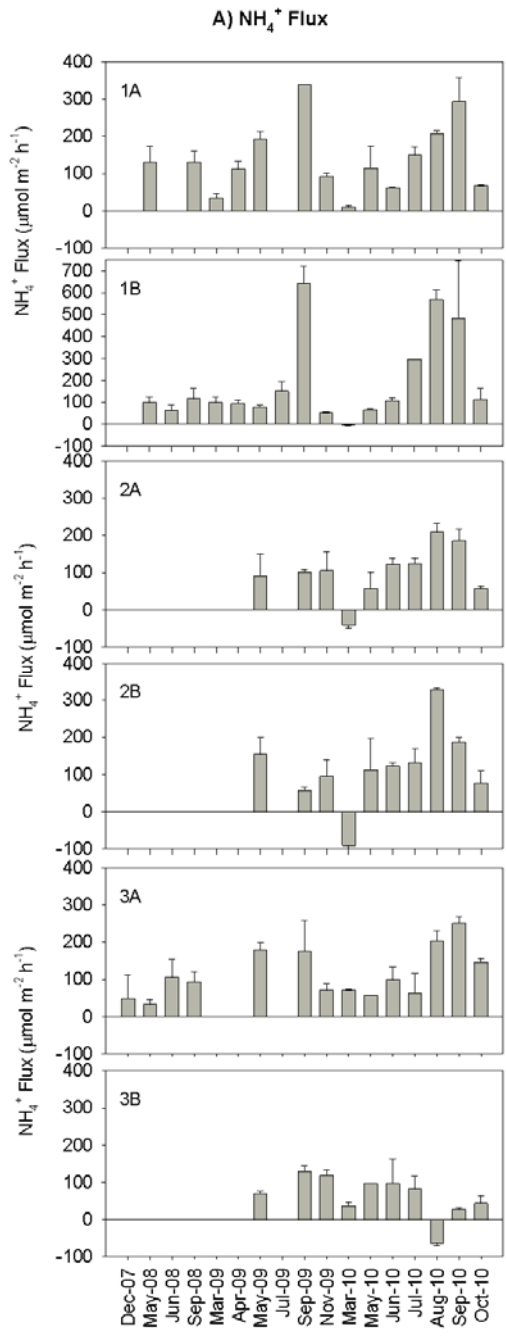


Figure 3-6 Effects of light and dark incubation on N remineralization ( $\text{DIN} = \sum \text{NH}_4^+ + \text{NO}_3^- + \text{N}_2\text{-N}$ ) through denitrification ( $\text{N}_2$  flux) of the fine-grained sediments. The slope indicates the mean ( $\pm$  SE) of denitrification efficiency in light ( $P = 0.03$ ,  $R^2 = 0.85$ ) and dark ( $P < 0.001$ ,  $R^2 = 0.97$ ). Data estimated from flux measurements in September 2009 and June 2010.





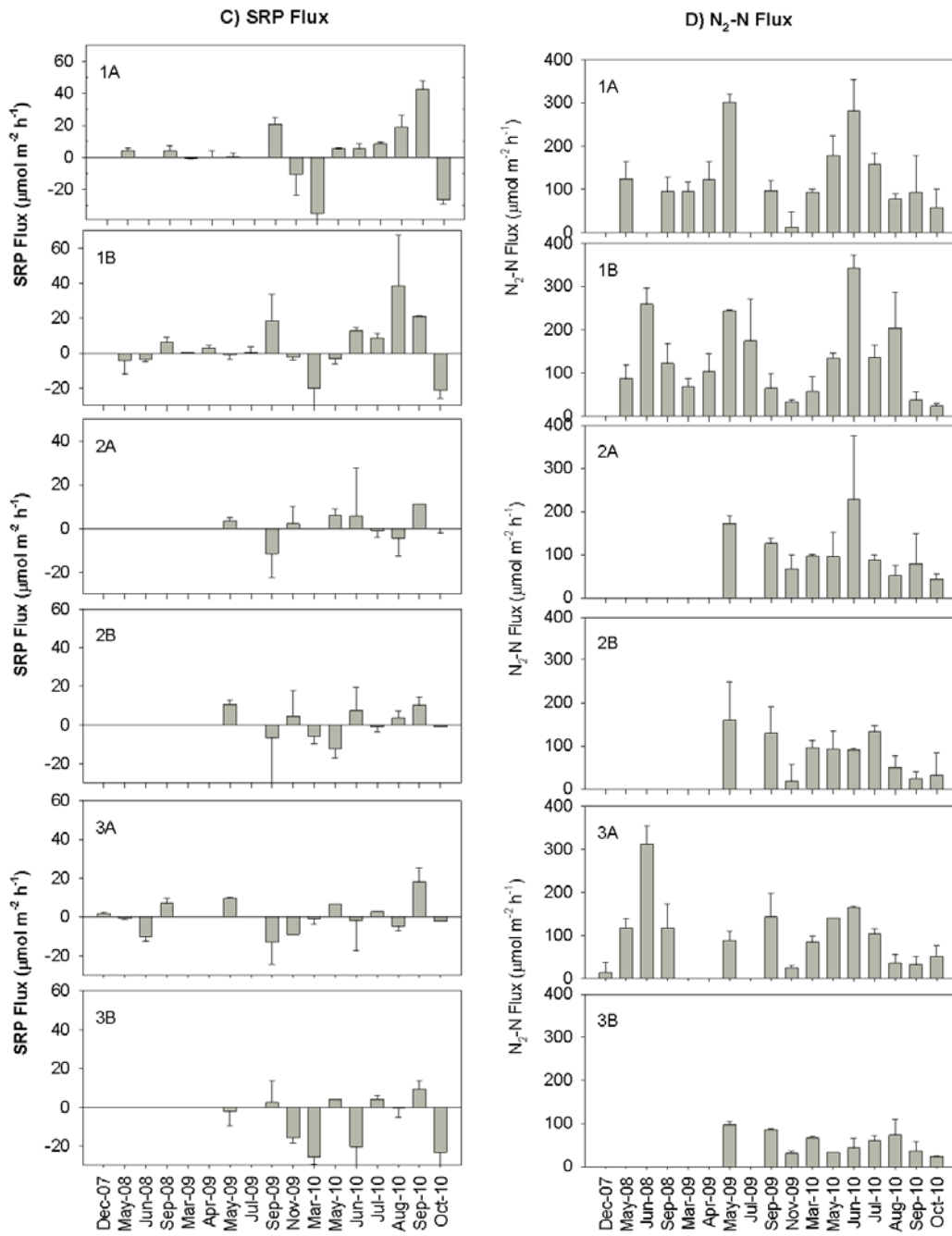


Figure 3-7 Flux rates of  $\text{NH}_4^+$  (A),  $\text{NO}_3^-$  (B), SRP (C) and  $\text{N}_2$  (D) of sediments from the upper SassafRAS River during Dec. 2007 to Oct. 2010. Flux measurements in darkness. Bar presents mean  $\pm$  standard deviation,  $n = 2 - 5$ .

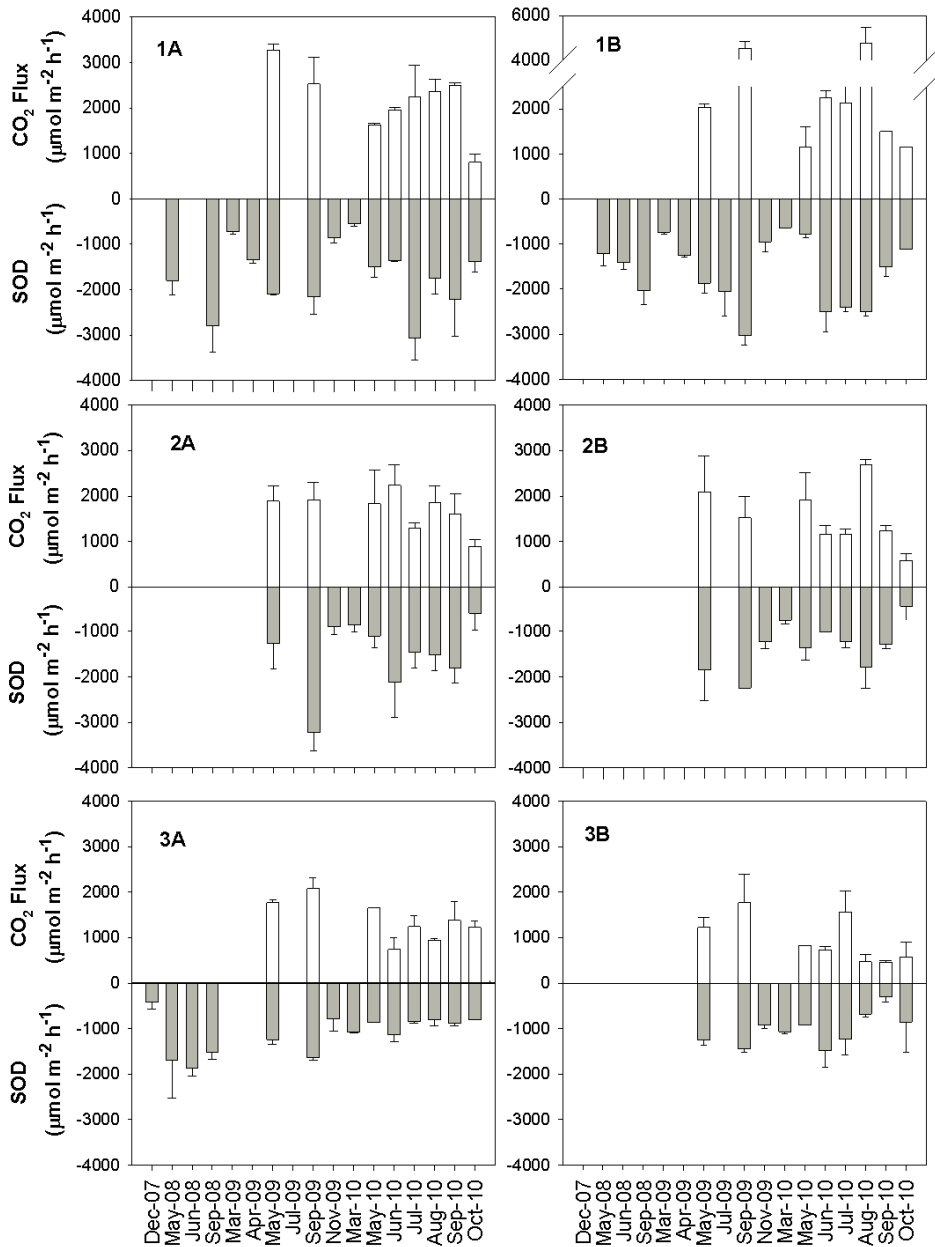
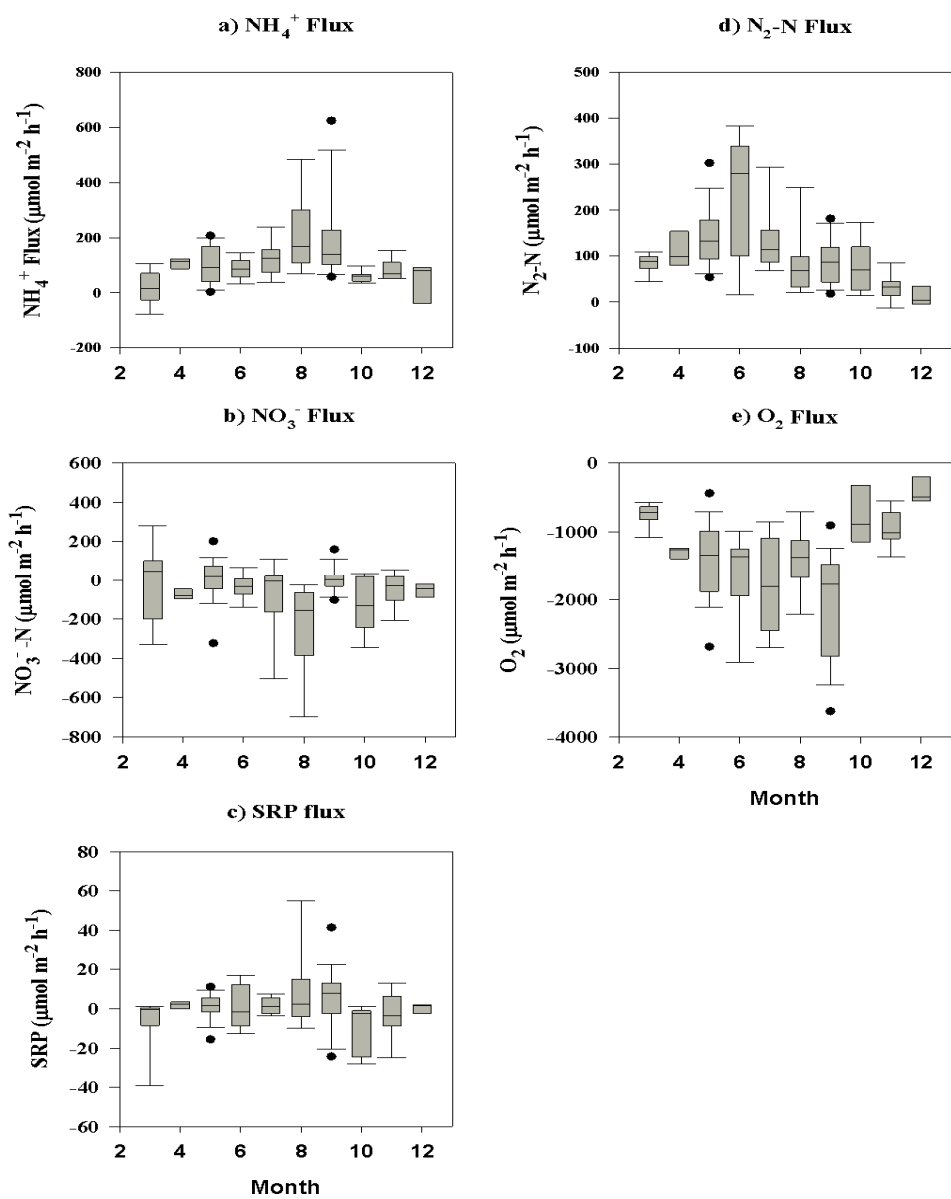


Figure 3-8 Comparison of mean of sediment oxygen demand (SOD ± standard deviation) and CO<sub>2</sub> flux (± standard deviation) in dark incubation of sediments from the upper Sassafra River. Respiration measurements were conducted during the summer of 2009 and 2010. Blank indicates missing data.

### Silty sediments



### Sandy Sediments

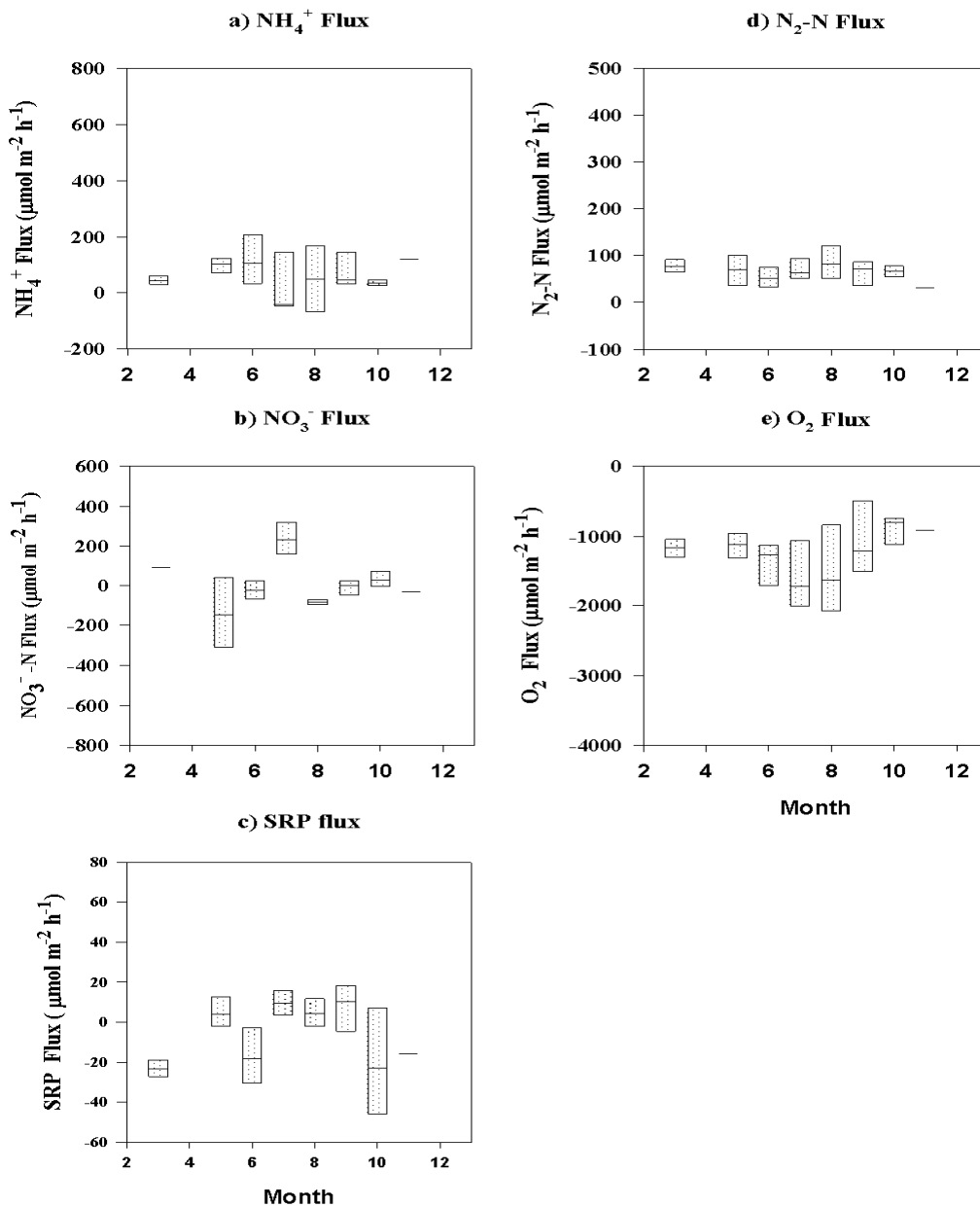


Figure 3-9 Box and whisker plots of monthly  $\text{NH}_4^+$ ,  $\text{NO}_3^-$ , SRP,  $\text{O}_2$  and denitrification fluxes in fine-grained sediments (stations 1A to 3A) and the sandy sediments (station 3B). Data shown are dark flux measurements in Figure 7 and 8. Dash bar presents the average monthly flux rates; the vertical box means the difference between the interquartile ranging from 25% and 75% and vertical bar from 10% to 90%.

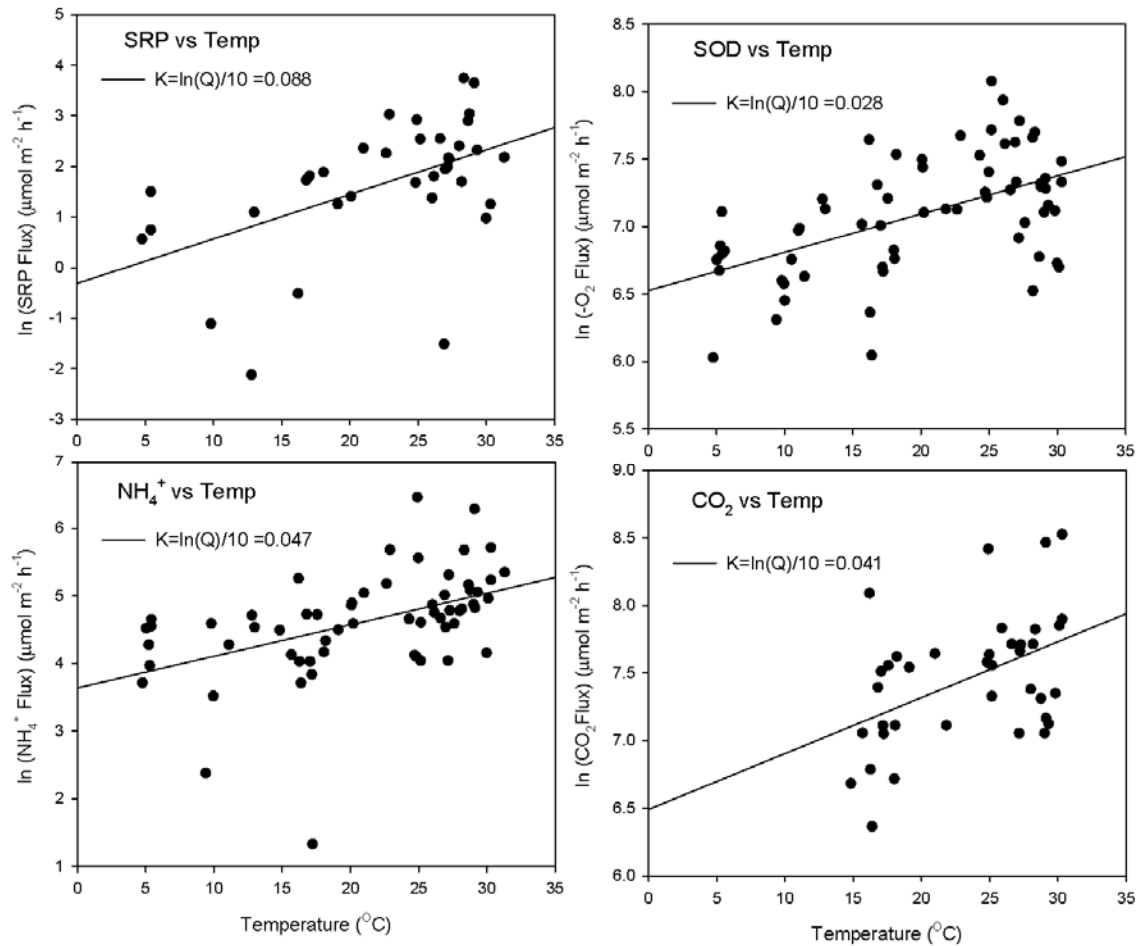


Figure 3-10 Linear regressions of temperature and the natural logarithm of flux rates. These relationships are significantly positive for SRP flux ( $P = 0.002$ ,  $R^2 = 0.35$ ),  $\text{NH}_4^+$  flux ( $P = 0.002$ ,  $R^2 = 0.45$ ), SOD ( $P < 0.001$ ,  $R^2 = 0.28$ ) and  $\text{CO}_2$  ( $P < 0.001$ ,  $R^2 = 0.22$ ). Estimated from dark-incubated cores of the fine-clay sediments (1A-3A) during 2007-2010. Estimated  $Q_{10}$  is 2.3 for SRP, 1.47 for  $\text{NH}_4^+$ , and 1.3 for SOD and 1.5 for  $\text{CO}_2$ .

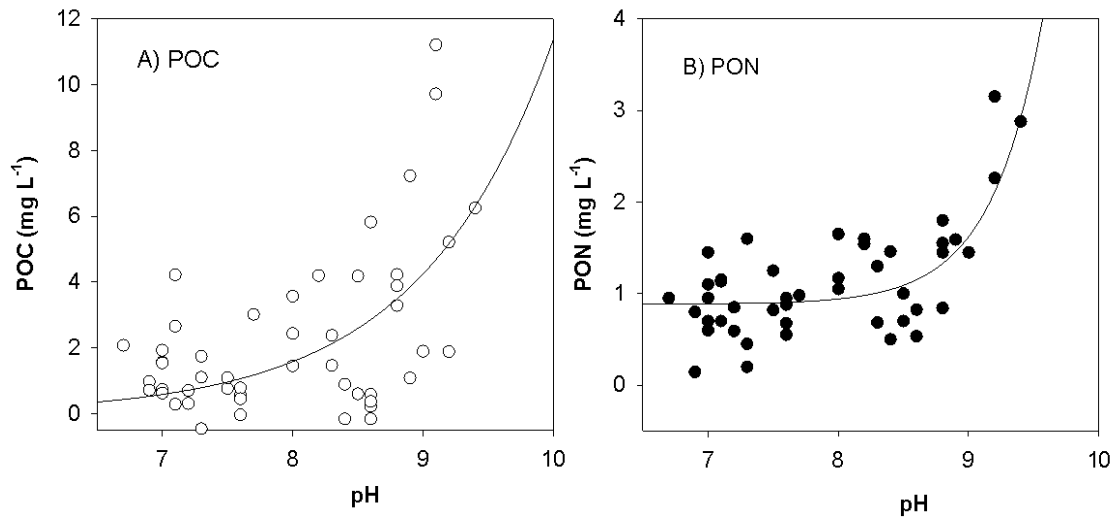


Figure 3-11 Concentration of particulate organic carbon (POC) and particulate organic nitrogen (PON) as a correlation of pH in water column. The regression of  $POC = -0.6 \times 10^{-3} \times \exp(0.98 \times pH)$  ( $n = 49$ ,  $P < 0.001$ ) and  $PON = -0.88 + 8.78 \times 10^{-11} \times \exp(2.54 \times pH)$  ( $n = 43$ ,  $P < 0.001$ ). Data shown from Chesapeake Bay Program records at Drawbridge during June to September for the year of 1986-1998 ([www.chesapeakebay.net/data\\_waterquality.aspx](http://www.chesapeakebay.net/data_waterquality.aspx)).

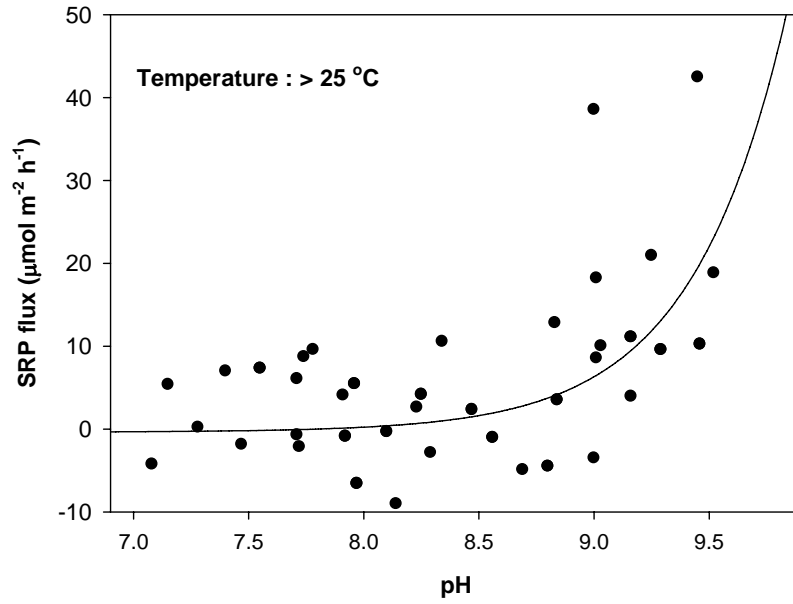


Figure 3-12 pH effects on SRP flux rates in fine-grained sediments with dark incubation. The solid line presents the regression:  $SRP = 8.8483E-009 \times \exp(pH \times 2.2644)$  ( $n=79$ ,  $P < 0.01$ ). Data are ambient pH's (shown in Figure 2) and flux rates of SRP (shown in Figure 7) when water temperature  $> 25$  °C.



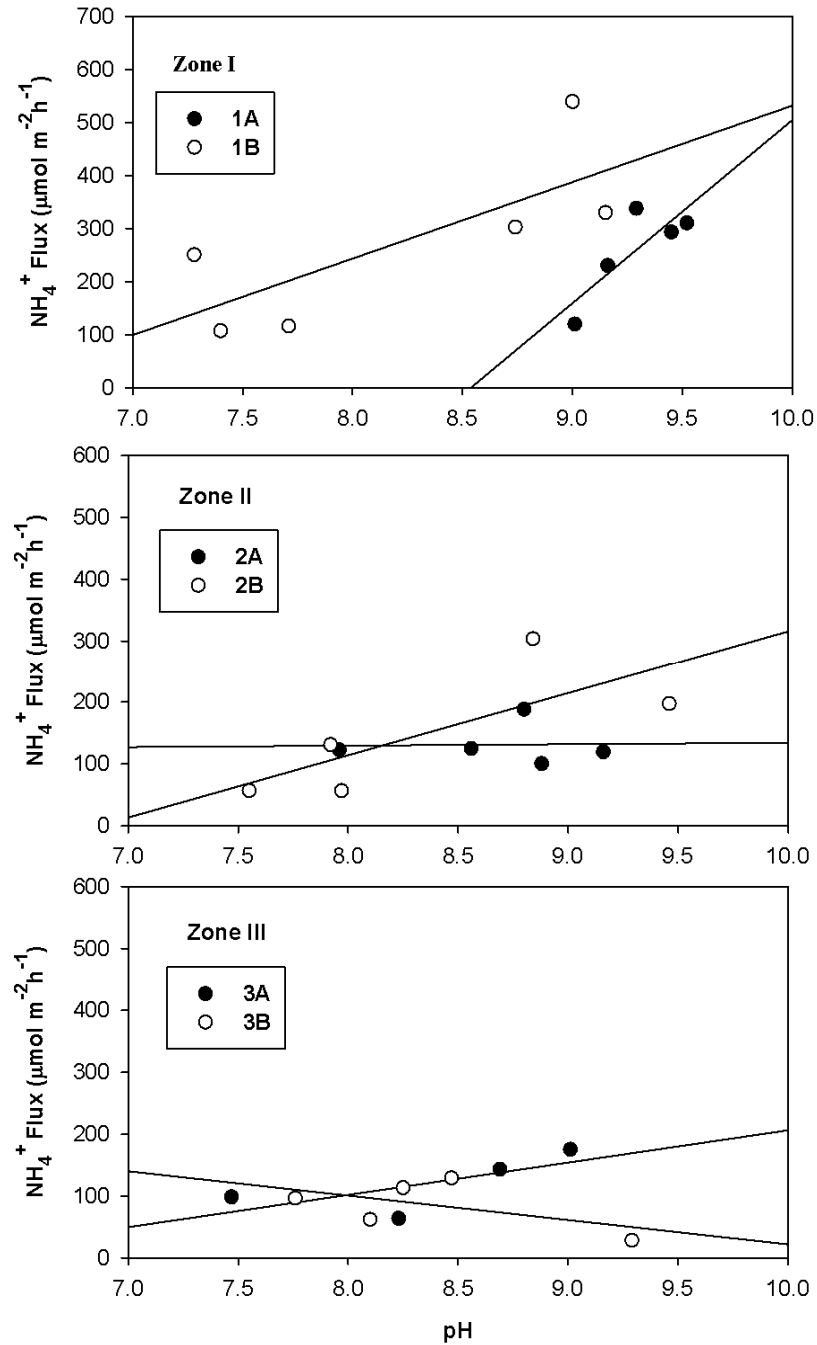


Figure 3-13 The spatial variation of pH and average  $\text{NH}_4^+$  flux rates of sediment cores, taken from the bloom region (Zone I), transitional region (Zone II) and stations outside of bloom (Zone III). Data shown are flux rates of  $\text{NH}_4^+$  in dark (Figure 7) and ambient pH values (Figure 2) at temperature  $> 25^\circ\text{C}$ . The positive linear regressions between pH (x) and  $\text{NH}_4^+$  flux (y) are as follows: in sediment 1A  $y=144.2x - 193.9$  ( $R^2=0.65$ ,  $P < 0.05$ ,  $n = 5$ ); in 1B  $y= 345.2x - 1023.1$  ( $R^2=0.68$ ,  $P < 0.01$ ,  $n = 6$ ); in 1C:  $y = 100.7x - 691.5$  ( $R^2=0.65$ ,  $P < 0.05$ ,  $n = 5$ ). No significant influence existed outside the bloom region.

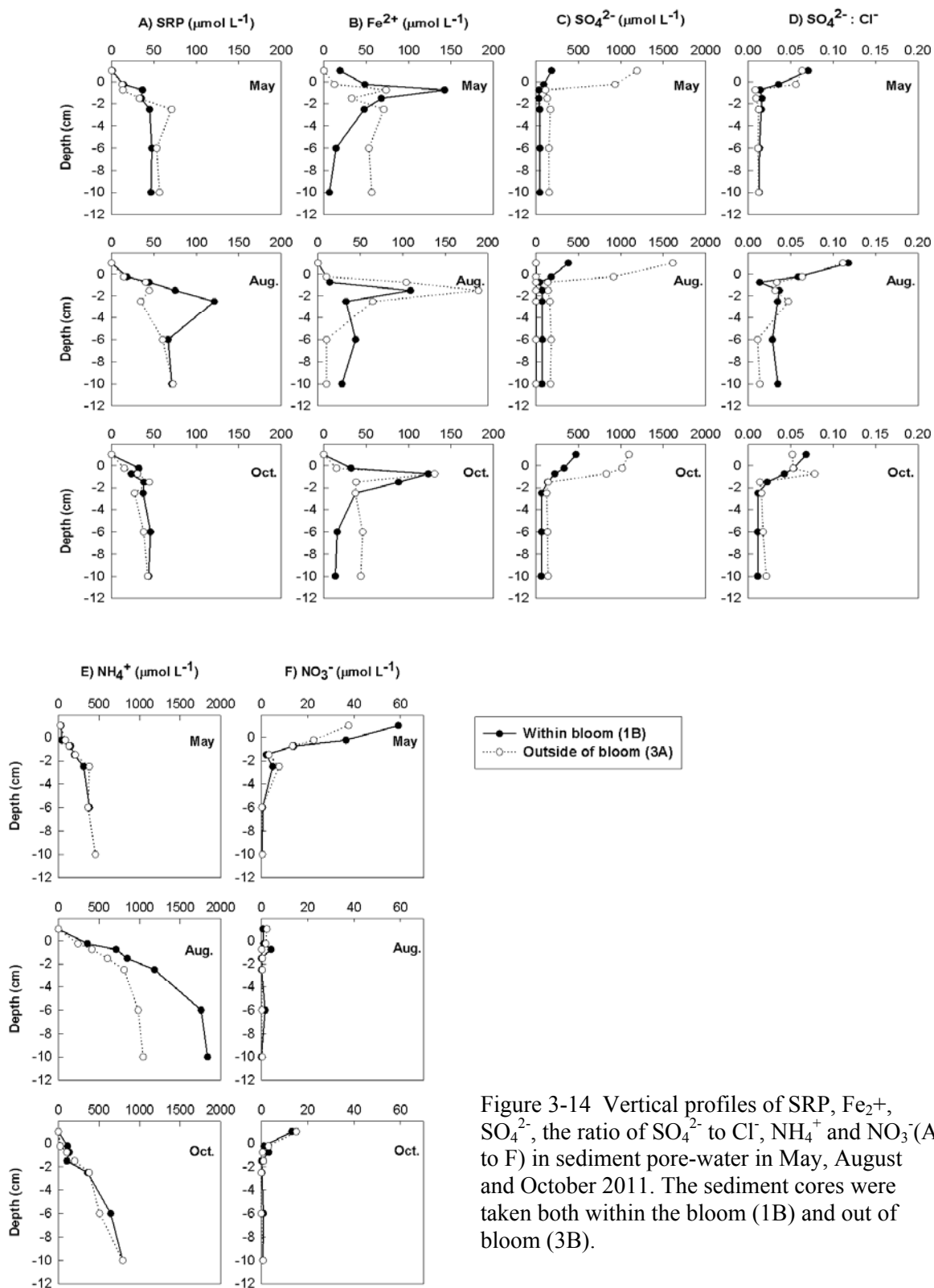


Figure 3-14 Vertical profiles of SRP,  $\text{Fe}_2^+$ ,  $\text{SO}_4^{2-}$ , the ratio of  $\text{SO}_4^{2-}$  to  $\text{Cl}^-$ ,  $\text{NH}_4^+$  and  $\text{NO}_3^-$  (A to F) in sediment pore-water in May, August and October 2011. The sediment cores were taken both within the bloom (1B) and out of bloom (3B).

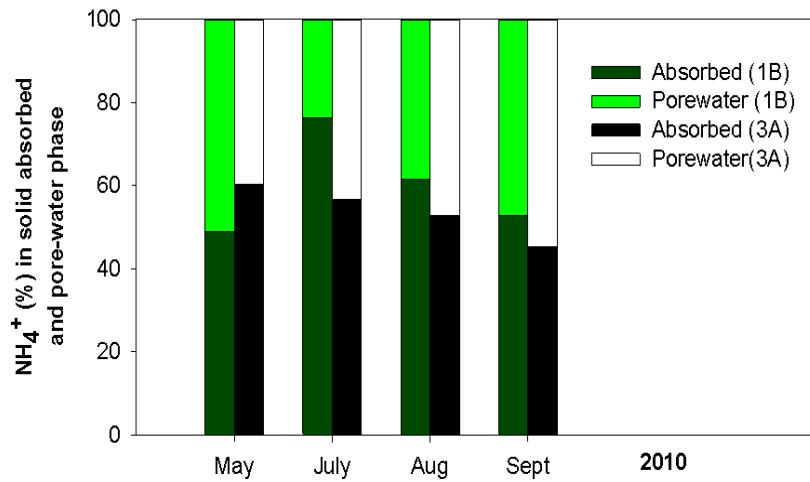


Figure 3-15 The fraction of adsorbed and pore-water  $\text{NH}_4^+$  in the surface sediments from station 1B (within bloom) and 3A (out of bloom). Pore water  $\text{NH}_4^+$  presented in dark green for stations within bloom and in black for stations outside of bloom. Adsorbed  $\text{NH}_4^+$  in solid phase presented in light green and in white for stations within and outside of bloom, respectively. Data calculated as the average changes in top 0-2 cm sediments, taken from May to September in 2010 (Appendix table 1).

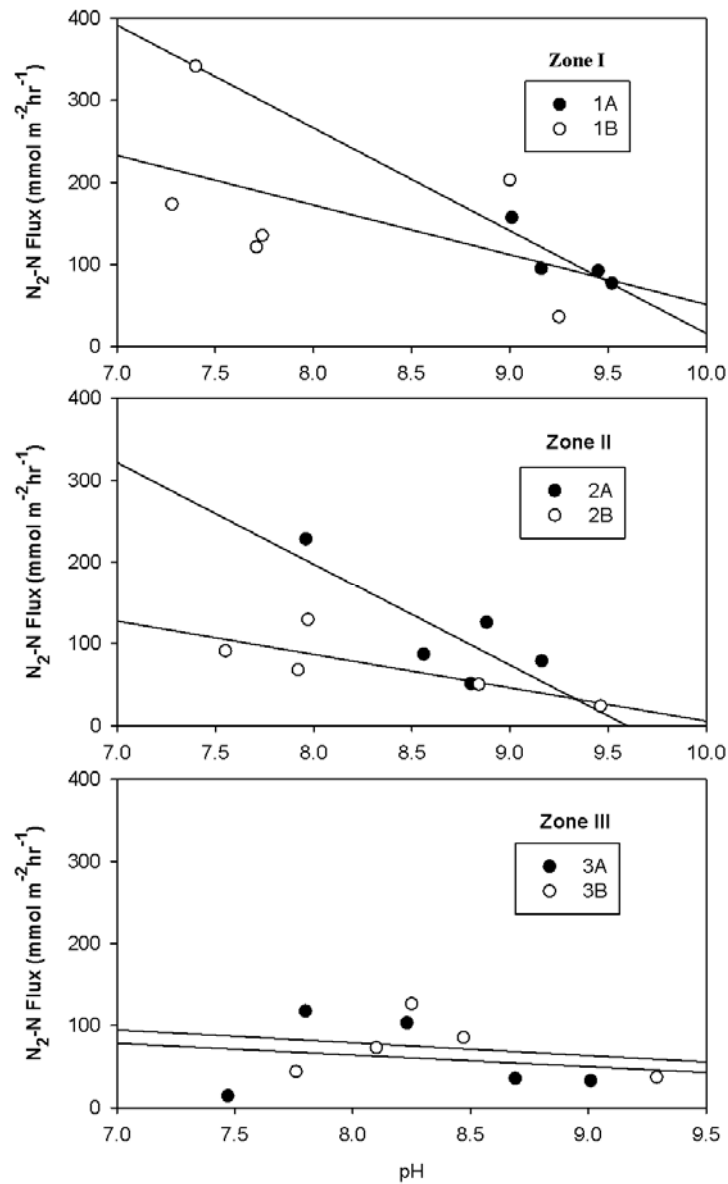


Figure 3-16 The spatial variation of denitrification rates ( $N_2-N$  flux) of sediment cores, taken from the bloom region (Zone I), transitional region (Zone II) and stations out of the bloom (Zone III). Denitrification rates shown are from dark incubations at  $T > 25\ ^\circ C$  during 2007-2010. pH (x) were negatively related to  $N_2$  flux (y) in Zone I and Zone II. The linear regression for 1A :  $y = -125.20x + 1267.95$  ( $R^2 = 0.72$ ,  $P = 0.15$ ,  $n = 4$ ); for 1B:  $y = -60.51x + 656.46$  ( $R^2 = 0.26$ ,  $P = 0.31$ ,  $n = 6$ ); for 2A:  $y = -12.387x + 1188.5962$  ( $R^2 = 0.65$ ,  $P = 0.097$ ,  $n = 4$ ); for 2B:  $y = -40.69x + 412.28$  ( $R^2 = 0.62$ ,  $P = 0.11$ ,  $n = 4$ ).

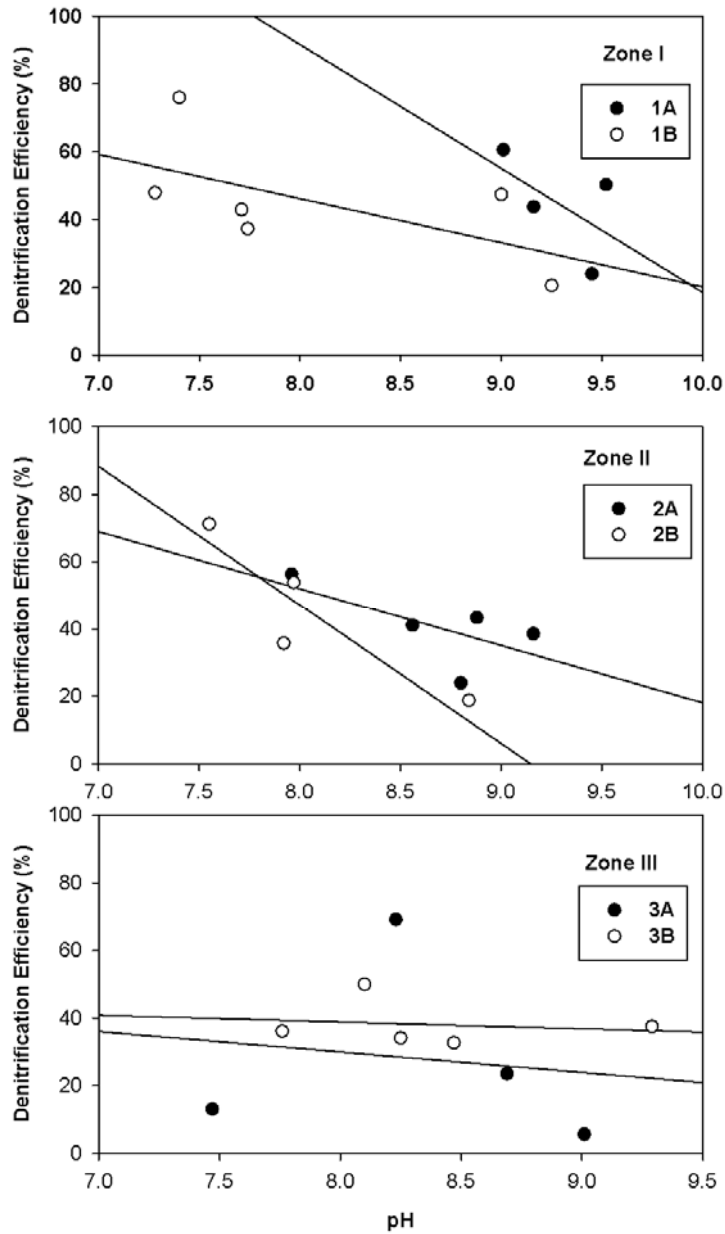


Figure 3-17 Denitrification efficiency (DE%) response to pH elevation in the bloom region (Zone I), transitional region (Zone II) and stations out of bloom (Zone III), when sediments were taken at temperature > 25 °C. DE% (y) is calculated as the percentage of N<sub>2</sub>-N flux to the net DIN flux in dark incubation during 2007-2010. The linear regression for 1A :  $y = -36.58x + 384.38$  ( $R^2 = 0.57$ ,  $P = 0.14$ ,  $n = 5$ ); for 1B:  $y = -13.02x + 150.33$  ( $R^2 = 0.36$ ,  $P = 0.20$ ,  $n = 6$ ); for 2A:  $y = -16.94x + 187.62$  ( $R^2 = 0.43$ ,  $P = 0.22$ ,  $n = 4$ ); for 2B:  $y = -41.06x + 375.72$  ( $R^2 = 0.36$ ,  $P = 0.0085$ ,  $n = 4$ ).

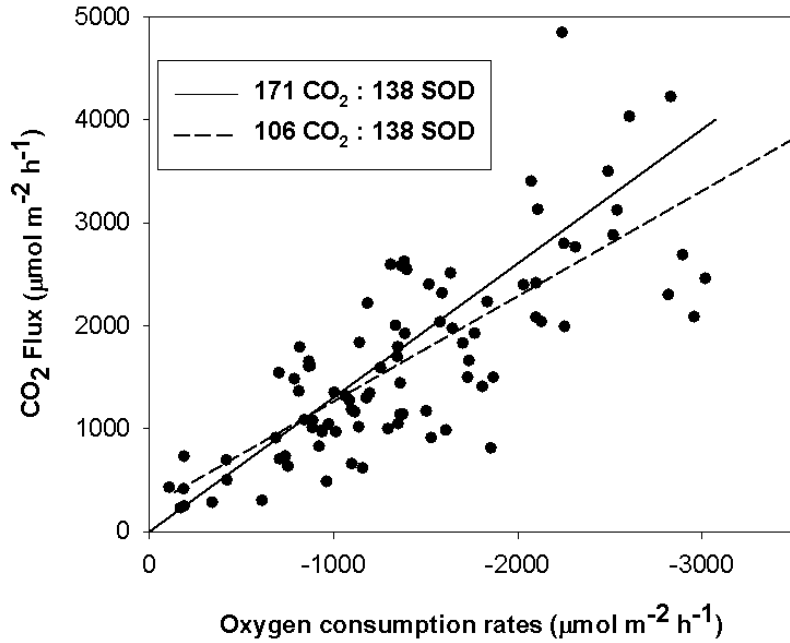


Figure 3-18 The linear relationship of the dark-incubated CO<sub>2</sub> flux rates and sediment oxygen consumption rates ( $K = 1.24$ ,  $P < 0.05$ ) from spring to summer in 2009 and 2010. The estimated slope of CO<sub>2</sub> versus SOD (solid line) is 171: 138, which generally exceeds the predicted stoichiometry that every 106 mol CO<sub>2</sub> production is generated from 138 mol oxygen consumption (dashed line).

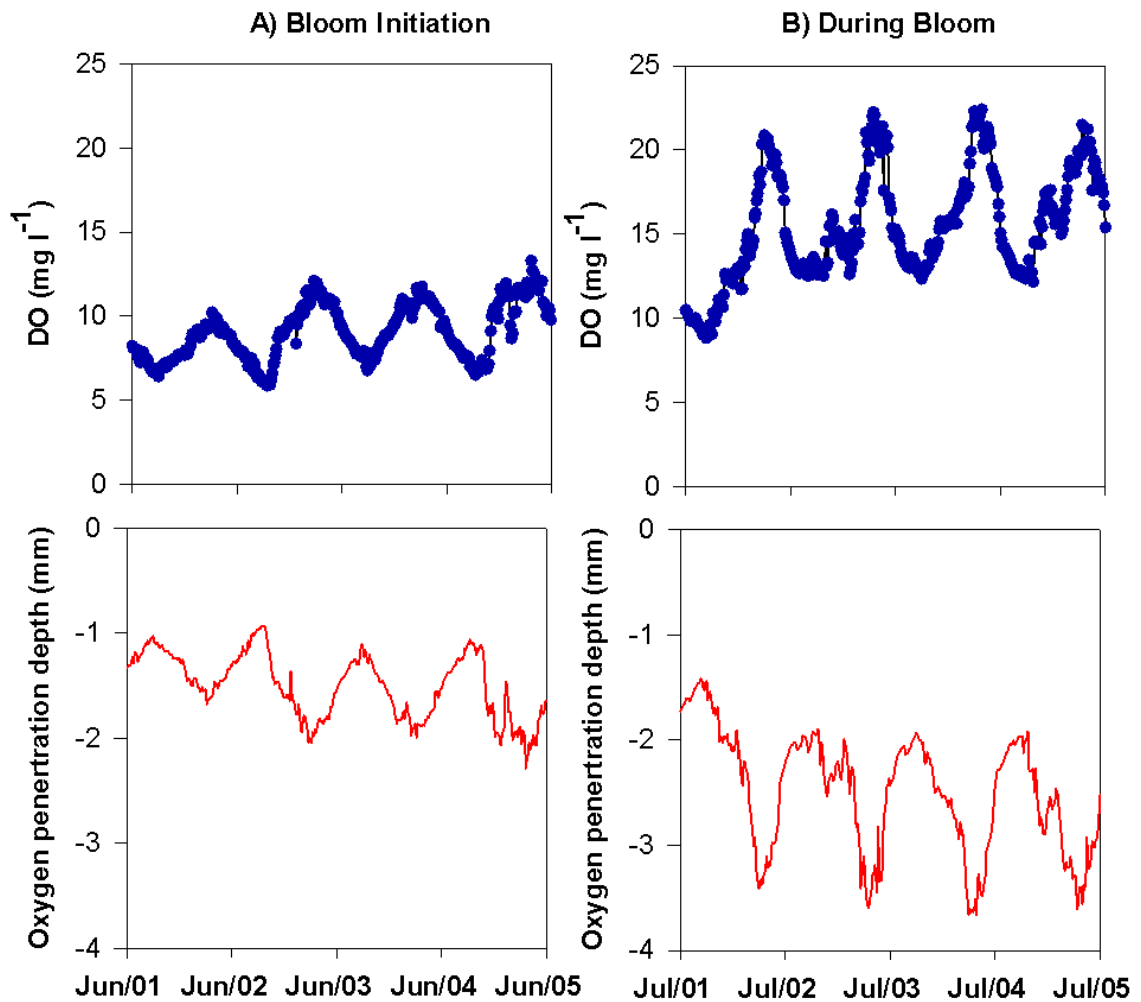


Figure 3-19 Response of oxygen penetration depth to the diel changes of oxygen in the bottom water. DO concentration is the real time measurement in the Budd's Landing (eyesonthebay.com); oxygen penetration depth is estimated from DO diffusion from the bottom water into sediment and oxygen consumption rates of sediment (SOD, measured in June 4<sup>st</sup> and July 1<sup>st</sup>, 2010).

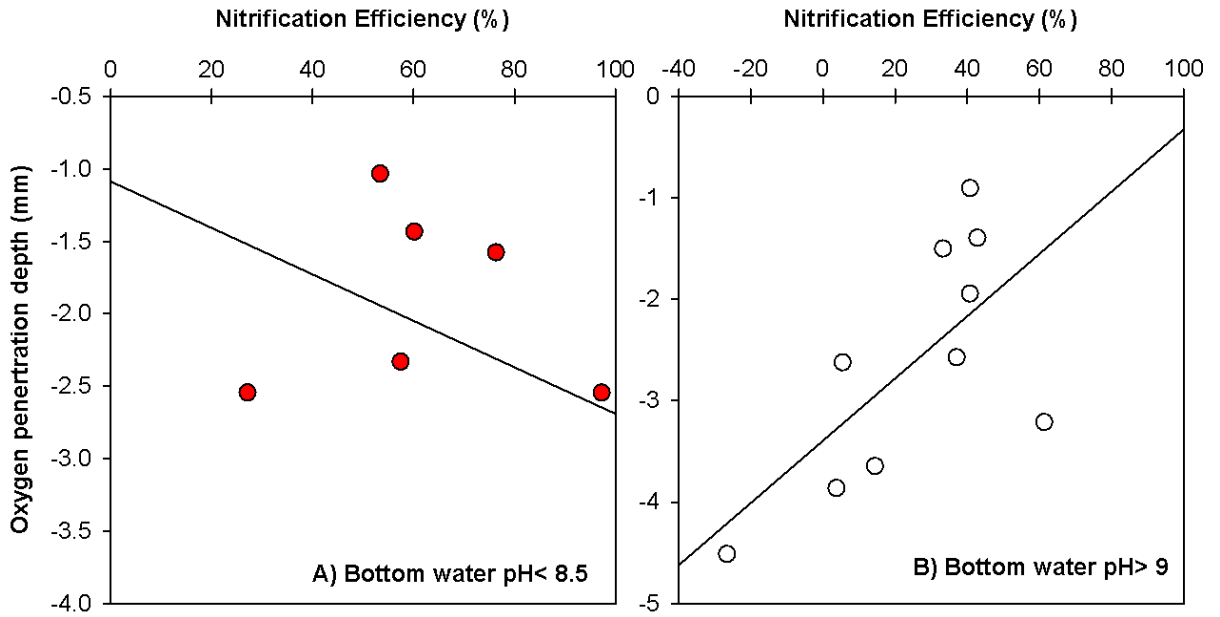


Figure 3-20 Oxygen penetration effects on nitrification efficiency during non-bloom (A) and bloom periods (B). Nitrification efficiency were estimated from flux rates of  $\text{NO}_3^-$  and  $\text{N}_2$  as well as the N remineralization rates from respiration rates when  $\text{NO}_3^-$  concentration in the water is less than  $25 \mu\text{M}$ . The linear regressions of nitrification % (x) to depth of oxic zone (y) are  $y = -1.60x - 1.08$  ( $P = 0.29$ ;  $R^2 = 0.21$ ) and  $y = 3.06x - 3.39$  ( $P = 0.036$ ;  $R^2 = 0.44$ ).

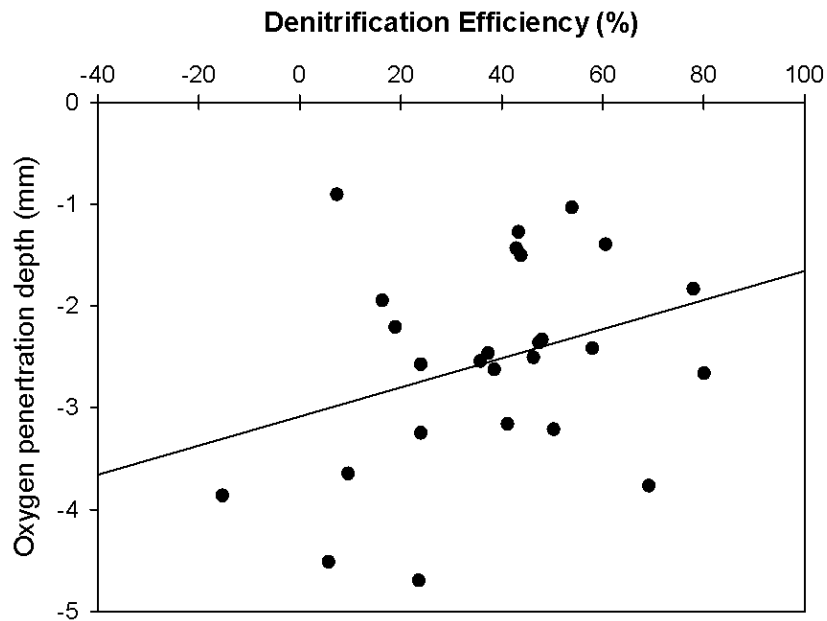


Figure 3-21 Oxygen penetration depth effects on denitrification rates (DE %). Data shown are similar to nitrification efficiency in the whole pH range of 7– 9.52 in the bottom water during the sediment core sampling. DE % is the proportion of  $\text{N}_2$  flux in the estimated N remineralization



rates from SOD. DE % is weekly related to the depth of aerobic zone as a function of  $y = 0.014x - 3.08$  ( $P = 0.11$ ;  $R^2 = 0.10$ ).

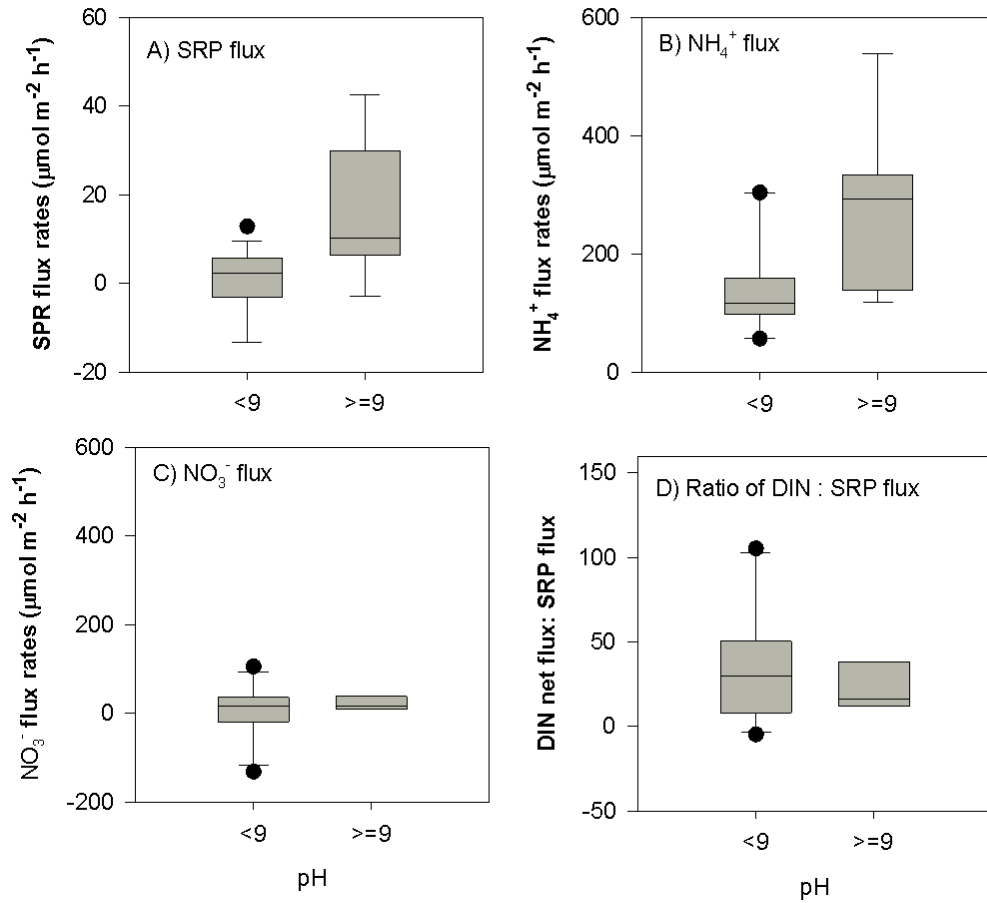


Figure 3-22 The box-whisker of the bioavailable inorganic nutrient release (A-C) and the ratio of DIN: SRP flux rates (D) at high and low pH. Data shown from dark-incubated flux rates on fine-grained sediment during 2007- 2010 ( $T > 25^\circ\text{C}$ ). Horizontal line presents the average value; the vertical box means the difference between the interquartile ranging from 25% and 75% and vertical bar from 10% to 90% confident interval.

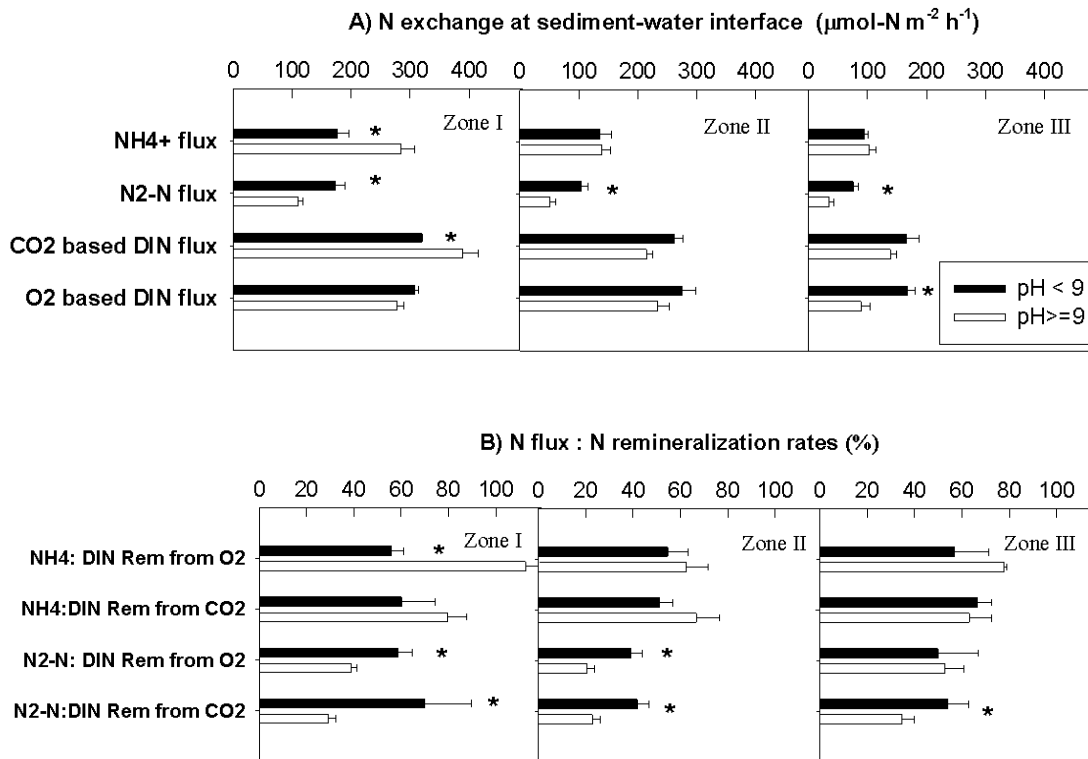


Figure 3-23 Mean ( $\pm$  SE) of A) the estimated N flux across the sediment-water interface and the predicted remineralization rates B) the contribution of  $\text{NH}_4^+$  and  $\text{N}_2$ -N release to total remineralization at bottom water pH < 9 and  $\geq$  9. Dark-incubated sediments flux rates at temperature  $> 25^\circ\text{C}$ , varying from locations within bloom (I), transition zone (II) and out of bloom (III). The oxygen-based remineralization (REM) was converted to  $\text{NH}_4^+$  and  $\text{N}_2$ -N flux rates in 2007-2010 by assuming an  $\text{O}_2$ : DIN ratio of 8.62.  $\text{CO}_2$ - based remineralization for to  $\text{NH}_4^+$  and  $\text{N}_2$ -N flux in 2009-2010 was based on the theoretical  $\text{CO}_2$ : DIN ratio of 6.625. The significant influence of high and low pH on N regeneration was noted in each group (\*,  $P < 0.05$ , Student's t - test).

## Chapter 4      Photosynthesis and nitrogen fixation during cyanobacterial blooms in an oligohaline / tidal fresh estuary

### **Abstract**

Cyanobacteria blooms have frequently been described in eutrophic, freshwater regions of Chesapeake Bay, but estimation of nitrogen (N) fixation and its response to constraining ecological factors are limited. In this study, we estimated cyanobacterial biomass, species composition, photosynthetic and N<sub>2</sub>- fixation rates with increasing light irradiance during cyanobacterial blooms in the Sassafras River, a tidal tributary of Chesapeake Bay, USA. N<sub>2</sub>-fixing cyanobacterial blooms are likely to be triggered by rising temperatures and the switch to low dissolved inorganic N: P ratios in late spring and early summer. Domination of diazotrophic cyanobacteria was taken by heterocystous *Anabaena* spp., reaching a peak biomass of 10.5 mg C L<sup>-1</sup> from June to August; followed by the non-heterocystous *Pseudanabaena* sp. in late August to early September. The unicellular diazotroph *Synechococcus* sp. persisted with a low biomass of < 1 mg C L<sup>-1</sup> from July through the end of the bloom in September. Carbon (C) fixation rates based on Chl *a* were positively related to irradiance in the experimental incubations. N<sub>2</sub> fixation rates, normalized to the biomass of diazotrophic cyanobacteria, generally

increased with increasing irradiances associated with C fixation, with the exception of an extremely high pH and DO period (Jun 30 - July 14 and early Sept. in 2010) caused by high photosynthetic removal of dissolved inorganic carbon (DIC). The constraint of oxygen on nitrogenase activity and C limitation on photosynthesis appeared to inhibit N<sub>2</sub> fixation in the light. Nevertheless, alleviation of oxygen stress by respiration in darkness along with the presence of a night time N<sub>2</sub> fixer *Synechococcus* sp. enhanced dark N<sub>2</sub>-fixation rates, accounting for up to 40% of total N<sub>2</sub> fixation during the dense bloom periods when pH and DO were extremely high.

### **Introduction**

In temperate and eutrophic estuaries, cyanobacterial harmful blooms have been reported widely and frequently (Paerl and Pinckney 1996; Piehler et al. 2002), often causing degradation in water quality and posing threat of toxicity (Codd et al. 2005). Moreover, cultural eutrophication and climate changes in estuaries may create the suitable environments for cyanobacteria, such as nutrient enrichment, warmer water temperatures and associated intensification of stratification in summer. These changes may cause global expansion of cyanobacterial blooms and increase the likelihood of blooms in temperate estuaries (Anderson et al. 2002; Paerl 2008).

One important attribute of some, but not all, bloom-forming cyanobacteria is nitrogen fixation. N<sub>2</sub> fixing cyanobacteria have evolved divergent strategies to protect nitrogenase from oxygen inhibition, reflecting different N fixation mechanisms among species and in light-dark phase (Bothe et al. 2010; Fay 1992). N<sub>2</sub> fixation in heterocystous cyanobacteria (e.g., *Anabaena flos-aquae*) can occur in light by protecting

nitrogenase within the specialized heterocysts (Milligan et al. 2007). Most non-heterocystous cyanobacteria (e.g., *Trichodesmium*) can fix N<sub>2</sub> in light by the combination of temporal and spatial separation of photosynthesis and N<sub>2</sub> fixation (Bergman et al. Berman-Frank et al. 2001; Levitan et al. 2007). But some of diazotrophic cyanobacteria, such as *Oscillatoria* sp. strain 23 (Stal and Krumbein 1985) and *Lyngbya majuscula* (Watkinson et al. 2005), showed nitrogenase activity in both light and dark phase. Unicellular cyanobacteria (e.g., *Synechococcus* and *Synechocystis*) temporally separate the two processes, N<sub>2</sub> fixation occurring in darkness and photosynthesis in light (Falcon et al. 2004; Rippka et al. 1971).

Dissolved N<sub>2</sub> can be reduced to form ammonium and organic nitrogen by diazotrophic cyanobacteria through the catalytic action of enzyme nitrogenase, and provide 'new' N to support primary productivity in N limited waters (Paerl and Zehr 2000). For instance, non-heterocystous filamentous cyanobacteria (e.g. *Trichodesmium*) have been found to support 50% of new production in tropical and subtropical ocean areas where they are common (Mulholland 2007). Unicellular N<sub>2</sub>-fixing cyanobacteria may be distributed globally and responsible for 10% of new production in the oceans (Montoya et al. 2004).

In contrast to ocean, estuarine N<sub>2</sub> fixation rates are generally thought to be low due to the high N loadings, and thus not been considered in ecosystem analyses and modeling of N dynamics (Boynton and Kemp 2009). However, cyanobacterial blooms occur frequently at the tidal-fresh and oligohaline zone of the tributaries and main channel in Chesapeake Bay (Tango and Butler 2008). Association of diazotrophic cyanobacteria within *Microcystis* blooms has been observed in summer months (O'Neil

unpublished data). Nitrogenase has been detected in many regions of the Chesapeake Bay with a remarkable diversity in speciation and nitrogenase gene sequences (Jenkins et al. 2004; Short and Zehr 2007). Nevertheless, the mechanisms for cyanobacterial persistence and N<sub>2</sub> fixation are poorly understood.

Nutrients in estuaries have a complicated influence on the growth of N<sub>2</sub> fixing cyanobacteria (Lehtimäki et al. 1997). Generally, N<sub>2</sub> fixing cyanobacteria prefer to use ammonium (NH<sub>4</sub><sup>+</sup>), nitrate (NO<sub>3</sub><sup>-</sup>), urea or other available organic sources of N over energetically costly N<sub>2</sub>-fixation (Capone and Ferrier 1994; Paerl and Pinckney 1996). Nutrient loading into estuaries may enhance primary productivity but may also alter N to phosphorus (P) ratios. Increases in inorganic and organic N inputs can lead to a decline in N<sub>2</sub> fixation rates, absence of N<sub>2</sub>-fixing cyanobacteria, and speciation changes in the phytoplankton community (Howarth et al. 1988). Reductions in N but not P loading may enhance N<sub>2</sub> fixation and favor cyanobacteria over eukaryotic phytoplankton (Paerl 2008).

In estuaries, temperature, salinity and associated physical changes are critical to determine cyanobacterial magnitude and distribution. Rising temperatures can promote cyanobacterial growth (Lewis 1984), and increase their competitive advantage (Coles and Jones 2000). Enhancement in the frequency, strength, and duration of stratification with temperature, which may minimize the availability of remineralized nutrient in surface water, may benefit buoyant cyanobacteria that access nutrients in the hypolimnion (Paerl 2008; Wagner and Adrian 2009). With different salinity tolerance among species, cyanobacterial growth, photosynthesis and nitrogenase activity vary greatly with salinity increase (Tonk et al. 2007). Salinity changes in estuaries may

consequently impact the spatial and temporal distribution of cyanobacterial blooms as well as species composition (Moisander et al. 2010; Sellner et al. 1988).

Beyond direct regulation of environmental factors on cyanobacterial blooms, photosynthesis during agglomerated blooms also can dramatically enhance intracellular oxygen concentrations and release oxygen into water column (Badger et al. 2006), which can suppress nitrogenase activity in many cyanobacteria (Bergman et al. 1997; Capone et al. 2008).

Reduction of dissolved inorganic carbon (DIC) and elevated pH due to their photosynthetic carbon removal may exert effects on their physiological responses. Although the net acquisition of inorganic carbon ( $\text{CO}_2$  and  $\text{HCO}_3^-$ ) can support photosynthetic  $\text{CO}_2$  fixation, only  $\text{CO}_2$  can serve as the substrate for ribulose biphosphate carboxylase-oxygenase (RuBisco).  $\text{CO}_2$  availability is often limited by its interception from the atmosphere and the water column diffusion rate, which is  $10^4$  times slower than in the atmosphere (Price et al. 2008; Stumm and Morgan 1996). With low carbonate buffering in freshwater and oligohaline environments, further increases in pH from photosynthesis quickly reduces  $\text{CO}_2$  (the main component of DIC in pH range of 7-8.5) and drives the chemical equilibrium from  $\text{HCO}_3^-$  to  $\text{CO}_3^{2-}$ . Taking advantage of  $\text{CO}_2$ -concentrating-mechanisms (CCM) that improve their photosynthetic performance (Price et al. 2008), cyanobacteria (e. g. *Nodularia spumigena*) may competitively survive under DIC limited concentrations and out compete non-CCM eukaryotic phytoplankton in mixed cultures and in situ (Mogelhoj et al. 2006).

However, the limited carbon availability may exert negative effects on C and  $\text{N}_2$  fixation (Bothe et al. 2010; Fay 1992). Once DIC availability is outside the range of

CCM mechanisms, the combined pH and inorganic carbon limitation may negatively affect photosynthesis, growth rate and cause changes in community composition (Carrasco et al. 2008; Hansen 2002). These pH and DIC mediated changes in photosynthetic physiology and in species composition of cyanobacterial blooms can in turn influence N<sub>2</sub> fixation, diel cycles and the cellular C: N ratio of cyanobacteria (Engel et al. 2008; Fu et al. 2008; Gattuso et al. 2010).

In this study, investigations on cyanobacteria blooms were carried out in the upper Sassafras River, where many cyanobacteria possess the capacity to fix N<sub>2</sub> (O'Neil, unpublished data). Following bloom development in 2010, we measured cyanobacterial abundance and speciation, physiological C and N<sub>2</sub> fixation as well as other regulating factors in water quality. Questions are addressed of how changes in environmental variables affect cyanobacterial abundance and species composition and their physiological responses in N<sub>2</sub> fixation. Assuming high irradiance combined with high photosynthetic biomass can lead to high rates of photosynthesis, pH elevation, and carbon depletion (Burton 1987; Hansen 2002; Jones and Stanley 2003), C and N<sub>2</sub> fixation rates were measured at different irradiance levels in laboratory experiments.

### **Materials and Methods**

Sampling was conducted weekly or biweekly from May 10<sup>th</sup> to September 15<sup>th</sup> in 2010 at two adjacent areas in the upper Sassafras River, Budds' Landing (BL) and Drawbridge (DB, Fig. 1). Cyanobacterial blooms have occurred at both locations during most summers in the past decade (MD DNR, Butler, unpublished). BL is located near the head of the river, and DB is a short distance down river close to a marina and sewage



treatment plant in Georgetown, MD. Subsamples were taken for Chlorophyll (Chl *a*), cyanobacterial biomass and species composition as well as and particulate C N P. Laboratory experiments were conducted for N<sub>2</sub> fixation and primary production (H<sup>14</sup>CO<sub>3</sub><sup>-</sup> fixation) rates in samples from the Sassafras River. Dissolved oxygen (DO), pH, dissolved inorganic nutrient and dissolved inorganic carbon (DIC) were measured from the incubations.

#### 4.1.1 *In situ* measurements

Temperature, salinity, DO and pH were measured with a YSI sensor (LI-1000). Photosynthetically active radiance (PAR) was measured at depth intervals of 0.2 m from the surface to bottom depths using a Li-Cor underwater PAR light sensor (Li-192). Data were also obtained for the real time changes of pH, temperature, salinity and DO at BL from the Maryland Department of Natural Resource (MD DNR) (Fig. 3). This monitoring sensor at BL was located in the middle of the 2m water column. Samples were collected from 10 cm below the surface in 10 L carboys and returned for processing to the Horn Point Laboratory within 2 hours. Samples were held overnight at close to *in situ* conditions and used the following day (within 24 hours of collection) for incubations to measure C and N<sub>2</sub> fixation as a function of irradiance.

#### 4.1.2 Chl *a* and cyanobacterial biomass

Samples for Chl *a* were filtered onto 25mm GF/F filters and then stored frozen at -20 °C until analyses. Filters were extracted in 10 ml 90% acetone overnight at -20°C and Chlorophyll *a* was then determined by fluorescence using standard techniques (Parsons et al. 1984). Triplicate samples for cyanobacterial biomass and identification were fixed

with 2.5% glutaraldehyde and enumerated via epi-fluorescence microscopy (Nikon Eclipse E800; filter set for Ex 465-495, DM 505 and BA 515-555). Based on geometric approximations (Hillebrand et al. 1999), biomass was calculated by a regression model for 1-1000  $\mu\text{m}^3$  cells preserved in glutaraldehyde (Verity et al. 1992).

$$\log C = -0.363 + 0.863 \times \log (BV)$$

where C and BV is carbon content of biomass ( $\text{pg cell}^{-1}$ ) and biovolume ( $\mu\text{m}^3 \text{ cell}^{-1}$ ), respectively.

#### 4.1.3 Dissolved and particulate nutrients

Triplicate samples for dissolved inorganic nutrients were filtered through 0.45  $\mu\text{m}$  cellulose acetate syringe filters and frozen at  $-4\text{ }^\circ\text{C}$  for the subsequent analysis of nitrate ( $\text{NO}_3^-$ ), ammonium ( $\text{NH}_4^+$ ) and soluble reactive phosphate (SRP). Concentration of  $\text{NH}_4^+$  was determined using the phenol hypochlorite method (Parsons 1984). Analysis of  $\text{NO}_3^-$  and nitrite ( $\text{NO}_2^-$ ) were conducted with iron chronometry (Kopp and Mckee 1983). SRP concentrations were determined with a UV-spectrophotometer following the procedure of Murphy and Riley (1962). Samples (10-20 ml) for particulate C, N and P were filtered onto pre-combusted ( $450\text{ }^\circ\text{C}$ , 4h) GF/F filters and stored at  $-20\text{ }^\circ\text{C}$ . Particulate C and N were analyzed by CE-440 Elemental Analyzer (Exeter Analytical Inc.) at Horn Point Laboratory Analytical Services (Lane et al. 2011). Particulate P was extracted by HCl solution and analyzed by the colorimetric method (Parsons et al. 1984).

#### 4.1.4 Laboratory measurement of pH, DO and DIC

The measurement of pH, DO and DIC were carried out immediately before and after the 24 h incubations. pH was recorded by a standard Radiometer glass pH electrode

(sensitivity 0.01), calibrated (3 point) with buffers of pH 4, 7 and 10. Dissolved gas samples for DO and DIC were collected in 7 ml test tubes with ground glass stoppers and 5 ml DIC samplers, respectively.  $\text{HgCl}_2$  was immediately added into the dissolved gas samples at a final concentration of  $10 \text{ mg L}^{-1}$  to inhibit microbial activity. Gas samples were sealed and stored under water until analysis. DO values were determined by the  $\text{O}_2$ : Ar method using membrane inlet mass spectrum analysis (MIMS) (Kana et al. 1994; Kana and Weiss 2004). DO concentrations were corrected by dissolved Ar concentrations at  $25^\circ\text{C}$  and ambient salinities (Kana and Weiss 2004). Total DIC concentrations were determined by automatically injecting 0.75 ml samples with phosphoric acid. The DIC pool resulting from the conversion of the three carbon components ( $\text{H}_2\text{CO}_3$ ,  $\text{HCO}_3^-$  and  $\text{CO}_3^{2-}$ ) was qualified with LI-7000 DIC/ $\text{H}_2\text{O}$  analyzer (Model A5-C3). During the 24 h laboratory incubations, changes in pH and DO were also monitored continuously using pH and DO microsensors (NexSens Technology, Inc.). Micro-sensors of pH were calibrated with pH standards. Additional DO subsamples were measured by MIMS at the beginning and the end of 24 h incubation on Jun. 2, Jun. 10, Jul. 28, Aug. 10 and Sept. 15. The results of DO sensors were compared with MIMS measurement and found to be similar.

#### 4.1.5 C and $\text{N}_2$ fixation

We examined C and  $\text{N}_2$  fixation rates at different irradiance to generate the combination of pH elevation and DIC reduction in samples, based on the consumption that carbon removal rates increase with irradiance by photosynthesis. Water samples were acclimated around 2 hours after the samples were brought back to the laboratory in the late afternoon. Triplicates subsamples, used for primary production and  $\text{N}_2$  fixation, were

gently mixed and dispensed into 125 ml glass bottles. To keep their natural diel cycle, subsamples were incubated in a light: dark cycles of 14 h: 10 h at 25 °C, close to the average water temperature of  $26 \pm 3$  °C during the sampling season.

A preliminary incubation of 4 h was conducted to find the irradiance range that was not inhibitory for subsequent experiments. Based on these results, the irradiance levels were 0, 62.5, 125 and 250  $\mu\text{mol photons m}^{-2} \text{s}^{-1}$  in the diel incubations. C fixation rates were measured by phytoplankton incorporation of  $^{14}\text{C}$ -bicarbonate (Parsons et al. 1984). All C fixation rates were calculated with the initial DIC concentrations.  $\text{N}_2$  fixation rates were estimated for the same time periods by the acetylene reduction method using flame ionization detector (FID) gas chromatography (GC-8A) (Capone 1995). The production of ethylene was corrected by the Bunsen gas solubility coefficient (Breitbarth et al. 2004), and then a theoretical ratio of 3:1 was used to convert ethylene production to  $\text{N}_2$  fixation (Capone 1995).

#### 4.1.6 Data analysis

The effects of light on C and  $\text{N}_2$  fixation rates were assessed using a nested ANOVA at the level of sampling time for BL and DB. A Pearson correlation was used to examine co-variation of pH, DO and DIC with irradiance during incubations. Linear regressions were used to quantify the influence of irradiance on both C and  $\text{N}_2$  fixation in each sample. A forward stepwise regression was used to analyze the effects of environmental variation (e.g. nutrients, pH, DIC, DO and irradiance) on photosynthesis and  $\text{N}_2$  fixation rates for samples spanning the whole bloom season. All data analyses were conducted with SAS system for windows (9.0) (Delwiche and Slaughter 2003; Quinn and Keough 2002).

## Results

### 4.1.7 *In situ* conditions

The upper Sassafras River is a turbid, tidal freshwater and shallow estuary. Light attenuation coefficient ( $K_d$ ), calculated from the light flux at different depths, was 3- 5.8  $m^{-1}$ . Cyanobacteria were not concentrated in or near surface layers but were relatively uniformly distributed in the water column, partly as a result of tidal mixing and freshwater flushing. This is consistent with the long-term observations of non- significant differences in Chl *a* concentration between the surface and bottom water depths (unpublished data from Chesapeake Bay Program). The water temperature, ranging from 20 to 32 °C, indicated an increase from spring to summer and decrease after September (Fig. 3). Salinity was generally less than 1 in summer and gradually increased in autumn with a clear spatial pattern, slightly lower salinity at up river (< 1, BL) than the further downstream (0 – 2, DB) (Fig. 1).

### 4.1.8 Cyanobacterial bloom development and succession

Development of cyanobacterial blooms, as indicated by cyanobacterial biomass, DO and pH, can be divided into three stages: stage I (the bloom initiation period, May to mid-June); stage II (first bloom, from mid-June to mid-August), and stage III (second bloom, after late August). The dominant cyanobacteria switched from non-N<sub>2</sub> fixing species of eukaryotic phytoplankton and *Microcystis* spp. to the diazotrophic cyanobacteria, varying in speciation and abundance. Diazotrophic filamentous heterocystous *Anabaena* spp. and non-heterocystous *Pseudanabaena* sp. biomass peaked

in stage II and III, respectively. Unicellular *Synechocystis* spp. were present during both blooms (Table 1 and Fig. 4).

The cyanobacterial bloom is initiated in stage I, with the cyanobacterial domination changing from the non-N<sub>2</sub> fixing genera *Microcystis* spp. to heterocystous N<sub>2</sub>-fixers, including *Anabaena circinalis*, *Anabaena planctonica* and *Anabaena flos-aquae* (Table 1). Concentrations of Chl *a* increased from ~20 µg L<sup>-1</sup> to ~80 µg L<sup>-1</sup> without significant difference between the two stations (Fig. 2). The biomass of *Microcystis* increased by ~ 1 mg C L<sup>-1</sup> from May to Mid-June, but the abundance and proportion of *Anabaena* in the total phytoplankton biomass were slightly different at BL and DB sites (Fig. 4). The biomass of *Anabaena* spp. rapid increased to an estimated 7 mg C L<sup>-1</sup> at BL and 4 mg C L<sup>-1</sup> at DB, respectively. This indicates a increasing tendency of *Anabaena* spp. domination, growing from a small fraction (12- 24%) of the total phytoplankton biomass in May to approximate 95% at BL and over 60% at DB by the end of stage I (Fig.4). The daily average of pH and DO from the monitoring records were similar to *in situ* observations at BL. In correspondence with bloom development, pH gradually rose from 7 to 9 at both stations. The diel fluctuation in DO was large but the daily average DO was relatively constant at 300 – 400 µmol L<sup>-1</sup> (Fig. 3).

In stage II, the N<sub>2</sub>-fixer, *Anabaena* dominated fully developed blooms and peaked in July, reaching 10.5 mg C L<sup>-1</sup> upriver at BL and 6.2 mg C L<sup>-1</sup> at further downstream (DB). The unicellular N-fixer, *Synechocystis*, presented at a relatively low and constant biomass (< 0.8 mg C L<sup>-1</sup>) from July to the end of the bloom season in September. Chl *a* concentration increased rapidly and was generally higher at the relatively up-river station (BL) than DB. At the upriver station, pH increased dramatically

to 10.3, with the daily average of pH > 9.2 for several weeks. The daily average DO almost doubled, with a similar maximum DO from field monitoring (732.9  $\mu\text{mol L}^{-1}$ ) and laboratory observation (643.4  $\mu\text{mol L}^{-1}$ ) (Fig. 3 and Fig. 10). During the same period, no significant increase of Chl *a*, pH nor DO was observed *in situ* at the downstream DB station. The highest value for Chl *a* (112.4  $\mu\text{g L}^{-1}$ ) occurred in early July at DB. The daily maximum of pH was 9.6 and of DO was 454.7  $\mu\text{mol L}^{-1}$  at DB during light experiments (Fig. 2 and Fig 10).

The second cyanobacterial bloom (stage III) occurred after heavy precipitation from August 13 to Aug. 17 (Fig. 2). After the decline of the *Anabaena* dominated blooms, a general increase of *Pseudanabaena* biomass was observed and reached up to 11.2 mg C L<sup>-1</sup> at BL and 6.1 mg C L<sup>-1</sup> at early September (Fig. 4). The diazotroph, *Pseudanabaena* sp., along with a small fraction of *Synechococcus* sp., became prevalent and comprised up to 94% at BL and 42.2 % at DB of the total phytoplankton biomass (Fig. 4). A sharp increase in Chl *a*, pH and DO occurred again, with larger increases at BL than at DB (Fig. 2, 3 and 11). In early September, Chl *a* increased up to 158.2 at BL and 124.7  $\mu\text{g L}^{-1}$  at DB, respectively (Fig.2); the maximum of pH and DO were similar to the highest observation during stage II. Blooms rapidly dissipated at both stations at the end of September, which was followed by the both decrease in pH and DO concentrations (Fig. 3).

#### 4.1.9 Dissolved inorganic nutrients and particulate C, N, P

Dissolved inorganic nutrients decreased with bloom development from spring to summer (Fig. 5). During May to August, concentration of  $\text{NO}_3^-$  and  $\text{NH}_4^+$  at BL declined rapidly from above 40  $\mu\text{mol L}^{-1}$  to less than 1.2  $\mu\text{mol L}^{-1}$  and from 2.1  $\mu\text{mol L}^{-1}$  to the

detection limit, respectively. Similar pattern of DIN concentrations were found at DB, but were generally higher than at the BL. SRP concentrations at both stations declined from 0.5~ 0.6  $\mu\text{mol L}^{-1}$  to 0.03 ~ 0.2  $\mu\text{mol L}^{-1}$ . After the bloom initiation in May, the ratio of DIN: SRP decreased from > 100 to 3 ~ 30 during summers and early autumn, except for an abruptly increased DIN: SRP (> 40) in September at BL (Fig. 5).

The ratio of C: N, N: P and C: P in particulate organic matter varied with time and location (Fig. 6). At the upriver station, particulate C: N ranged from 6 to 12, C: N from 18 to 32 and C: P from 84 to 265. Ratios were generally higher than the Redfield ratio during bloom stage I, and below or close to the Redfield ratio during bloom stage II and III. At DB, the ratios of C: P and N: P declined from above 250 and 20~38, respectively, during stage I to below the Redfield ratio in stage III. The ratios of C: N varied from 6 to 10, which is higher than the Redfield ratio.

#### 4.1.10 Photosynthesis experiments

In the preliminary experiment, photoinhibition of C fixation was not observed in the irradiance range of 0 to 500  $\mu\text{mol photons m}^{-2} \text{ s}^{-1}$ ; therefore irradiances  $\leq 250 \mu\text{mol photons m}^{-2} \text{ s}^{-1}$  were used for subsequent incubations (Fig. 7).

There was a positive correlation of average pH and DO with incubation irradiance and an inverse relationship with DIC during the 24 hour incubations (Table 6). With increased irradiance, enhanced pH and decreased DIC were observed in samples during all incubations (Fig. 8 and Fig.10). With samples in incubations at 250  $\mu\text{mol photons m}^{-2} \text{ h}^{-1}$  from the river head (BL), the daily average pH rose from ~ 7.2 in stage I to ~10.5 in stage II. The daily average DIC concentration coincidentally decreased from over 800  $\mu\text{M}$  to ~300  $\mu\text{M}$  (Fig 10). With samples from DB, pH was enhanced to 9.6 during the bloom



and DIC declined to values as low as  $\sim 500 \mu\text{M}$ . When the bloom died out at both pH during incubations decreased to 7.5  $\sim$  8.6 and DIC increased to around  $800 \mu\text{M}$  (Fig. 10).

As expected, Chl *a*-normalized C fixation rates increased linearly with irradiance (Table 2); however, the linear regression coefficients ( $\alpha^{\text{chl}}$ , photosynthetic efficiency) changed with bloom development (Table 3). The estimated  $\alpha^{\text{chl}}$  decreased from stage I ( $>20 \text{ mg C (mg Chl } a)^{-1} (\mu\text{mol photon}^{-1} \text{ m}^{-2} \text{ s}^{-1}) \text{ h}^{-1}$ ) to a minimum in stage II ( $< 8.5 \text{ mg C (mg Chl } a)^{-1} (\mu\text{mol photon}^{-1} \text{ m}^{-2} \text{ s}^{-1}) \text{ h}^{-1}$ ), and then rose again to above  $9 \text{ mg C (mg Chl } a)^{-1} (\mu\text{mol photon}^{-1} \text{ m}^{-2} \text{ s}^{-1}) \text{ h}^{-1}$  at the end of stage III. During stage II, the correlation of photosynthesis with irradiance was non-significant in 3 out of 4 incubations under the conditions of low DIC and elevated pH (Fig 8 and 10). Moreover, C fixation rates at  $250 \mu\text{mol photons m}^{-2} \text{ h}^{-1}$  declined from  $6.2\text{-}7.8 \text{ mg C (mg Chl } a)^{-1} \text{ h}^{-1}$  in stage I, reached a minimum of less than  $1 \text{ mg C (mg Chl } a)^{-1} \text{ h}^{-1}$  in stage II, and then rose to  $2\text{-}4 \text{ mg C (mg Chl } a)^{-1} \text{ h}^{-1}$  in stage III. Net C uptake rates were below  $2 \text{ mg C mg (mg Chl } a)^{-1} \text{ h}^{-1}$  and did not significantly increase with irradiance when DIC concentrations were  $< 540 \mu\text{mol L}^{-1}$  (Fig. 9). Above this level, photosynthetic rates were positively related to DIC supply and irradiance with  $\alpha^{\text{chl}}$  ranging from  $65.3$  to  $117.1 \text{ mg C (mg Chl } a)^{-1} (\mu\text{mol photon}^{-1} \text{ m}^{-2} \text{ s}^{-1}) \text{ h}^{-1}$ .

#### 4.1.11 $\text{N}_2$ fixation

$\text{N}_2$  fixation was first detected in mid-June when the ratio of DIN: SRP had decreased from over 100 to  $< 30$ . According to a preliminary experiment,  $250 \mu\text{mol photons m}^{-2} \text{ s}^{-1}$  was determined to be close to the light saturation for photosynthesis but

was not high enough to inhibit N<sub>2</sub> fixation in laboratory incubations. N<sub>2</sub> fixation was inhibited at incubation irradiances of 500 μmol photons m<sup>-2</sup> s<sup>-1</sup> (Fig. 7).

In the range of 0 to 250 μmol photons m<sup>-2</sup> s<sup>-1</sup>, irradiance usually significantly enhanced N<sub>2</sub> fixation rates based on N<sub>2</sub>-fixing cyanobacterial biomass for samples taken from both stations (Table 4 and Table 8). However, in samples from BL in stage II and from DB in stage III, biomass specific N<sub>2</sub> fixation did not significantly increase as a function of irradiance (Table 4).

In the bloom initiation period (stage I), N<sub>2</sub> fixation rates incubated at 250 μmol photons m<sup>-2</sup> s<sup>-1</sup> could reach up to 1600 pmol N mg C<sup>-1</sup> d<sup>-1</sup> in the samples from BL and up to 540 pmol N mg C<sup>-1</sup> d<sup>-1</sup> in the samples from DB. Dark N<sub>2</sub> fixation rates were below 36 pmol N mg C<sup>-1</sup> d<sup>-1</sup> and sometimes undetectable.

Stage II and III of the bloom were characterized by elevated pH / DO and low DIC and SRP concentrations (Fig.3 and 5). In comparison with stage I, N<sub>2</sub> fixation rates were generally lower in stage II and III, and tended to decrease with rising pH and DO during blooms (Fig. 10). In samples taken during the intensive bloom at BL on June 30 and July 14 and from both stations on Sept 2, N<sub>2</sub> fixation rates dropped below 200 pmol N mg C<sup>-1</sup> d<sup>-1</sup> at an incubation irradiance of 250 μmol photons m<sup>-2</sup> s<sup>-1</sup>.

There was a positive relationship between N<sub>2</sub> fixation rates and irradiance in most of the incubated samples as determined by linear regression (Table 4), but the correlations were usually weak or non-significant during bloom stage II and III at BL and stage III at DB (Table 4). Although N<sub>2</sub> fixation rates remained higher during the light: dark = 14 : 10 incubation than the 24 h dark treatment, dark period N<sub>2</sub> fixation increased up to 60 pmol N mg C<sup>-1</sup> d<sup>-1</sup> during the dense bloom periods. Assuming that N<sub>2</sub> fixation

rate in the 24 h dark incubation was similar to the rates during the dark period of light: dark incubation, dark period N<sub>2</sub> fixation could account for 40 – 62% of daily N<sub>2</sub> fixation in samples of stage II from upriver and for 20 – 45% of daily N<sub>2</sub> fixation in samples from downstream when the bloom expanded during the *Pseudanabaena* bloom (stage III) (Fig. 12).

#### 4.1.12 The environmental effects on C and N<sub>2</sub> fixation rates

The environmental effects on both C and N<sub>2</sub> fixation rates were estimated using a forward stepwise regression analysis (Table 7 and 8). Both C and N<sub>2</sub> fixation rates were positively related to irradiance and SRP concentration. DIC concentration had a positive effect on C fixation; while DO had a negative effects on N<sub>2</sub> fixation rates. In this study, DIN was usually limiting for cyanobacterial blooms relative to SRP (Fig. 4). N: P ratios were negatively correlated with N<sub>2</sub> fixation rates (Table 8).

## **Discussion**

#### 4.1.13 Bloom Stage I

The cyanobacterial blooms in the Sassafras River may be initiated by seasonal increases in water temperature (Fig. 3). In the culture experiments, rising temperatures were positively related to growth and photosynthetic rates of cyanobacteria (e.g. *M. aeruginosa*, *M. ichthyoblabe* and *A. aphanizomenoides*) (Coles and Jones 2000; Sabour et al. 2009). Cyanobacteria appeared to become more successful competitors than diatoms and green algae as temperatures approach and exceed 20 °C (> 20<sup>0</sup>C) (Amirbahman et al. 2003; Coles and Jones 2000). This is likely a result that the growth

rates of freshwater eukaryotic phytoplankton generally stabilize or decrease while growth rates of many cyanobacteria increase, providing a competitive advantage (O'neil et al. 2011; Paerl and Huisman 2009).

Moreover, the decreased DIN: SRP ratios during May to June (Fig.5) favor the diazotrophic cyanobacteria, evidenced by the increased cyanobacterial biomass and the succession of *Microcystis* spp. toward *Anabaena* spp. dominance in phytoplankton community by June (Fig. 4). In spring DIN and SRP are higher than other seasons due to the maximum freshwater run-off and low nutrient consumption in the water during this period. Non-N fixers were dominant at DIN: SRP > 50 in May. However, dissolved N limitation after June in the water column (Fig. 5) promoted the dominance by *Anabaena* spp., which may satisfy its need for N by dinitrogen reduction. Besides, N<sub>2</sub> fixation possibly supported the growth of co-occurring non-N<sub>2</sub> fixing cyanobacteria, such as *M. wesenbergii* and *M. aeruginosa* (Howarth et al. 1988). Evidence suggests the release of fixed N from diazotrophic cyanobacteria into the water as NH<sub>4</sub><sup>+</sup>, amino acids or other organic N compounds (Carpenter et al. 1999; Glibert et al. 2004), and this could support the growth of the bacteria and other phytoplankton (Mulholland 2007; Mulholland et al. 2004).

Consistent with previous studies (Coles and Jones 2000; Lewis 1984), photosynthesis generally increases with light in stage I (Fig. 8). The maximum rates of photosynthesis, at 250 μmol photons m<sup>-2</sup> h<sup>-1</sup> in each experimental incubation, were below or close to the maximum photosynthetic rates reported from cultures of cyanobacteria, 2.9 – 3.8 mg C mg Chl a<sup>-1</sup> h<sup>-1</sup> observed for *A. flos-aquae* at 20 °C (Oh et al. 1991; Sabour et al. 2009), 6.8 mg C mg Chl a<sup>-1</sup> h<sup>-1</sup> observed for *M. aeruginosa* at 25 °C (Coles and

Jones 2000; Oh et al. 1991). The average photosynthetic rates were  $6.98 \text{ mg C mg Chl } a^{-1} \text{ h}^{-1}$ , in the range of  $1.4 - 24.5 \text{ mg C mg Chl } a^{-1} \text{ h}^{-1}$  during a cyanobacterial summer bloom in the tidal freshwater zone of Potomac River, another Chesapeake Bay tributary (Jones 1998). The increase in photosynthesis rates within our experimental light irradiances (8), estimated by photosynthetic efficiency ( $\alpha^{\text{chl}}$ ), was consistent with observation of  $2.79 - 14.4 \text{ mg C} \cdot \text{mg Chl } a^{-1} \text{ h}^{-1} \cdot \mu\text{mol photon}^{-1} \text{ m}^{-2} \text{ s}^{-1}$  in the Potomac river (Jones 1998).

The dominance of cyanobacteria (Fig. 4) and light dependent C fixation (Fig. 8) were consistent with previous study for their adaption, succession and dominance in phytoplankton community when water column  $\text{CO}_2$  concentrations are drawn down and pH are enhanced with bloom development (Oliver and Ganf 2000). Although photosynthesis driven-pH elevation from 7 to 9 resulted in DIC decrease and speciation changes from  $\text{CO}_2$  to mainly  $\text{HCO}_3^-$ , cyanobacteria may benefit from carbon concentrating mechanisms (CCM) and buoyancy. All cyanobacteria have CCM mechanisms that improve the efficiency of  $\text{CO}_2$  fixation by multiple  $\text{C}_i$  transporter and carbonic anhydrates to enhance  $\text{HCO}_3^-$  affinity and transportation (Beardall et al. 1998; Ogawa and Kaplan 2003). Partition of Rubisco into micro-compartments within cyanobacteria, known as Carboxysomes, can increase efficiency of CCM mechanisms by generating a high concentration of  $\text{CO}_2$  around the Rubisco enzyme (Badger et al. 2006; Beardall and Giordano 2002). In addition, surface-dwelling cyanobacteria (e.g., *Anabaena*, *Pseudanabaena*, *Microcystis*) may have an advantage over other phytoplankton due to their closer proximity to atmospheric  $\text{CO}_2$  that may rapidly diffuse into surface waters and promote their growth (O'neil et al. 2011; Oliver 1994; Paerl and Huisman 2009).

The increase in N<sub>2</sub> fixation rates with irradiance (Table 3 and Fig. 10) were consistent with the field study of N<sub>2</sub> fixation by Severin and Stal (2008) during the *Anabaena* spp. dominated blooms. The low dark N<sub>2</sub> fixation rates may be a result of the *Anabaena* spp. dominance, with co-occurrence of oxygenic photosynthesis and N<sub>2</sub> fixation in the day time. Heterocysts have lost photosystem II and hence the capacity of oxygenic photosynthesis (Adams and Duggan 1999). Moreover, the cell envelope of heterocysts represents a gas diffusion barrier and any O<sub>2</sub> that enters the cell is scavenged by an efficient and high-affinity respiratory system (Walsby, 2007). Hence, *Anabaena* spp. can spatially separate photosynthesis in the vegetative cells from N<sub>2</sub> fixation in the heterocysts (Milligan et al. 2007).

N<sub>2</sub> fixation in each experiment with irradiances below 250 μmol photons m<sup>-2</sup> s<sup>-1</sup>, and the positive relationship between C and N<sub>2</sub> fixation in the bloom stage I suggests a co-dependence (Table 5). Cyanobacteria can meet the high energy demand of N<sub>2</sub> fixation, which requires ATP and reductants to convert N<sub>2</sub> to ammonium (Bothe et al. 2010), and photosynthetically produced carbon skeletons to assimilate fixed nitrogen (Cox 1969). Formation of ammonium through N<sub>2</sub> reduction to, in return, supports growth and photosynthesis of the cyanobacterial community.

#### 4.1.14 Bloom Stage II

During June to August, the cyanobacterial bloom was more intense at BL, with the Chl *a* maximum 48% higher than at DB (Fig. 2). The increase in biomass of N<sub>2</sub>-fixing cyanobacteria may have been stimulated by a deficiency in N and concomitant sufficiency in P. The ratio of DIN: SRP in stage II was in the range of 3 – 20 (95% confidence limit), supporting the dominance of N<sub>2</sub>-fixing species (Fig. 4 and Fig. 5).

ranging from 0.18 – 4.2  $\mu\text{mol L}^{-1}$ , may not be a strong limiting factor for N and C fixation in this tributary when high pH is maintained in the water column (Fig. 5). Inorganic P input from land erosion and agriculture runoff is an important seasonal input of P to the Sassafra River (Sassafra River Association 2010). Additionally, cyanobacteria may alleviate their P limitation through physiological functions such as the luxury uptake and storage of P (Krauk et al. 2006); the ability to utilize P from the dissolved organic P pool (Dyhrman et al. 2006; Dyhrman and Haley 2006; Dyhrman and Ruttenberg 2006); and use of surface-adsorbed phosphate (Sanudo-Wilhelmy et al. 2004).

The persistence of cyanobacteria may benefit from the high pH that was maintained from July to August in the poorly buffered brackish water of the upper Sassafra River. Even though SRP concentration in the water decreased from spring to summer with increases in nutrient assimilation and less land input of P during the summer drought period, P consumption by cyanobacteria in the water column may be quickly compensated for by pH-driven P release from sediment and suspended particles (Seitzinger 1991). Phosphate release due to high pH can constitute a high fraction (30 – 100%) of P demand during cyanobacterial blooms in lakes and oligohaline estuaries (Seitzinger 1991; Xie and Xie 2003). In addition, cyanobacteria associated with high pH may also relieve grazing pressure by some small sized zooplankton on themselves. These may benefit the persistence of *Anabaena* spp. and appearance of unicellular *Synechococcus* sp. (Fig. 4). When large cyanobacteria (*Anabaena flos-aquae*, *Aphanizomenon flos-aquae*, large *Microcystis* colonies) were abundant, some *Daphnia* spp. showed reduced reproduction and development due to toxin production from

cyanobacteria (Burns 1987). High pH (9-10.6) also suppresses the growth of *Daphnia longispina*, *Bosmina longirostris* and *Chydorus sphaericus* (Hansen et al. 1991).

However, the photosynthetic carbon consumption that occurred during dense bloom periods caused dramatic elevations of pH and reduction of DIC at BL (Fig. 3 and 8). The rapid rise of pH shifted the DIC equilibrium away from  $\text{HCO}_3^-$  towards  $\text{CO}_3^{2-}$ , and even caused depletion in available inorganic carbon ( $\text{CO}_2$  and  $\text{HCO}_3^{2-}$ ). Although  $\text{CO}_2$  production via dark respiration, supplement from air-water exchange and CCM mechanisms may alleviate carbon limitation for cyanobacteria maintenance in high biomass (Beardall et al. 1998; Ogawa and Kaplan 2003), the limited DIC concentrations reduce photosynthetic carbon uptake efficiency (Fig 10 and Table 3). In previous studies, carbon limitation and high pH were found to inhibit growth, cell division and photosynthesis of cyanobacteria such as *M. aeruginosa* and *A. cylindrica* (Qiu and Gao 2002; Yamamoto and Nakahara 2005). Alternatively, *Anabaena* biomass increased ~20 fold after  $\text{Na}_2\text{CO}_3$  enrichment and became competitive in a mixed phytoplankton community in a high pH and N-limited lake (Unrein et al. 2010).

During the mid-bloom, oxygen produced by photosynthesis resulted in super-saturated DO values and extremely high pH up to above 10, which showed a similar range of pH and DO values observed in the 24 h incubations (Fig. 10) to the field diel fluctuation (Fig. 3). High DO concentration can inhibit the activity of nitrogenase, the enzyme responsible for the reduction of  $\text{N}_2$  to ammonium (Paerl and Zehr 2000). Even though irradiance increase can slightly promote Chl *a*-specific C fixation rates, the response of  $\text{N}_2$  fixation rates was reduced in the light and turned into dark fixation from end of June to July (Fig. 10 and 11), partly as a result of light-stimulated oxygen



accumulation, carbon limitation as well as their different tolerance among cyanobacterial species (Boyd et al. 2010).

Biomass specific  $N_2$  fixation rates to irradiance became weaker in July (Table 4), obviously reflecting the constraint of carbon limitation, high pH, and oxygen depression during dense bloom.  $N_2$  fixation has a high-energy demand (16 mol ATP for the reduction of 1 mol  $N_2$ ) (Bergman et al. 1997), and requires the photosynthetic production of ‘assimilatory power’ (ATP and reducing equivalents in the form of NADPH or reduced ferredoxin). Several culture studies that used changing  $pCO_2$  to adjust water column DIC concentration have suggested that the lower DIC availability, the more limitation on growth, C fixation and  $N_2$  fixation rates of *Trichodesmium* and *Crocospaera* (Fu et al. 2008; Levitan et al. 2007) . This, in return, may constrain carbon uptake by cyanobacteria that starved for nitrogen.

In addition, high pH also leads to precipitation of essential elements (Cu, Fe, Mo) for photosynthesis and  $N_2$  fixation (Gallon 1992; Strauss et al. 2002). All diazotrophic organisms need Mo nitrogenase either exclusively or together with other alternative forms (Schmidt 2006). Limitation of Fe may reduce growth rates and nitrogenase activity by regulating different  $N_2$ -fixing strategies among diazotrophs, such as the filamentous non-heterocystous *Trichodesmium*, the filamentous heterocystous *Anabaena*, and the unicellular *Cyanothece* (Berman-Frank et al. 2007; Fu et al. 2008; Mahaffey et al. 2005).

Shift of  $N_2$  fixation from light to dark possibly minimized the deleterious effects of  $O_2$  on nitrogenase activity, possibly a consequence of changes in species composition of diazotrophic cyanobacteria associated with heterotrophic bacteria. Dark  $N_2$  fixation increased with bloom progression and contributed up to a calculated ~ 60% of total  $N_2$

fixation, especially when pH was > 9.5 and DO super-saturated (Fig. 12). Unicellular N<sub>2</sub>-fixing cyanobacteria *Synechococcus* sp., which occurred within the aggregates of heterocystous N<sub>2</sub>-fixers, may have been largely responsible for the dark N<sub>2</sub> fixation. In unicellular cyanobacteria, nitrogenase activity and *nifH* activity usually are engaged at night to temporally separate them from O<sub>2</sub> production in day time (Gallon 1992; Mohr et al. 2010). On the other hand, increases of dark N<sub>2</sub> fixation were possibly contributed by species that could fix N<sub>2</sub> in light. After switching from light to dark, dark respiration may alleviate oxygen stress by consuming intracellular O<sub>2</sub> and decreasing DO concentrations in the water (Fay 1992). Excess energy produced during the light period may also be available and cover part of the energy demand of N<sub>2</sub> fixation in the dark (Paerl 1996). Relatively higher N<sub>2</sub> fixation rates were found in the beginning of dark incubation for heterocystous *Anabaena* spp. and non-heterocystous *Oscillatoria limosa*, *Limnothrix aestuarii* and *Lyngbya aestuarii* (Bergman et al. 1997; Severin and Stal 2008).

Although no direct measurements were made in this study, heterotrophic bacteria were proved to maintain optimal growth and nitrogen-fixing potential for the cyanobacterial community in a previous study. Paerl (1978) found that nitrogenase activity of *Anabaena* with attached heterotrophic bacteria on its heterocysts can be higher or that they can recover quicker than axenic cultures under oxygen pressure. Under high pH conditions in photosynthetic periods, bacteria association may provide zones of increased CO<sub>2</sub> availability coupled with O<sub>2</sub> removal through mineralization of organics, which may provide protection from O<sub>2</sub> inhibition of nitrogenase activity and relax DIC limitation. In turn, diazotrophs may release surplus nitrogen to the heterotrophic community (Ploug 2008). In spite of low N<sub>2</sub> fixing for bacteria relative to cyanobacterial

diazotrophs, some of heterocystous bacteria may fix nitrogen both in light and darkness when DIN is limiting (Stevenson and Waterbury 2006; Zehr et al. 1995).

Particulate C: N ratios under high pH /low DIC decreased to approximately Redfield ratio values, which is possibly due to carbon limitation (Burkhardt et al. 1999). However, N<sub>2</sub> fixers can balance their assimilation of C and N during blooms by accessing atmospheric dissolved reservoirs of N<sub>2</sub> and CO<sub>2</sub> (Klemer et al. 1996). The low particulate N: P ratio during stage II is consistent with N limitation in water column and SRP enrichment due to pH elevation.

#### 4.1.15 Bloom Stage III

The filamentous bloom-forming cyanobacteria *Pseudanabaena* spp., which are closely related to *Limnothrix* (Acinas et al. 2009), are capable of fixing N<sub>2</sub> during the daytime (Bergman et al. 1997). At the peak biomass of *Pseudanabaena* spp. in early September, the enhancement of dark N<sub>2</sub> fixation occurred again and potentially comprised a large fraction of new N input (Fig. 12).

High photosynthesis and biomass of cyanobacteria (mainly *Pseudanabaena* spp.) evidently led to drawdown of SRP at both stations (Fig. 5). Especially at BL, there was a clear excess of DIN relative to SRP at the end of the bloom. The increase in DIN: SRP (Fig. 3) may end the domination of diazotrophic cyanobacterial blooms (Perakis et al. 1996). SRP supply becomes more critical for bloom persistence, as evidenced by the high particulate N: P ratio (Fig. 6). The fixation rates of DIC and N<sub>2</sub> were gradually reduced in the whole water (Fig. 8 and 11). Decrease of temperature and the slight increase of salinity may have suppressed cyanobacterial growth, photosynthesis (Moisander et al.

2002) and N<sub>2</sub> fixation (Fu et al. 2007; Moisander et al. 2002), ending the bloom by late September.

### **Conclusions**

During the summer of 2010, dense diazotrophic cyanobacterial blooms were dominant in the Sassafras River, a tidal-fresh/ oligohaline and eutrophic tributary of the Chesapeake Bay. The occurrence of non-diazotrophic and diazotrophic cyanobacteria resulted from a variety of interactions among constraining environmental factors, such as temperature, salinity and the low ratio of bioavailable N : P. Interestingly, the consequences of their high photosynthetic metabolism (e. g. low DIC concentration, extremely high pH) may favor their persistence. Negative feedbacks on cyanobacterial growth occur due to their own metabolism (e. g. low DIC concentration, extremely high pH and the supersaturated dissolve oxygen) which may cause reduction and diel variations in the biomass-specific N<sub>2</sub> fixation rates. Dark N<sub>2</sub> fixation, mediated by diazotrophic species succession and their various physiological adaptations, appeared to supply the lack of nitrogen during dense blooms.

### **References**

- Acinas, S. G., T. H. A. Haverkamp, J. Huisman, and L. J. Stal. 2009. Phenotypic and genetic diversification of *Pseudanabaena* spp. (cyanobacteria). *ISME J.* **3**: 31-46.
- Adams, D. G., and P. S. Duggan. 1999. Heterocyst and akinete differentiation in cyanobacteria. *New Phytol.* **144**: 3-33.

- Amirbahman, A., A. R. Pearce, R. J. Bouchard, S. A. Norton, and J. S. Kahl. 2003. Relationship between hypolimnetic phosphorus and iron release from eleven lakes in Maine, USA. *Biogeochemistry* **65**: 369-385.
- Anderson, D. M., P. M. Glibert, and J. M. Burkholder. 2002. Harmful algal blooms and eutrophication: Nutrient sources, composition, and consequences. *Estuaries* **25**: 704-726.
- Badger, M. R., G. D. Price, B. M. Long, and F. J. Woodger. 2006. The environmental plasticity and ecological genomics of the cyanobacterial CO<sub>2</sub> concentrating mechanism. *J. Exp. Bot.* **57**: 249-265.
- Beardall, J., and M. Giordano. 2002. Ecological implications of microalgal and cyanobacterial CO<sub>2</sub> concentrating mechanisms, and their regulation. *Funct. Plant Biol.* **29**: 335-347.
- Beardall, J., A. Johnston, and J. Raven. 1998. Environmental regulation of CO<sub>2</sub> concentrating mechanisms in microalgae. *Canadian Journal of Botany-Revue Canadienne De Botanique* **76**: 1010-1017.
- Bergman, B., J. R. Gallon, A. N. Rai, and L. J. Stal. 1997. N<sub>2</sub> fixation by non-heterocystous cyanobacteria. *FEMS Microbiol. Rev.* **19**: 139-185.
- Berman-Frank, I. and others 2001. Segregation of nitrogen fixation and oxygenic photosynthesis in the marine cyanobacterium *Trichodesmium*. *Science* **294**: 1534-1537.
- Berman-Frank, I., A. Quigg, Z. V. Finkel, A. J. Irwin, and L. Haramaty. 2007. Nitrogen-fixation strategies and Fe requirements in cyanobacteria. *Limnol. Oceanogr.* **52**: 2260-2269.
- Bothe, H., O. Schmitz, M. G. Yates, and W. E. Newton. 2010. Nitrogen fixation and hydrogen metabolism in cyanobacteria. *Microbiol. Mol. Biol. Rev.* **74**: 529-551.
- Boyd, P. W., R. Strzepek, F. X. Fu, and D. A. Hutchins. 2010. Environmental control of open-ocean phytoplankton groups: Now and in the future. *Limnol. Oceanogr.* **55**: 1353-1376.
- Boynton, W., and M. Kemp. 2009. Estuaries, p. 809-866. *In* D. Capone, D. Bronk, M. Mulholland and E. Carpenter [eds.], *Nitrogen in the marine environment*. Elsevier.

- Burkhardt, S., I. Zondervan, and U. Riebesell. 1999. Effect of CO<sub>2</sub> concentration on C : N : P ratio in marine phytoplankton: A species comparison. *Limnol. Oceanogr.* **44**: 683-690.
- Burns, C. W. 1987. Insights into zooplankton-cyanobacteria interactions derived from enclosure studies. *N. Z. J. Mar. Freshw. Res.* **21**: 477-482.
- Burton, R. F. 1987. On Calculating Concentrations of HCO<sub>3</sub> from pH and PCO<sub>2</sub>. *Comparative Biochemistry and Physiology a-Physiology* **87**: 417-422.
- Capone, D. G. 1995. Determination of nitrogenase activity in aquatic samples using the acetylene reduction procedure, p. 621-610. *In* P. Kemp, B. Sherr, E. Sherr and J. Cole [eds.], *Handbook of methods in aquatic microbial ecology*. Lewis.
- Capone, D. G., D. Bronk, M. Mulholland, and E. J. Carpenter. 2008. *Nitrogen in the Marine Environment*, 2nd edition. . Academic Press/ Elsevier.
- Capone, D. G., and M. D. Ferrier. 1994. Amino acid cycling in colonies of the planktonic marine cyanobacterium *Trichodesmium thiebautii*. *Appl. Environ. Microbiol.* **60**: 3989-3995.
- Carpenter, E. J., J. P. Montoya, J. Burns, M. R. Mulholland, A. Subramaniam, and D. G. Capone. 1999. Extensive bloom of a N<sub>2</sub>-fixing diatom/cyanobacterial association in the tropical Atlantic Ocean. *Mar. Ecol. Prog. Ser.* **185**: 273-283.
- Carrasco, M., J. M. Mercado, and F. X. Niell. 2008. Diversity of inorganic carbon acquisition mechanisms by intact microbial mats of *Microcoleus chthonoplastes* (Cyanobacteriae, Oscillatoriaceae). *Physiol. Plant* **133**: 49-58.
- Codd, G. A., L. F. Morrison, and J. S. Metcalf. 2005. Cyanobacterial toxins: risk management for health protection. *Toxicol. Appl. Pharmacol.* **203**: 264-272.
- Coles, J. F., and R. C. Jones. 2000. Effect of temperature on photosynthesis-light response and growth of four phytoplankton species isolated from a tidal freshwater river. *J. Phycol.* **36**: 7-16.
- Cox, R. M. 1969. Special aspects of nitrogen fixation by blue-green algae. *Proceedings of the Royal Society B: Biological Sciences* **172**: 357-366.
- Delwiche, L., and S. Slaughter. 2003. *The little SAS book: a primer*. SAS Press.

- Dyhrman, S. T. and others 2006. Phosphonate utilization by the globally important marine diazotroph *Trichodesmium*. *Nature* **439**: 68-71.
- Dyhrman, S. T., and S. T. Haley. 2006. Phosphorus scavenging in the unicellular marine diazotroph *Crocospaera watsonii*. *Appl. Environ. Microbiol.* **72**: 1452-1458.
- Dyhrman, S. T., and K. C. Ruttenberg. 2006. Presence and regulation of alkaline phosphatase activity in eukaryotic phytoplankton from the coastal ocean: Implications for dissolved organic phosphorus remineralization. *Limnol. Oceanogr.* **51**: 1381-1390.
- Engel, A., K. G. Schulz, U. Riebesell, R. Bellerby, B. Delille, and M. Schartau. 2008. Effects of CO<sub>2</sub> on particle size distribution and phytoplankton abundance during a mesocosm bloom experiment (PeECE II). *Biogeosciences* **5**: 509-521.
- Falcon, L. I., E. J. Carpenter, F. Cipriano, B. Bergman, and D. G. Capone. 2004. N<sub>2</sub> fixation by unicellular bacterioplankton from the Atlantic and Pacific oceans: Phylogeny and in situ rates. *Appl. Environ. Microbiol.* **70**: 765-770.
- Fay, P. 1992. Oxygen relations of nitrogen-fixation in cyanobacteria. *Microbiol. Rev.* **56**: 340-373.
- Fu, F. X. and others 2008. Interactions between changing pCO<sub>2</sub>, N<sub>2</sub> fixation, and Fe limitation in the marine unicellular cyanobacterium *Crocospaera*. *Limnol. Oceanogr.* **53**: 2472-2484.
- Fu, F. X., M. E. Warner, Y. H. Zhang, Y. Y. Feng, and D. A. Hutchins. 2007. Effects of increased temperature and CO<sub>2</sub> on photosynthesis, growth, and elemental ratios in marine *Synechococcus* and *Prochlorococcus* (Cyanobacteria). *J. Phycol.* **43**: 485-496.
- Gallon, J. R. 1992. Reconciling the incompatible : N<sub>2</sub> fixation and O<sub>2</sub>. *New Phytol.* **122**: 571-609.
- Gattuso, J. P., J. W. Liu, M. G. Weinbauer, C. Maier, and M. H. Dai. 2010. Effect of ocean acidification on microbial diversity and on microbe-driven biogeochemistry and ecosystem functioning. *Aquat. Microb. Ecol.* **61**: 291-305.
- Glibert, P. M. and others 2004. Evidence for dissolved organic nitrogen and phosphorus uptake during a cyanobacterial bloom in Florida Bay. *Mar. Ecol. Prog. Ser.* **280**: 73-83.

- Hansen, A. M., J. V. Christensen, and O. Sortkajer. 1991. Effect of high pH on zooplankton and nutrients in fish-free enclosures. *Archiv Fur Hydrobiologie* **123**: 143-164.
- Hansen, P. J. 2002. Effect of high pH on the growth and survival of marine phytoplankton: implications for species succession. *Aquat. Microb. Ecol.* **28**: 279-288.
- Howarth, R. W., R. Marino, J. Lane, and J. J. Cole. 1988. Nitrogen-fixation in fresh-water, estuarine, and marine ecosystems .1. Rates and importance. *Limnol. Oceanogr.* **33**: 669-687.
- Jenkins, B. D., G. F. Steward, S. M. Short, B. B. Ward, and J. P. Zehr. 2004. Fingerprinting diazotroph communities in the Chesapeake Bay by using a DNA macroarray. *Appl. Environ. Microbiol.* **70**: 1767-1776.
- Jones, J. B., and E. H. Stanley. 2003. Long-term decline in carbon dioxide supersaturation in rivers across the contiguous United States. *Geophysical Research Letter* **30**: 1495-1499.
- Jones, R. C. 1998. Seasonal and spatial patterns in phytoplankton photosynthetic parameters in a tidal freshwater river. *Hydrobiologia* **364**: 199-208 Part: Part 192.
- Kana, T. M., C. Darkangelo, M. D. Hunt, J. B. Oldham, G. E. Bennett, and J. C. Cornwell. 1994. Membrane inlet mass spectrometer for rapid high-precision determination of N<sub>2</sub>, O<sub>2</sub>, and Ar in environmental water samples. *Anal. Chem.* **66**: 4166-4170.
- Kana, T. M., and D. L. Weiss. 2004. Comment on "comparison of isotope pairing and N<sub>2</sub>: Ar methods for measuring sediment denitrification" by B. D. Eyre, S. Rysgaard, T. Dalsgaard, and P. Bondo Christensen. 2002. *estuaries* 25 : 1077-1087". *Estuaries* **27**: 173-176.
- Klemer, A. R., J. J. Cullen, M. T. Mageau, K. M. Hanson, and R. A. Sundell. 1996. Cyanobacterial buoyancy regulation: The paradoxical roles of carbon. *J. Phycol.* **32**: 47-53.
- Kopp, J. F., and G. D. Mckee. 1983. *Methods for Chemical Analysis of Water and Wastes.* United States Environmental Protection analysis Agency.
- Krauk, J., T.A., J. A. Villareal, J. P. M. Sohm, and D. G. Capone. 2006. Plasticity of N:P ratios in laboratory and field populations of *Trichodesmium* spp. *Aquat. Microb. Ecol.* **42**: 243-253.



- Lane, L., S. Rhoades, C. Thomas, and L. Van Heukelem. 2011. Standard Operating procedures 2000. Technical report NO.TS-264-00.
- Lehtimäki, J., P. Moisaner, K. Sivonen, and K. Kononen. 1997. Growth, nitrogen fixation, and nodularin production by two Baltic Sea cyanobacteria. *Appl. Environ. Microbiol.* **63**: 1647-1656.
- Levitan, O. and others 2007. Elevated CO<sub>2</sub> enhances nitrogen fixation and growth in the marine cyanobacterium *Trichodesmium*. *Global Change Biology* **13**: 531-538.
- Lewis, W. M. 1984. The light response of nitrogen fixation in Lake Valencia, Venezuela. *Limnol. Oceanogr.* **29**: 894-900.
- Mahaffey, C., A. F. Michaels, and D. G. Capone. 2005. The conundrum of marine N<sub>2</sub> fixation. *Am. J. Sci.* **305**: 546-595.
- Milligan, A. J., I. Berman-Frank, Y. Gerchman, G. C. Dismukes, and P. G. Falkowski. 2007. Light-dependent oxygen consumption in nitrogen-fixing cyanobacteria plays a key role in nitrogenase protection. *J. Phycol.* **43**: 845-852.
- Mogelhoj, M., P. Hansen, P. Henriksen, and N. Lundholm. 2006. High pH and not allelopathy may be responsible for negative effects of *Nodularia spumigena* on other algae. *Aquat. Microb. Ecol.* **43**: 43-53.
- Moisaner, P. H. and others 2010. Unicellular cyanobacterial distributions broaden the oceanic N<sub>2</sub> fixation domain. *Science* **327**: 1512-1514.
- Moisaner, P. H., E. McClinton, and H. W. Paerl. 2002. Salinity effects on growth, photosynthetic parameters, and nitrogenase activity in estuarine planktonic cyanobacteria. *Microb. Ecol.* **43**: 432-442.
- Montoya, J. P., C. M. Holl, J. P. Zehr, A. Hansen, T. A. Villareal, and D. G. Capone. 2004. High rates of N<sub>2</sub> fixation by unicellular diazotrophs in the oligotrophic Pacific Ocean. *Nature* **430**: 1027-1031.
- Mulholland, M. R. 2007. The fate of nitrogen fixed by diazotrophs in the ocean. *Biogeosciences* **4**: 37-51.
- Mulholland, M. R., D. A. Bronk, and D. G. Capone. 2004. Dinitrogen fixation and release of ammonium and dissolved organic nitrogen by *Trichodesmium* IMS101. *Aquat. Microb. Ecol.* **37**: 85-94.

- Murphy, J., and J. P. Riley. 1962. A modified single solution method for determination of phosphates in natural water. *Anal. Chim. Acta* **27**: 31-36.
- O'neil, J. M., T. W. Davis, M. A. Burford, and C. J. Gobler. 2011. The rise of harmful cyanobacteria blooms: The potential roles of eutrophication and climate change. *Harmful Algae* **Accepted**.
- Ogawa, T., and A. Kaplan. 2003. Inorganic carbon acquisition systems in cyanobacteria. *Photosynth. Res.* **77**: 105-115.
- Oh, H., J. Maeng, and G. Rhee. 1991. Nitrogen and carbon fixation by *Anabaena* sp. isolated from a rice paddy and grown under P and light limitations. *J. Appl. Phycol.* **3**: 335-343.
- Oliver, R. 1994. Floating and sinking in gas-vacuolate cyanobacteria. *J. Phycol.* **30**: 161-173.
- Oliver, R. L., and G. G. Ganf. 2000. Freshwater blooms, p. 149-194. *In* B. A. Whitton, Potts, M. [ed.], *The Ecology of Cyanobacteria*. Dordrecht.
- Paerl, H. 2008. Nutrient and other environmental controls of harmful cyanobacterial blooms along the freshwater-marine continuum, p. 217-237. *In* K. Hudnell [ed.], *Cyanobacterial Harmful Algal Blooms: State of the Science and Research Needs*. Springer.
- Paerl, H., and J. P. Zehr. 2000. Marine nitrogen fixation, p. 387-418. *In* D. Kirchman [ed.], *Microbial Ecology of the Oceans*. Wiley-Liss, Inc.
- Paerl, H. W. 1978. Role of Heterotrophic Bacteria in Promoting N<sub>2</sub>-Fixation by *Anabaena* in Aquatic Habitats. *Microb. Ecol.* **4**: 215-231.
- . 1996. Microscale physiological and ecological studies of aquatic cyanobacteria: macroscale implications. *Microsc. Res. Tech.* **33**: 47-72.
- Paerl, H. W., and J. Huisman. 2009. Climate change: a catalyst for global expansion of harmful cyanobacterial blooms. *Env Microbiol Rep* **1**: 27-37.
- Paerl, H. W., and J. L. Pinckney. 1996. A mini-review of microbial consortia: Their roles in aquatic production and biogeochemical cycling. *Microb. Ecol.* **31**: 225-247.

- Parsons, T. R., Y. Maita, and C. M. Lalli. 1984. Fluorometric determination of chlorophylls, p. 107-108. *In* T. R. Parsons [ed.], *A Manual of Chemical and Biological Methods for Seawater Analysis*. Pergamon Press.
- Perakis, S. S., E. B. Welch, and J. M. Jacoby. 1996. Sediment-to-water blue-green algal recruitment in response to alum and environmental factors. *Hydrobiologia* **318**: 165-177.
- Piehler, M. F., J. Dyble, P. H. Moisander, J. L. Pinckney, and H. W. Paerl. 2002. Effects of modified nutrient concentrations and ratios on the structure and function of the native phytoplankton community in the Neuse River Estuary, North Carolina, USA. *Aquat. Ecol.* **36**: 371-285.
- Ploug, H. 2008. Cyanobacterial surface blooms formed by *Aphanizomenon* sp and *Nodularia spumigena* in the Baltic Sea: Small-scale fluxes, pH, and oxygen microenvironments. *Limnol. Oceanogr.* **53**: 914-921.
- Price, G. D., M. R. Badger, F. J. Woodger, and B. M. Long. 2008. Advances in understanding the cyanobacterial CO<sub>2</sub>-concentrating-mechanism (CCM): functional components, Ci transporters, diversity, genetic regulation and prospects for engineering into plants. *J. Exp. Bot.* **59**: 1441-1461.
- Qiu, B. S., and K. S. Gao. 2002. Effects of CO<sub>2</sub> enrichment on the bloom-forming cyanobacterium *Microcystis aeruginosa* (Cyanophyceae): Physiological responses and relationships with the availability of dissolved inorganic carbon. *J. Phycol.* **38**: 721-729.
- Quinn, G., and M. Keough. 2002. *Experimental design and data analysis for biologists*. Cambridge University Press.
- Rippka, R., A. Neilson, R. Kunisawa, and C. G. 1971. Nitrogen fixation by unicellular blue-green algae. *Arch. Mikrobiol.* **76**: 341-348.
- Sabour, B., B. Sbiyyaa, M. Loudiki, B. Oudra, M. Belkoura, and V. Vasconcelos. 2009. Effect of light and temperature on the population dynamics of two toxic bloom forming cyanobacteria - *Microcystis ichthyoblabe* and *Anabaena aphanizomenoides*. *Chemistry and Ecology* **25**: 277-284.
- Sanudo-Wilhelmy, S. A., A. Tovar-Sanchez, F. X. Fu, D. G. Capone, E. J. Carpenter, and D. A. Hutchins. 2004. The impact of surface-adsorbed phosphorus on phytoplankton Redfield stoichiometry. *Nature* **432**: 897-901.

- Schmidt, T. 2006. Topics in Ecological and Environmental Microbiology. Elsevier Inc.
- Seitzinger, S. P. 1991. The effect of pH on the release of phosphorus from Potomac estuary sediments - implications for blue-green-algal blooms. *Estuar. Coast. Shelf Sci.* **33**: 409-418.
- Sellner, K. G., R. V. Lacouture, and C. R. Parrish. 1988. Effects of increasing salinity on a cyanobacteria bloom in the Potomac River estuary. *J. Plankton Res.* **10**: 49-61.
- Severin, I., and L. J. Stal. 2008. Light dependency of nitrogen fixation in a coastal cyanobacterial mat. *ISEM Journal: Multidisciplinary Journal of Microbial Ecology* **2**: 1077-1088.
- Short, S. M., and J. P. Zehr. 2007. Nitrogenase gene expression in the Chesapeake Bay Estuary. *Environ. Microbiol.* **9**: 1591-1596.
- Stal, L. J., and W. E. Krumbein. 1985. Nitrogenase activity in the non-heterocystous cyanobacterium *Oscillatoria* sp. grown under alternating light-dark cycles. *Arch. Microbiol.* **143**: 67-71.
- Stevenson, B. S., and J. B. Waterbury. 2006. Isolation and identification of an epibiotic bacterium associated with heterocystous *Anabaena* cells. *Biol. Bull.* **210**: 73-77.
- Strauss, E. A., N. L. Mitchell, and G. A. Lamberti. 2002. Factors regulating nitrification in aquatic sediments: effects of organic carbon, nitrogen availability, and pH. *Can. J. Fish. Aquat. Sci.* **59**: 554-563.
- Stumm, W., and J. Morgan. 1996. *Aquatic Chemistry: Chemical Equilibria and Rates in Natural Waters*. John Wiley & Sons, Inc.
- Tango, P. J., and W. Butler. 2008. Cyanotoxins in tidal waters of Chesapeake Bay. *Northeast. Nat.* **15**: 403-416.
- Tonk, L., K. Bosch, P. Visser, and J. Huisman. 2007. Salt tolerance of the harmful cyanobacterium *Microcystis aeruginosa*. *Aquat. Microb. Ecol.* **46**: 117-123.
- Unrein, F., I. O'farrell, I. Izaguirre, R. Sinistro, M. D. Afonso, and G. Tell. 2010. Phytoplankton response to pH rise in a N-limited floodplain lake: relevance of N<sub>2</sub>-fixing heterocystous cyanobacteria. *Aquatic Sciences* **72**: 179-190.
- Verity, P. G., C. Y. Robertson, C. R. Tronzo, M. G. Andrews, J. R. Nelson, and M. E. Sieracki. 1992. Relationships between Cell-Volume and the Carbon and Nitrogen-

Content of Marine Photosynthetic Nanoplankton. *Limnol. Oceanogr.* **37**: 1434-1446.

Wagner, and Adrian. 2009. Cyanobacteria dominance: Quantifying the effects of climate change. *Limnol. Oceanogr.* **54**: 2460-2468.

Watkinson, A. J., J. M. O'neil, and W. C. Dennison. 2005. Ecophysiology of the marine cyanobacterium, *Lyngbya majuscula* (*Oscillatoriaceae*) in Moreton Bay, Australia. *Harmful Algae* **4**: 697-715.

Xie, L. Q., and P. Xie. 2003. Enhancement of dissolved phosphorus release from sediment to lake water by *Microcystis* blooms - an enclosure experiment in a hyper-eutrophic, subtropical Chinese lake. *Environ. Pollut.* **122**: 391-399.

Yamamoto, Y., and H. Nakahara. 2005. Competitive dominance of the cyanobacterium *Microcystis aeruginosa* in nutrient-rich culture conditions with special reference to dissolved inorganic carbon uptake. *Phycol. Res.* **53**: 201-208.

Zehr, J. P., M. Mellon, S. Braun, W. Litaker, T. Steppe, and H. W. Paerl. 1995. Diversity of Heterotrophic Nitrogen-Fixation Genes in a Marine Cyanobacterial Mat. *Appl. Environ. Microbiol.* **61**: 2527-2532.

## Tables

Table 4-1 The Cyanobacterial species and N<sub>2</sub> fixers observed in the summer of 2010.

Latin name	Ref: N <sub>2</sub> fixer
<i>Microcystis aeruginosa</i>	
<i>Microcystis botrys</i>	
<i>Microcystis wesenbergii</i>	
<i>Merismopedia glauca</i>	
<i>Merismopedia</i>	
<i>Anabaena circinalis</i>	1
<i>Anabaena crassa</i>	1,2
<i>Anabaena flos-aque</i>	1,2
<i>Anabaena planctonica</i>	1
<i>Anabaena spiroides</i>	1
<i>Anabaena Oscillarioides</i>	1
<i>Anabaena sp.</i>	1
<i>Lyngbya sp.</i>	1, 4
<i>Pseudanabaena sp.</i>	3, 4, 5
<i>Chroococcus sp.</i>	4, 6
<i>Synechococcus sp.</i>	1

Note : the species identification and N<sub>2</sub> fixation record from 1. John et al. 2002; 2. Fay 1992; 3. Singh et al. 1987; 4. Bergman et al. 1997; 5. Staal et al. 2003; 6. Rippka et al. 1971

Table 4-2 Three-level nested analysis of variance of effects of station (n= 2), sampling date (n=5 for C and n= 9 for N) and irradiance (n=4) on carbon and nitrogen fixation in laboratory incubations. Data are shown in Fig 8 (C fixation) and Fig 11 (N-fixation).

<b>Dependent variable: C fixation rate (mean of 3 triplicates)</b>					
<b>Source of variation</b>	<b>DF</b>	<b>Sum of Squares</b>	<b>Mean Square</b>	<b>F Value</b>	<b>Pr &gt; F</b>
Model	19	3.89E+08	2.05E+07	10.82	<.0001 ***
Error	18	3.41E+07	1.89E+06		
Corrected Total	37	4.23E+08			
<b>Source of variation</b>	<b>DF</b>	<b>Type III SS</b>	<b>Mean Square</b>	<b>F Value</b>	<b>Pr &gt; F</b>
All	1	3.62E+05	3.62E+05	0.19	0.667
Dates within stations	8	9.19E+06	1.15E+06	0.61	0.7607
Irradiance within stations and dates	10	1.79E+08	1.79E+07	9.44	<.0001 ***
<b>Dependent variable: N<sub>2</sub> fixation rate (mean of 3 triplicates)</b>					
<b>Source of variation</b>	<b>DF</b>	<b>Sum of Squares</b>	<b>Mean Square</b>	<b>F Value</b>	<b>Pr &gt; F</b>
Model	39	7.58E+06	1.94E+05	20.26	<.0001 ***
Error	39	3.74E+05	9.59E+03		
Corrected Total	78	7.95E+06			
<b>Source of variation</b>	<b>DF</b>	<b>Type III SS</b>	<b>Mean Square</b>	<b>F Value</b>	<b>Pr &gt; F</b>
All	1	4.45E+03	4.45E+03	0.46	0.4996
Dates within stations	18	2.12E+05	1.18E+04	1.23	0.2872
Irradiance within stations and dates	20	2.89E+06	1.44E+05	15.06	<.0001 ***

Table 4-3 Photosynthetic efficiency ( $\alpha^{chl}$ , mg C mg Chl  $a^{-1} h^{-1}$  ( $\mu\text{mol photon}^{-1} \text{m}^{-2} \text{s}^{-1}$ )), in laboratory incubation of samples collected during bloom stage I, II and III at 2 stations on the upper Sassafras River in 2010. Data are shown in Figure 8.

Phase	Date	Budds Landing			Drawbridge					
		$\alpha^{chl}$	SE	P	$\alpha^{chl}$	SE	t	P		
Stage I	6/10	41.94	16.24	0.04	*	45.97	10.00	4.60	0.04	**
	6/15	19.14	4.89	0.059		24.20	8.61	2.81	0.11	
Stage II	6/30	8.28	5.83	0.39		3.60	3.97	0.91	0.53	
	7/14	1.63	0.29	0.030	*	1.86	0.25	7.42	0.02	**
Stage III	9/14	15.21	3.18	0.041	*	9.67	1.91	5.05	0.04	*

Note: \*  $P \leq 0.05$ ; \*\*  $P \leq 0.01$ ; \*\*\*  $P \leq 0.001$ .

Table 4-4 Response of N-fixation to irradiance in laboratory incubations of samples collected during bloom stage I, II and III at 2 stations on the upper Sassafras River in 2010. Regression coefficient (Cof) = (mg N mg Chl  $a^{-1} h^{-1}$  ( $\mu\text{mol photon}^{-1} \text{m}^{-2} \text{s}^{-1}$ )). Data are shown in Figure 11. '-' = undetectable data.

Phase	Date	Budds Landing			Drawbridge				
		Cof	SE	P	Cof	SE	P		
Stage I	5/25	-			-				
	6/10	6.70	1.52	0.05	*	2.62	0.59	0.05	*
	6/15	1.52	0.25	0.03	*	3.96	0.59	0.02	*
Stage II	6/25	0.29	0.10	0.10		0.14	0.02	0.02	*
	6/30	-0.16	0.39	0.72		1.16	0.28	0.05	*
	7/14	-0.42	0.31	0.41		0.23	0.04	0.03	*
	8/9	2.98	0.41	0.02	*	1.36	0.24	0.03	*
Stage III	8/26	0.78	0.17	0.05	*	0.57	0.47	0.35	
	9/1	0.04	0.05	0.47		0.63	1.26	0.66	
	9/14	0.90	0.15	0.03	*	0.56	0.16	0.08	

Note: \*  $P \leq 0.05$ ; \*\*  $P \leq 0.01$ ; \*\*\*  $P \leq 0.001$ .

Table 4-5 Response of N-fixation to C fixation in the laboratory incubation of samples collected during bloom stage I, II, and III at 2 stations in the upper Sassafras River in 2010. K is the correlation between N fixation and C fixation rates. Data are shown in Figure 11.



Phase	Date	Budds Landing			Drawbridge		
		K	SE	Pr> t	K	SE	Pr> t
Stage I	6/10	0.14	0.02	0.02 *	0.06	0.01	0.01 **
	6/15	0.07	0.01	0.02 *	0.13	0.05	0.12
Stage II	6/30	-0.05	0.00	0.02 *	0.03	0.02	0.39
	7/14	0.68	0.47	0.07	0.74	0.08	0.01 *
Stage III	9/14	0.05	0.02	0.12	0.05	0.03	0.20

Note: \*  $P \leq 0.05$ ; \*\*  $P \leq 0.01$ ; \*\*\*  $P \leq 0.001$ .

Table 4-6 Correlation among pH, dissolved oxygen (DO), dissolved inorganic carbon (DIC) and irradiance in 24 h incubations of samples collected from Budds Landing and Drawbridge. Corr is Pearson correlation coefficient; N is the sample size and P is the significant level.

		<b>pH</b>	<b>DO</b>	<b>DIC</b>	<b>Irradiance</b>
<b>pH</b>	<b>Corr</b>	1	0.61	-0.05	0.41
	<b>P</b>		<.001 ***	0.8	0.009 **
	<b>n</b>	76	69	69	74
<b>DO</b>	<b>Corr</b>		1	-0.56	0.70
	<b>P</b>			0.002 **	<.0001 ***
	<b>n</b>		79	68	68
<b>DIC</b>	<b>Corr</b>			1	-0.44
	<b>P</b>				0.004 **
	<b>n</b>			78	68
<b>Irradiance</b>	<b>Corr</b>				1
	<b>P</b>				
	<b>n</b>				74

Note: \*  $P \leq 0.05$ ; \*\*  $P \leq 0.01$ ; \*\*\*  $P \leq 0.001$ .

Table 4-7 Multiple linear relationship between C fixation rates and environmental parameters, estimated by forward stepwise regression. Independent variables are from the daily average value of DO, DIC, pH, SRP,  $\text{NO}_3^-$  and  $\text{NH}_4^+$ . SE is standard error. Dates for Chl *a*-normalized C fixation rates shown in Figure 8.

<b>Parameters</b>	<b>Slope</b>	<b>SE</b>	<b>Type II SS</b>	<b>F</b>	<b>P &gt; F</b>	
<b>Intercept</b>	-3047.44	1398.97	1.81E+07	4.75	0.04	*
<b>DIC</b>	8.21	1.60	1.01E+08	26.38	<.0001	***
<b>Irradiance</b>	24.15	5.67	6.93E+07	18.14	0.0002	***
<b>DO</b>	-13.23	4.09	4.00E+07	10.47	0.0031	**
<b>SRP</b>	7425.74	3616.94	1.61E+07	4.21	0.0495	*
<b>N: P ratio</b>	38.71	22.34	1.15E+07	3.00	0.09	
<b><math>\text{NH}_4^+</math></b>	824.22	621.85	6.71E+06	1.76	0.1957	
<b><math>\text{NO}_3^-</math></b>	-191.47	152.65	6.01E+06	1.57	0.2201	

Note: \*  $P \leq 0.05$ ; \*\*  $P \leq 0.01$ ; \*\*\*  $P \leq 0.001$

Table 4-8 Multiple linear relationship of N<sub>2</sub> fixation rates with changes in water column, estimated by forward stepwise regression. Independent variables from the daily average value of DO, DIC, pH, SRP, NO<sub>3</sub><sup>-</sup> and NH<sub>4</sub><sup>+</sup>. Date for C- specific N<sub>2</sub> fixation rates shown in Figure 11. SE is standard error.

Variable	Slope	SE	Type II SS	F	Pr > F	
<b>Intercept</b>	371.9	159.8	408434	5.4	0.0228	*
<b>Irradiance</b>	2.2	0.4	1883573	25.0	<.0001	***
<b>DO</b>	-1.4	0.4	817279	10.8	0.0015	**
<b>NO<sub>3</sub><sup>-</sup></b>	-14.1	4.5	746205	9.9	0.0024	**
<b>SRP</b>	599.3	287.8	327131	4.3	0.0409	*
<b>N: P ratio</b>	-1.5	1.2	121748	1.6	0.208	

Note: \* P ≤ 0.05; \*\* P ≤ 0.01; \*\*\* P ≤ 0.001

## Figures

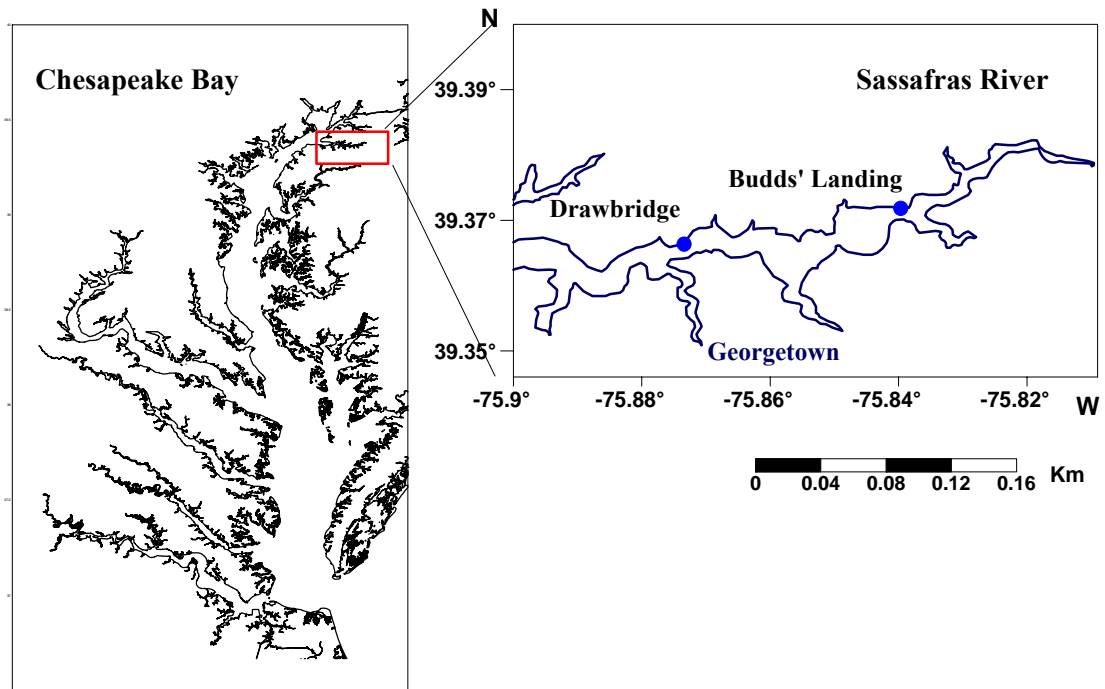


Figure 4-1 Sampling stations in the upper Sassafra River, Maryland, USA. Budds Landing (BL) and Drawbridge (DB) are located on the upper river, with BL close to the river head and DB slightly downstream from BL.

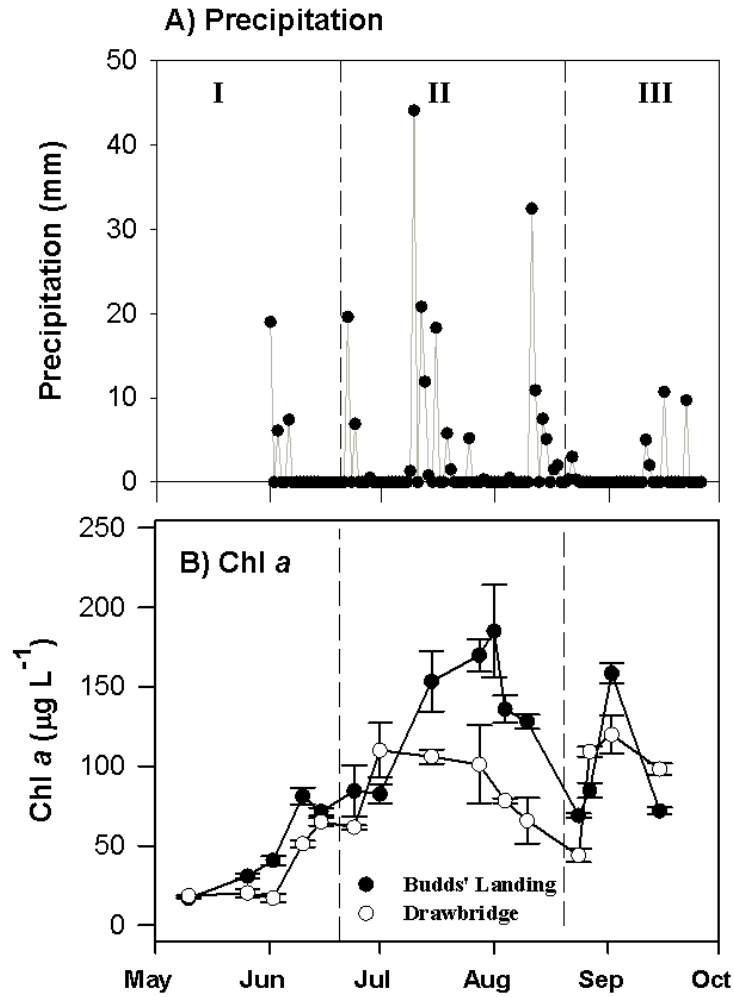


Figure 4-2 The variation in precipitation at Georgetown, Maryland (A) and Chl *a* concentrations (B) at Budds Landing (BL, upstream) and Drawbridge (DB, downstream site) from early May to Mid September in 2010. Data are shown for the bloom stage I, II and III.

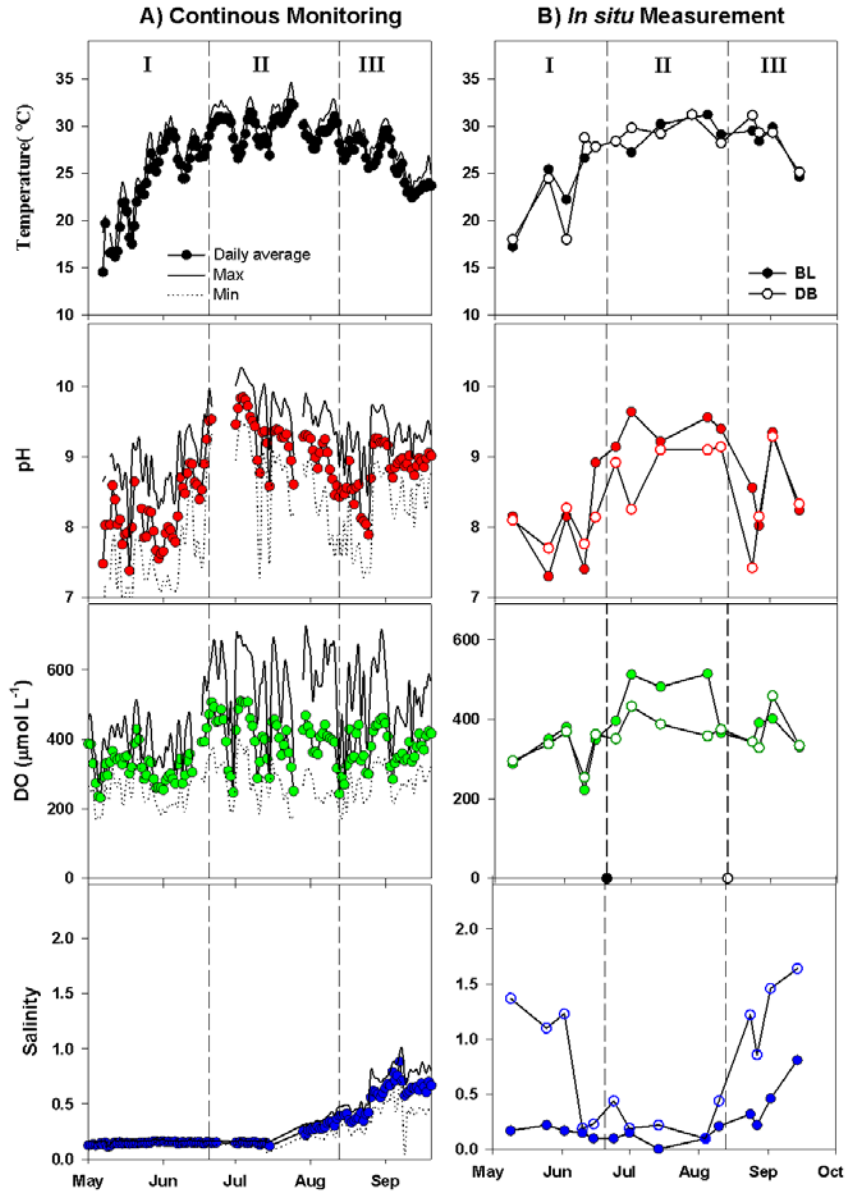


Figure 4-3 The seasonal patterns of temperature, pH, dissolved oxygen and salinity in the Sassafras River. A) the continuous changes at Budds Landing in 2010. Circles represent the daily average of the continuous records. The daily maximum and minimum values are indicated with solid line and dash lines, respectively (Maryland Department of Natural Resources). B) *In situ* measurements at Budds Landing (solid circles) and Drawbridge (empty circles). Data are shown for the bloom stage I, II and III.

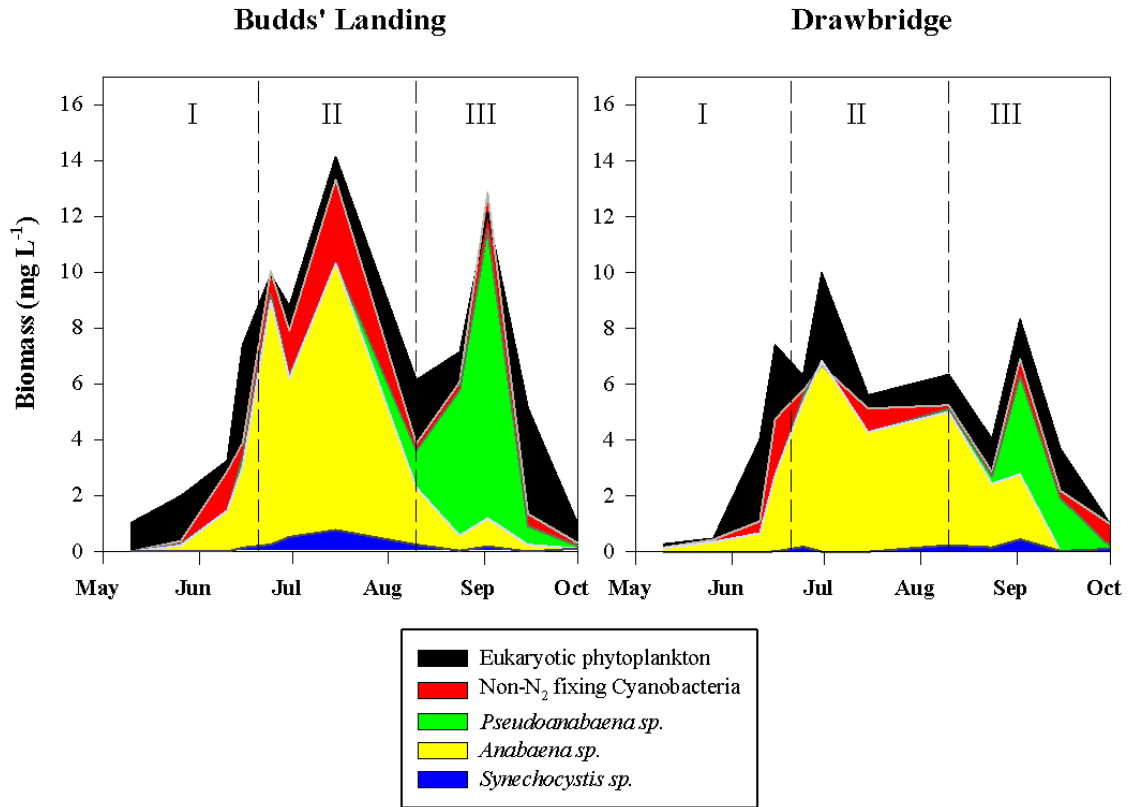


Figure 4-4 The estimated biomass of phytoplankton at Budds Landing (BL) and Drawbridge (DB) in 2010, including non-diazotrophic cyanobacteria (mostly *Microcystis sp.*) diazotrophic cyanobacteria (heterocystous *Anabaena sp.*, unicellular *Synechocystis sp.*, filamentous non-heterocystous *Pseudoanabaena sp.*) and eukaryotic phytoplankton. Data are shown for the bloom stages I, II and III.



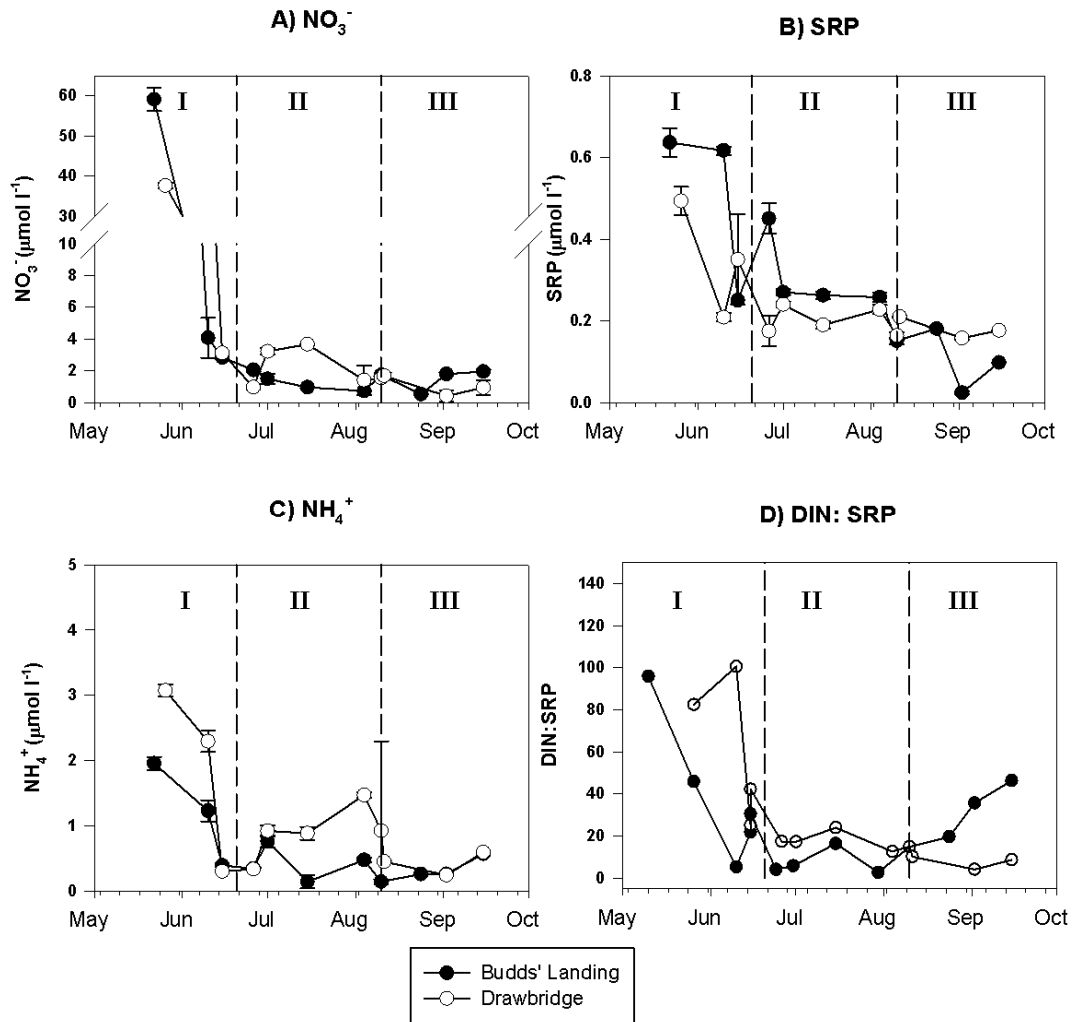


Figure 4-5 Weekly or biweekly inorganic nutrient concentrations ( $\text{NH}_4^+$ ,  $\text{NO}_3^-$ , SRP) and the ratio of dissolved inorganic nitrogen to SRP (DIN: SRP) at Budds Landing (BL) and Drawbridge (DB) in 2010. Data presented as the mean  $\pm$  SE for nutrients during the bloom stage I, II and III.

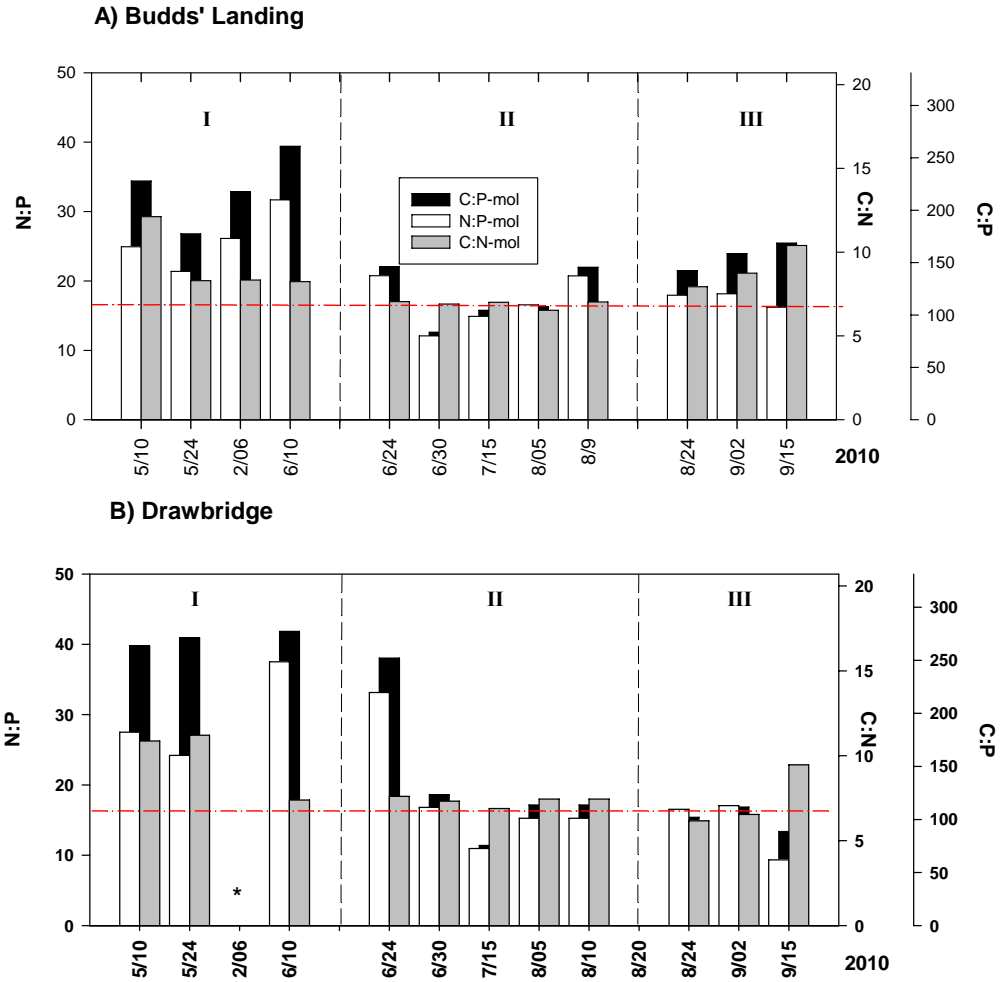


Figure 4-6 Particulate molar ratio of C: N: P at Budds Landing (BL) and Drawbridge (DB) in 2010. \* = missing data. Dotted line= the Redfield ratio. Data are shown for bloom stage I, II and III.

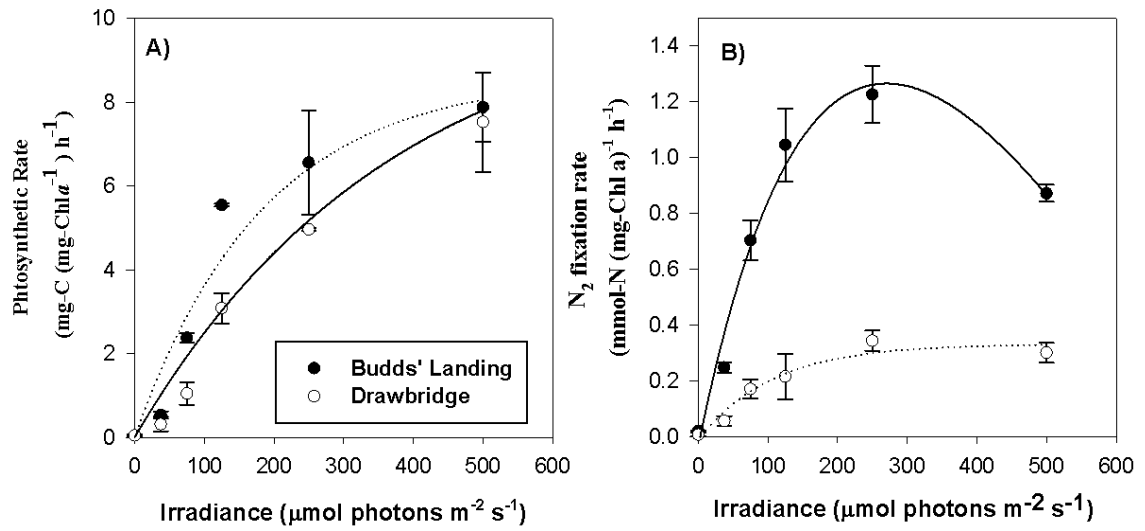


Figure 4-7 Photosynthesis and N<sub>2</sub> fixation rates as a function of irradiance in laboratory incubations of samples collected from Budds Landing (BL) and Drawbridge (DB) on June 10, 2010.

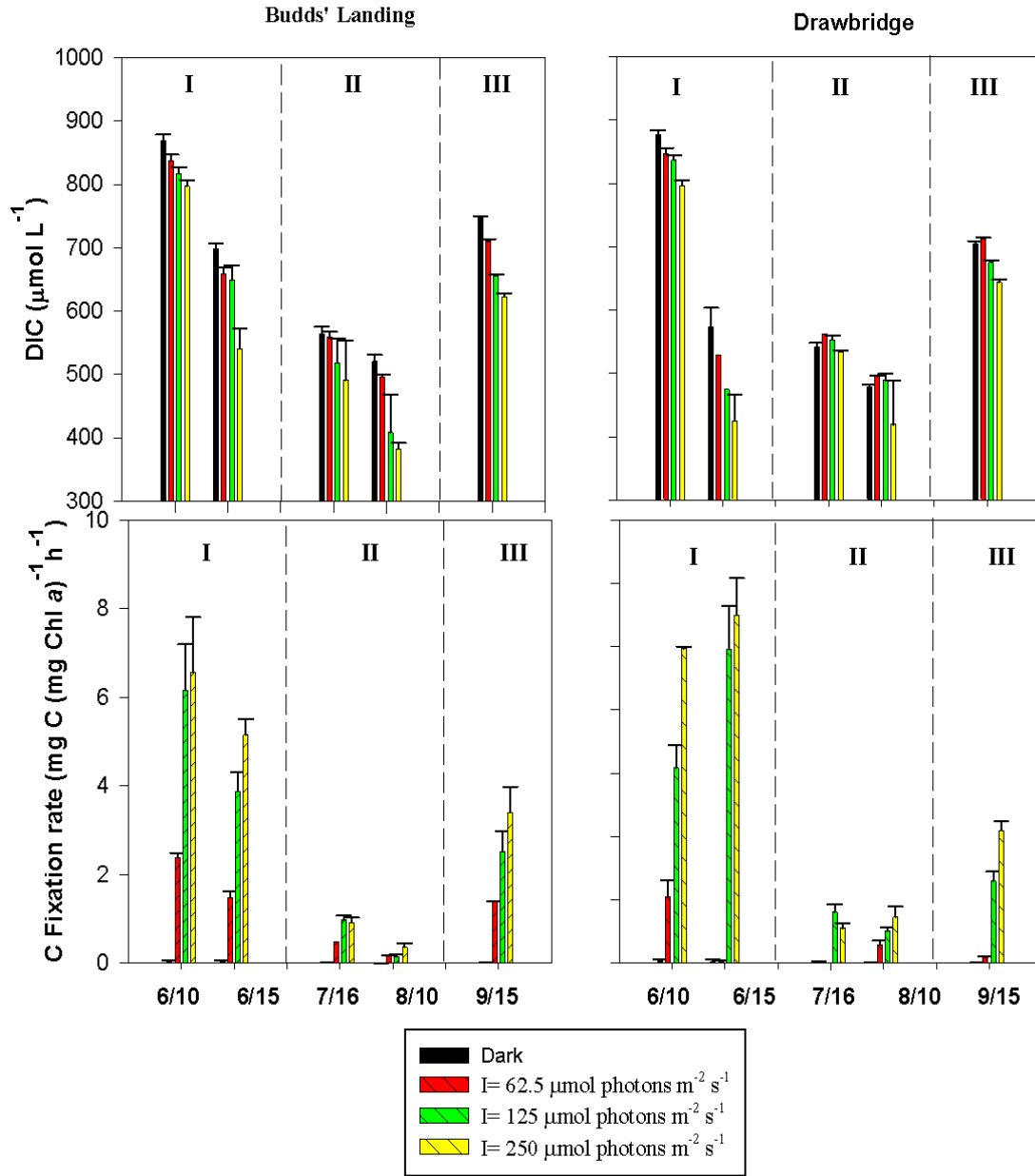


Figure 4-8 The mean ( $\pm$  standard deviation) of DIC concentration and carbon fixation rates in laboratory incubations of samples from Budds Landing (BL) and Drawbridge (DB). Samples were taken during bloom Stage I (on June 11 and June 15), Stage II (on July 16 and August 15), and the end of bloom stage III (on September 15).

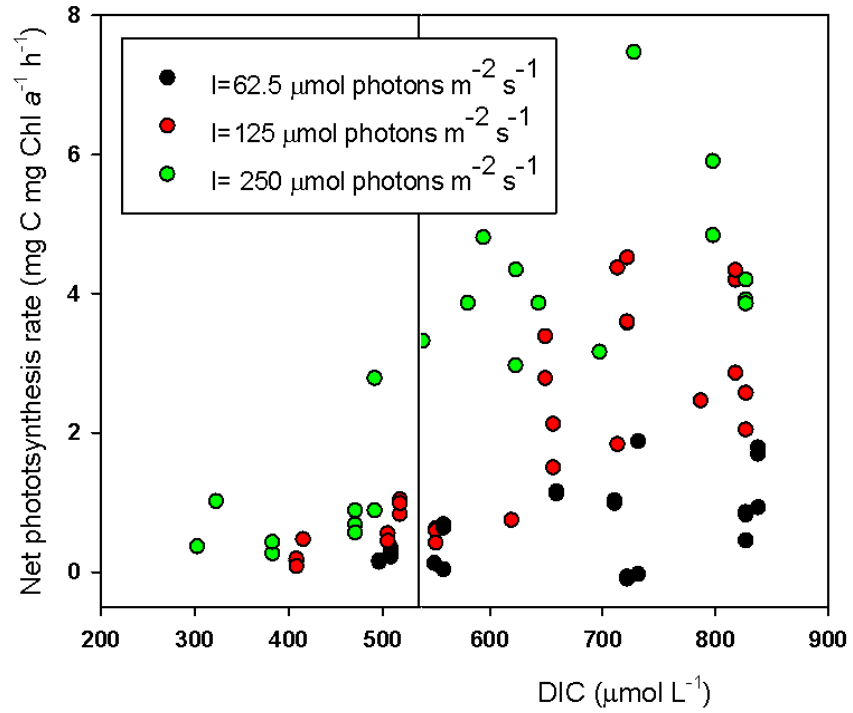
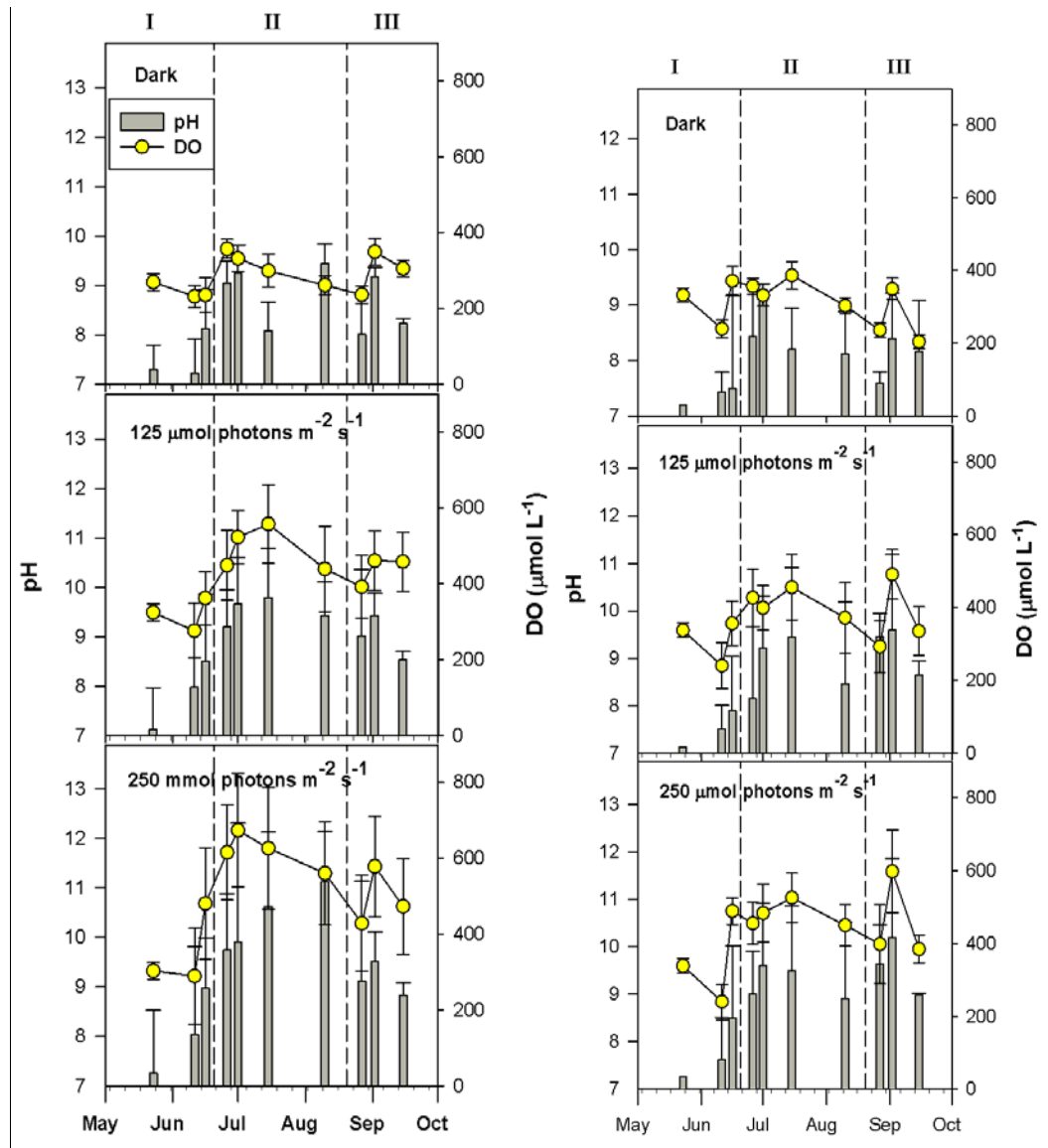


Figure 4-9 Net photosynthetic rate as a function of average DIC concentration at incubation irradiances of 62.5, 125, 250 μmol photons m<sup>-2</sup> h<sup>-1</sup>. At DIC concentrations below 540 μmol L<sup>-1</sup> (indicated by vertical line), photosynthetic rates did not increase with irradiance.



**A) Budds Landing**

**B) Drawbridge**

Figure 4-10 The average of pH and dissolved oxygen (DO) in the laboratory incubations of samples from Budds Landing (BL) and Drawbridge (DB). The bars are pH ± SE; the circles are DO ± SE. Data are shown for the bloom stage I, II and III.

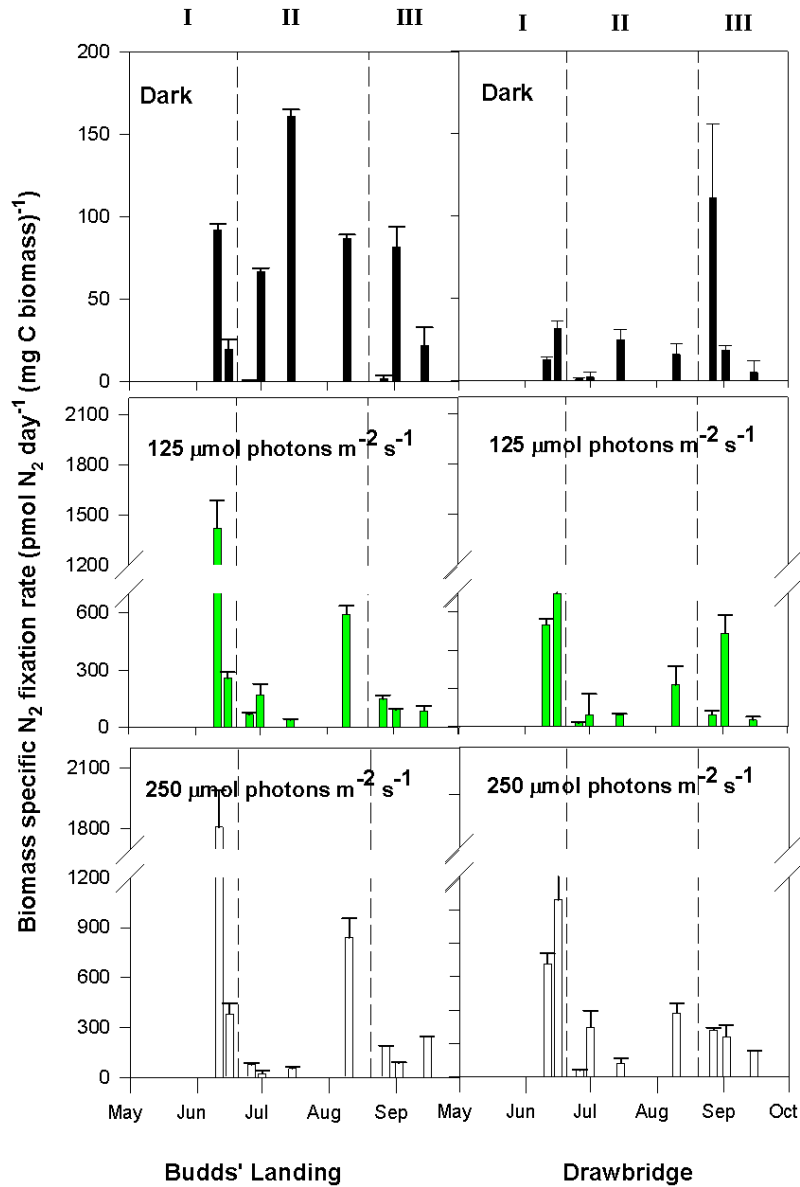


Figure 4-11  $N_2$  fixation rates of at Budds Landing (BL) and Drawbridge (DB), including 24 hr dark and dark-light incubation at irradiance of 125 and 250  $\mu\text{mol photons m}^{-2} \text{h}^{-1}$ . Note difference in y-axis scales. Data are shown for the bloom stage I, II and III.

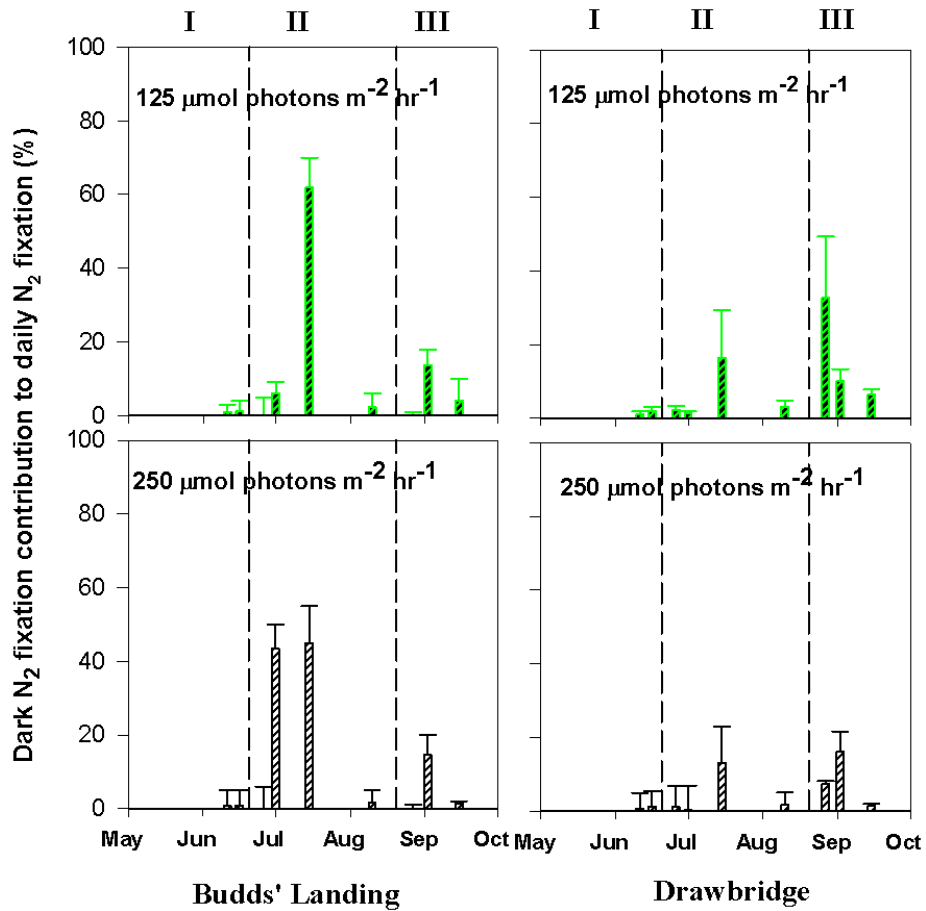


Figure 4-12 Contribution of dark N<sub>2</sub> fixation to daily N<sub>2</sub> fixation at Budds Landing (BL) and Drawbridge (DB). Assuming N<sub>2</sub> fixation rate in 24 h dark incubation was equal to that in dark period at the 24 hr D: L incubation, accumulation of fixed N in the 10 hr dark was compared with the daily N fixation in D: L incubation at each light level. Data are shown for the bloom stage I, II and III.



## Chapter 5      Summary and Conclusions: Factors contribution to cyanobacterial blooms in the Sassafras River, Maryland

In many years, cyanobacteria cause massive blooms in the tidal-fresh and oligohaline region of the upper Sassafras River, which can result in toxic events and degradation of water quality (Tango and Butler 2008). In recent decades, diazotrophic cyanobacteria dominated blooms have increased in magnitude and have reached abundances up to  $4.2 \times 10^6$  cells  $\text{ml}^{-1}$  (Fig.1). In order to understand why these undesirable blooms occur in estuarine-tidal fresh waters such as the Sassafras River, data were assembled on nutrient input and burial, nutrient regeneration through biogeochemical recycling, and  $\text{N}_2$  fixation, as well as on the factors that may control cyanobacterial bloom initiation, persistence and termination (Table 1).

### **Nutrient loading from watershed**

Eutrophication can strongly influence and sustain harmful cyanobacterial blooms in estuarine ecosystems (Kemp et al. 2005; Richardson 1997). Land use in the Sassafras River watershed is 59% agricultural, 24% forested and 5% developed (residential and industrial) (Sassafras River Association). In the counties around the Sassafras River (Kent and Cecil Counties in Maryland, and New Castle County in Delaware), human population has increased about 17% (from  $46 \times 10^3$  to  $54 \times 10^3$ ) between 1980 and 2008, likely increasing nutrient loading. However, the most dramatic increase in a potential

source of nutrient loading has been in chicken growing operations. Total chicken inventory and sales increased by 40% from 1997 to 2007 in these counties (National Agriculture Association). Estuaries are experiencing nutrient enrichment through land runoff, land erosion and waste water input. Based on estimates from modeling of point and non-point sources in the Sassafras watershed (Shenk and Boynton, results of Chesapeake Bay Watershed model), the yearly loading rate of total nitrogen (N) and total phosphate (P) has increased 2-3 fold and 3-4 fold, respectively, during 1985 to 2005 (Fig. 2). Similar increases in nutrient loading are reported for other Chesapeake Bay tributaries including the Potomac River, Choptank River and Patuxent River (Boynton et al. 1995; Fisher et al. 2006a; Testa et al. 2008).

### **Hydrological influences**

In the Sassafras River, flow rates decline from winter-spring to summer-fall and are positively related to DIN and DIP input (Fig. 3). Paerl (2008) has suggested that elevated winter-spring rainfall and flushing events followed by prolonged summer droughts might promote cyanobacterial blooms in estuaries. Winter-spring rainfall would tend to increase nutrient availability for bloom initiation. During prolonged droughts, cyanobacteria may out-compete eukaryotic algae because they may be better at recycling and retaining nutrients. In addition, the long water residence times during droughts may favor relatively slow growing cyanobacterial species.

We found that in summer, flow has a negative effect on cyanobacterial abundance in the upper Sassafras River (Fig. 4), which is similar to the Potomac River and other estuaries (Bennett et al. 1986). Cell densities of cyanobacteria were 5-10 times higher during the dry years (2002 and 2005) than the wet years (2003 and 2004, Fig. 8A).

Moreover, diazotrophic cyanobacteria accounted for 70-98% of the cyanobacterial abundance when the monthly average river flow was below  $2 \text{ m}^3 \text{ s}^{-1}$  in summer; while < 10% of the cyanobacteria were diazotrophic in the summer of 2003, a wet, stormy year (Fig. 8B). Soluble N input from fields into the river may be reduced in summer due to nutrient uptake with crop growth and evaporation that usually exceeds rainfall (Fisher et al. 2006a). Particularly during drought, the constant input of sewage effluent with low N : P ratio (5-8) may cause N limitation (Staver et al. 1996). Intense precipitation, which is usually consistent with increased river discharge, may bring more nutrients into the water (Bennett et al. 1986). However, rapid river discharge increases turbidity and decreases light penetration in the water column due to resuspension and higher input of terrestrially derived particulates, potentially decreasing the growth rate of cyanobacteria. Rising flow rates also decrease the residence time of water; if residence times are lower than the growth rate of cyanobacteria, cyanobacterial populations will decrease. Accumulated cyanobacteria colonies in the water may be flushed from the system. This scenario suggests that although high flow delivers more nutrients, it might still discourage bloom formation (Paerl 2008).

The seasonal increase in nutrient release from sediments and  $\text{N}_2$  fixation are important for supporting massive blooms. From spring to summer, nutrient loading rates declined from  $1.5$  to  $0.5 \text{ mmol m}^{-2} \text{ d}^{-1}$  of DIN and  $0.8$  to  $0.2 \text{ mmol m}^{-2} \text{ d}^{-1}$  of DIP (Fig. 5). In contrast, release of  $\text{NH}_4^+$  and SRP from sediment increased in the same time frame (Fig. 7). In summer, sediment fluxes of DIN and SRP provide 5-20 times more N and 2-9 times more P than nutrient loading from land to the estuary. In addition,  $\text{N}_2$  fixation may be important to meet the nitrogen demand of phytoplankton in N limited conditions.

### **Sediment N and P burial in the Sassafras River estuary**

We took sediment cores in the upper Sassafras River to estimate sedimentation rates and nutrient burial in the sediments (Fig. 6). Based on radiometric  $^{210}\text{Pb}$  geochronology dating techniques (Armentano and Woodwell 1975b), sedimentation rates were calculated with the mass accumulation amounts at depth and a modified equation for the first-order decay in sediment (Robbins et al. 1978). The estimated sedimentation rate ( $1.5 \text{ kg m}^{-2} \text{ y}^{-1}$ ) in the upper Sassafras River was similar to those obtained from cores from other tidal fresh regions of Chesapeake Bay, such as the rates of 2.9-4.4  $\text{kg m}^{-2} \text{ y}^{-1}$  in the Patuxent River (Hartzell, 2009), 1.8-8.4  $\text{kg m}^{-2} \text{ y}^{-1}$  for the subtidal region in the Corsica River (Palinkas and Cornwell, in press), and 1-3  $\text{kg m}^{-2} \text{ y}^{-1}$  in the main channel of the upper Chesapeake Bay (Cooper and Brush 1993; Cornwell et al. 1996). Based on the N and P content of sediments integrated over the last 30 years (top ~10 cm sediment) in the Sassafras River cores, N and P burial rates are 1.8 and 6.6  $\text{g m}^{-2} \text{ y}^{-1}$ , respectively. These results are close to the nutrient burial rates in the tidal-fresh and subtidal regions in the Patuxent River and Corsica River (Hartzell et al. 2010; Merrill 1999).

Sediments trapped a substantial fraction of nutrients entering the Sassafras River. During 1985-2005, the input of TN from point and diffusive sources averaged 10.9  $\text{g N m}^{-2} \text{ y}^{-1}$ , and ranged from 5.8-15  $\text{g N m}^{-2} \text{ y}^{-1}$ . Meanwhile, TP input varied from 0.2 to 2.2  $\text{g P m}^{-2} \text{ y}^{-1}$  with a mean of 0.86  $\text{g P m}^{-2} \text{ y}^{-1}$ . Assuming the atmospheric deposition in this river is similar to that of the Choptank River, which is covered with 65% of agriculture, forest and 6% urban, direct atmospheric deposition were 0.16  $\text{g N m}^{-2} \text{ y}^{-1}$  and 1.1  $\text{g P m}^{-2} \text{ y}^{-1}$  for the watershed (Fisher et al. 2006b). Therefore, approximately 50% of TN delivered from the watershed and atmospheric deposition was temporarily sequestered in

sediment; TP retention in sediments accounted for 80% - 200 % of external nutrient High P storage efficiency has been suggested by a whole Chesapeake mass balance (Boynton 1995).

Although the whole watershed model estimation of nutrient loading might differ from the 'real' input in our study region, the N and P retention in sediments reasonably reflects nutrient accumulation and regeneration. In agriculturally dominated regions, application of fertilizer to soils may enrich soil P content, and enhance particulate P input through bank erosion, rain events and land runoff (Fisher et al. 2006a). Phosphorus input, mainly as particulate form, may be deposited in sediments, especially during periods of low river discharge. In contrast to P, the dominant input of N is dissolved N, which may be directly taken up by phytoplankton or flushed downstream. In addition, N regenerated from particulate decomposition in sediments has a high turnover rate due to ammonium release, nitrification and denitrification (Kemp and Boynton 1984; Vouve et al. 2000). In contrast, P release is usually hindered by re-adsorption and co-precipitation with iron oxides in surface sediment under aerobic water. Once triggered by the suitable conditions (e.g. temperature, redox condition, and pH), the efflux of N and P from sediments can support primary production in the water column.

### **Contribution of sediment nutrient flux and N<sub>2</sub> fixation in supporting cyanobacteria blooms**

Nutrient release from sediments and N<sub>2</sub> fixation might support most of N and P demand by summer cyanobacterial blooms (Table 3). *In situ* primary productivity and N<sub>2</sub> fixation were measured every 2-4 hours for 24 hours at Budds Landing (BL) during a massive cyanobacterial bloom in July 30, 2010. Daily rates of primary production and N<sub>2</sub>

fixation were measured, and integrated with depth and incubation time in the field. The N demand and fixed N through nitrogenase activity were estimated from net primary production with a ratio of 106C : 16N, and N<sub>2</sub> fixation estimated from nitrogenase activity (Carpenter and Price 1977). N<sub>2</sub> fixation is estimated to have contributed 3.3 mmol N m<sup>-2</sup> d<sup>-1</sup> and to have accounted for 21% of the N supply for cyanobacterial growth on this date (Table 3B and Fig. 8).

Flux measurements within the bloom zone suggest that dissolved nutrient fluxes from sediment into the water might support a substantial fraction of primary production. In sediments taken near station Budds Landing, net DIN release was 8.3 mmol m<sup>-2</sup> d<sup>-1</sup> in July and 11.4 mmol m<sup>-2</sup> d<sup>-1</sup> in early August, 2010. SRP release from Budds Landing was 0.2 to 0.9 mmol m<sup>-2</sup> d<sup>-1</sup> from July to August (Fig. 7). If we disregard soluble nutrient transport downriver, release from sediment may contribute 52% to 72% of N and 20% to 91% of P needed to support summer cyanobacterial bloom nutrient demand (Fig. 8).

### **Factors influencing sediment nutrient regeneration**

Several environmental factors may favor sediment nutrient regeneration and release of nutrients to the water column (Tab. 2). Rising temperatures increase the efficiency of bacterially mediated decomposition of organic matter, and thus enhance remineralization of N and P as well as their release into water (Cowan and Boynton 1996; Kim et al. 2006). The temperature coefficient (Q<sub>10</sub>) reflects the change in rates as a consequence of increasing temperature by 10 °C. The estimated Q<sub>10</sub> in the Sassafras River is 2.3 for SRP, 1.47 for NH<sub>4</sub><sup>+</sup>, 1.3 for SOD and 1.5 for CO<sub>2</sub>.

Benthic and pelagic processes in shallow water estuaries are tightly coupled with organic matter production in the water-column, fueling sediment nutrient recycling

(Cowan and Boynton 1996). Partly due to the low freshwater discharge, sediments within the bloom region received higher deposition of phytodetritus than sediments further downstream, where cyanobacteria density was generally low.

Both experimental and field observations suggest that photosynthesis-driven pH elevation impacts nutrient exchange at the sediment-water interface. During dense cyanobacterial blooms, high pH is maintained for several weeks in the shallow waters of the upper Sassafras River ([www.eyesonthebay.com](http://www.eyesonthebay.com)), allowing progressive pH penetration into the sediment. In the N-rich sediment of a tidal fresh estuary (Kithome et al. 1998), conversion of  $\text{NH}_4^+$  to  $\text{NH}_3$  as pH increases results in desorption of exchangeable ammonium, increased ammonium concentrations in the pore water, vertical gradients of both  $\text{NH}_4^+$  and  $\text{NH}_3$ , and increased ammonium flux rates. The high  $\text{NH}_4^+$  flux rates in the bloom areas compared to that outside the bloom (Fig. 7) might be attributable to the high labile organic matter input and high pH in the bloom area (Newell et al. 2009).

Nitrification can be inhibited by the toxic effects of  $\text{NH}_3$  and high pH in the thin oxic layer ~ 2 mm of sediments; inhibition can occur once the water column pH is above the optimal range of 6.5-8.5 of nitrification (Anthonisen et al. 1976; Cuhel et al. 2010). Bloom induced changes in biogeochemical processes can limit the supply of  $\text{NO}_3^-$  for denitrification, either from nitrification or diffusion from the overlying water. The combined toxic effects of pH and  $\text{NH}_3$  can reduce the activity of denitrifying bacteria and thus  $\text{NO}_3^-$  availability (Park et al. 2010).

Photosynthesis and dark respiration by cyanobacteria can result in great variability in environmental conditions during the diel cycle that affect biogeochemical

processes. As a consequence of oxygen penetration from the overlying water into sediment, the redox boundary layer may move up in light and downward in dark, which may result in a decline in denitrification with bloom development (Fig. 7). The elevated pH and DO fluctuations during blooms favor the remineralization of N through benthic  $\text{NH}_4^+$  release, rather than loss of N from the system, and thus provide bioavailable N in the N-limited bloom water.

In addition, elevated pH (> 9) triggers massive P release from Fe-bonded P compounds, which are usually preserved due to particulate precipitation and re-adsorptions of soluble P at the oxic sediment surface. In experimental core incubations, as the pH increased from neutral to 9.5, SRP flux rates dramatically increased by 5-10 fold. Unlike the constant pH conditions used in the laboratory simulations, the pH in sediments may change with the diel changes of pH in the overlying water. High pH effects on SRP fluxes from sediments were only found when high pH in the water column persisted for days during the massive bloom in summer. The high pH kept moving downward into sediment, leading to further desorption of P and continued SRP release from sediment into the water column. The maximum SRP flux rates were  $23.7 \pm 4.3$  and  $42.5 \pm 5.2 \mu\text{mol m}^{-2} \text{h}^{-1}$  at sites 1A and 1B, respectively, during the high pH period. Ratios of DIN: SRP flux rates during the high pH period were generally < 16 (the Redfield Ratio). Relative to DIN flux, high SRP tends to favor the diazotrophic cyanobacterial blooms.

### **Factors influencing $\text{N}_2$ fixation rates**

Although cyanobacteria may take advantage of  $\text{N}_2$  fixation when DIN supply is insufficient during summer (Capone et al. 2005),  $\text{N}_2$  fixation rates varied greatly both



spatially and temporally during our multiple year investigation. Dissolved nutrient concentrations and N to P ratios in estuaries are more influenced by land input and episodic rain events than these parameters in oceanic waters, which lead to more complex changes in N<sub>2</sub> fixing activity in estuaries than in the ocean. However, a number of environmental factors have a predictable influence on the diazotrophic response to N deficiency (Table 2). The biomass of N<sub>2</sub>-fixing cyanobacteria and nitrogenase activity in 2010 generally increased from spring to summer, which was partly due to rising temperature and decrease in N: P ratios in the water.

Increases in irradiance can promote both C and N fixation as cyanobacterial blooms develop. Once cyanobacteria become dense enough to cause unusually high pH and DO in a tidal freshwater estuary, limitation of DIC (in the available form of CO<sub>2</sub> and HCO<sub>3</sub><sup>-</sup>) may inhibit carbon uptake and subsequently reduce N fixation rates; oxygenic photosynthesis may also inhibit nitrogenase activity. N<sub>2</sub>-fixation rates were generally low in high pH /DO water during 2010 blooms. However, cyanobacteria tended to adapt to high pH and DO by changes in species composition which appeared to be related to their diel pattern of nitrogenase activity. Unicellular *Synechococcus* was usually in lower biomass than *Anabaena* and *Pseudanabaena* spp., but in the dark, it is estimated that it could contribute 60 – 80% of the total daily N-fixation. However, limited SRP and the high pH-induced trace metal (e.g. Fe, Mo) precipitation may constrain N<sub>2</sub> fixation due to a greater demand for these elements by N<sub>2</sub>-fixers. In early autumn, the gradual increase in salinity, reduction in water temperature and decrease in daily irradiance probably contributed to the termination of the cyanobacterial bloom.

### **Advantages of cyanobacteria over eukaryotic phytoplankton**

Cyanobacteria are more competitive than most eukaryotic phytoplankton when high pH causes limitation of inorganic carbon (Mogelhoj et al. 2006). Cyanobacteria can take up  $\text{HCO}_3^-$  to provide  $\text{CO}_2$  for photosynthesis through an efficient carbon concentration mechanism (CCM) that elevates the concentration of  $\text{CO}_2$  around Rubisco and increases enzyme activity (Badger et al. 2006; Kaplan et al. 1980). Gas-vacuolated cyanobacteria, *Microcystis*, *Anabaena* and *Pseudanabaena*, can carry out vertical migration to the surface layer where the higher irradiance and dissolved  $\text{CO}_2$  may support a high rate of photosynthesis (Klemer et al. 1996; Walsby et al. 1997). Thus, CCM and buoyancy can help cyanobacteria survive and continue to take up inorganic C at higher pH levels than most phytoplankton, and thus allows them to maintain high pH in the water column and promote nutrient release in shallow water estuaries.

Cyanobacteria may be relatively resistant to grazing by zooplankton and other small grazers, which may potentially increase the chance for cyanobacteria to outcompete other phytoplankton in the community (Buskey 2008; Lampert 1987). Lampert (1987) suggested that large colonies of *Aphanizomenon*, *Anabaena* and *Microcystis* were hard to handle by zooplankton. Cyanobacterial toxins provide another positive feedback for their growth by reducing the filtration, growth, reproduction and survival of zooplankton (Thostrup and Christoffersen 1999). High pH ( $> 9.5$ ) causes death of most protozooplankton and pH  $> 9$  reduces the biomass of heterotrophic protists in estuarine and coastal waters (Pedersen and Hansen 2003). Thus, high pH driven by photosynthesis of cyanobacterial assemblages may reduce mortality of cyanobacteria due to grazing.

Some studies suggest a linkage between the persistence of cyanobacteria blooms in certain areas and storage of “seed” populations of cyanobacteria and polyphosphates in sediment. Some species of cyanobacteria (e.g. *Microcystis*) that help form summer blooms can survive overwinter in the sediment as vegetative cells, rather than forming special akinetes (Brunberg and Bostrom 1992). In spring, when conditions are suitable for cyanobacterial growth, recruitment can occur from this benthic ‘seed’ population. Polyphosphates stored by cyanobacteria (e.g. *Synechocystis* spp., *Synechococcus* spp.) under P sufficient conditions may help them to survive under P deficiency (Grillo and Gibson 1979; Lawrence et al. 1998). When cyanobacteria containing polyphosphates settle to the bottom in oxic waters, polyphosphates are found at the sediment surface which may then influence P release from sediment (Sannigrahi and Ingall 2005).

### **Conclusions**

Increased inputs of nutrients from land and low N: P ratios in the water column, combined with high winter-spring flow and summer drought, can create conditions that favor cyanobacterial blooms in shallow fresh-oligohaline tidal waters. Once established, cyanobacterial blooms “bioengineer” the ecosystem to support their persistence and growth during the warm season. Most notably, this includes sustained increases in water column pH, which in shallow waters cause changes in sediment biogeochemistry that result in increased nutrient fluxes from the sediments into the water column, thus supporting the bloom. The high pH may also inhibit competitors and grazers on the cyanobacteria. In addition to the pH-driven effects on nutrient biogeochemistry and community ecology, cyanobacteria increase N availability through N<sub>2</sub>-fixation and inhibition of denitrification. This can result in changes in the estuarine ecosystem that

favor eutrophication, retention of nutrients, and persistent and recurrent cyanobacterial blooms.

## References

- Anthonisen, A. C., R. C. Loehr, T. B. S. Prakasam, and E. G. Srinath. 1976. Inhibition of nitrification by ammonia and nitrous-acid. *Journal Water Pollution Control Federation* **48**: 835-852.
- Armentano, T. V., and G. M. Woodwell. 1975. Sedimentation rates in a Long Island marsh determined by  $^{210}\text{Pb}$  dating. *Limnol. Oceanogr.* **20**: 452-456.
- Badger, M. R., G. D. Price, B. M. Long, and F. J. Woodger. 2006. The environmental plasticity and ecological genomics of the cyanobacterial  $\text{CO}_2$  concentrating mechanism. *J. Exp. Bot.* **57**: 249-265.
- Bennett, J. P., J. W. Woodward, and D. J. Shultz. 1986. Effect of discharge on the chlorophyll a distribution in the tidally-influenced Potomac River. *Estuaries* **9**: 250-260.
- Boynton, W. R., J. H. Garber, R. Summers, and W. M. Kemp. 1995. Inputs, transformations, and transport of nitrogen and phosphorus in Chesapeake Bay and selected tributaries. *Estuaries* **18**: 285-314.
- Brunberg, A. K., and B. Bostrom. 1992. Coupling between benthic biomass of *Microcystis* and phosphorus release from the sediments of a highly eutrophic lake. *Hydrobiologia* **235**: 375-385.
- Buskey, E. J. 2008. How does eutrophication affect the role of grazers in harmful algal bloom dynamics? *Harmful Algae* **8**: 152-157.
- Capone, D. G. and others 2005. Nitrogen fixation by *Trichodesmium* spp.: An important source of new nitrogen to the tropical and subtropical North Atlantic Ocean. *Global Biogeochem. Cycles* **19**: GB2024.
- Carpenter, E. J., and C. C. Price. 1977. Nitrogen fixation, distribution, and production of *Oscillatoria (Trichodesmium)* spp. in the western Sargasso and Caribbean Seas. *Limnol. Oceanogr.* **22**: 60-72.
- Cooper, S. R., and G. S. Brush. 1993. A 2,500 year history of anoxia and eutrophication in Chesapeake Bay. *Estuaries* **16**: 617-626.

- Cornwell, J. C., D. J. Conley, M. Owens, and J. C. Stevenson. 1996. A sediment chronology of the eutrophication of Chesapeake Bay. *Estuaries* **19**: 488-499.
- Cowan, J. L. W., and W. R. Boynton. 1996. Sediment-water oxygen and nutrient exchanges along the longitudinal axis of Chesapeake Bay: Seasonal patterns, controlling factors and ecological significance. *Estuaries* **19**: 562-580.
- Cuhel, J. and others 2010. Insights into the effect of soil pH on N<sub>2</sub>O and N<sub>2</sub> emissions and denitrifier community size and activity. *Appl. Environ. Microbiol.* **76**: 1870-1878.
- Fisher, T. R., J. A. Benitez, K. Y. Lee, and A. J. Sutton. 2006a. History of land cover change and biogeochemical impacts in the Choptank River basin in the mid-Atlantic region of the US. *Int. J. Remote Sens.* **27**: 3683-3703.
- Fisher, T. R., J. D. Hagy, W. R. Boynton, and M. R. Williams. 2006b. Cultural eutrophication in the Choptank and Patuxent estuaries of Chesapeake Bay. *Limnol. Oceanogr.* **51**: 435-447.
- Grillo, J. F., and J. Gibson. 1979. Regulation of phosphate accumulation in the unicellular cyanobacterium *synechococcus*. *J. Bacteriol.* **140**: 508-517.
- Hartzell, J. L., T. E. Jordan, and J. C. Cornwell. 2010. Phosphorus burial in sediments along the salinity gradient of the Patuxent River, a subestuary of the Chesapeake Bay (USA). *Estuar. Coast.* **33**: 92-106.
- Kaplan, A., M. R. Badger, and J. A. Berry. 1980. Photosynthesis and the intracellular inorganic carbon pool in the blue green alga *Anabaena variabilis* - response to external CO<sub>2</sub> concentration. *Planta* **149**: 219-226.
- Kemp, W. M., and W. R. Boynton. 1984. Spatial and temporal coupling of nutrient inputs to estuarine primary production - the role of particulate transport and decomposition. *Bull. Mar. Sci.* **35**: 522-535.
- Kemp, W. M. and others 2005. Eutrophication of Chesapeake Bay: historical trends and ecological interactions. *Mar. Ecol. Prog. Ser.* **303**: 1-29.
- Kim, D. J., D. I. Lee, and J. Keller. 2006. Effect of temperature and free ammonia on nitrification and nitrite accumulation in landfill leachate and analysis of its nitrifying bacterial community by FISH. *Bioresour. Technol.* **97**: 459-468.

- Kithome, M., J. W. Paul, L. M. Lavkulich, and A. A. Bomke. 1998. Kinetics of ammonium adsorption and desorption by the natural zeolite clinoptilolite. *Soil Sci. Soc. Am. J.* **62**: 622-629.
- Klemer, A. R., J. J. Cullen, M. T. Mageau, K. M. Hanson, and R. A. Sundell. 1996. Cyanobacterial buoyancy regulation: The paradoxical roles of carbon. *J. Phycol.* **32**: 47-53.
- Lampert, W. 1987. Laboratory studies on zooplankton-cyanobacteria interactions. *New Zealand Journal of Marine and Freshwater* **21**: 483-490.
- Lawrence, B. A., C. Suarez, A. Depina, E. Click, N. H. Kolodny, and M. M. Allen. 1998. Two internal pools of soluble polyphosphate in the cyanobacterium *Synechocystis* sp. strain PCC 6308: An in vivo P-31 NMR spectroscopic study. *Arch. Microbiol.* **169**: 195-200.
- Merrill, J. 1999. Tidal freshwater marshes as nutrient sinks: particulate nutrient burial and denitrification. *Marine and Estuarine Science*.
- Mogelhoj, M., P. Hansen, P. Henriksen, and N. Lundholm. 2006. High pH and not allelopathy may be responsible for negative effects of *Nodularia spumigena* on other algae. *Aquat. Microb. Ecol.* **43**: 43-53.
- Newell, R. I. E., R. R. Holyoke, and J. C. Cornwell. 2009. Biogeochemical responses of shallow water sediments to enrichment by eastern oyster (*Crassostrea virginica*) biodeposits. *J. Shellfish Res.* **28**: 717-718.
- Paerl, H. 2008. Nutrient and other environmental controls of harmful cyanobacterial blooms along the freshwater-marine continuum, p. 217-237. *In* K. Hudnell [ed.], *Cyanobacterial Harmful Algal Blooms: State of the Science and Research Needs*. Springer.
- Park, S., W. Bae, and B. E. Rittmann. 2010. Operational boundaries for nitrite accumulation in nitrification based on minimum/maximum substrate concentrations that include effects of oxygen limitation, pH, and free ammonia and free nitrous acid inhibition. *Environ. Sci. Technol.* **44**: 335-342.
- Pedersen, M. F., and P. J. Hansen. 2003. Effects of high pH on a natural marine planktonic community. *Mar. Ecol. Prog. Ser.* **260**: 19-31.

- Richardson, K. 1997. Harmful or exceptional phytoplankton blooms in the marine ecosystem. *Advances In Marine Biology*, Vol 31 Book Series: *Advances In Marine Biology* **31**: 301-385.
- Robbins, J. A., D. N. Edgington, and A. L. W. Kemp. 1978. Comparative  $^{210}\text{Pb}$ ,  $^{137}\text{Cs}$  and pollen geochronologies of sediments from Lakes Ontario and Erie. *Quaternary Research* **10**: 256-278.
- Sannigrahi, P., and E. Ingall. 2005. Polyphosphates as a source of enhanced P fluxes in marine sediments overlain by anoxic waters: Evidence from P-31 NMR. *Geochem. Trans.* **6**: 52-59.
- Staver, L. W., K. W. Staver, and J. C. Stevenson. 1996. Nutrient inputs to the Choptank River estuary: Implications for watershed management. *Estuaries* **19**: 342-358.
- Tango, P. J., and W. Butler. 2008. Cyanotoxins in tidal waters of Chesapeake Bay. *Northeast. Nat.* **15**: 403-416.
- Testa, J. M., W. M. Kemp, W. R. Boynton, and J. D. Hagy. 2008. Long-term changes in water quality and productivity in the Patuxent River estuary: 1985 to 2003. *Estuar. Coast.* **31**: 1021-1037.
- Thostrup, L., and K. Christoffersen. 1999. Accumulation of microcystin in *Daphnia magna* feeding on toxic *Microcystis*. *Archiv für Hydrobiologie* **145**: 447-467.
- Vouve, F., G. Guiraud, C. Marol, M. Girard, P. Richard, and M. J. C. Laima. 2000.  $\text{NH}_4^+$  turnover in intertidal sediments of Marennes-Oleron Bay (France): effect of sediment temperature. *Oceanologica Acta* **23**: 575-584.
- Walsby, A. E., P. K. Hayes, R. Boje, and L. J. Stal. 1997. The selective advantage of buoyancy provided by gas vesicles for planktonic cyanobacteria in the Baltic Sea. *New Phytol.* **136**: 407-417.



## Tables

Table 5.1 Data on cyanobacterial bloom, nutrient inputs and biogeochemical processes in the Sassafras River.

	<b>General description</b>	<b>Location</b>	<b>Time</b>	<b>Measurement frequency</b>	<b>Source</b>
Nutrient land input	Includes diffuse TN, TP, TIN and TIP loads from all point and non-point sources in the basin	The whole Sassafras River	1985-2005	monthly	Bay program HSPG model (Hank and Boynton 2009)
Burial rates and sedimentation	Mass accumulation of C, N and P; <sup>210</sup> Pb dating technique in the top 100 cm sediment	The upper river	June 2009	1	
Nutrient conc.	Dissolved nutrient concentrations of NH <sub>4</sub> <sup>+</sup> , NO <sub>3</sub> <sup>-</sup> , and SRP in water column	Budds Landing	2007-2009	bi-week or monthly	Chesapeake Bay Program
Cell conc.	Species composition and abundance of phytoplankton, including cyanobacteria	Budds Landing Drawbridge	2007-2009 2000-2009	monthly	Maryland DNR
pH and DO	Continuous monitoring of pH, DO, salinity, temperature in water column	Budds Landing	2006-2010	Continuous April to October	eyesonthebay.net (Maryland DNR)
Primary production and N <sub>2</sub> fixation	The diel measurement of the vertical changes in primary productivity and N <sub>2</sub> fixation	Budds Landing	July 30, 2010	One time	Field incubation

Note: sediment releases were measured in Chapter 3; atmospheric deposition rates were estimation in Choptank River (Fisher 2010), a similar estuary in the Chesapeake Bay.

Table 5.2 Positive (+) and negative (-) effects of environmental factors in water column on N<sub>2</sub> fixation by cyanobacteria and nutrient release from sediment into the water column.

	Temperature	Light	pH	DO	NH <sub>4</sub> <sup>+</sup>	NO <sub>3</sub> <sup>-</sup>	SRP	N: P
<b>N<sub>2</sub> fixation</b>	+	+	-	-	-	-	+	-
<b>Nutrient exchange at sediment-water interface</b>								
<b>NH<sub>4</sub><sup>+</sup> flux</b>	+	-	+	?				
<b>NO<sub>3</sub><sup>-</sup> flux</b>	-	+	-	+				
<b>N<sub>2</sub> flux</b>	+	-	-	-				
<b>SRP flux</b>	+	-	+	-				

Table 5.3 Net primary production (A, N=3) and N<sub>2</sub> fixation (B, N=3) incubations at Budds Landing (BL). Water samples were taken from the surface 0.1 - 0.2 m and incubated at depths of 0.1, 0.3, 0.5 and 1 m in July 30, 2010. The 1.0 m incubation is close to the bottom. Primary production was calculated from the difference of oxygen production between the light and dark bottles. N<sub>2</sub> fixation was measured by acetylene reduction.

A)	Incubation			Mean of net primary production ( $\mu\text{mmol O}_2 \text{ L}^{-1} \text{ h}^{-1}$ )				Stand Error				Adjusted $\Delta\text{T}(\text{h})$	Net PP ( $\mu\text{mmol O}_2 \text{ m}^{-2} \text{ h}^{-1}$ )
	Initial	End	$\Delta\text{T}$ (h)	0-0.2m	0.2-0.4m	0.4-0.6m	>0.6m	0-0.2m	0.2-0.4m	0.4-0.6m	>0.6m		
T1	8:10	10:05	1.9	108.0	34.3	43.8	31.4	12.7	0.4	2.19	0.4	1.92	2159.3
T2	9:35	11:10	1.6	187.9	158.7	104.0	-2.7	7.0	5.2	5.20	1.4	1.08	28053.9
T3	10:50	14:15	3.4	120.5	60.9	84.1	65.3	7.9	0.4	4.21	0.1	3.08	2409.1
T4	14:15	17:00	2.8	149.5	109.5	117.6	66.9	7.5	1.4	5.88	50.1	2.75	20667.4
T5	17:30	20:50	3.3	7.9	7.9	-3.9	-13.8	2.9	2.9	0.20	2.8	3.83	315.5
T6	17:30	5:10	11.7	0.0	0.0	0.0	0.0	0.0	0.0	0.00	0.5	8.33	0.0
T7	6:00	8:30	2.5	33.3	20.0	24.2	16.2	1.0	3.1	1.21	1.5	3.33	1550.5
T8	8:15	11:05	2.8	65.9	12.6	14.1	0.0	8.6	0.3	0.71	0.2		
<b>Total of net primary production (<math>\mu\text{mmol O}_2 \text{ L}^{-1} \text{ d}^{-1}</math>)</b>													<b>105171.3</b>

Note: Adjusted  $\Delta\text{T}$  is calculated from the difference of the initial to the end incubation for T1 and from the ending point of adjacent incubation for rest of time periods.

B)	Incubation			Mean of N <sub>2</sub> fixation rates ( $\mu\text{mol N}_2\text{-N L}^{-1}\text{ h}^{-1}$ )				Stand Error				Adjusted $\Delta\text{T}$ (h)	$\Sigma\text{N}_2$ fixation ( $\mu\text{mol N}_2\text{-N m}^{-2}\text{ h}^{-1}$ )
	Time Initial	Time End	$\Delta\text{T}$ (h)	0-0.2m	0.2-0.4m	0.4-0.6m	>0.6m	0-0.2m	0.2-0.4m	0.4-0.6m	>0.6m		
T1	8:10	10:05	1.9	4.25	2.68	2.48	1.43	0.1	0.0	0.02	0.0	1.92	289.1
T2	9:35	11:10	1.6	6.19	4.79	5.54	-0.78	0.1	0.0	0.07	0.0	1.08	190.6
T3	10:50	14:15	3.4	2.37	1.70	3.95	0.02	0.0	0.0	0.04	0.0	3.08	138.2
T4	14:15	17:00	2.8	0.49	1.58	3.52	0.02	0.0	0.0	0.02	0.0	2.75	109.3
T5	17:30	20:50	3.3	0.04	0.04	0.04	0.04	0.0	0.0	0.05	0.0	3.83	6.4
T6	17:30	5:10	11.7	0.80	0.93	0.51	0.39	0.1	0.1	0.06	0.1	8.33	76.1
T7	6:00	8:30	2.5	4.92	5.04	2.58	0.04	0.1	0.0	0.01		3.33	206.1
T8	8:15	11:05	2.8	5.02	5.85	3.18	0.03	0.0	0.0	0.01	0.0		
<b>N<sub>2</sub>-N fixation rates (<math>\mu\text{mol N}_2\text{-N L}^{-1}\text{ d}^{-1}</math>)</b>												<b>3352.9</b>	

Note: Adjusted  $\Delta\text{T}$  is calculated from the difference of the initial to the end incubation for T1 and from the ending point of adjacent incubation for rest of time periods.

Figures

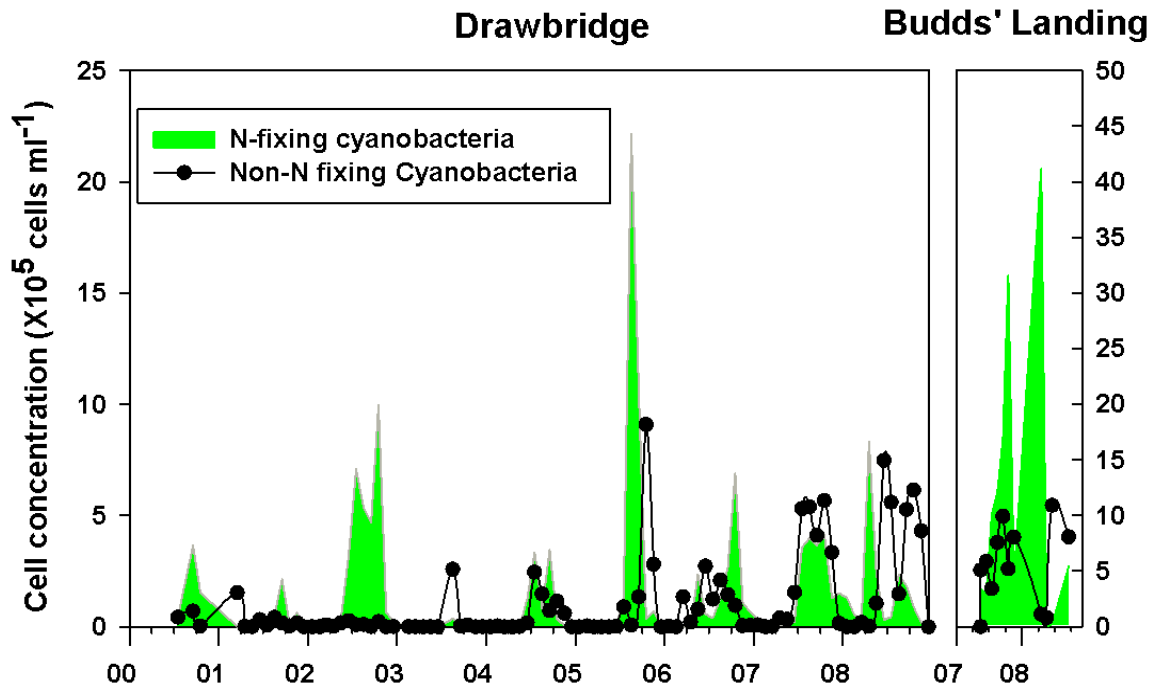


Figure 5-1 Cyanobacterial blooms of Drawbridge (DB) and Budds Landing (BL) in the upper Sassafras River, a tributary of Chesapeake Bay. Data shown are from Maryland Department of Natural Resource (Butler and Michael). Note: changes in y-axis scale between the two sites.

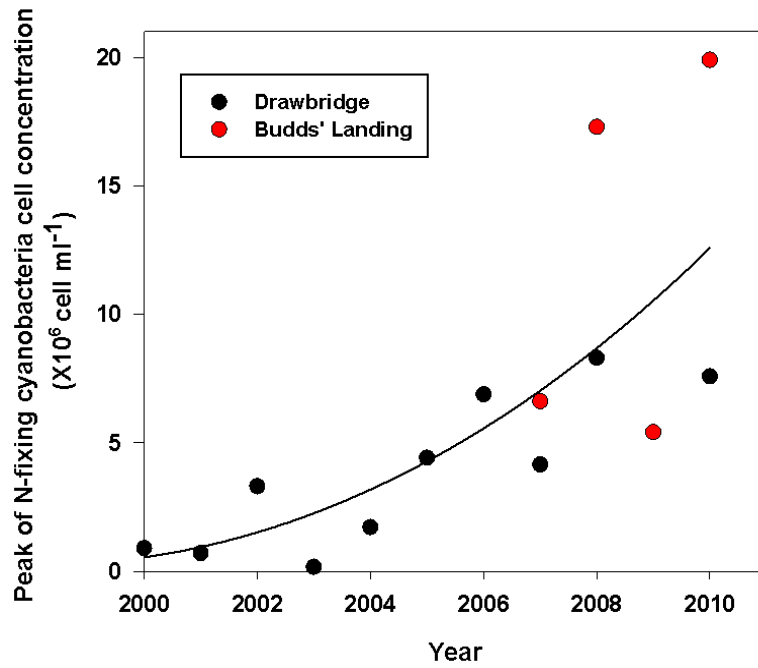


Figure 5-2 Annual maximum cell density of N<sub>2</sub>-fixing cyanobacteria at two stations on the upper Sassafras River: Drawbridge (DB, 2000 – 2010) and Budds Landing (BL, 2007 – 2010) (MD DNR and our samples in 2009 – 2010).

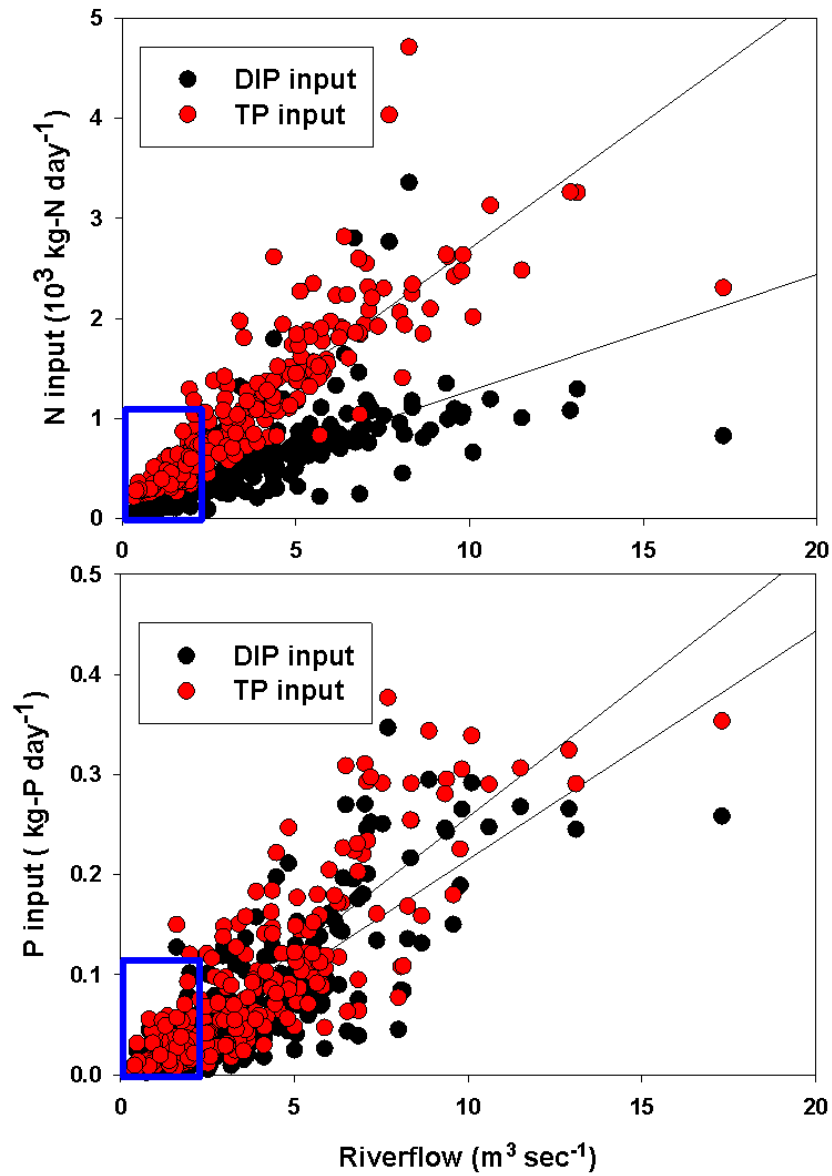


Figure 5-3 The relationship of nutrient loading and river flow. The linear regression coefficient (K) are 252.2 for TN ( $P < 0.001$ ;  $R^2 = 0.87$ ), 116.4 for DIN ( $P < 0.001$ ;  $R^2 = 0.69$ ), 26.9 for TP ( $P < 0.001$ ;  $R^2 = 0.84$ ) and 22.8 for DIP ( $P < 0.001$ ;  $R^2 = 0.82$ ). The monthly average of nutrient inputs include non-point and point source release into this tidal-fresh water estuarine system (model results from Dr. Walter Boynton, UMCES, CBL).

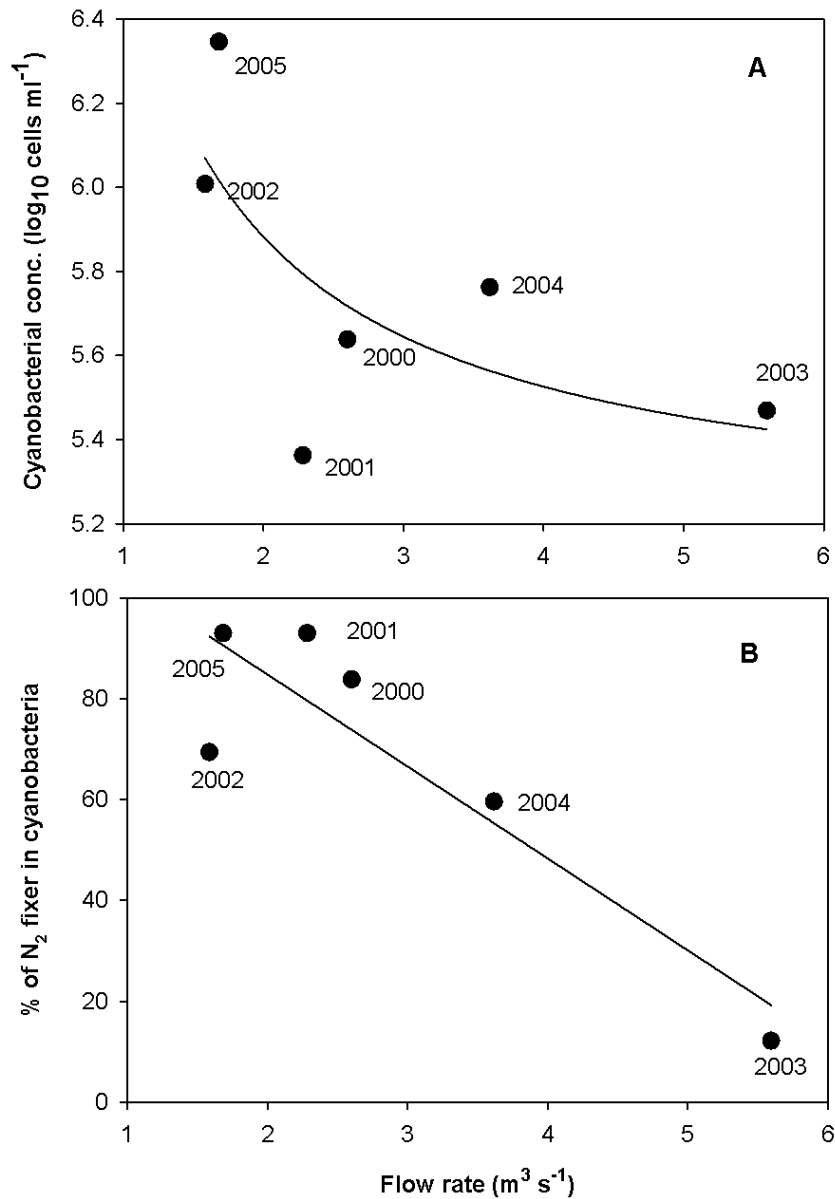


Figure 5-4 Flow rate effects on cyanobacterial abundance (A) and the percentage of diazotrophic cyanobacteria of total cyanobacteria (B). The flow rates are the mean of monthly river flow during June to September in 2000-2005. The maximum cyanobacteria cell concentration ( $y_1$ ) during summer is functional related to flow rates ( $y_1 = 5.16 + 1.42/x$ ,  $R^2 = 0.69$ ,  $P = 0.12$ ); % of diazotrophic cyanobacteria is calculated from the fraction of diazotrophic cyanobacteria in total phytoplankton community when blooms had the highest density. The proportion of  $\text{N}_2$  fixer ( $y_2$ ) is negatively related to flow rates as a function of  $y_2 = 1.21 - 0.18x$  ( $R^2 = 0.90$ ,  $P = 0.014$ ).



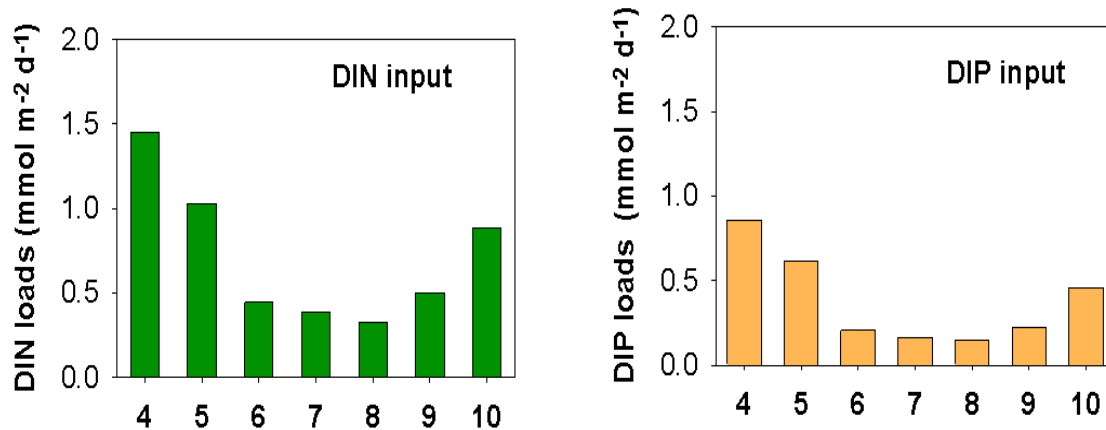


Figure 5-5 Mean of monthly input of DIN and DIP from the point source and nonpoint diffusion into the SassafRAS River. The data shown are the average monthly inputs in 2000-2005, excluding the wet years, 2003 and 2004.

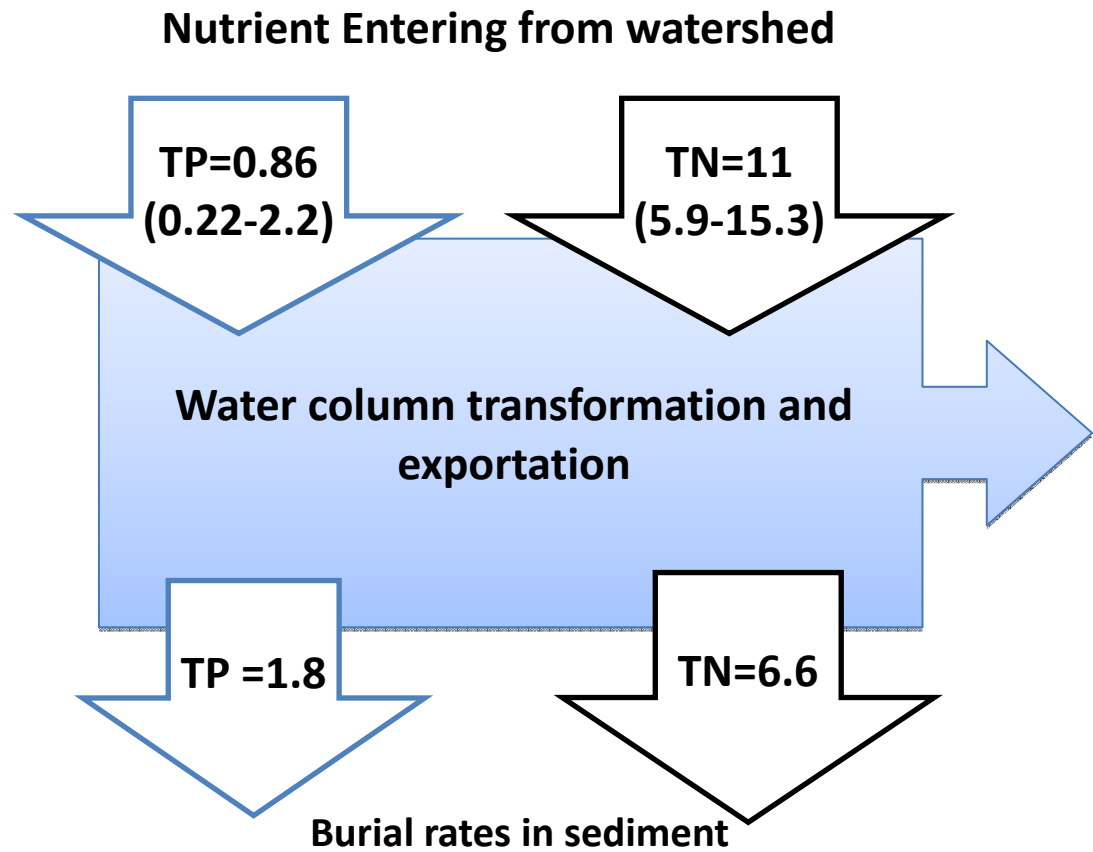


Figure 5-6 The balance between nutrient input from land use and burial rate into the upper Sassafras River. The rates of input and burial are  $\text{g m}^{-2} \text{y}^{-1}$ . A one meter sediment core was taken at the upper Sassafras River ( $39^{\circ}22.310'$ ,  $75^{\circ}50.380'$ ) in June 2009. After section into intervals of 2.0 cm at the top 20cm, of 5.0 cm at 30-60 cm depth, and of 10.0 cm until to the end, sediment samples were analyzed using a sequential extraction technique for  $^{210}\text{Pb}$  ( $T_{1/2}=22.3$  yr) and its daughter radionuclide  $^{210}\text{Po}$  ( $T_{1/2}=138$  days) (Armentano and Woodwell 1975a). Sediment nutrients (C, N and P) were used to quantify burial rates in recent 100 year scale (Nittrouer et al. 1979).

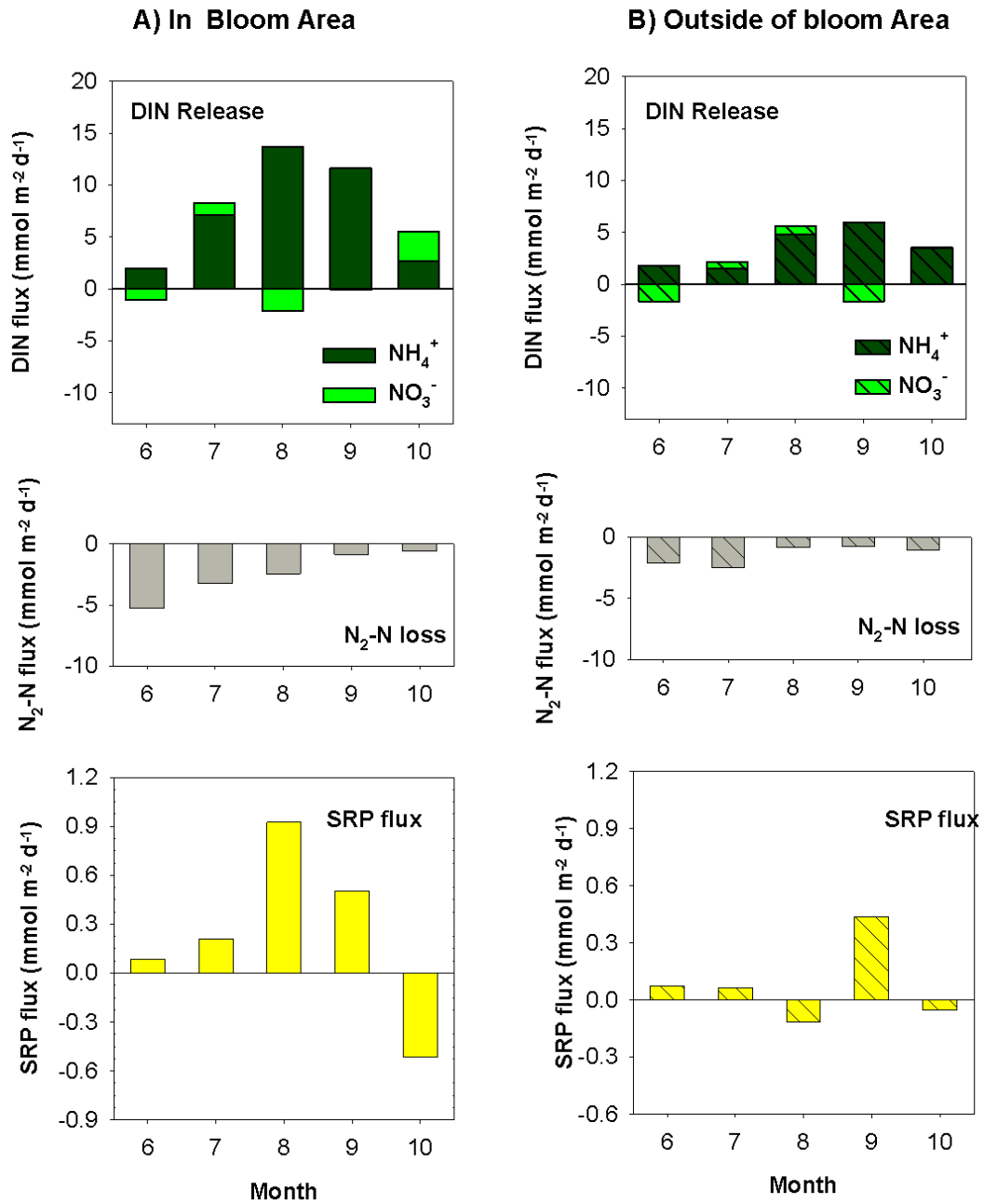


Figure 5-7 Nutrient release (+) and loss (-) to the shallow water column from sediment due to biogeochemical processes within and outside of bloom area during June to September 2010. Data shown are from the seasonal investigation in SR\_2 and SR\_5 (Chap 4).

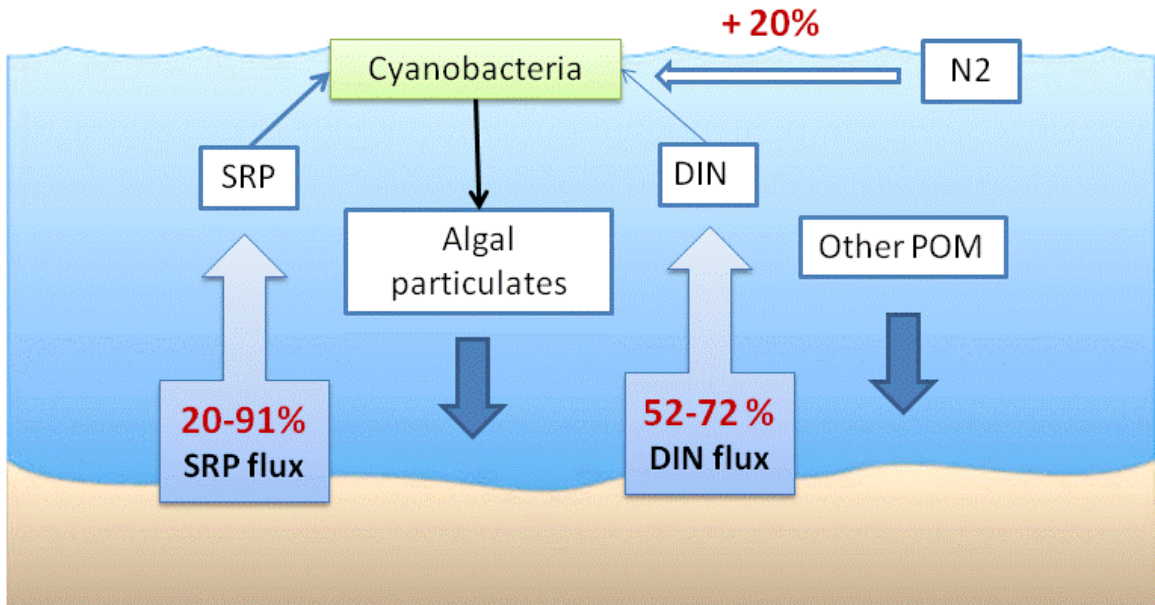


Figure 5-8 The summary of mass balance for SRP and DIN demands by a cyanobacterial bloom, accounting from benthic nutrient fluxes and N<sub>2</sub> fixation. The rates of nutrient demands were estimated from cyanobacterial C uptake (Table 5.3) based on N: P Redfield ratio. N<sub>2</sub> fixation rates and nutrient release from sediments were integrated from the field investigation on June 30, 2010 (Table 5.3) and average flux rates within bloom zone in July and August (Figure 5.7), respectively.

## Complete References

- Acinas, S. G., T. H. A. Haverkamp, J. Huisman, and L. J. Stal. 2009. Phenotypic and genetic diversification of *Pseudanabaena* spp. (cyanobacteria). *ISME J.* **3**: 31-46.
- Adams, D. G., and P. S. Duggan. 1999. Heterocyst and akinete differentiation in cyanobacteria. *New Phytol.* **144**: 3-33.
- Amirbahman, A., A. R. Pearce, R. J. Bouchard, S. A. Norton, and J. S. Kahl. 2003. Relationship between hypolimnetic phosphorus and iron release from eleven lakes in Maine, USA. *Biogeochemistry* **65**: 369-385.
- An, S. 2001. Enhancement of coupled nitrification-denitrification by benthic photosynthesis in shallow estuarine sediments. *Limnol. Oceanogr.* **46**: 62-74.
- Andersen, J. M. 1975. Influence of pH on release of phosphorus from lake sediments. *Archiv für Hydrobiologie* **76**: 411-419.
- Anderson, D. M., P. M. Glibert, and J. M. Burkholder. 2002. Harmful algal blooms and eutrophication: Nutrient sources, composition, and consequences. *Estuaries* **25**: 704-726.
- Anschutz, P., S. J. Zhong, B. Sundby, A. Mucci, and C. Gobeil. 1998. Burial efficiency of phosphorus and the geochemistry of iron in continental margin sediments. *Limnol. Oceanogr.* **43**: 53-64.
- Anthonisen, A. C., R. C. Loehr, T. B. S. Prakasam, and E. G. Srinath. 1976. Inhibition of nitrification by ammonia and nitrous-acid. *Journal Water Pollution Control Federation* **48**: 835-852.
- Armentano, T. V., and G. M. Woodwell. 1975a. Sedimentation-Rates in a Long Island Marsh Determined by Pb-210 Dating. *Limnology and Oceanography* **20**: 452-456.
- . 1975b. Sedimentation rates in a Long Island marsh determined by <sup>210</sup>Pb dating. *Limnol. Oceanogr.* **20**: 452-456.
- Badger, M. R., G. D. Price, B. M. Long, and F. J. Woodger. 2006. The environmental plasticity and ecological genomics of the cyanobacterial CO<sub>2</sub> concentrating mechanism. *J. Exp. Bot.* **57**: 249-265.

- Bailey, E., M. Owens, W. Boynton, and J. Cornwell. 2006. Sediment phosphorus flux: pH interaction in the tidal freshwater Potomac River estuary. Interstate Commission on the Potomac River Basin, UMCES report TS-505-08-CBL: 1-91.
- Baldock, J. A., C. A. Masiello, Y. Gelinas, and J. I. Hedges. 2004. Cycling and composition of organic matter in terrestrial and marine ecosystems. *Mar. Chem.* **92**: 39-64.
- Baumann, B., M. Snozzi, A. J. B. Zehnder, and J. R. Vandermeer. 1996. Dynamics of denitrification activity of *Paracoccus denitrificans* in continuous culture during aerobic-anaerobic changes. *J. Bacteriol.* **178**: 4367-4374.
- Beardall, J., and M. Giordano. 2002. Ecological implications of microalgal and cyanobacterial CO<sub>2</sub> concentrating mechanisms, and their regulation. *Funct. Plant Biol.* **29**: 335-347.
- Beardall, J., A. Johnston, and J. Raven. 1998. Environmental regulation of CO<sub>2</sub> concentrating mechanisms in microalgae. *Canadian Journal of Botany-Revue Canadienne De Botanique* **76**: 1010-1017.
- Bennett, J. P., J. W. Woodward, and D. J. Shultz. 1986. Effect of discharge on the chlorophyll a distribution in the tidally-influenced Potomac River. *Estuaries* **9**: 250-260.
- Bergman, B., J. R. Gallon, A. N. Rai, and L. J. Stal. 1997. N<sub>2</sub> fixation by non-heterocystous cyanobacteria. *FEMS Microbiol. Rev.* **19**: 139-185.
- Berman-Frank, I. and others 2001. Segregation of nitrogen fixation and oxygenic photosynthesis in the marine cyanobacterium *Trichodesmium*. *Science* **294**: 1534-1537.
- Berman-Frank, I., A. Quigg, Z. V. Finkel, A. J. Irwin, and L. Haramaty. 2007. Nitrogen-fixation strategies and Fe requirements in cyanobacteria. *Limnol. Oceanogr.* **52**: 2260-2269.
- Boers, P. C. M. 1991. The influence of pH on phosphate release from lake-sediments. *Water Res.* **25**: 309-311.
- Boers, P. C. M., W. Van Raaphorst, and D. T. Van Der Molen. 1998. Phosphorus retention in sediments. *Water Sci. Technol.* **37**: 31-39.

- Bothe, H., O. Schmitz, M. G. Yates, and W. E. Newton. 2010. Nitrogen fixation and hydrogen metabolism in cyanobacteria. *Microbiol. Mol. Biol. Rev.* **74**: 529-551.
- Boudreau, B. P. 1997. *Diagenetic Models and Their Implementation: Modeling Transport and Reactions in Aquatic Sediments*. Springer.
- Boyd, E. S. and others 2011. Diversity, abundance, and potential activity of nitrifying and nitrate-reducing microbial assemblages in a subglacial ecosystem. *Appl. Environ. Microbiol.* **77**: 4778-4787.
- Boyd, P. W., R. Strzepek, F. X. Fu, and D. A. Hutchins. 2010. Environmental control of open-ocean phytoplankton groups: Now and in the future. *Limnol. Oceanogr.* **55**: 1353-1376.
- Boynton, W., and M. Kemp. 2009. Estuaries, p. 809-866. *In* D. Capone, D. Bronk, M. Mulholland and E. Carpenter [eds.], *Nitrogen in the marine environment*. Elsevier.
- Boynton, W. R. 1996. Sediment-water oxygen and nutrient exchanges along the longitudinal axis of Chesapeake Bay: Seasonal patterns, controlling factors and ecological significance. *Estuar. Coast.* **19**: 562-580.
- Boynton, W. R., J. H. Garber, R. Summers, and W. M. Kemp. 1995. Inputs, transformations, and transport of nitrogen and phosphorus in Chesapeake Bay and selected tributaries. *Estuaries* **18**: 285-314.
- Boynton, W. R. and others 2008. Nutrient budgets and management actions in the Patuxent River estuary, Maryland. *Estuar. Coast.* **31**: 623-651.
- Bray, J. T., O. P. Bricker, and B. N. Troup. 1973. Phosphate in interstitial waters of anoxic sediments - oxidation effects during sampling procedure. *Science* **180**: 1362-1364.
- Brunberg, A. K., and B. Bostrom. 1992. Coupling between benthic biomass of *Microcystis* and phosphorus release from the sediments of a highly eutrophic lake. *Hydrobiologia* **235**: 375-385.
- Burkhardt, S., I. Zondervan, and U. Riebesell. 1999. Effect of CO<sub>2</sub> concentration on C : N : P ratio in marine phytoplankton: A species comparison. *Limnol. Oceanogr.* **44**: 683-690.

- Burns, C. W. 1987. Insights into zooplankton-cyanobacteria interactions derived from enclosure studies. *N. Z. J. Mar. Freshw. Res.* **21**: 477-482.
- Burton, R. F. 1987. On Calculating Concentrations of  $\text{HCO}_3$  from pH and  $\text{PCO}_2$ . *Comparative Biochemistry and Physiology a-Physiology* **87**: 417-422.
- Buskey, E. J. 2008. How does eutrophication affect the role of grazers in harmful algal bloom dynamics? *Harmful Algae* **8**: 152-157.
- Cabrera, F., P. Dearambarri, L. Madrid, and C. G. Toca. 1981. Desorption of phosphate from iron-oxides in relation to equilibrium pH and porosity. *Geoderma* **26**: 203-216.
- Caffrey, J. M., and L. G. Miller. 1995. A comparison of two nitrification inhibitors used to measure nitrification rates in estuarine sediments. *FEMS Microbiol. Ecol.* **17**: 213-220.
- Cai, J., and F. L. Sayles. 1996. Oxygen penetration depths and fluxes in marine sediments. *Mar. Chem.* **52**: 123-131.
- Cai, W. J., G. W. Luther, J. C. Cornwell, and A. E. Giblin. 2010. Carbon cycling and the coupling between proton and electron transfer reactions in aquatic sediments in Lake Champlain. *Aquat. Geochem.* **16**: 421-446.
- Capone, D., D. Bronk, M. Mulholland, and E. Carpenter. 2009. Nitrogen in the marine environment. Elsevier.
- Capone, D. G. 1995. Determination of nitrogenase activity in aquatic samples using the acetylene reduction procedure, p. 621-610. *In* P. Kemp, B. Sherr, E. Sherr and J. Cole [eds.], *Handbook of methods in aquatic microbial ecology*. Lewis.
- Capone, D. G., D. Bronk, M. Mulholland, and E. J. Carpenter. 2008. Nitrogen in the Marine Environment, 2nd edition. . Academic Press/ Elsevier.
- Capone, D. G. and others 2005. Nitrogen fixation by *Trichodesmium* spp.: An important source of new nitrogen to the tropical and subtropical North Atlantic Ocean. *Global Biogeochem. Cycles* **19**: GB2024.
- Capone, D. G., and M. D. Ferrier. 1994. Amino acid cycling in colonies of the planktonic marine cyanobacterium *Trichodesmium thiebautii*. *Appl. Environ. Microbiol.* **60**: 3989-3995.



- Carini, S. A., and S. B. Joye. 2008. Nitrification in Mono Lake, California: Activity and community composition during contrasting hydrological regimes. *Limnol. Oceanogr.* **53**: 2546-2557.
- Carpenter, E. J., J. P. Montoya, J. Burns, M. R. Mulholland, A. Subramaniam, and D. G. Capone. 1999. Extensive bloom of a N<sub>2</sub>-fixing diatom/cyanobacterial association in the tropical Atlantic Ocean. *Mar. Ecol. Prog. Ser.* **185**: 273-283.
- Carpenter, E. J., and C. C. Price. 1977. Nitrogen fixation, distribution, and production of *Oscillatoria (Trichodesmium)* spp. in the western Sargasso and Caribbean Seas. *Limnol. Oceanogr.* **22**: 60-72.
- Carrasco, M., J. M. Mercado, and F. X. Niell. 2008. Diversity of inorganic carbon acquisition mechanisms by intact microbial mats of *Microcoleus chthonoplastes* (Cyanobacteria, Oscillatoriaceae). *Physiol. Plant* **133**: 49-58.
- Codd, G. A., L. F. Morrison, and J. S. Metcalf. 2005. Cyanobacterial toxins: risk management for health protection. *Toxicol. Appl. Pharmacol.* **203**: 264-272.
- Coles, J. F., and R. C. Jones. 2000. Effect of temperature on photosynthesis-light response and growth of four phytoplankton species isolated from a tidal freshwater river. *J. Phycol.* **36**: 7-16.
- Cooper, A. B. 1983. Population ecology of nitrifiers in a stream receiving geothermal inputs of ammonium. *Appl. Environ. Microbiol.* **45**: 1170-1177.
- Cooper, S. R., and G. S. Brush. 1993. A 2,500 year history of anoxia and eutrophication in Chesapeake Bay. *Estuaries* **16**: 617-626.
- Cornwell, J., and K. Kana. 1999. Denitrification in coastal ecosystems: methods, environmental controls, and ecosystem level controls, a review. *Aquat. Ecol.* **33**: 41-54.
- Cornwell, J., and M. Owens. 2011. Quantifying sediment nitrogen releases associated with estuarine dredging. *Aquat. Geochem.* **17**: 499-517.
- Cornwell, J. C., D. J. Conley, M. Owens, and J. C. Stevenson. 1996. A sediment chronology of the eutrophication of Chesapeake Bay. *Estuaries* **19**: 488-499.
- Cornwell, J. C., W. M. Kemp, and T. M. Kana. 1999. Denitrification in coastal ecosystems: environmental controls and aspects of spatial and temporal scale. *Aquat. Ecol.* **33**: 41-54.

- Cowan, J. L. W., and W. R. Boynton. 1996. Sediment-water oxygen and nutrient exchanges along the longitudinal axis of Chesapeake Bay: Seasonal patterns, controlling factors and ecological significance. *Estuaries* **19**: 562-580.
- Cowan, J. L. W., J. R. Pennock, and W. R. Boynton. 1996. Seasonal and interannual patterns of sediment-water nutrient and oxygen fluxes in Mobile Bay, Alabama (USA): Regulating factors and ecological significance. *Mar. Ecol. Prog. Ser.* **141**: 229-245.
- Cox, R. M. 1969. Special aspects of nitrogen fixation by blue-green algae. *Proceedings of the Royal Society B: Biological Sciences* **172**: 357-366.
- Cuhel, J. and others 2010. Insights into the effect of soil pH on N<sub>2</sub>O and N<sub>2</sub> emissions and denitrifier community size and activity. *Appl. Environ. Microbiol.* **76**: 1870-1878.
- Delwiche, L., and S. Slaughter. 2003. *The little SAS book: a primer*. SAS Press.
- Dittmann, E. 2005. Genetic contributions to the risk assessment of microcystin in the environment. *Toxicol. Appl. Pharmacol.* **203**: 192-200.
- Dyhrman, S. T. and others 2006. Phosphonate utilization by the globally important marine diazotroph *Trichodesmium*. *Nature* **439**: 68-71.
- Dyhrman, S. T., and S. T. Haley. 2006. Phosphorus scavenging in the unicellular marine diazotroph *Crocospaera watsonii*. *Appl. Environ. Microbiol.* **72**: 1452-1458.
- Dyhrman, S. T., and K. C. Ruttenberg. 2006. Presence and regulation of alkaline phosphatase activity in eukaryotic phytoplankton from the coastal ocean: Implications for dissolved organic phosphorus remineralization. *Limnol. Oceanogr.* **51**: 1381-1390.
- Eckert, W., A. Nishri, and R. Parparova. 1997. Factors regulating the flux of phosphate at the sediment-water interface of a subtropical calcareous lake: A simulation study with intact sediment cores. *Water Air Soil Pollut.* **99**: 401-409.
- Elliston, K., and J. O'neil. 2005. Nitrogen fixation in various estuarine environments of Chesapeake Bay. Research experiences for undergraduate student (REU) program report.

- Engel, A., K. G. Schulz, U. Riebesell, R. Bellerby, B. Delille, and M. Schartau. 2008. Effects of CO<sub>2</sub> on particle size distribution and phytoplankton abundance during a mesocosm bloom experiment (PeECE II). *Biogeosciences* **5**: 509-521.
- Falcon, L. I., E. J. Carpenter, F. Cipriano, B. Bergman, and D. G. Capone. 2004. N<sub>2</sub> fixation by unicellular bacterioplankton from the Atlantic and Pacific oceans: Phylogeny and in situ rates. *Appl. Environ. Microbiol.* **70**: 765-770.
- Fay, P. 1992. Oxygen relations of nitrogen-fixation in cyanobacteria. *Microbiol. Rev.* **56**: 340-373.
- Filimonenkov, A. A., R. A. Zvyagilskaya, T. V. Tikhonova, and V. O. Popov. 2010. Isolation and characterization of nitrate reductase from the halophilic sulfur-oxidizing bacterium *Thioalkalivibrio nitratireducens*. *Biochemistry* **75**: 744-751.
- Fisher, T. R., J. A. Benitez, K. Y. Lee, and A. J. Sutton. 2006a. History of land cover change and biogeochemical impacts in the Choptank River basin in the mid-Atlantic region of the US. *Int. J. Remote Sens.* **27**: 3683-3703.
- Fisher, T. R., P. R. Carlson, and R. T. Barber. 1982. Sediment nutrient regeneration in 3 north-carolina estuaries. *Estuar. Coast. Shelf Sci.* **14**: 101-116.
- Fisher, T. R., J. D. Hagy, W. R. Boynton, and M. R. Williams. 2006b. Cultural eutrophication in the Choptank and Patuxent estuaries of Chesapeake Bay. *Limnol. Oceanogr.* **51**: 435-447.
- Fisher, T. R., L. W. Harding, D. W. Stanley, and L. G. Ward. 1988. Phytoplankton, nutrients, and turbidity in the Chesapeake, Delaware, and Hudson estuaries. *Estuar. Coast. Shelf Sci.* **27**: 61-93.
- Fisher, T. R., E. R. Peele, J. W. Ammerman, and L. W. Harding. 1992. Nutrient limitation of phytoplankton in Chesapeake Bay. *Mar. Ecol. Prog. Ser.* **82**: 51-63.
- Folk, R. 1974. *Petrology of Sedimentary Rocks*. Hemphill Publishing Company.
- Fu, F. X. and others 2008. Interactions between changing pCO<sub>2</sub>, N<sub>2</sub> fixation, and Fe limitation in the marine unicellular cyanobacterium *Crocospaera*. *Limnol. Oceanogr.* **53**: 2472-2484.
- Fu, F. X., M. E. Warner, Y. H. Zhang, Y. Y. Feng, and D. A. Hutchins. 2007. Effects of increased temperature and CO<sub>2</sub> on photosynthesis, growth, and elemental ratios in

- marine *Synechococcus* and *Prochlorococcus* (Cyanobacteria). *J. Phycol.* **43**: 485-496.
- Gallon, J. R. 1992. Reconciling the incompatible : N<sub>2</sub> fixation and O<sub>2</sub>. *New Phytol.* **122**: 571-609.
- Garcia-Ruiz, R., S. N. Pattinson, and B. A. Whitton. 1998. Denitrification in river sediments: relationships between process rate and properties of water and sediment. *Freshw. Biol.* **39**: 467-476.
- Gardner, W., and M. Mccarthy. 2009. Nitrogen dynamics at the sediment-water interface in shallow, sub-tropical Florida Bay: why denitrification efficiency may decrease with increased eutrophication. *Biogeochemistry* **95**: 185-198.
- Gardner, W. S., M. J. Mccarthy, S. M. An, D. Sobolev, K. S. Sell, and D. Brock. 2006. Nitrogen fixation and dissimilatory nitrate reduction to ammonium (DNRA) support nitrogen dynamics in Texas estuaries. *Limnol. Oceanogr.* **51**: 558-568 Part 552.
- Gardner, W. S., S. P. Seitzinger, and J. M. Malczyk. 1991. The effects of sea salts on the forms of nitrogen released from estuarine and fresh-water sediments - Does ion-pairing affect ammonium flux. *Estuaries* **14**: 157-166.
- Gattuso, J. P., J. W. Liu, M. G. Weinbauer, C. Maier, and M. H. Dai. 2010. Effect of ocean acidification on microbial diversity and on microbe-driven biogeochemistry and ecosystem functioning. *Aquat. Microb. Ecol.* **61**: 291-305.
- Gibb, M. M. 1979. A simple method for the rapid determination of iron in natural waters. *Water Res.* **13**: 295-297.
- Glibert, P. M. and others 2004. Evidence for dissolved organic nitrogen and phosphorus uptake during a cyanobacterial bloom in Florida Bay. *Mar. Ecol. Prog. Ser.* **280**: 73-83.
- Glibert, P. M. F., D.; Burkholder, J. M.; Cornwell, J. C.; Kana, T. M. 2011. Ecological stoichiometry, biogeochemical cycling, invasive species, and aquatic food webs: San Francisco estuary and comparative systems. *Rev. Fish. Sci.* **19**: 1-60.
- Grillo, J. F., and J. Gibson. 1979. Regulation of phosphate accumulation in the unicellular cyanobacterium *synechococcus*. *J. Bacteriol.* **140**: 508-517.

- Hansen, A. M., J. V. Christensen, and O. Sortkajer. 1991. Effect of high pH on zooplankton and nutrients in fish-free enclosures. *Archiv Fur Hydrobiologie* **123**: 143-164.
- Hansen, P. J. 2002. Effect of high pH on the growth and survival of marine phytoplankton: implications for species succession. *Aquat. Microb. Ecol.* **28**: 279-288.
- Hartzell, J. L., T. E. Jordan, and J. C. Cornwell. 2010. Phosphorus burial in sediments along the salinity gradient of the Patuxent River, a subestuary of the Chesapeake Bay (USA). *Estuar. Coast.* **33**: 92-106.
- Havens, K. E. 2008. Cyanobacterial harmful algal blooms: state of the science and research needs. *Adv. Exp. Med. Biol.* **619**: 733-747.
- Heggie, D. T., G. A. Logan, C. S. Smith, D. J. Fredericks, and D. Palmer. 2008. Biogeochemical processes at the sediment-water interface, Bombah Broadwater, Myall Lakes. *Hydrobiologia* **608**: 49-67.
- Henriksen, K., J. I. Hansen, and T. H. Blackburn. 1981. Rates of nitrification, distribution of nitrifying bacteria, and nitrate fluxes in different types of sediment from danish waters. *Mar. Biol.* **61**: 299-304.
- Henriksen, K., and M. J. Kemp. 1988. Nitrification in estuarine and coastal marine sediments: Methods, patterns and regulating factors, p. 207- 249. *In* H. Blackburn and J. Sorensen [eds.], *Nitrogen cycling in coastal marine environments*. Wiley.
- Hinga, K. R. 2002. Effects of pH on coastal marine phytoplankton. *Mar. Ecol. Prog. Ser.* **238**: 281-300.
- Hopkinson, C. S., A. E. Giblin, J. Tucker, and R. H. Garritt. 1999. Benthic metabolism and nutrient cycling along an estuarine salinity gradient. *Estuaries* **22**: 863-881.
- Howarth, R. W. 2006. Nitrogen as the limiting nutrient for eutrophication in coastal marine ecosystems: Evolving views over three decades. *Limnol. Oceanogr.* **51**: 364-376.
- Howarth, R. W., R. Marino, J. Lane, and J. J. Cole. 1988. Nitrogen-fixation in fresh-water, estuarine, and marine ecosystems .1. Rates and importance. *Limnol. Oceanogr.* **33**: 669-687.
- Huisman, J., and H. Matthijs. 2011. *Harmful Cyanobacteria*. Springer.

- Hutchins, C. M., P. R. Teasdale, J. Lee, and S. L. Simpson. 2007. The effect of manipulating sediment pH on the porewater chemistry of copper- and zinc-spiked sediments. *Chemosphere* **69**: 1089-1099.
- Isnansetyo, A., N. D. Thien, and M. Seguchi. 2011. Potential of mud sediment of the Ariake Sea tidal flat and the individual effect of temperature, ph, salinity and ammonium concentration on its nitrification rate. *Res. J Environ. Earth Sci.* **3**: 587-599.
- Jenkins, B. D., G. F. Steward, S. M. Short, B. B. Ward, and J. P. Zehr. 2004. Fingerprinting diazotroph communities in the Chesapeake Bay by using a DNA macroarray. *Appl. Environ. Microbiol.* **70**: 1767-1776.
- Jenkins, M. C., and W. M. Kemp. 1984. The coupling of nitrification and denitrification in two estuarine sediments. *Limnol. Oceanogr.* **29**: 609-619.
- Jones, J. B., and E. H. Stanley. 2003. Long-term decline in carbon dioxide supersaturation in rivers across the contiguous United States. *Geophysical Research Letter* **30**: 1495-1499.
- Jones, R. C. 1998. Seasonal and spatial patterns in phytoplankton photosynthetic parameters in a tidal freshwater river. *Hydrobiologia* **364**: 199-208 Part: Part 192.
- Kana, T. M., J. C. Cornwell, and L. J. Zhong. 2006. Determination of denitrification in the Chesapeake Bay from measurements of N<sub>2</sub> accumulation in bottom water. *Estuar. Coast.* **29**: 222-231.
- Kana, T. M., C. Darkangelo, M. D. Hunt, J. B. Oldham, G. E. Bennett, and J. C. Cornwell. 1994. Membrane inlet mass spectrometer for rapid high-precision determination of N<sub>2</sub>, O<sub>2</sub>, and Ar in environmental water samples. *Anal. Chem.* **66**: 4166-4170.
- Kana, T. M., M. B. Sullivan, J. C. Cornwell, and K. Groszkowski. 1998. Denitrification in estuarine sediments determined by membrane inlet mass spectrometry. *Limnol. Oceanogr.* **42**: 334-339.
- Kana, T. M., and D. L. Weiss. 2004. Comment on "comparison of isotope pairing and N<sub>2</sub>: Ar methods for measuring sediment denitrification" by B. D. Eyre, S. Rysgaard, T. Dalsgaard, and P. Bondo Christensen. 2002. *estuaries* 25 : 1077-1087". *Estuaries* **27**: 173-176.

- Kaplan, A., M. R. Badger, and J. A. Berry. 1980. Photosynthesis and the intracellular inorganic carbon pool in the blue green alga *Anabaena variabilis* - response to external CO<sub>2</sub> concentration. *Planta* **149**: 219-226.
- Karl, D. and others 2002. Dinitrogen fixation in the world's oceans. *Biogeochemistry* **57**: 47-98.
- Kater, B. J., and M. Dubbeldam. 2006. Ammonium toxicity at high pH in a marine bioassay using corophium volutator. *Arch. Environ. Contam. Toxicol.* **51**: 347-351.
- Kemp, M. J., and W. K. Dodds. 2001. Centimeter-scale patterns in dissolved oxygen and nitrification rates in a prairie stream. *J. North. Am. Benthol. Soc.* **20**: 347-357.
- Kemp, W. M., and W. R. Boynton. 1984. Spatial and temporal coupling of nutrient inputs to estuarine primary production - the role of particulate transport and decomposition. *Bull. Mar. Sci.* **35**: 522-535.
- Kemp, W. M. and others 2005. Eutrophication of Chesapeake Bay: historical trends and ecological interactions. *Mar. Ecol. Prog. Ser.* **303**: 1-29.
- Kemp, W. M., J. Faganelli, S. Puskarick, E. M. Smith, and W. R. Boynton. 1999. Pelagic-benthic coupling and nutrient cycling. *Ecosystems at the Land-Sea Margin* **55**: 295-339.
- Kemp, W. M., P. Sampou, J. Caffrey, M. Mayer, K. Henriksen, and W. R. Boynton. 1990. Ammonium recycling versus denitrification in Chesapeake Bay sediments. *Limnol. Oceanogr.* **35**: 1545-1563.
- Killham, K. 1994. *Soil Ecology*. Cambridge University Press.
- Kim, D. J., D. I. Lee, and J. Keller. 2006. Effect of temperature and free ammonia on nitrification and nitrite accumulation in landfill leachate and analysis of its nitrifying bacterial community by FISH. *Bioresour. Technol.* **97**: 459-468.
- Kithome, M., J. W. Paul, L. M. Lavkulich, and A. A. Bomke. 1998. Kinetics of ammonium adsorption and desorption by the natural zeolite clinoptilolite. *Soil Sci. Soc. Am. J.* **62**: 622-629.
- Klemer, A. R., J. J. Cullen, M. T. Mageau, K. M. Hanson, and R. A. Sundell. 1996. Cyanobacterial buoyancy regulation: The paradoxical roles of carbon. *J. Phycol.* **32**: 47-53.

- Koop, K., W. R. Boynton, F. Wulff, and R. Carman. 1990. Sediment-water oxygen and nutrient exchanges along a depth gradient in the Baltic sea. *Mar. Ecol. Prog. Ser.* **63**: 65-77.
- Kopp, J. F., and G. D. Mckee. 1983. *Methods for Chemical Analysis of Water and Wastes*. United States Environmental Protection analysis Agency.
- Krauk, J., T.A., J. A. Villareal, J. P. M. Sohm, and D. G. Capone. 2006. Plasticity of N:P ratios in laboratory and field populations of *Trichodesmium* spp. *Aquat. Microb. Ecol.* **42**: 243-253.
- Krausejensen, D., K. Mcglathery, S. Rysgaard, and P. B. Christensen. 1996. Production within dense mats of the filamentous macroalga *Chaetomorpha linum* in relation to light and nutrient availability. *Mar. Ecol. Prog. Ser.* **134**: 207-216.
- Krogmann, D. W., R. Butalla, and J. Sprinkle. 1986. Blooms of Cyanobacteria on the Potomac River. *Plant Physiol.* **80**: 667-671.
- Laima, M. J. C. 1992. Extraction and seasonal variation of  $\text{NH}_4^+$  pools in different types of coastal marine sediments. *Mar. Ecol. Prog. Ser.* **82**: 75-84.
- Laima, M. J. C. and others 1999. Distribution of adsorbed ammonium pools in two intertidal sedimentary structures, Marennes-Oleron Bay, France. *Mar. Ecol. Prog. Ser.* **182**: 29-35.
- Lamontagne, M., V. Astorga, A. E. Giblin, and I. Valiela. 2002. Denitrification and the stoichiometry of nutrient regeneration in Waquoit Bay, Massachusetts. *Estuaries* **25**: 272-281.
- Lampert, W. 1987. Laboratory studies on zooplankton-cyanobacteria interactions. *New Zealand Journal of Marine and Freshwater* **21**: 483-490.
- Lane, L., S. Rhoades, C. Thomas, and L. Van Heukelem. 2011. Standard Operating procedures 2000. Technical report NO.TS-264-00.
- Lawerence, B. A., C. Suarez, A. Depina, E. Click, N. H. Kolodny, and M. M. Allen. 1998. Two internal pools of soluble polyphosphate in the cyanobacterium *Synechocystis* sp. strain PCC 6308: An in vivo P-31 NMR spectroscopic study. *Arch. Microbiol.* **169**: 195-200.



- Lehtimäki, J., P. Moisanter, K. Sivonen, and K. Kononen. 1997. Growth, nitrogen fixation, and nodularin production by two Baltic Sea cyanobacteria. *Appl. Environ. Microbiol.* **63**: 1647-1656.
- Levitan, O. and others 2007. Elevated CO<sub>2</sub> enhances nitrogen fixation and growth in the marine cyanobacterium *Trichodesmium*. *Global Change Biology* **13**: 531-538.
- Lewis, W. M. 1984. The light response of nitrogen fixation in Lake Valencia, Venezuela. *Limnol. Oceanogr.* **29**: 894-900.
- Liikanen, A., L. Flojt, and P. Martikainen. 2002. Gas dynamics in eutrophic lake sediments affected by oxygen, nitrate, and sulfate. *J. Environ. Qual.* **31**: 338-349.
- Liu, B. B., P. T. Morkved, A. Frostegard, and L. R. Bakken. 2010. Denitrification gene pools, transcription and kinetics of NO, N<sub>2</sub>O and N<sub>2</sub> production as affected by soil pH. *FEMS Microbiol. Ecol.* **72**: 407-417.
- Mackin, J. E., and R. C. Aller. 1984. Ammonium adsorption in marine sediments. *Limnol. Oceanogr.* **29**: 250-257.
- Magalhaes, C. M., A. A. Bordalo, and W. J. Wiebe. 2002. Temporal and spatial patterns of intertidal sediment-water nutrient and oxygen fluxes in the Douro River estuary, Portugal. *Mar. Ecol. Prog. Ser.* **233**: 55-71.
- Magni, P., and S. Montani. 2006. Seasonal patterns of pore-water nutrients, benthic chlorophyll a and sedimentary AVS in a macrobenthos-rich tidal flat. *Hydrobiologia* **571**: 297-311.
- Mahaffey, C., A. F. Michaels, and D. G. Capone. 2005. The conundrum of marine N<sub>2</sub> fixation. *Am. J. Sci.* **305**: 546-595.
- Martens, C. S., and J. V. Klump. 1980. Biogeochemical cycling in an organic-rich coastal marine basin .1. methane sediment-water exchange processes. *Geochim. Cosmochim. Acta* **44**: 471-490.
- Martin, L. A., P. J. Mulholland, J. R. Webster, and H. M. Valett. 2001. Denitrification potential in sediments of headwater streams in the southern Appalachian Mountains, USA. *J. North. Am. Benthol. Soc.* **20**: 505-519.
- Martin, W. R., and G. T. Banta. 1992. The measurement of sediment irrigation rates - a comparison of the br-tracer and <sup>222</sup>Rn/<sup>226</sup>Ra disequilibrium techniques. *Journal of Marine Research* **50**: 125-154.

- Mayer, M., K. Henriksen, and W. R. Boynton. 1990. Ammonium recycling versus denitrification in Chesapeake Bay sediments. *Limnol. Oceanogr.* **35**: 1545-1563.
- Merrill, J. 1999. Tidal freshwater marshes as nutrient sinks: particulate nutrient burial and denitrification. *Marine and Estuarine Science*.
- Milligan, A. J., I. Berman-Frank, Y. Gerchman, G. C. Dismukes, and P. G. Falkowski. 2007. Light-dependent oxygen consumption in nitrogen-fixing cyanobacteria plays a key role in nitrogenase protection. *J. Phycol.* **43**: 845-852.
- Mogelhoj, M., P. Hansen, P. Henriksen, and N. Lundholm. 2006. High pH and not allelopathy may be responsible for negative effects of *Nodularia spumigena* on other algae. *Aquat. Microb. Ecol.* **43**: 43-53.
- Moisander, P. H. and others 2010. Unicellular cyanobacterial distributions broaden the oceanic N<sub>2</sub> fixation domain. *Science* **327**: 1512-1514.
- Moisander, P. H., E. McClinton, and H. W. Paerl. 2002. Salinity effects on growth, photosynthetic parameters, and nitrogenase activity in estuarine planktonic cyanobacteria. *Microb. Ecol.* **43**: 432-442.
- Montoya, J. P., C. M. Holl, J. P. Zehr, A. Hansen, T. A. Villareal, and D. G. Capone. 2004. High rates of N<sub>2</sub> fixation by unicellular diazotrophs in the oligotrophic Pacific Ocean. *Nature* **430**: 1027-1031.
- Morin, J., and J. W. Morse. 1999. Ammonium release from resuspended sediments in the Laguna Madre estuary. *Mar. Chem.* **65**: 97-110.
- Morse, J. W., and J. Morin. 2005. Ammonium interaction with coastal marine sediments: influence of redox conditions on K\*. *Mar. Chem.* **95**: 107-112.
- Mulholland, M. 2008. Gaseous nitrogen compounds (NO, N<sub>2</sub>O, N<sub>2</sub>, NH<sub>3</sub>) in the ocean, p. 52-123. *In* D. Capone, M. Mulholland and E. Carpenter [eds.], *Nitrogen in the Marine Environment*. Elsevier.
- Mulholland, M. R. 2007. The fate of nitrogen fixed by diazotrophs in the ocean. *Biogeosciences* **4**: 37-51.
- Mulholland, M. R., D. A. Bronk, and D. G. Capone. 2004. Dinitrogen fixation and release of ammonium and dissolved organic nitrogen by *Trichodesmium* IMS101. *Aquat. Microb. Ecol.* **37**: 85-94.

- Murphy, J., and J. P. Riley. 1962. A modified single solution method for determination of phosphates in natural water. *Anal. Chim. Acta* **27**: 31-36.
- Newell, R. I. E., J. C. Cornwell, and M. S. Owens. 2002. Influence of simulated bivalve biodeposition and microphytobenthos on sediment nitrogen dynamics: A laboratory study. *Limnol. Oceanogr.* **47**: 1367-1379.
- Newell, R. I. E., R. R. Holyoke, and J. C. Cornwell. 2009. Biogeochemical responses of shallow water sediments to enrichment by eastern oyster (*Crassostrea virginica*) biodeposits. *J. Shellfish Res.* **28**: 717-718.
- Nittrouer, C. A., R. W. Sternberg, R. Carpenter, and J. T. Bennett. 1979. Use of Pb-210 Geochronology as a Sedimentological Tool - Application to the Washington Continental-Shelf. *Marine Geology* **31**: 297-316.
- Nixon, S. W. and others 1996. The fate of nitrogen and phosphorus at the land sea margin of the North Atlantic Ocean. *Biogeochemistry* **35**: 141-180.
- O'neil , J. M., T. W. Davis, M. A. Burford, and C. J. Gobler. 2011. The rise of harmful cyanobacteria blooms: The potential roles of eutrophication and climate change. *Harmful Algae* **Accepted**.
- Oakes Jm Oakes, J. M., B. D. Eyre, and D. J. Ross. 2011. Short-term enhancement and long-term suppression of denitrification in estuarine sediments receiving primary- and secondary-treated paper and pulp mill discharge. *Environ. Sci. Technol.* **45**: 3400-3406.
- Ogawa, T., and A. Kaplan. 2003. Inorganic carbon acquisition systems in cyanobacteria. *Photosynth. Res.* **77**: 105-115.
- Oh, H., J. Maeng, and G. Rhee. 1991. Nitrogen and carbon fixation by *Anabaena* sp. isolated from a rice paddy and grown under P and light limitations. *J. Appl. Phycol.* **3**: 335-343.
- Okeefe, J. 2007. Sediment biogeochemistry across the Patuxent River estuarine gradient: Geochronology and Fe-S-P interactions. Master Thesis.
- Oliver, R. 1994. Floating and sinking in gas-vacuolate cyanobacteria. *J. Phycol.* **30**: 161-173.
- Oliver, R. L., and G. G. Ganf. 2000. Freshwater blooms, p. 149-194. *In* B. A. Whitton, Potts, M. [ed.], *The Ecology of Cyanobacteria*. Dordrecht.

- Paerl, H. 2008. Nutrient and other environmental controls of harmful cyanobacterial blooms along the freshwater-marine continuum, p. 217-237. *In* K. Hudnell [ed.], *Cyanobacterial Harmful Algal Blooms: State of the Science and Research Needs*. Springer.
- Paerl, H., and J. P. Zehr. 2000. Marine nitrogen fixation, p. 387-418. *In* D. Kirchman [ed.], *Microbial Ecology of the Oceans*. Wiley-Liss, Inc.
- Paerl, H. W. 1978. Role of Heterotrophic Bacteria in Promoting N<sub>2</sub>-Fixation by *Anabaena* in Aquatic Habitats. *Microb. Ecol.* **4**: 215-231.
- . 1996. Microscale physiological and ecological studies of aquatic cyanobacteria: macroscale implications. *Microsc. Res. Tech.* **33**: 47-72.
- Paerl, H. W., and J. Huisman. 2009. Climate change: a catalyst for global expansion of harmful cyanobacterial blooms. *Env Microbiol Rep* **1**: 27-37.
- Paerl, H. W., and J. L. Pinckney. 1996. A mini-review of microbial consortia: Their roles in aquatic production and biogeochemical cycling. *Microb. Ecol.* **31**: 225-247.
- Park, S., W. Bae, and B. E. Rittmann. 2010. Operational boundaries for nitrite accumulation in nitrification based on minimum/maximum substrate concentrations that include effects of oxygen limitation, pH, and free ammonia and free nitrous acid inhibition. *Environ. Sci. Technol.* **44**: 335-342.
- Parsons, T. R., Y. Maita, and C. M. Lalli. 1984. Fluorometric determination of chlorophylls, p. 107-108. *In* T. R. Parsons [ed.], *A Manual of Chemical and Biological Methods for Seawater Analysis*. Pergamon Press.
- Pedersen, M. F., and P. J. Hansen. 2003. Effects of high pH on a natural marine planktonic community. *Mar. Ecol. Prog. Ser.* **260**: 19-31.
- Perakis, S. S., E. B. Welch, and J. M. Jacoby. 1996. Sediment-to-water blue-green algal recruitment in response to alum and environmental factors. *Hydrobiologia* **318**: 165-177.
- Pfenning, K. S., and P. B. McMahon. 1997. Effect of nitrate, organic carbon, and temperature on potential denitrification rates in nitrate-rich riverbed sediments. *Journal of Hydrology* **187**: 283-295.
- Piehler, M. F., J. Dyble, P. H. Moisander, J. L. Pinckney, and H. W. Paerl. 2002. Effects of modified nutrient concentrations and ratios on the structure and function of the

- native phytoplankton community in the Neuse River Estuary, North Carolina, USA. *Aquat. Ecol.* **36**: 371-285.
- Ploug, H. 2008. Cyanobacterial surface blooms formed by *Aphanizomenon* sp and *Nodularia spumigena* in the Baltic Sea: Small-scale fluxes, pH, and oxygen microenvironments. *Limnol. Oceanogr.* **53**: 914-921.
- Pommerening-Röser, A., and H. P. Koops. 2005. Environmental pH as an important factor for the distribution of urease positive ammonia-oxidizing bacteria. *Microbiol. Res.* **160**: 27-35.
- Price, G. D., M. R. Badger, F. J. Woodger, and B. M. Long. 2008. Advances in understanding the cyanobacterial CO<sub>2</sub>-concentrating-mechanism (CCM): functional components, Ci transporters, diversity, genetic regulation and prospects for engineering into plants. *J. Exp. Bot.* **59**: 1441-1461.
- Qiu, B. S., and K. S. Gao. 2002. Effects of CO<sub>2</sub> enrichment on the bloom-forming cyanobacterium *Microcystis aeruginosa* (Cyanophyceae): Physiological responses and relationships with the availability of dissolved inorganic carbon. *J. Phycol.* **38**: 721-729.
- Quinn, G., and M. Keough. 2002. *Experimental design and data analysis for biologists.* Cambridge University Press.
- Rao, A. M. F., and R. A. Jahnke. 2004. Quantifying porewater exchange across the sediment-water interface in the deep sea with in situ tracer studies. *Limnol. Oceanogr. - Method* **2**: 75-90.
- Rauch, M., and L. Denis. 2008. Spatio-temporal variability in benthic mineralization processes in the eastern English Channel. *Biogeochemistry* **89**: 163-180.
- Rich, J. J., O. R. Dale, B. Song, and B. B. Ward. 2008. Anaerobic ammonium oxidation (anammox) in Chesapeake Bay sediments. *Microb. Ecol.* **55**: 311-320.
- Richardson, K. 1997. Harmful or exceptional phytoplankton blooms in the marine ecosystem. *Advances In Marine Biology*, Vol 31 Book Series: *Advances In Marine Biology* **31**: 301-385.
- Rippka, R., A. Neilson, R. Kunisawa, and C. G. 1971. Nitrogen fixation by unicellular blue-green algae. *Arch. Mikrobiol.* **76**: 341-348.

- Risgaard-Petersen, N. 2003. Coupled nitrification-denitrification in autotrophic and heterotrophic estuarine sediments: On the influence of benthic microalgae. *Limnol. Oceanogr.* **48**: 93-105.
- Risgaardpedersen, N., S. Rysgaard, L. P. Nielsen, and N. P. Revsbech. 1994. Diurnal-variation of denitrification and nitrification in sediments colonized by benthic microphytes. *Limnol. Oceanogr.* **39**: 573-579.
- Robbins, J. A., D. N. Edgington, and A. L. W. Kemp. 1978. Comparative  $^{210}\text{Pb}$ ,  $^{137}\text{Cs}$  and pollen geochronologies of sediments from Lakes Ontario and Erie. *Quaternary Research* **10**: 256-278.
- Rosenfeld, J. K. 1979. Ammonium adsorption in nearshore anoxic sediments. *Limnol. Oceanogr.* **24**: 356-364.
- Ruhl, H. a. R., N. B. 2010. Long-term reductions in anthropogenic nutrients link to improvements in Chesapeake Bay habitat. *Proceedings of the National Academy of Society* **174**: 16566 -16570.
- Rysgaard, S., P. B. Christensen, and L. P. Nielsen. 1995. Seasonal-variation in nitrification and denitrification in estuarine sediment colonized by benthic microalgae and bioturbating infauna. *Mar. Ecol. Prog. Ser.* **126**: 111-121.
- Rysgaard, S., N. Risgaard-Petersen, and N. P. Sloth. 1994. Oxygen regulation of nitrification and denitrification in sediments. *Limnol. Oceanogr.* **39**: 1643-1652.
- Sabour, B., B. Sbiyyaa, M. Loudiki, B. Oudra, M. Belkoura, and V. Vasconcelos. 2009. Effect of light and temperature on the population dynamics of two toxic bloom forming cyanobacteria - *Microcystis ichthyoblabe* and *Anabaena aphanizomenoides*. *Chemistry and Ecology* **25**: 277-284.
- Sannigrahi, P., and E. Ingall. 2005. Polyphosphates as a source of enhanced P fluxes in marine sediments overlain by anoxic waters: Evidence from P-31 NMR. *Geochem. Trans.* **6**: 52-59.
- Sanudo-Wilhelmy, S. A., A. Tovar-Sanchez, F. X. Fu, D. G. Capone, E. J. Carpenter, and D. A. Hutchins. 2004. The impact of surface-adsorbed phosphorus on phytoplankton Redfield stoichiometry. *Nature* **432**: 897-901.
- Schmidt, T. 2006. *Topics in Ecological and Environmental Microbiology*. Elsevier Inc.

- Schulz, K. G., U. Riebesell, B. Rost, S. Thoms, and R. E. Zeebe. 2006. Determination of the rate constants for the carbon dioxide to bicarbonate inter-conversion in pH-buffered seawater systems. *Mar. Chem.* **100**: 53-65.
- Scott, J. T., M. J. McCarthy, W. S. Gardner, and R. D. Doyle. 2008. Denitrification, dissimilatory nitrate reduction to ammonium, and nitrogen fixation along a nitrate concentration gradient in a created freshwater wetland. *Biogeochemistry* **87**: 99-111.
- Seitzinger, S. 1987a. The effect of pH on the release of phosphorus from Potomac River sediment, p. 1-46. Chesapeake Bay program.
- Seitzinger, S. 1988. Denitrification in freshwater and coastal marine ecosystems: ecological and geochemical significance. *Limnol. Oceanogr.* **33**: 702-724.
- Seitzinger, S. P. 1987b. The effect of pH on the release of phosphorus from Potomac River sediment, p. 1-46. Chesapeake Bay Program Report.
- . 1991. The effect of pH on the release of phosphorus from Potomac estuary sediments - implications for blue-green-algal blooms. *Estuar. Coast. Shelf Sci.* **33**: 409-418.
- Seitzinger, S. P., W. S. Gardner, and A. K. Spratt. 1991. The effect of salinity on ammonium sorption in aquatic sediments - implications for benthic nutrient recycling. *Estuaries* **14**: 167-174.
- Sellner, K. G., R. V. Lacouture, and C. R. Parrish. 1988. Effects of increasing salinity on a cyanobacteria bloom in the Potomac River estuary. *J. Plankton Res.* **10**: 49-61.
- Severin, I., and L. J. Stal. 2008. Light dependency of nitrogen fixation in a coastal cyanobacterial mat. *ISEM Journal: Multidisciplinary Journal of Microbial Ecology* **2**: 1077-1088.
- Sharp, J. H. and others 2009. A Biogeochemical view of estuarine eutrophication: seasonal and spatial trends and correlations in the Delaware estuary. *Estuar. Coast.* **32**: 1023-1043.
- Short, S. M., and J. P. Zehr. 2007. Nitrogenase gene expression in the Chesapeake Bay Estuary. *Environ. Microbiol.* **9**: 1591-1596.
- Simek, M., L. Jisova, and D. W. Hopkins. 2002. What is the so-called optimum pH for denitrification in soil? *Soil Biol. Biochem.* **34**: 1227-1234.

- Simon, N. S., and M. M. Kennedy. 1987. The distribution of nitrogen species and adsorption of ammonium in sediments from the tidal Potomac River and estuary. *Estuar. Coast. Shelf Sci.* **25**: 11-26.
- Slomp, C. P., J. F. P. Malschaert, and W. Van Raaphorst. 1998. The role of adsorption in sediment-water exchange of phosphate in North Sea continental margin sediments. *Limnol. Oceanogr.* **43**: 832-846.
- Sloth, N. P., H. Blackburn, L. S. Hansen, N. Risgaardpetersen, and B. A. Lomstein. 1995. Nitrogen cycling in sediments with different organic loading. *Mar. Ecol. Prog. Ser.* **116**: 163-170.
- Smith, E. M., and W. M. Kemp. 2001. Size structure and the production/respiration balance in a coastal plankton community. *Limnol. Oceanogr.* **46**: 473-485.
- Soetaert, K., A. F. Hofmann, J. J. Middelburg, F. J. R. Meysman, and J. Greenwood. 2007. The effect of biogeochemical processes on pH (Reprinted from *Marine Chemistry*, vol 105, pg 30-51, 2007). *Mar. Chem.* **106**: 380-401.
- Staal, M., S. T. L. Hekkert, F. J. M. Harren, and L. J. Stal. 2003. Effects of O<sub>2</sub> on N<sub>2</sub> fixation in heterocystous cyanobacteria from the Baltic Sea. *Aquat. Microb. Ecol.* **33**: 261-270.
- Stainton, M. P. 1973. Syringe gas-stripping procedure for gas-chromatographic determination of dissolved inorganic and organic carbon in fresh water and carbonates in sediments. *J. Fish. Res. Board Can.* **30**: 1441-1445.
- Stal, L. J., and W. E. Krumbein. 1985. Nitrogenase activity in the non-heterocystous cyanobacterium *Oscillatoria* sp. grown under alternating light-dark cycles. *Arch. Microbiol.* **143**: 67-71.
- Staner, R. Y. D., M.; Adelberg, E. A. 1970. Other groups of gram-negative nonphotosynthetic true bacteria, p. 873. *The microbial world*. Prentice-Hall, Inc.
- Staver, L. W., K. W. Staver, and J. C. Stevenson. 1996. Nutrient inputs to the Choptank River estuary: Implications for watershed management. *Estuaries* **19**: 342-358.
- Stevenson, B. S., and J. B. Waterbury. 2006. Isolation and identification of an epibiotic bacterium associated with heterocystous *Anabaena* cells. *Biol. Bull.* **210**: 73-77.



- Stief, P., D. De Beer, and D. Neumann. 2002. Small-scale distribution of interstitial nitrite in freshwater sediment microcosms: The role of nitrate and oxygen availability, and sediment permeability. *Microb. Ecol.* **43**: 367-378.
- Strauss, E. A., N. L. Mitchell, and G. A. Lamberti. 2002. Factors regulating nitrification in aquatic sediments: effects of organic carbon, nitrogen availability, and pH. *Can. J. Fish. Aquat. Sci.* **59**: 554-563.
- Stumm, W., and J. Morgan. 1996. *Aquatic Chemistry: Chemical Equilibria and Rates in Natural Waters*. John Wiley & Sons, Inc.
- Sundback, K., and A. Miles. 2000. Balance between denitrification and microalgal incorporation of nitrogen in microtidal sediments, NE Kattegat. *Aquat. Microb. Ecol.* **22**: 291-300.
- Tango, P. J., and W. Butler. 2008. Cyanotoxins in tidal waters of Chesapeake Bay. *Northeast. Nat.* **15**: 403-416.
- Tank, S. E., L. F. W. Lesack, and D. J. Mcqueen. 2009. Elevated pH regulates bacterial carbon cycling in lakes with high photosynthetic activity. *Ecology* **90**: 1910-1922.
- Testa, J. M., W. M. Kemp, W. R. Boynton, and J. D. Hagy. 2008. Long-term changes in water quality and productivity in the Patuxent River estuary: 1985 to 2003. *Estuar. Coast.* **31**: 1021-1037.
- Thostrup, L., and K. Christoffersen. 1999. Accumulation of microcystin in *Daphnia magna* feeding on toxic *Microcystis*. *Archiv für Hydrobiologie* **145**: 447-467.
- Tiedje, J. M., S. Simkins, and P. M. Groffman. 1989. Perspectives on measurement of denitrification in the field including recommended protocols for acetylene based methods. *Plant Soil* **115**: 261-284.
- Tomaszek, J. A., and E. Czerwieniec. 2003. Denitrification and oxygen consumption in bottom sediments: factors influencing rates of the processes. *Hydrobiologia* **504**: 59-65.
- Tonk, L., K. Bosch, P. Visser, and J. Huisman. 2007. Salt tolerance of the harmful cyanobacterium *Microcystis aeruginosa*. *Aquat. Microb. Ecol.* **46**: 117-123.
- Tortell, P. D., C. Payne, C. Gueguen, R. F. Strzepek, P. W. Boyd, and B. Rost. 2008. Inorganic carbon uptake by Southern Ocean phytoplankton. *Limnol. Oceanogr.* **53**: 1266-1278.

- Trimmer, M., D. Nedwell, and D. Sivyer. 1998. Nitrogen fluxes through the lower estuary of the river Great Ouse, England: the role of the bottom sediments. *Mar. Ecol. Prog. Ser.* **163**: 109-124.
- Unrein, F., I. O'farrell, I. Izaguirre, R. Sinistro, M. D. Afonso, and G. Tell. 2010. Phytoplankton response to pH rise in a N-limited floodplain lake: relevance of N<sub>2</sub>-fixing heterocystous cyanobacteria. *Aquatic Sciences* **72**: 179-190.
- Van Hulle, S. W. H., E. I. P. Volcke, J. L. Teruel, B. Donckels, M. C. M. Van Loosdrecht, and P. A. Vanrolleghem. 2007. Influence of temperature and pH on the kinetics of the Sharon nitrification process. *J. Chem. Technol. Biotechnol.* **82**: 471-480.
- Verity, P. G., C. Y. Robertson, C. R. Tronzo, M. G. Andrews, J. R. Nelson, and M. E. Sieracki. 1992. Relationships between Cell-Volume and the Carbon and Nitrogen-Content of Marine Photosynthetic Nanoplankton. *Limnol. Oceanogr.* **37**: 1434-1446.
- Vouve, F., G. Guiraud, C. Marol, M. Girard, P. Richard, and M. J. C. Laima. 2000. NH<sub>4</sub><sup>+</sup> turnover in intertidal sediments of Marennes-Oleron Bay (France): effect of sediment temperature. *Oceanologica Acta* **23**: 575-584.
- Wagner, and Adrian. 2009. Cyanobacteria dominance: Quantifying the effects of climate change. *Limnol. Oceanogr.* **54**: 2460-2468.
- Walsby, A. E., P. K. Hayes, R. Boje, and L. J. Stal. 1997. The selective advantage of buoyancy provided by gas vesicles for planktonic cyanobacteria in the Baltic Sea. *New Phytol.* **136**: 407-417.
- Wang, F. L., and A. K. Alva. 2000. Ammonium adsorption and desorption in sandy soils. *Soil Sci. Soc. Am. J.* **64**: 1669-1674.
- Watkinson, A. J., J. M. O'neil, and W. C. Dennison. 2005. Ecophysiology of the marine cyanobacterium, *Lyngbya majuscula* (*Oscillatoriaceae*) in Moreton Bay, Australia. *Harmful Algae* **4**: 697-715.
- Weston, N. B., A. E. Giblin, G. T. Banta, C. S. Hopkinson, and J. Tucker. 2010. The effects of varying salinity on ammonium exchange in estuarine sediments of the Parker River, Massachusetts. *Estuar. Coast.* **33**: 985-1003.

- Wood, P. 1988. Monooxygenase and free radical mechanisms for biological ammonia oxidation, p. 219–243. *In* J. Cole and S. Ferguson [eds.], *The Nitrogen and Sulphur Cycles*. Cambridge University Press.
- Xie, L. Q., and P. Xie. 2003. Enhancement of dissolved phosphorus release from sediment to lake water by *Microcystis* blooms - an enclosure experiment in a hyper-eutrophic, subtropical Chinese lake. *Environ. Pollut.* **122**: 391-399.
- Yamamoto, Y., and H. Nakahara. 2005. Competitive dominance of the cyanobacterium *Microcystis aeruginosa* in nutrient-rich culture conditions with special reference to dissolved inorganic carbon uptake. *Phycol. Res.* **53**: 201-208.
- Zehr, J. P., M. Mellon, S. Braun, W. Litaker, T. Steppe, and H. W. Paerl. 1995. Diversity of Heterotrophic Nitrogen-Fixation Genes in a Marine Cyanobacterial Mat. *Appl. Environ. Microbiol.* **61**: 2527-2532.